ROYAUME DU MAROC

Université Mohammed V - RABAT -

جامعة محمد الخامس – الرباط –

Faculté des sciences

كلية العلوم

CENTRE D'ETUDES DOCTORALES - SCIENCES ET TECHNOLOGIES

N° d'ordre 3889

THESE

En vue de l'obtention du : ***DOCTORAT***

Centre de Recherche : ***GEOPAC Research Center***
Structure de Recherche : ***Geophysics and Natural Hazards Laboratory***
Discipline : ***Sciences de l'Ingénieur***
Spécialité : ***Sciences et Technologies de l'Espace***

Présentée et soutenue le 29/12/2023 par :

Badr BEN HICHOU

Le titre de la thèse

Geoinformation Technologies for Environmental Monitoring and Modeling: A Multi-Faceted Approach

JURY

Jamal CHAO	PES, Faculté de Sciences de Kenitra, Université Ibn Tofail	Président
Oumnia HIMMI	PES, Institut Scientifique de Rabat. Université Mohammed V	Rapporteuse/ Examinatrice
Rachid ALAOUI	PH, Ecole Supérieure de Technologie de Salé, Université Mohammed V	Rapporteur/ Examinateur
Hicham EL BELRHITI	PH, Institut Agronomique et Vétérinaire Hassan-II	Rapporteur/ Examinateur
Rachid EL MRABET	HDR, Directeur Général, INNOREM Group	Examinateur
Mohamed DAKKI	PES, Institut Scientifique de Rabat, Université Mohammed V	Invité d'honneur
Nadia MHAMMDI	PES, Institut Scientifique de Rabat. Université Mohammed V	Directrice de Thèse

Année Universitaire : 2023/2024

✉ Faculté des Sciences, avenue Ibn Battouta, BP. 1014 RP, Rabat –Maroc
☎ 00212 (05) 37 77 18 76 🖷 00212(05) 37 77 42 61; http://www. fsr.um5.ac.ma

Dedication

I dedicate this thesis, and all my academic achievements, to my parents, my wife, my daughter, my brother and my entire family.

I wish to express my heartfelt gratitude to my parents ***Mano & Bano***, to my wife ***Hayat***, and to my daughter ***Joud***, for their unwavering support and encouragement throughout my academic journey. Their love and belief in me have been the cornerstone of my accomplishments, and I am profoundly blessed to have them as my pillars of strength. I am also grateful to my extended family and friends for their constant support of my dreams.

Acknowledgments

I would like to express my deep gratitude and sincere appreciation to Geophysics and Natural Hazards Laboratory, and GEOPAC Research Center. I extend my heartfelt thanks to **Professor Mohamed DAKKI**, my former thesis advisor, for his exceptional mentorship and invaluable support throughout my academic journey. His guidance and expertise were instrumental in cultivating my passion for scientific research and honing my skills. Professor DAKKI taught me the fundamentals of scientific research, inspired me to pursue excellence, and supported me through challenges and opportunities. Even after his retirement, his influence continues to resonate in my academic and professional achievements.

I am equally grateful to **Professor Nadia MHAMMDI**, my current advisor, for her support and valuable guidance. Her mentorship has been crucial in reaching the stage where I am ready to defend my thesis, and for that, I am deeply thankful.

I would like to extend my sincere gratitude to the President of the jury **Professor Jamal CHAO**, whose leadership and oversight were pivotal in the evaluation of my work. His commitment to maintaining high academic standards is greatly appreciated. My deepest thanks to the reporters and examiners of my thesis, whose thorough evaluations and constructive feedback have significantly contributed to the refinement and quality of my research.

I am profoundly grateful to **Professor Oumnia HIMMI** as examiner and reporter for her thorough evaluation and constructive feedback. Her expertise and attention to detail have been invaluable in refining the quality of my research.

My sincere thanks to **Professor Rachid ALAOUI** as examiner and reporter for his critical assessment and valuable suggestions. His insights have significantly contributed to enhancing the depth and rigor of my work.

My heartfelt appreciation goes to **Professor Hicham EL BELRHITI** as examiner and reporter for his comprehensive review and constructive comments. His guidance has played a crucial role in shaping the final form of my thesis.

I am deeply thankful to **Doctor Rachid EL MRABET** as examiner for his insightful feedback and expert evaluation. His contributions have been instrumental in ensuring the academic integrity and quality of my research.

I would also like to thank the guests who have shown interest in my research and have been supportive throughout this journey. Your presence and encouragement mean a lot to me.

Finally, I want to acknowledge my family, friends, and colleagues, whose constant support and encouragement have been my driving force. Their belief in me has been a source of strength and motivation throughout this journey. Thank you so much!

Abstract

In an era marked by swift urbanization, industrial growth, and escalating resource demands, the world confronts significant challenges in reconciling human advancement with environmental well-being. Global issues such as environmental degradation, natural disasters, and ecosystem loss demand innovative solutions. This extensive thesis embarks on a journey to explore the multifaceted applications of geoinformation technologies, including remote sensing, GIS, and GeoAI, in environmental monitoring, modeling, and territorial management through five distinct research studies. Our investigations intricately examine various aspects, including tracking the spread of forest fires, conducting in-depth studies on wetland hydrology in arid regions, assessing vulnerabilities to soil degradation, predicting sediment yield and delivery ratio of a dam, prioritizing conservation efforts using advanced models, and classifying estuarine ecosystems. These studies actively contribute to the realization of the United Nations Sustainable Development Goals, underscoring the crucial role of spatial information technologies in comprehending and effectively managing environmental dynamics to uphold a natural balance.

Key Words: Geoinformation Technologies, Environmental Monitoring, Territorial Management, Natural Hazards, Remote Sensing, GIS.

Résumé

Dans une ère caractérisée par une urbanisation rapide, une industrialisation croissante et des demandes de ressources en augmentation, notre monde fait face à des défis profonds pour harmoniser le progrès humain avec le bien-être environnemental. La dégradation de l'environnement, les catastrophes naturelles et la perte d'écosystèmes sont des préoccupations mondiales pressantes qui nécessitent des solutions innovantes. Au sein des pages de cette thèse exhaustive, nous nous lançons dans un voyage pour explorer les applications diverses des technologies de géoinformation telles que la télédétection, les SIG et la géo-IA dans la surveillance et la modélisation environnementales, ainsi que dans la gestion territoriale à travers cinq études de recherche distinctes. Nous analysons méticuleusement et suivons la propagation des incendies de forêt, menons des études détaillées sur l'hydrologie des zones humides dans les régions arides, quantifiant les sols sensibles à l'érosion hydrique, prédisons le rendement en sédiments et le rapport de livraison de sédiments d'un barrage, priorisons les efforts de conservation en utilisant des modèles avancés, et classifions les écosystèmes estuariens. Ces études contribuent à la réalisation des objectifs de développement durable des Nations Unies et soulignent le rôle essentiel des technologies de l'information spatiale dans la compréhension et la gestion efficaces des dynamiques environnementales, tout en maintenant un équilibre naturel.

Mot clés : Technologies de la Géo-Information, Surveillance de l'environnement, Gestion du territoire, Risques naturels, Télédétection, SIG.

✉ Faculté des Sciences, avenue Ibn Battouta, BP. 1014 RP, Rabat - Maroc
☎ 00212 (05) 37 77 18 76 🖷 00212(05) 37 77 42 61; http://www. fsr.um5.ac.ma

ملخص

في عصر يتسم بالتحضر السريع والنمو الصناعي وزيادة الطلب على الموارد، يواجه العالم تحديات كبيرة في التوفيق بين تقدم الإنسان ورفاهية البيئة. قضايا عالمية مثل تدهور البيئة والكوارث الطبيعية وفقدان النظام البيئي تتطلب حلاً مبتكرًا. في هذه الأطروحة، نستكشف التطبيقات الواسعة لتقنيات المعلومات المكانية مثل الاستشعار عن بعد بالأقمار الاصطناعية ونظم المعلومات الجغرافية والذكاء الاصطناعي في مراقبة البيئة وإدارة المجال من خلال خمس دراسات بحثية متميزة. تحليلنا يتناول بعناية جوانب متنوعة، بما في ذلك تتبع وتحليل انتشار حرائق الغابات اعتمادا على تكنولوجيا الاستشعار عن بعد، وإجراء دراسات مفصلة حول هيدرولوجيا الأراضي الرطبة في المجال الصحراوي بالاعتماد على تقنيات النمذجة المحاكية للواقع، وتقدير قابلية التربة للانجراف في حوض الجريان السطحي من مستجمعات المياه للسد بتحديد كم التربة الحساسة والمحتمل تدهورها اعتمادا على نظم المعلومات الجغرافية والخصائص الفيزيائية للمجالات الطبيعية، مع إعطاء الأولوية لجهود الحفاظ عليها باستخدام نماذج متقدمة، وإجراء دراسة أخرى لتوقع نسبة الأوحال التي تترسب في السد أثناء انتقالها مع المياه السطحية عبر الوديان ومياه الأمطار، وكذا تصنيف مصبات الأنهار في البحر اعتمادا على تقنيات النمذجة الهيدرولوجية. تسهم هذه الدراسات في تحقيق أهداف التنمية المستدامة للأمم المتحدة، مؤكدة الدور الحيوي لتقنيات المعلومات المكانية في فهم وإدارة الديناميات البيئية بفعالية، والحفاظ على التوازن الطبيعي.

الكلمات الرئيسية: تقنيات المعلومات المكانية، مراقبة البيئة، إدارة الأراضي، الكوارث الطبيعية، الاستشعار عن بعد، نظم المعلومات الجغرافية

Résumé détaillé

Dans un monde marqué par une urbanisation rapide, une industrialisation croissante et une demande accrue de ressources, la dégradation de l'environnement, les catastrophes naturelles et la perte des écosystèmes posent des défis significatifs. Cette thèse explore le rôle des technologies de géoinformation, telles que la télédétection, les SIG et la GeoIA, dans la surveillance et la modélisation environnementales pour répondre à ces préoccupations mondiales.

L'objectif principal de cette thèse est d'explorer et de démontrer les applications multiples des technologies de géoinformation dans la surveillance, la modélisation environnementale et la gestion territoriale à travers cinq études de recherche distinctes. Ces études visent à contribuer à la compréhension, à la gestion et à l'atténuation des problèmes environnementaux tout en soutenant les Objectifs de Développement Durable (ODD) des Nations Unies.

La première étude analyse et suit la propagation des incendies de forêt et les changements de couverture terrestre associés. En utilisant la télédétection et les techniques SIG pour surveiller les incendies de forêt actifs et cartographier les zones brûlées, cette étude offre une analyse spatiotemporelle détaillée de la propagation des incendies et de la sévérité des brûlures. Les informations fournies sont cruciales pour la gestion post-incendie et soulignent le rôle des technologies géospatiales dans la préservation des écosystèmes forestiers.

La deuxième étude se concentre sur l'hydrologie de la zone humide saharienne d'Imlili Sebkha. Elle utilise les SIG et les données satellites pour étudier les dynamiques hydrologiques de cette zone dans les régions arides. L'intégration des données orohydrographiques et des traitements géospatiaux permet d'estimer les volumes d'eau reçus par la zone humide. Cette étude met en évidence les défis de la maintenance de l'hydrologie des zones humides dans les environnements arides et fournit des données cruciales pour la gestion durable des ressources en eau.

La troisième étude évalue l'impact des barrages artificiels sur l'érosion des sols et le rendement sédimentaire, en se concentrant sur le réservoir Hassan Ad-Dakhil. Utilisant les SIG, la télédétection et le modèle RUSLE pour estimer les taux annuels de sédiments, cette étude offre des insights sur les dynamiques hydro-sédimentaires. Les résultats soutiennent l'évaluation de l'impact environnemental et la gestion durable des écosystèmes aquatiques.

La quatrième étude cartographie les zones sensibles à la dégradation des sols dans le bassin du barrage Sidi Mohamed Ben Abdellah en utilisant le modèle MEDALUS. L'intégration des données Sentinel 2 dans un système SIG permet d'évaluer divers

indices de qualité, tels que le climat, le sol, la végétation et la gestion. Cette étude crée une carte complète de la sensibilité à la désertification, fournissant un cadre pour prioriser les efforts de conservation.

Enfin, la cinquième étude se concentre sur la classification des écosystèmes estuariens de la bande côtière du Yémen. En appliquant des algorithmes de classification modernes et des données satellites, cette étude identifie et classe les environnements estuariens. Elle améliore la compréhension de la relation entre les caractéristiques des bassins versants et les écosystèmes estuariens, aidant ainsi à une classification et une gestion efficaces.

Cette thèse contribue de manière significative aux Objectifs de Développement Durable (ODD). Elle promeut la gestion responsable des ressources en eau (ODD 6), soutient le développement urbain durable (ODD 11), évalue les risques environnementaux et développe des stratégies de mitigation (ODD 13), priorise la conservation et la restauration des écosystèmes (ODD 15), et encourage la collaboration entre divers acteurs pour avancer les objectifs de développement durable (ODD 17).

Cette thèse souligne le rôle indispensable des technologies de géoinformation dans la surveillance, la modélisation et la gestion environnementales. Les études de recherche contribuent collectivement à une compréhension plus large des dynamiques environnementales et démontrent le potentiel des technologies de l'information spatiale pour relever les défis environnementaux mondiaux. Les résultats mettent en avant la nécessité d'une innovation continue et d'une collaboration pour gérer et protéger efficacement les ressources naturelles de notre planète.

Figures list

Chapter I

Chapter II

Chapter III

Chapter IV

Chapter V

List of Tables

Table of Contents

Chapter I: Introduction

I.1. Background and Context

The integration of information technologies has revolutionized the fields of ecology and environmental science. Classic studies laid the foundational principles, while modern approaches, enhanced by advanced technologies, allow for more comprehensive, precise, and impactful research. This transformation has enabled scientists to address complex environmental challenges with unprecedented accuracy and efficiency, facilitating better conservation strategies and policy decisions.

In an age marked by rapid urbanization, expanding industrialization, and an ever-increasing demand for resources, our planet faces unprecedented challenges in maintaining the delicate balance between human progress and environmental sustainability and climate change. Environmental degradation, natural disasters, and the loss of critical ecosystems have become pressing global concerns, necessitating innovative solutions and a deeper understanding of the complex interactions between the environment and human activities. It is within this context that the role of geoinformation technologies, encompassing remote sensing, Geographic Information Systems (GIS), and GeoAI, has taken center stage in the field of environmental monitoring and territorial management.

This thesis embarks on a multifaceted journey to explore the dynamic and versatile applications of geoinformation technologies as powerful tools for understanding, managing, and mitigating environmental issues. Our research endeavors delve into five distinct studies, each shedding light on critical aspects of environmental dynamics and their implications for our planet's well-being.

The first study offers a meticulous examination of forest fires, a perilous natural phenomenon with profound consequences. By seamlessly integrating geomatics techniques and remote sensing data, we unveil the intricacies of forest fire propagation and the associated changes in land cover. The study's findings provide invaluable insights for post-fire management, emphasizing the pivotal role of geospatial technologies in safeguarding our critical forest ecosystems.

Turning our attention to the arid landscapes of southern Morocco, the second study explores the hydrology of a Saharan wetland, the Imlili Sebkha. Through the lens of GIS and satellite data, we delve into the challenges of maintaining wetland hydrology in arid regions, where water resources are scarce and precious.

In the third study, GIS, Remote Sensing, and the RUSLE, along with Williams' (1977) equation, are employed to estimate the yearly sediment rate influenced by the Hassan

Ad-Dakhil Dam in South-East Morocco. This inventive methodology offers valuable insights into hydro-sedimentary dynamics, supporting environmental impact assessment and fostering sustainable management of aquatic ecosystems and dam infrastructure.

Our fourth study harnesses the power of the MEDALUS model to map areas susceptible to soil degradation, focusing on the Sidi Mohamed Ben Abdellah dam watershed. This comprehensive approach considers multiple factors and offers a roadmap for prioritizing conservation and management efforts in the region.

Shifting our gaze to the estuarine ecosystems of Yemen, the fifth and study employs satellite data and modern classification algorithms to classify these vital environments. Through this research, we unravel the intricate relationship between watershed characteristics and the diverse nature of estuaries, shedding light on the challenges of obtaining sea data for classification.

These five studies underscore the multifaceted and indispensable role of geoinformation technologies in the realms of environmental monitoring, modeling, and management. They offer a valuable mosaic of insights that contribute to our broader understanding of the intricate dance between the natural environment and human activities, while also serving as a testament to the power of cutting-edge technologies in safeguarding our planet's future.

I.2. Sustainable Development Goals and Their Relevance to the Research

A global call to action to solve a number of urgent concerns was issued by the United Nations in 2015 with the adoption of the 17 Sustainable Development Goals (SDGs). By 2030, this set of objectives offers a thorough plan for creating a more just, resilient, and sustainable world. They place a strong emphasis on how interconnected economic, social, and environmental aspects are, acknowledging how improvements in one area are closely related to those in others.

This thesis's research strongly connects with multiple SDGs, demonstrating the work's worldwide relevance through its exploration of geoinformation technologies. For SDG 6, it studies the hydrology of the Imlili Sebkha wetland, using GIS and satellite data to promote responsible water resource management in arid regions. For SDG 11, it highlights the role of these technologies in urban sustainability by examining forest fire propagation and land cover changes. Addressing SDG 13, the research assesses environmental risks and develops strategies for mitigation, focusing on soil degradation and sediment yield prediction. For SDG 15, it prioritizes conservation through advanced modeling, emphasizing the protection and restoration of ecosystems. Finally, for SDG 17, the research promotes collaboration between stakeholders, exemplifying interdisciplinary partnerships for sustainable development.

The covered SDGs are specifically covered in this study:

Table I. 1: Covered Sustainable Development Goals of the Thesis

SDG 6: Clean Water and Sanitation	This research contributes to SDG 6 by examining the sustainable management of water resources, particularly in arid regions. It seeks to understand the dynamics of water sources and their environmental implications, offering insights into responsible water resource usage.
SDG 11: Sustainable Cities and Communities	The utilization of geoinformation technologies and environmental monitoring supports the creation of sustainable and resilient urban communities, a central theme in SDG 11. By focusing on the management and conservation of territories and resources, this research directly contributes to sustainable urbanization.
SDG 13: Climate Action	The core of this research revolves around the assessment of environmental risks and the development of strategies for mitigation. In doing so, it directly supports the objectives of SDG 13, which call for urgent measures to combat climate change and its impacts.
SDG 15: Life on Land	The research endeavors to preserve terrestrial ecosystems and biodiversity. By addressing wetlands, forest fires, and habitat diversity, it aligns with the central aims of SDG 15, which seeks to protect, restore, and sustainably use life on land.
SDG 17: Partnerships for the Goals	Collaboration and partnerships are essential for achieving the SDGs. This research fosters collaboration between various stakeholders, including academia, government agencies, and environmental organizations, to advance these global goals. It exemplifies the spirit of SDG 17 by promoting cooperative action for sustainable development.

I.3. Environmental Monitoring and Modeling: Literature Review

The rapid growth of technology has caused significant changes in society, the economy, and the environment in the twenty-first century. As a defining characteristic of this time period, climate change stands out because it has a direct or indirect worldwide impact on both human existence and the natural world. The effects of this phenomenon include changes in many different climate patterns, an increase in the average world temperature, local rises in sea levels, and the progressive thawing of polar ice, among others. Consequences of these changes include altered biodiversity within ecosystems, changes in natural processes, and an increase in the frequency of natural disasters (figure I.1).

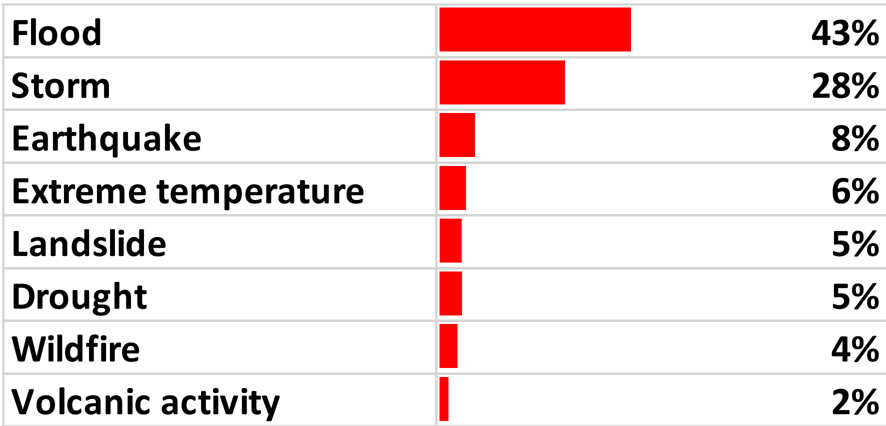

Figure I. 1: Percentage of natural disasters by kind between 1995 and 2015 (Wahlstrom et al. 2015)

The creation and use of contemporary, highly effective tools, which have surfaced in conjunction with the current increase in technology and scientific advancements related to environmental monitoring and modeling and climate change, is a critical component of addressing and responding to this emerging reality. Over the past ten years, the scientific community and decision-makers have focused on studying, controlling, and responding to natural disasters and processes. These initiatives are especially important in view of the current environmental, social, and economic issues (Figure I.2), which are principally brought on by climate change. Accurately forecasting natural catastrophes and defending susceptible areas against their rising threat and mounting effects are two of the most serious concerns.

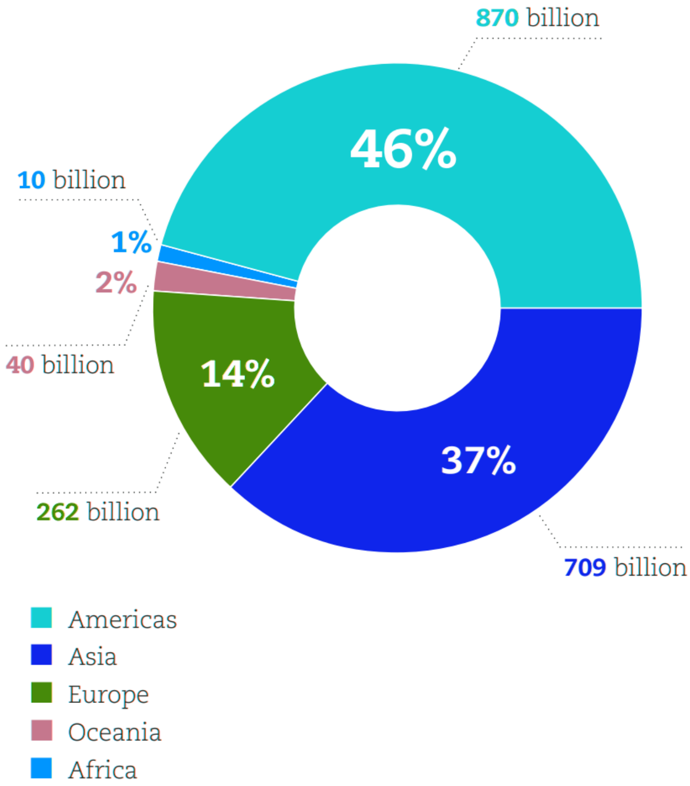

Figure I. 2: Total losses by continent (in US dollars) (1994–2015)

The European Union Directive 2007/60, which attempts to update and improve flood prevention, management, and rehabilitation procedures throughout its member states, is a notable example of this proactive strategy. Additionally, this directive aims to set environmental goals for member states' water management plans with a focus on groundwater, which is threatened by both natural and human overuse, leading to degradation in both quantity and quality. Similar programs have been carried out all over the world, and they have resulted in noteworthy achievements in the pursuit of sustainable environmental management.

Due to the impressive advancements made in science and technology over the past few decades, there is a growing demand for cutting-edge solutions and techniques in the field of environmental monitoring and modeling, design, and management. This trajectory of development has ushered in a transformational era in the geosciences, particularly in the complex fields of natural processes, risks, and disasters, and it shows no indications of slowing down in the near future. Geographic Information Systems (GIS) and Remote Sensing have emerged as two important innovation pillars that serve as compass points in this evolution.

The field of environmental research and management has undergone significant change as a result of the dynamic and quick advancements in these two disciplines. They have changed the methods and instruments used by contemporary scientists and practitioners in addition to broadening the field of study. The effects of this breakthrough are extensive, touching on a wide range of environmental issues that are extremely relevant to modern humans' daily lives.

The growth of satellite systems for Earth monitoring on a global basis has been nothing short of amazing. Whether acting independently or in cooperation with others, a large number of nations have started ambitious efforts to create satellite systems that are specifically suited to certain needs and purposes. These systems are made to examine a wide range of events, both artificial and natural. Passive optical satellites like Landsat and active RADAR satellites, designed specifically to achieve a range of environmental goals, are leading the charge in this attempt.

These systems are made to examine a wide range of events, both artificial and natural. Passive optical satellites like Landsat and active RADAR satellites like Sentinel-1, designed specifically to achieve a range of environmental goals, are leading the charge in this attempt. These include, but are not limited to, mapping flooded areas, forest fire management, seismic activity monitoring through sophisticated interferometric analysis of satellite data, and vegetation assessment. Additionally, as technology advances, the quality of satellite data continues to improve in terms of temporal frequency and spatial resolution, giving researchers a more detailed and granular understanding of the Earth's processes.

Tools for geoprocessing and analysis have experienced a comparable revolution in parallel with these developments in satellite technology. They have incorporated innovative approaches and strategies while expanding their reach and user-friendliness. Notably, open-source software alternatives, like QGIS, have grown to be strong rivals to proprietary software programs like ArcGIS. These open-source platforms enable academics to design custom tools that match their particular needs and work conditions. As a result, not only is flexibility increased, but data analysis and result extraction expenses and times are significantly reduced. These methods also solve difficulties that were previously intractable in conventional field research, such as accessibility to distant and otherwise inaccessible locations and the capability to operate productively in poor weather conditions.

These advances in science and technology have important consequences. The geo-environmental issues of the twenty-first century are not insurmountable impediments anymore; rather, they offer chances for investigation, comprehension, and efficient mitigation. We will begin a thorough investigation of a variety of thematic topics relating to environmental monitoring as we go further into the following sections. These encompass the investigation of floods, soil erosion, forest fires, hydrology, and sea level rise, each of which poses distinct research and management difficulties and opportunities.

In-depth discussions of tools and methods like GIS and Earth Observation (EO) will be provided, providing priceless insights into how they can be used to monitor, assess, and control these intricate environmental phenomena. By doing this, we hope to shed light on how modern environmental science and technology are advancing and helping us to meet the issues of our day with ever-greater accuracy and understanding.

I.3.1. Role of Earth Observation in Managing Natural Disasters

In the era of climate change, the escalating frequency and intensity of natural disasters have emerged as a paramount concern in scientific research, primarily due to their widespread and devastating impact on our planet (Gillespie et al., 2007; Colson et al., 2018; Whyte et al., 2018). As the world grapples with these increasingly complex challenges, various scientific approaches are being harnessed to mitigate the catastrophic consequences of natural disasters, taking into account their unique characteristics.

Earth observation has risen to prominence as an indispensable asset in disaster management, offering a versatile toolset for quantifying and detecting the spatiotemporal distribution and variability of myriad environmental hazards across diverse scales (Whyte et al., 2018; Srivastava et al., 2019). The EO sector has witnessed substantial growth over recent decades, rendering it increasingly capable of assessing the impacts of disasters on terrestrial landscapes, aquatic ecosystems, vegetation, and public health during these catastrophic events. The advent of satellite-based EO technology has firmly established it as the principal means of mapping and monitoring the dynamic spatial information related to disasters in real time, regardless of prevailing weather conditions (Evans et al., 2018; Pandey et al., 2020).

The domain of satellite remote sensing has progressively become the preferred instrument for managing disasters, chiefly owing to its capacity to furnish comprehensive information over vast geographic areas at short intervals. Moreover, the data gleaned from both historical and real-time observations empower experts to identify alterations in Earth's surface and underpin the formulation of effective management and mitigation strategies (Amos et al., 2019). EO datasets are the cornerstone of diverse geospatial analyses, enabling the retrieval, mapping, tracking, simulation, and representation of disaster-related events with remarkable efficiency and precision, all without necessitating physical site visits. The scientific and technical strengths of EO introduce a wide array of innovative capabilities for assessing and monitoring environmental variables (Dalezios et al., 2020). Consequently, remote sensing for forecasting, nowcasting, monitoring, and assessing environmental hazards has gained considerable traction, given the consistent availability of high-resolution data that spans vast geographic extents (Karamesouti et al., 2016).

The scope of EO encompasses satellites with variable spatial and temporal resolutions, available in both geostationary and polar orbits. These two orbit types complement each other, providing optimal choices for disaster management. Polar-orbiting satellites, positioned at low altitudes (<1000 km above Earth's surface), yield data with high spatial resolution but comparatively lower temporal resolution. Conversely, geostationary satellites orbit at higher altitudes (approximately 36,000 km above Earth's surface) and offer data with lower spatial resolution but significantly higher temporal resolution, sometimes with updates in mere minutes (Jeyaseelan, 2003; Petropoulos et al., 2012; Petropoulos et al., 2012). A multitude of satellite platforms incorporates multiple sensors that capture spectral information across the electromagnetic spectrum, encompassing the visible, infrared, thermal, and microwave regions. Numerous studies, including those conducted by (Gillespie et al., 2007; Joyce et al., 2009; Tralli et al., 2005), have explored the utility of various EO sensor types in addressing a wide array of natural hazards. Depending on the interaction between electromagnetic waves and atmospheric constituents, as well as Earth's surface features, EO sensors operating at various wavelengths are deployed to collect data on a range of geophysical phenomena. Over time, the monitoring of natural disasters has unveiled the prominent use of optical and microwave (MW) technologies within the EO domain (Volpi et al., 2013; Said et al., 2015).

The efficacy of predicting natural disasters hinges on the availability of suitable EO data products, which can be amassed through both short-term and long-term monitoring efforts (Kosmopoulos et al., 2018; Knorr et al., 2011). A continuous and frequent supply of EO data equips researchers with high spatiotemporal data that proves invaluable for studying both past and present phenomena. A wealth of EO data sources are now accessible for tracking natural hazards, encompassing ocean floor buoys, atmospheric tracking stations, aircraft observations, and orbital satellites positioned worldwide. Optical sensors, characterized by their consistent enhancements in both spatial and spectral resolution (Colson et al., 2018; Petropoulos et al., 2012; Ireland et al., 2015), offer invaluable resources for hazard mapping. Notable examples include optical sensors such as MODIS (Xin et al., 2013), ASTER (Liu et al., 2009; Huang et al., 2012), Hyperion (Forkuo, 2011), and OLI (Petropoulos et al., 2012; McNeil et al., 2007), all of which have demonstrated their efficacy in mapping hazards. However, their utility may be constrained by adverse weather conditions. In contrast, microwave sensors come to the fore in scenarios where optical observations are hindered by factors like cloud cover. Prominent examples of such sensors deployed in disaster mapping include radio direction and ranging (RADAR), radiometers, scatterometers, and radar altimeters (Whyte et al., 2018).

Successful mitigation of natural disasters hinges on the availability of detailed information regarding the anticipated frequency, characteristics, and magnitude of natural hazards over specific geographic areas (Amarnath, 2014). Disaster management encompasses three pivotal phases in which EO can make a substantial contribution: (1) the preparedness phase, which unfolds well before an event and entails risk prediction and the identification of risk zones; (2) the prevention phase, which is undertaken just prior to or during the event and includes early warning/forecasting, monitoring, and the preparation of contingency plans; and (3) the response and mitigation phase, which centers on damage assessment and relief management in the immediate aftermath of the event (Ireland & Petropoulos, 2015). Information required during any of these phases can be readily accessed through EO sensors covering extensive areas, whether mounted on aircraft or satellites. This information can be subsequently processed within a Geographic Information System (GIS) environment, where suitable geospatial analysis techniques are employed to yield valuable insights for devising effective disaster management plans that optimize preparedness and response strategies (Evans et al., 2018; Petropoulos et al., 2012; Kalivas et al., 2013). The integration of EO data with image manipulation techniques not only facilitates disaster mitigation but also enhances preparedness by providing systematic observations that feed into risk modeling (Evans et al., 2018; Poser & Dransch, 2010). The geospatial analysis of land surface conditions, combined with various spatial and non-spatial data, aids in efficient management and the development of effective mitigation plans. The diverse array of data, each with distinct characteristics, enables the identification of surface and subsurface ground conditions and supports rapid and thorough analysis. However, certain limitations persist in the use of EO for addressing natural disasters. For example, EO cannot provide information about subsurface ground features beyond certain depths, and EO data predictions may exhibit biases, necessitating ground truth observations for calibration and validation purposes to assess the accuracy of these predictions.

I.3.2. Technical Specifications of Earth Observation Satellites

The methods, techniques, and tools presented in this work are not ordinary resources but rather an advanced arsenal for contemporary research, management, and environmental monitoring. These tools serve as the forefront in combating various geo-environmental hazards that afflict our world, including droughts, floods, soil erosion, groundwater depletion, frost, and the rising sea levels. Additionally, they play an important role in safeguarding our invaluable natural resources.

What distinguishes these tools and makes them even more essential is their inherent adaptability. They possess the ability to evolve with the changing times, a characteristic deeply rooted in their modern origins. Their development and structure incorporate the latest advancements in software, data analytics, and modern techniques. As a result, they continue to grow and are capable of incorporating the expanding body of scientific knowledge and technological progress.

Speaking of technological advancements, satellite programs offer a fascinating range of earth observation imagery. These images can be broadly categorized into two main types: Passive and Active imagery. Passive imagery includes panchromatic, multi-spectral, pan-sharpened, hyper-spectral, microwave radiometry, and more. On the other hand, Active imagery encompasses remarkable technologies such as Synthetic Aperture Radar (SAR), LIDAR, Radar Altimetry, GNSS-R, and Radar Scatterometry.

The resolution of these images significantly impacts their usefulness. Low-resolution images have a Ground Sample Distance (GSD) exceeding 300 meters, while medium-resolution images range from 300 meters to 30 meters. High-resolution imagery provides a GSD within the 30 to 5-meter range, and very high resolution (VHR) imagery offers details at a level below 5 meters.

The selection of an appropriate resolution is contingent upon the specific requirements of an application or research investigation. In addition to resolution, satellite programs also differ in terms of revisit time. For instance, the COMS satellite offers a swift revisit time of merely 1 hour, albeit with a coarser Ground Sample Distance (GSD) of 500 meters. On the other hand, the SPOT-5 satellite has a longer revisit time of 26 days, but provides a finer GSD of 2.5 meters. Furthermore, the number of bands varies across different satellites, with some having 1, 2, or 3 bands, such as the Himawari 8, while others, like the Sentinel 3 A/B, boast an impressive 21 bands.

Consequently, researchers and application developers have a plethora of options available to them when it comes to selecting the most suitable satellite sensor or platform for their specific needs. The choice ultimately hinges upon the unique demands of each individual application or research inquiry.

To streamline this selection process, Table I.2, presented below, furnishes a comprehensive overview of some of the most renowned earth observation satellites. This table outlines their key characteristics, including launch year, number of bands, spatial resolution, altitude, and revisit days. By consulting this comprehensive reference guide, individuals can make well-informed decisions, ensuring that they possess the necessary tools to effectively address the challenges and opportunities presented by our ever-evolving world.

The following Table I.2, offers an overview of the prominent Earth Observation satellites, along with their primary attributes, including launch year, band count, spatial resolution, altitude, and revisit intervals.

Table I. 2: Characteristics of earth observation satellites

Satellite Name	Launch Year	No of Bands	Spatial Resolution (m)	Altitude (km)	Revisit Time (days)
SPOT 1	1986	3	20	832	2–3
SPOT 2	1990	3	20	832	2–3
SPOT 3	1993	2	20	832	2–3
SPOT 4	1998	4	20	832	2–3
SPOT 5	2002	4	10	822	2–3
SPOT 6	2012	4	6	694	1
SPOT 7	2014	4	6	694	1
MODIS	1999	36	250–1000	705	1
Landsat 1	1972	4	80	917	18
Landsat 2	1975	4	80	917	18
Landsat 3	1978	4	80	917	18
Landsat 4	1982	6	80	705	16
Landsat 5	1984	6	30	705	16
Landsat 6	1993		30	705	16
Landsat 7	1999	6	30	705	16
Landsat 8	2013	9	30	705	4.5
Sentinel 1	2016	C	2	693	12
Sentinel 2	2015	13	10–60	290	5–10
Sentinel 3	2016	21	300	814	100 (min)
SeaSAT	1978	L	20		24
ENVISAT	2002	C	25–50		35
Radarsat-1	1995	C	20–30		24
Radarsat-2	2007	C	20-–30		24

ALOS-1	2006	L	9–30	46
ALOS-2	2014	L	6–10	14
COSMO-SkyMED	2007	X	3–15	1–8
TerraSAR-X	2007	X	1–3	11

Nonetheless, a multifaceted challenge looms on the horizon in the realm of satellite programs, revolving around the time-consuming process of amalgamating downloads and generating essential data. This crucial endeavor involves not only the launch and deployment of new satellites but also the seamless integration of these satellites into existing constellations. Simultaneously, it calls for efforts to enhance the spatial resolution of satellite receivers, thereby refining the quality and granularity of the products they produce. Achieving this ambitious goal requires the development of a new generation of sensor technology, encompassing both transmitters and receivers, which will propel the capabilities of satellite equipment into the future.

Looking ahead, one of the primary objectives in the field of environmental surveillance products is to strive for a reduction in the errors that inevitably accompany the data. These errors undergo continuous evolution, with meticulous documentation and scrutiny for improvement. The ongoing commitment to validate and enhance this data is exemplified by collaborative efforts that involve co-processing ground measurements collected from monitoring stations across various European Union countries. These concerted endeavors extend beyond mere error adjustment through measurement comparisons; they also encompass a comprehensive assessment of the distinct climatic and geographical conditions inherent to each region.

In essence, the journey into the future of satellite programs entails not only the expansion of their technical capabilities but also a steadfast dedication to enhancing data accuracy and reliability. This dynamic evolution represents a collective commitment to harnessing the potential of advanced technology for the betterment of environmental monitoring and the understanding of our planet.

I.3.3. Monitoring and Modeling for Environmental Assessment

Environmental monitoring and modeling are now at the forefront of environmental science and management, and they are essential for understanding, protecting, and minimizing the effects of the changing environmental scene. Environmental monitoring, a key component of these initiatives, entails the methodical gathering of information on various environmental indicators. This process produces priceless insights into the wellbeing and security of human populations, the sustainability of resource management, and the health and condition of ecosystems. Such information is essential for understanding environmental dynamics as well as serving as a foundational source for scientific inquiry, supporting efforts to elucidate the workings of ecological systems, evaluate environmental dangers, and create sensible environmental policy.

Simulating and predicting complex environmental behaviors and responses is one way that environmental modeling enhances and complements the importance of monitoring. These models act as a portal to the future, allowing us to predict outcomes under many circumstances thanks to the strength of computer algorithms and data integration. This predictive ability is crucial for risk assessment, policy formation, and informed decision-making across a variety of fields, from climate forecasting to catastrophe planning and mitigation. The combination of monitoring and modeling is strengthened by the rapidly changing technological environment. High-resolution data may be found in abundance thanks to Geographic Information Systems (GIS), remote sensing, and sophisticated computer methods. This integration equips scientists, policymakers, and environmental managers with more potent tools to navigate the multifaceted environmental challenges of our time, delivering precision and efficacy in the quest to address issues ranging from climate change and biodiversity preservation to air and water quality control. In essence, the collective force of monitoring and modeling serves as a linchpin in our endeavors to preserve our environment and respond adeptly to emerging environmental complexities, thereby nurturing a more resilient and environmentally aware future.

With the development of modern technologies such as Geographic Information Systems (GIS), remote sensing, and artificial intelligence, which offer a plethora of high-resolution environmental data, the integration of monitoring and modeling is becoming more seamless. We are better able to manage the complex and changing environmental world as we continue to hone our abilities to gather, analyze, and model environmental data, enabling a more resilient and ecologically conscientious future. Our efforts to protect our environment and successfully address new environmental concerns rely heavily on the combined power of monitoring and modeling.

I.3.3.1. Forest Fire Monitoring and Modeling

The global landscape is bearing witness to an alarming surge in the destruction of its forests, driven by two formidable forces: intensive cultivation practices and the unrelenting scourge of wildfires. The magnitude of this ecological calamity is staggering. Since the inception of the 21st century, the world's forested regions have dwindled by a disheartening 50%. This distressing trend is further exacerbated by the escalating temperatures and prolonged droughts perpetuated by the overarching challenge of climate change. The year 2021 stands out as an exemplar of this crisis, with a staggering 9 million hectares of lush forest land succumbing to the relentless march of flames. To put this in perspective, this expanse of scorched earth is tantamount to the entire landmass of Portugal in Europe. The weight of this tragedy is most prominently borne by three formidable nations: Russia, Canada, and the United States, who together accounted for a staggering 7.8 million hectares of forest loss. Yet, even regions that may seem geographically removed from this catastrophe, such as Italy in the Mediterranean area, are not spared. Over the course of the preceding 14 years, Italy has witnessed the agonizing incineration of 723,924 hectares of its precious forested lands. In the year 2021 alone, a devastating 159,437 hectares of forest fell prey to the voracious flames. This relentless assault on our forests and ecosystems is emblematic of a world that, year after year, intensifies its exploitation of natural resources, a cause for grave concern (Kimbrough, 2022).

The pernicious specter of forest fires, in all their multidimensionality, stands as a grave and formidable threat to our forests and land ecosystems, demanding immediate attention and a resolute, proactive response. The repercussions of these fires are far-reaching and traverse the ecological, economic, and societal realms, leaving extensive devastation in their wake, not merely within our forested domains but beyond.

The genesis of forest fires comprises an amalgamation of natural and human-induced factors. Natural igniters include lightning strikes, volcanic eruptions, and even spontaneous combustion. Yet, it is the human-induced causes that loom most prominently in this crisis, encompassing uncontrolled agricultural practices, transformations in land use, arson, and actions driven by neglect. The looming specter of climate change forms an ominous backdrop to the intensifying conditions that have propelled the frequency and severity of wildfires to unprecedented levels (U.S. EPA, 2016).

Ecologically, the repercussions of forest fires are profound and far-reaching. The loss of biodiversity ranks as a chief casualty, as habitats are obliterated, and plant and animal species face peril. In the aftermath of these fires, soil degradation emerges as another disconcerting facet, marked by erosion, depletion of essential nutrients, and a decline in fertility. Furthermore, the fires disrupt crucial ecological processes, notably nutrient cycling, and introduce transformative shifts in patterns of ecological succession and regeneration. In this upheaval, ecosystems are rendered vulnerable to the invasion of disruptive alien species, further amplifying the challenges faced by our natural world (Pellegrini et al., 2017).

Forest fires have far-reaching effects on terrestrial ecosystems, permanently altering the fragile balance of nature. Deforestation and the destruction of natural ecosystems are the results of these catastrophic catastrophes, which have serious ramifications for the complex web of life that lives in these surroundings. In addition to causing large amounts of smoke and flames, forest fires also significantly contribute to the worldwide problem of climate change by increasing the threat of global warming by releasing copious amounts of carbon emissions into the atmosphere (Oris et al., 2014). Their effects go beyond, upsetting the complex hydrological cycles and water supplies, which causes issues with water quality, less clean water available, and diminished watershed functions. Socioeconomically speaking, forest fires have disastrous effects on the areas they destroy, including the loss of livelihoods, the forcible relocation of communities, and severe financial losses.

Effective fire management measures are essential to combating this ubiquitous threat. Systems for early detection and quick response are at the forefront of monitoring and surveillance, allowing for prompt and effective action to reduce the harm these fires inflict. Fire risk can be significantly reduced by taking steps to prevent fires, including controlled burning, fuel management, and public awareness programs. In order to quickly confine and put out flames, fire suppression approaches entail the strategic deployment of infrastructure and firefighting resources. In addition, encouraging community involvement and developing people's capacity promote the adoption of fire-safe practices and strengthen communities' ability to withstand these overwhelming obstacles. Collaborative approaches to fire control are further fostered by international cooperation and knowledge exchange, which makes it possible to leverage shared assets and experience.

Many scientific fields and tenets form the theoretical basis of wildfire detection and monitoring. Understanding the complexities of fire behavior and its spread, the critical function of remote sensing, the subtleties of data analysis, and the creation of advanced modeling approaches are important components.

Effective wildfire detection and monitoring requires a deep understanding of fire behavior and its complex spread. This entails delving deeply into the dynamics of fire, heat transfer, and combustion processes, among other physical aspects of fire. Scientists and practitioners can develop more accurate detection and monitoring systems by having a better understanding of how flames start, spread, and interact with their surroundings.

The use of remote sensing technology is essential for monitoring and detecting wildfires. Utilizing technologies like satellite images, aerial photography, and other sensor systems, it entails gathering information on fire incidents, smoke plumes, and affected regions. The utilization of remote sensing technology facilitates the detection and monitoring of wildfires across extensive geographical regions, furnishing crucial insights for well-informed decision-making and the efficient allocation of resources.

A key component of wildfire detection and monitoring is data analysis, which involves the processing and interpretation of information gleaned from a variety of sources, including meteorological stations, satellite imaging, and ground-based sensors (Ding et al., 2023). By using a variety of data analysis techniques, including as machine learning, statistical analysis, and image processing, it is possible to identify fire signs, detect anomalies, and promptly provide the information required for efficient fire control.

Another essential component of wildfire detection and monitoring is modeling, which makes use of computational and mathematical models (Andrews, 1986) to simulate fire behavior, forecast its spread, and evaluate its effects. In order to produce forecasts and assist in decision-making, these models consider factors including geography, fuel properties, and weather.

The theoretical basis of wildfire detection and monitoring depend on a thorough grasp of fire behavior, efficient use of remote sensing technologies, application of data analysis methods, and creation of advanced modeling tools for wildfire mapping, prediction and monitoring. By combining these theoretical underpinnings, scientists and professionals can significantly improve wildfire monitoring and detection systems' efficacy, which will ultimately result in more successful fire management and mitigation initiatives.

A fascinating new direction in the age of rapidly developing technology is the smooth assimilation of sophisticated Information and Communication Technology (ICT) systems into their surroundings to the point where these extremely sophisticated systems are integrated into the environment itself. Through this integration, the environment is improved and given new capabilities, mostly related to self-protection and self-monitoring. With this extra layer of intelligence, the environment may function in a proactive manner, putting its own preservation first and responding quickly to changes while immediately notifying the appropriate individuals.

This paradigm-shifting idea depicts an intelligent environment—that is, an intelligent environment that is self-aware, self-monitoring, and self-protecting. A thorough description, as given in (Stipanicev et al., 2007) by Stipanicev, D. et al., highlights this creative architectural strategy, which depends on a sophisticated sensor network called the observer network. The goal of this architectural concept is to provide a complete framework for the study of perception by expanding on the formal observation principles first presented by Bennet et al. in (Bennet et al., 1989). These ideas have led to the development of a mathematical model that has been applied in a variety of settings as a component of intelligent forest fire monitoring and detection systems.

However, it is imperative to recognize that forest fires provide a multitude of difficulties. Adaptive solutions are required due to the consequences of climate change and the consequent increase in fire danger. A range of strategies must be integrated and careful thought must be given to balancing conservation goals with socioeconomic demands. Traditional ecological knowledge and native fire management techniques can offer priceless insights that help create more potent methods. Notably, technological developments present encouraging opportunities for development, such as the development of creative fire suppression methods and early warning systems. Given that forest fires pose a threat that cuts beyond national boundaries, it is critical to enhance international collaboration and information sharing.

It is important to take prompt action in light of the significant threat that forest fires pose to terrestrial ecosystems and forests alike. To lessen the destructive effects of forest fires, proactive measures like strong policies, efficient fire prevention plans, and sustainable forest management techniques must be put into place. To protect our priceless forests and land ecosystems from this ubiquitous threat, international cooperation and coordinated measures are desperately needed.

As a proactive and long-term solution, prevention is essential in lowering the frequency and intensity of wildfires. Along with saving lives, preserving resources, and preserving ecosystems, it also preserves the livelihoods and general well-being of people at risk of wildfires. Fuel management for preventing wildfires frequently encounters issues with economic viability in areas like Southern Europe. Regarding this, Ascoli et al. (Ascoli et al., 2023) have conducted a thorough analysis of fuel management programs in Southern EU nations and have suggested viable remedies. To increase the value of fuel management goods and services, these creative projects usually enlist the cooperation of public and private resources.

Sousa et al. (Sousa et al., 2021) conducted a detailed study on wildfire propagation in Portugal, analyzing factors such as vegetation, climate, topography, and human influence. Employing spatial cluster analysis and regression models, their research aimed to comprehend the contribution of different elements to extensive fire spread, providing invaluable insights for tailored prevention strategies.

Furthermore, a study by Granville et al. (Granville et al., 2022) delved into fire growth distributions in Ontario's Crown forest areas from 1976 to 2019. In this case, industrial forestry operations in Ontario, Canada, were restricted to mitigate the risk of wildfires through the Modified Industrial Operations Protocol (MIOP). Their findings indicated iterative improvements in fire growth response over time, underscoring the effectiveness of MIOP in mitigating negative impacts. MIOP strikes a balance between operational flexibility and safe practices in industrial forestry operations, with the overarching aim of minimizing the adverse impact of fires resulting from industrial activities.

A significant and noteworthy effort is the pilot project on prescribed burning (PB) in Greece, as described by Athanasiou et al. (Athanasiou et al., 2022). The objective of this two-year project is to reintroduce controlled fire as a reliable and effective tool for wildfire prevention. The project encompasses planned field experiments to gather knowledge on fire behavior and its impact on soil, trees, and plant biodiversity. These experimental fires also serve as valuable training opportunities for firefighters, land managers, and researchers.

Other studies, such as the one conducted by McGee et al. (McGee & Cabling, 2022) among rural residents in the Edson forest area of Alberta, Canada, explore topics like examining fire use, fire permits, and safe burning practices. The survey in this study revealed that while most respondents used fire on their properties and were aware of the local fire risk, there was limited recognition of the contribution of agricultural fire use to wildfires.

Numerous studies have addressed similar issues in various parts of the world, including Australia, New Zealand, and Africa (Price, 2019). For instance, in (Hollingsworth, 2020), the authors present a mathematical treatment of backing fire, while in (Hegg, 2020), an operational methodology for directing and influencing the natural direction of a fire is discussed.

Forest fire monitoring, detection, and prevention rely on a diverse array of methodologies, systems, and sensors aimed at enhancing early detection, rapid response, and effective management of wildfires. These approaches encompass the utilization of remote sensing techniques, such as satellites and aerial platforms, to provide real-time data on fire hotspots, smoke plumes, and areas affected by the blaze. Geographic Information Systems (GIS) integrate spatial data to create risk maps and allocate resources effectively. Weather monitoring systems and prediction models are invaluable in producing fire weather forecasts and supporting early warning systems. Fire detection systems, which include both ground-based and satellite-based sensors, excel at identifying heat signatures, smoke, and flames, thus facilitating prompt response. Sensor networks, in a continuous fashion, monitor environmental conditions, while machine learning and artificial intelligence come to the forefront in the analysis of data for fire detection algorithms. In addition to these technological advancements, controlled burning and fuel management practices are instrumental in mitigating fire risk, and community engagement and public awareness programs play a pivotal role in promoting fire-safe practices and ensuring the early reporting of fire hazards.

A central aim of this thesis is to delve into the methodologies and prominent systems currently employed, supported by a wide range of sensor technology. Image analysis, a widely adopted procedure, can leverage static acquisition systems mounted on control towers or images sourced from satellites, as detailed in (Priya & Vani, 2019) by R. Shanmuga et al. More recently, there has been a surge in methodologies that employ drones, offering a faster and cost-effective approach compared to traditional satellite technology. For example, Zhentian Jiao et al. (Jiao et al., 2020) put forth the use of YOLO neural networks for real-time forest fire detection by processing data from a drone-mounted depth camera.

Scientific research continues to make significant strides in addressing these challenges. From the early 2000s to the present, a multitude of innovative alternatives and technological advancements have been proposed. For instance, cutting-edge tools for image analysis, underpinned by artificial intelligence techniques, have been applied to each frame of video footage, enabling the extraction of minute details associated with fire detection. Dongqing Shen et al. explore the application of the YOLO neural network in this context (Shen et al., 2018). Additionally, Barmpoutis et al. (Barmpoutis et al., 2020) describe how wireless sensors of this nature can be used in tandem with cameras to ascertain the presence and location of an actual fire. The development of newer communication networks has improved intra-node and node-to-gateway communication, extending coverage to even those areas that are challenging to reach via traditional radio signal methods.

This analysis underscores the strengths and advantages offered by different technologies used in fire detection and prevention. These include advanced image analysis, the utilization of Geospatial Artificial Intelligence (GeoAI) techniques, and the integration of sensor networks. These technological innovations are instrumental in enabling the timely detection of fire outbreaks, bolstering early warning systems, and allowing for proactive measures to be taken. However, it is essential to recognize the limitations of these technologies, including the requirement for continuous monitoring, the potential for false alarms, and the challenges associated with adapting them to diverse geographical contexts.

Furthermore, this section explores emerging technologies and approaches that have the potential to further enhance the effectiveness of fire management strategies. The Figure I.3 provides a comprehensive overview of the current state of technology, serving as an inspiration for future research and innovation in this critical field.

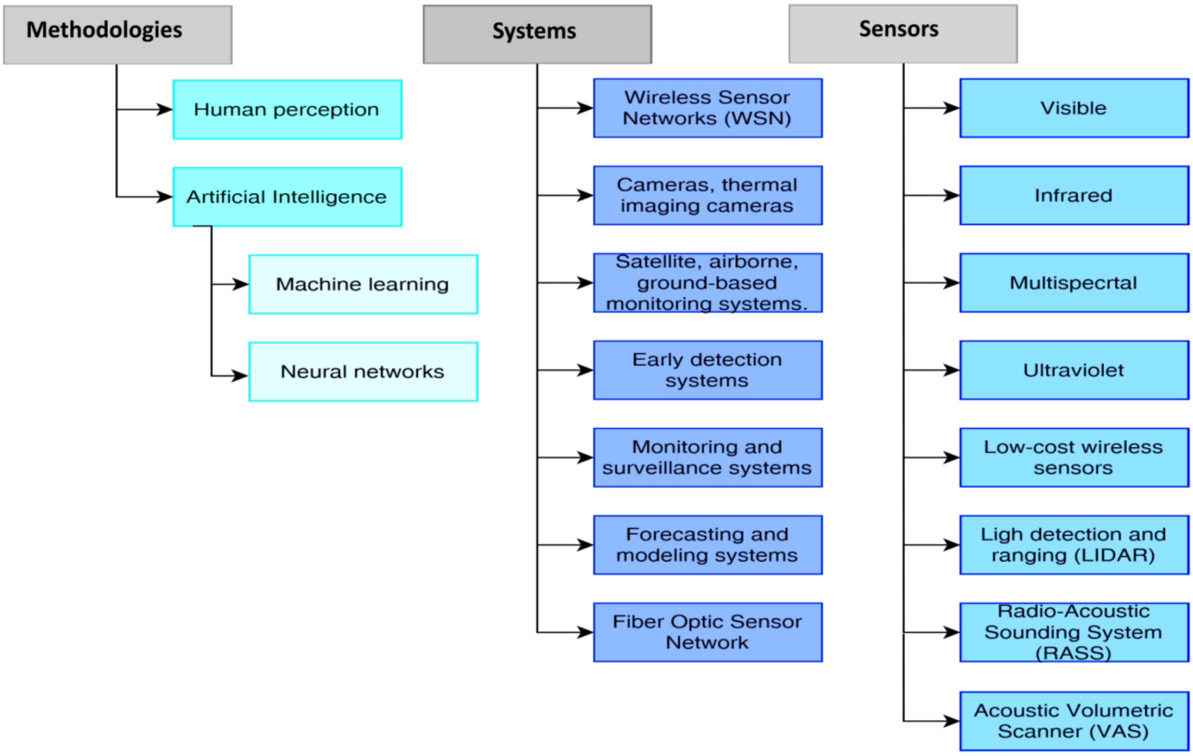

Figure I. 3: Summary of the primary methods for detecting and monitoring forest fires.

I.3.3.2. Soil Erosion Monitoring and Modeling

Soil erosion, a complex and dynamic environmental phenomenon, has a significant impact on numerous locations around the world. Following the rise in population, it is a major contributor to land degradation and one of the world's most pressing environmental concerns. Notably, statistics show that soil erosion occurs at an alarming rate in the United States, ten times quicker than natural replenishment, and at an even more startling rate in China and India, where figures range from 30 to 40 times the rate (Pimentel, 2006).

Globally, the extent of land affected by water-driven erosion spans 10,940,000 km^2, with a substantial 7,510,000 km^2 undergoing significant degradation (Lal, 2003). Annually, rivers worldwide transport sediment to the ocean, totaling an estimated 15 to 30 billion tonnes (Milliman & Syvitski, 1992; Walling & Webb, 1996). Soil erosion profoundly impacts the morphological characteristics of regions, influencing soil fertility, agricultural productivity, water quality, reservoir capacity, and the development of coastal areas within sedimentary environments (Polykretis et al., 2020; Lal, 2001; Xu et al., 2013).

The ongoing trajectory of erosion is inextricably linked to global warming, resulting in heightened hydrological activity in numerous regions. This manifests as increased precipitation, including more frequent and intense rainfall events. These changes in weather patterns, alongside shifts in temperature, solar radiation, and atmospheric

CO_2 concentrations, exert significant influence on rates of soil erosion. The dynamics of climate change's impact on water-induced soil erosion are multifaceted, encompassing shifts in rainfall volume and intensity, changes in the ratio of rain to snow, plant biomass production, decomposition rates of plant residues, evapotranspiration rates, and adjustments in land use practices necessitated by an evolving climate (Nearing et al., 2004).

Moreover, soil erosion detrimentally affects agricultural lands on a global scale, resulting in the loss of nutrient-rich topsoil, increased surface runoff in less permeable soil layers, and reduced water availability for plants (Ganasri & Ramesh, 2016). A staggering 85% of worldwide soil degradation stems from soil erosion, contributing to a substantial 17% decrease in crop productivity (Oldeman et al., 1990).

Effective monitoring, modeling, and analysis of soil erosion serve as essential tools for assessing the current state of erosion, identifying trends, and facilitating scenario analysis (Ganasri & Ramesh, 2016). Furthermore, these actions yield valuable insights for land management decisions, enabling the development of alternative land-use scenarios and their subsequent evaluation (Fistikoglu & Harmancioglu, 2002). Quantitative monitoring and evaluation (Kothyari, 1996) are often imperative to ascertain the scope and magnitude of soil erosion challenges, thereby aiding in the formulation of sound regional management strategies in conjunction with on-site measurements.

Soil erosion monitoring and analysis models fall into three primary categories: empirical, conceptual (partly empirical/mixed), and physical (Jha & Paudel, 2010). Noteworthy examples in these categories encompass the empirical model USLE and its derivatives, conceptual models like ANSWERS (Areal Nonpoint Source Watershed Environment Response Simulation), CREAMS (Chemicals, Runoff and Erosion from Agricultural Management Systems), and MODANSW (Modified ANSWERS), as well as physical models such as EUROSEM (European Soil Erosion Model) and MIKE SHE (European Hydrological System). Since the 1930s, soil experts and decision-makers have been developing and employing erosion models to monitor and estimate soil loss, resulting in the creation of over 80 such models until 2014 (Karydas et al., 2014).

One of the most widely used empirical models for erosion monitoring and estimation is the Universal Soil Loss Equation (USLE), conceived by Wischmeier and Smith in 1965 based on soil erosion data from the United States (Wischmeier & Smith, 1978). Originally designed for assessing soil erosion on arable land and slightly sloping terrains, USLE is still prevalent in numerous studies aimed at estimating soil loss (Abdelhadi Ouakil et al., 2022). The revised RUSLE, which considers upstream areas contributing to downstream surface runoff, is considered more predictive than USLE. The modified version, MUSLE, remains extensively utilized for soil loss assessment and monitoring in Europe (Ganasri & Ramesh, 2016; Lee & Lee, 2006; Van Remortel et al., 2001).

Recent years have witnessed a surge in efforts to spatially model soil erosion, spurred by advancements in GIS, remote sensing technology, and increased computational power. The widespread adoption of GIS and satellite data streamlines the development of erosion models by enabling the utilization of multiple data sources, easy model structure adjustments, and versatile scaling capabilities [67,68]. The integration of soil erosion models, field data, and remote sensing information via GIS proves particularly advantageous, enabling the visualization of erosion distribution through hazard maps, crucial for devising protective measures (Xu et al., 2013; Ganasri & Ramesh, 2016; Fernandez et al., 2018; Stathopoulos et al., 2017).

The significance of continuous soil erosion monitoring and the implementation of integrated river basin management practices has been further augmented by the independent and combined use of remote sensing data, such as aerial photos, LiDAR, UAV, and satellite data (e.g., Landsat, IRS-P6, ASTER GDEM, GeoEye, QuickBird, WorldView, MODIS, Hyperion), alongside various data types, including rain gauges, soil samples, and topographic maps, all within a GIS framework (Neugirg et al., 2016; Rayegani et al., 2016; Dewan et al., 2017; Chappell et al., 2018). An exemplary instance is the monthly soil erosion risk mapping for the Mauritius region developed by Nigel et al. (Rughooputh and Nigel, 2010), employing GIS, decision rules, rainfall and soil data, and SPOT satellite imagery, yielding high-resolution soil erosion monitoring maps.

The combined utilization of remote sensing data, GIS, and soil loss assessment models, such as USLE, RUSLE, RUSLE3D, USPED, PESERA, among others, has proven invaluable for monitoring and predicting soil erosion (Ganasri & Ramesh, 2016; Helmi, 2023; Gao et al., 2023; Aiello et al., 2015). Recent examples include the implementation of the G2 soil erosion model by Karydas et al. (Karydas & Panagos, 2018) in southeastern Europe and Cyprus, using a wealth of satellite data (e.g., Sentinel-2, MERIS, PROBA-V, SPOT-VGT) for monthly soil loss estimation. Additionally, Leh et al. (Leh et al., 2013) conducted land use allocation and soil erosion level predictions for a US catchment area up to 2030 by combining remote sensing, GIS, and modeling techniques, using Landsat satellite images over a 20-year period (1986–2006).

Further advancements in this line of research include the integration of data, models, and methods with techniques such as Frequency Ratio (FR), Analytical Hierarchy Process (AHP), Logistic Regression (LR), Multiple Linear Regression (MLR), Potential Erosion Index (PEI), Sediment Delivery Ratio (SDR), the GIS model GWLF, the TLSD function, and others (Park et al., 2011; Chowdary et al., 2013; Badar et al., 2013; Thomas et al., 2018). An illustrative contemporary case is the Environmental Fragility Index (EFI) developed by Macedo et al. (Macedo et al., 2018), which incorporates geoclimatic factors and anthropogenic pressures, utilizing geospatial, rainfall, and Landsat TM satellite data to monitor and predict sediment deposition in 148 rivers across Brazil.

In conclusion, considering the wealth of evidence presented, GIS and Remote Sensing stand as indispensable and potent tools for reliable soil erosion monitoring and estimation. These tools can draw from models like USLE/RUSLE, employ Multi-Criteria Evaluation Techniques, or combine various methods. Spatial information analysis remains a continually evolving approach, offering decision support in the monitoring, planning, management, and sustainable development of complex challenges like

soil erosion in river and lake basins. In recent years, GIS has emerged as a superior choice for supporting decisions in soil monitoring and land-use planning.

The vital role of soil erosion monitoring cannot be overstated, and the amalgamation of advanced technologies, modeling techniques, and comprehensive data analysis is crucial in tackling this pressing environmental challenge. These methods allow us to gain a more profound understanding of soil erosion processes, evaluate its impact on various regions, and ultimately make informed decisions for sustainable land management and environmental protection. As we continue to grapple with the effects of climate change and the intensification of hydrological cycles, the importance of soil erosion monitoring becomes increasingly evident. It is a vital tool in preserving our planet's precious soil resources, sustaining agriculture, and safeguarding the health of ecosystems and water bodies.

I.3.3.3. Flood Monitoring and Modeling

Countries around the world marked by natural disasters have left an unmistakable impact, unleashing their destructive fury on communities, resulting in widespread death, infrastructure damage, and huge population relocation. To make matters worse, the coming threat of climate change threatens to magnify these already severe effects in a number of countries, portending a future marked by even greater misery. Natural catastrophes continue to be unrelenting in their ability to inflict catastrophic economic and environmental effects, exacting a heavy toll in human lives on a worldwide scale, despite tremendous advances in technology and scientific knowledge that define our century. The dedicated research and monitoring of these occurrences, which has constantly revealed unsettling increasing patterns, has been a consistent thread in recent decades (Smith, 2009).

To effectively track, mitigate, and prepare for the impact of these natural calamities, the creation of hazard and risk maps for both natural and man-made environments stands as an imperative endeavor (Maantay & Maroko, 2009; Smith, 2001).

Amid the pantheon of natural disasters, few are as menacing and far-reaching as inundations, casting their shadow over more than 75 million people worldwide (Smith, 2001). Rapidly and effectively managing the magnitude of their impact, and the extent of land engulfed during extreme flood events, is of paramount importance (Wang, 2004). In this context, flood mapping and modeling emerge as invaluable tools, offering means to monitor, predict, protect, and enhance both short-term and long-term assistance to affected regions in the aftermath of disaster. As articulated by Lekkas (Lekkas, 2000), two primary categories of floods warrant our attention: upstream and downstream. Upstream floods manifest in the higher reaches of drainage areas, typically resulting from intense, short-term rainfall in localized areas. Conversely, downstream floods are born of protracted storms that saturate the soil, inundating larger expanses. The occurrence and scale of floods hinge on a multitude of factors, including the total amount and distribution of rainfall, the permeability of rock and soil, and the complex interplay of topographical features (Lekkas, 2000). Moreover, the distribution of land use, particularly in small drainage basins, exerts a significant influence on flood size and frequency. The risk of flooding in a watershed, in turn, depends on a complex interplay of factors such as land use, flood volume, intensity, and frequency, elevation and duration of flooding, seasonal variations, sediment deposition, and the effectiveness of monitoring, prediction, prevention, warning, and emergency response mechanisms (Lekkas, 2000).

The advent of emerging environmental challenges, such as rising temperatures, erratic precipitation patterns, the specter of desertification, and the omnipresent menace of extreme phenomena like storms, floods, landslides, and soil erosion, pose ominous threats to human life and the infrastructure that supports it. This escalating threat landscape has catalyzed a surge in interest in the monitoring and management of water resources. The need for optimal methods of monitoring and management is further accentuated by the rapid march of technology, which provides new tools and techniques for addressing these challenges. This dynamic and evolving environmental regime underscores the imperative of systematic research in related fields such as hydrology and hydraulics. The pursuit of methodological efficiency, comprehensive databases, state-of-the-art modeling developments, and a deeper understanding of events and phenomena of high contemporary significance emerges as a driving force for ongoing research. In this endeavor, modern geotechnologies, exemplified by Geographic Information Systems (GIS) and Remote Sensing, assume pivotal roles.

The early 1980s witnessed an intellectual debate among geographers, who argued that flood maps fell short in significantly influencing people's perception of floods and providing adequate support for research planning. Even the Canadian Flood Disaster Reduction Program reported that the increased awareness of flood effects among different groups was not solely attributed to the availability of maps (Handmer, 1981). To address this perceived inadequacy, researchers explored various approaches. One such approach hinged on the use of Remote Sensing (RS), an idea not entirely novel. In 1980, forward-thinking researchers championed the application of remote sensing in disaster monitoring and warning, encompassing tasks such as flood mapping and assessment (Deekshatulu et al., 1980). Over the ensuing decade, the utilization of Remote Sensing and GIS in flood monitoring and research became a firmly established practice. Passive and active sensors were brought into play and rigorously tested, as borne out by subsequent references. For instance, Hubert-Moy et al. (Hubert-Moy et al., 1992) highlighted the aptness of spatial analysis of Landsat Thematic Mapper (TM) data for scrutinizing floods in small catchments. The study also validated the capability of satellite image processing and flow analysis to replicate flood conditions, even days after the peak event, notwithstanding the satellite's limited repeatability. In contrast, a 1996 study delved into the utility of synthetic aperture radar (SAR) data. This study compared satellite data on river floods with photographic records captured from small aircraft, striving to demonstrate the accuracy of the SAR technique (Biggin, 1996).

As we advance into the 21st century, GIS, Remote Sensing, and other modern technologies have entrenched themselves as pivotal instruments in flood monitoring, analysis, mapping, and hydrological and hydraulic modeling. This ecosystem is characterized by a state of perpetual evolution and revolution, manifesting in the emergence of innovative applications. These applications combine hydrological and other models with Remote Sensing and GIS techniques to investigate and monitor a spectrum of issues related to surface runoff and flooding. Multiple hydrological models have been conceived and deployed, encompassing notable creations such as the HYDROTEL model [196], the SLURP model (Du et al., 2009; Lei et al., 2011), the SWAT model (Soil and Water Assessment Tool) (Abbaspour et al., 2007; Kalogeropoulos et al., 2011; Pissias et al., 2013; Kalogeropoulos & Chalkias, 2013), the HEC-HMS/RAS models (Knebl et al., 2005; Nikolaos et al., 2019; Amengual et al., 2007; Choudhari et al., 2014; Mendes & Maia, 2016; Al-Zahrani et al., 2017), the WEP-L hydrological model (Jia et al., 2006), the MIKE11 model (Ranaee et al., 2009), and the spatially distributed hydrological model LIS-Flood model (Van Der Knijff et al., 2010). These models, in tandem with Remote Sensing and GIS data, have proven instrumental in addressing diverse issues, including the complex challenge of urban sprawl (Weng, 2001; Stamellou et al., 2013).

The evolution of geographic-spatial analysis methods, with GIS at the forefront, has marked a transformation in the approach to flooding. This transformation is characterized by a shift away from purely mathematical-theoretical models and in situ research toward a more functional approach grounded in spatial analysis, spatial models, geostatistics, and various related techniques. These include methodologies like logistic regression and frequency analysis, among others (Stathopoulos et al., 2017; Melesse & Graham, 2004; Tehrany et al., 2013; Gioti et al., 2013), (Kalogeropoulos et al., 2013; Kalogeropoulos et al., 2013; Chalkias et al., 2016; Kalogeropoulos et al., 2020).

The ongoing improvements in remote sensing data, including expanded coverage, enhanced spatial resolution, and increased data frequency, are poised to further amplify their utility. Numerous scientists have been driven to harness hydrological, hydraulic, and other models, in conjunction with remote sensing and GIS data and techniques, to investigate and monitor issues related to surface runoff and flooding (Smith, 2004; Pulvirenti et al., 2011; Stancalie & Craciunescu, 2005; Kourgialas et al., 2010; Fugura et al., 2011; Pradhan, 2009). An illustration of the vast array of applications that combine hydrological and other models with Remote Sensing and GIS techniques can be found in the study of urban sprawl (Weng, 2001; Stamellou et al., 2013; Kalogeropoulos et al., 2020).

I.3.3.4. Predictive Modeling and Management of Sedimentation in Dams

Sediment transport, driven by overland flow exceeding soil cohesive strength, is a critical environmental phenomenon with widespread implications for river ecosystems and human activities (Li et al., 2020). The resulting sediments, influenced by weathering, are transported through natural pathways and often deposited in rivers during floods (Ben Hichou et al., 2023), significantly impacting hydraulic performance and posing challenges for sustainable river management (Ge et al., 2019; Xie et al., 2021). This thesis explores in a chapter IV the use of geoinformation technologies in monitoring and modeling transported sediments, with a focus on sediment rates in dams and their impact on the hydro-sedimentary regime, to address the complex interplay between sediment dynamics and river ecosystems.

The consequences of sediment transfer are far-reaching, contributing to increased flood heights, embankment instability, forward erosion, and environmental disturbances (Julien, 2018; Bizzi et al., 2015; Zhang et al., 2021). To comprehensively manage rivers sustainably, it is essential to have a deep understanding of inflow discharge, sediment transport, and sediment yield (Bhatti et al., 2021; Wheater et al., 1993). Various methodologies, including physical, conceptual, and experimental models, have been employed to estimate sediment output and transport ratios (Kulsoontornrat and Ongsomwang, 2021; Zhang et al., 2016; Bernardi and Schippa, 2014).

Mathematical models, often based on statistical approaches, have been developed to quantify sediment production. However, the complexity of the process, influenced by diverse factors such as geology, forestry, climatology, topography, geography, hydraulics, and pedology, poses significant challenges (Stone et al., 2021; Ferreira et al., 2009; Jang, 2017; Kang et al., 2021; Julien, 2018). Empirical models, relying on observed relationships between variables, have been utilized to predict sediment yield, emphasizing the importance of accurate measurements (Pierson-Wickmann et al., 2011; Shu et al., 2021; Setia et al., 2021). However, inconsistencies persist among experimental models, highlighting the need for more sophisticated predictive approaches.

Social, economic, and environmental considerations underscore the importance of effective sediment management in rivers (Quan et al., 2021; Yue et al., 2021; Zhao et al., 2020; Liu et al., 2022; Huang et al., 2019). The global geochemical cycle relies heavily on river-delivered sediment, influencing societies and environments differently based on regional variables (Liu et al., 2016). Historical agricultural practices, such as utilizing seasonal floods for nutrient deposition in the Nile floodplain, have given way to large-scale dams that alter sediment transport patterns and influence flooding dynamics (Fang et al., 2021; Wang et al., 2021).

The equilibrium of natural river reaches, crucial for the geochemical cycle and material transfer from land to sea, is disrupted by human activities like dam construction and deforestation (Yang et al., 2022). Approximately 50% of major rivers exhibit significant changes in sediment loads, often due to the presence of dams and river control structures (Walling and Fang, 2003). Managing sediment loads requires region-specific strategies, considering factors like soil and water conservation, river control structures, tree cover, topography, and land-use practices (Yang et al., 2022).

The proliferation of dams globally, surpassing 40,000, presents challenges in sediment management (Chen et al., 2022; Yin et al., 2022). Sedimentation rates in dry climates, reaching 6000 to 8000 m3/km2/year, result in the loss of 0.5–1.0% of the world's reservoir capacity annually (White, 2000). Sediment data integration with hydrological information is crucial for reservoir design, allowing for operational optimization and economic considerations (Chen et al., 2022; Yin et al., 2022). Sustainable basin water storage capacity expansion strategies involve preventing sediment intrusion, reservoir management, and exploring additional storage options (Haznedar et al. 2023). The World Bank advocates a life cycle management approach, encompassing social and environmental protection, dam decommissioning, sedimentation management, and economic optimization in the planning phase.

In the context of the Sediments & Habitats project, the focus is on understanding the impact of flood defense operations on habitats, sediments, and river conveyance. Geoinformation technologies play a crucial role in achieving this goal by providing real-time data and advanced modeling capabilities (Quan et al., 2021; Yue et al., 2021). Remote sensing technologies, such as satellite imagery and LiDAR, enable accurate monitoring of sediment transport patterns, allowing for a better understanding of the dynamics within dam environments (Zhao et al., 2020; Liu et al., 2022).

Furthermore, Geographic Information System (GIS) tools facilitate the integration of various spatial data layers, including topography, land use, and hydrological features, to create comprehensive models for predicting sediment transport in dams (Huang et al., 2019). These technologies offer a holistic approach to sediment management, enabling authorities to make informed decisions about dam operations and mitigate the adverse effects of sedimentation.

The Sediments & Habitats project emphasizes the importance of adaptive management strategies for sustainable river reaches (Quan et al., 2021; Yue et al., 2021). Geoinformation technologies provide the tools necessary for implementing such strategies by offering real-time data, predictive modeling, and decision support systems. Adaptive management involves continuous monitoring and adjustment based on the evolving conditions within dam environments, ensuring that sediment management practices remain effective and environmentally sustainable.

Chapter II: Integrated Geomatics and Remote Sensing Analysis of Forest Fire Propagation and Land Cover Change

II.1. Introduction

Forest fires present a multifaceted challenge that extends far beyond their immediate impact, casting a daunting shadow over both the environment and society. The repercussions of these fires are far-reaching, as they not only imperil the rich tapestry of biodiversity but also pose a significant threat to local communities and the delicate balance of ecosystems (Kala, 2023). In light of this ever-growing concern, it is paramount to acknowledge the pivotal role that remote sensing technologies now play in our efforts to monitor and manage forest fires on a global scale (Payra et al., 2023).

The synergy between technology and ecological preservation has never been more evident. A growing body of research underscores the undeniable significance of remote sensing methodologies, emphasizing their invaluable contributions to our understanding of fire dynamics and the assessment of the environmental consequences wrought by forest fires (Arjasakusuma et al., 2022; Nolè et al., 2022; Payra et al., 2023). This dynamic intersection between science and technology enables us to not only witness the destructive power of these infernos but also to empower us with the knowledge needed to combat them effectively.

To delve deeper into the capabilities of remote sensing, let's take a closer look at a compelling case study conducted in a Mediterranean region by Viana-Soto et al. (2020). In their research, the effectiveness of remote sensing in evaluating post-fire vegetation recovery and mapping burned areas became abundantly clear. Leveraging the power of Sentinel-2 imagery, the research team meticulously tracked the gradual evolution of vegetation cover in the aftermath of a forest fire event. This endeavor illuminated the critical importance of seamlessly integrating multispectral data with advanced Geographic Information Systems (GIS) techniques, serving as a testament to the pivotal role played by technology in accurately delineating the extents of burned areas and evaluating the regrowth of vegetation in the fire-affected region.

However, the relevance of these advancements in remote sensing is not confined to academic studies alone. Recently, the province of Berkane in Morocco (Figure II.1) faced a devastating forest fire that raged from July 16 to 18, 2023. This harrowing event necessitated the swift deployment of multiple response teams who worked tirelessly to combat the blaze and protect lives and property. In the aftermath of this catastrophic incident, it is imperative that we embark on comprehensive analyses aimed at unraveling the intricate dynamics of the fire and understanding its enduring impact on the landscape (Ben Hichou et al., 2023a). By doing so, we can continue to harness the power of remote sensing, further fortifying our ability to protect our natural world and the communities that depend on it.

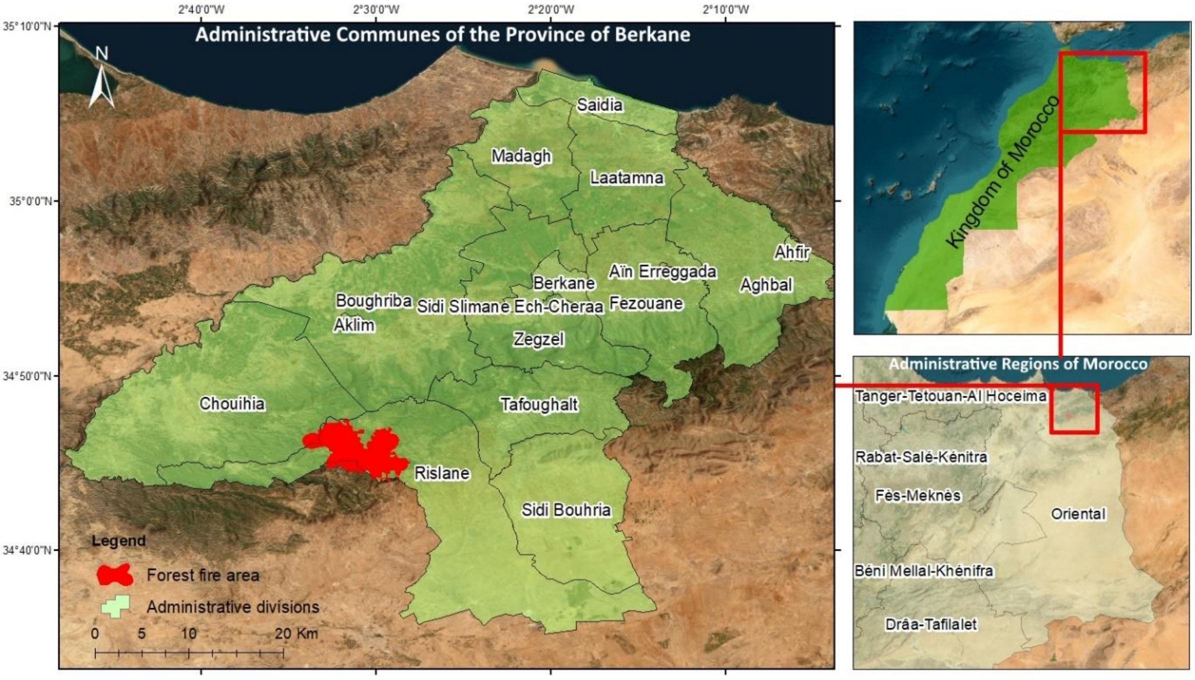

Figure II. 1 :Geographic location map of the study area

In light of the pressing need to address the multifaceted challenges posed by forest fires, our study was meticulously designed with two primary objectives in mind. Firstly, we aimed to provide critical insights into the spatiotemporal propagation of the active forest fires during the incident, thus offering invaluable support to the brave on-ground firefighting teams battling the blaze. Secondly, we aspired to detect and analyze changes in the vegetation cover resulting from the fire, ultimately creating a precise and comprehensive mapping of the burned area. To achieve these multifaceted objectives, our research harnessed the power of an integrated approach that seamlessly combined advanced geomatics methods with cutting-edge remote sensing data.

The utility of Geographic Information Systems (GIS) and remote sensing technologies in the assessment and management of forest fires cannot be overstated, as aptly noted by Duncan (2009). In our study, we harnessed the capabilities of these powerful tools by integrating data from various sources, including the NASA Fire Information for Resource Management System (FIRMS) database and high-resolution Sentinel-2 satellite imagery. This data integration facilitated a holistic and detailed analysis of the fire's behavior, its evolution over time, and the consequential impact on the surrounding environment. The Sentinel-2 imagery, captured both before and after the wildfire, served as a linchpin in providing critical information on the extent of the affected area, thereby allowing us to comprehend the spatial distribution and severity of the burned region with unparalleled precision.

Our research endeavors are aimed at making a significant contribution to the development of post-fire management strategies, which are undeniably pivotal in safeguarding the invaluable forest resources of the Province of Berkane. The accurate mapping of the burned area, coupled with the identification of changes in vegetation cover, will undoubtedly play a central role in the formulation of effective conservation and restoration plans, as highlighted by the work of Perkl (2016). These strategies, informed by our study, have the potential to minimize the ecological impact of forest fires and promote sustainable recovery efforts, aligning with the principles of ecological restoration as emphasized by Jenkins (2022).

As we delve deeper into the subsequent sections of this chapter, we will provide a thorough exploration of the methodology employed to achieve our multifaceted objectives. This will include a comprehensive discussion of the geomatics techniques and remote sensing analyses that formed the foundation of our research. Moreover, we will meticulously dissect the key findings and implications derived from our study, shedding light on the pivotal role of an integrated geomatics approach in understanding and mitigating the impact of forest fires, both within the context of the Province of Berkane as a case study and in broader, global terms.

Our fervent hope is that this research will not remain confined to the realm of academia. Instead, we aim for it to serve as a valuable and practical resource for the broader scientific community, policymakers, and local authorities alike. Armed with the knowledge and insights generated through our study, these stakeholders can better address the multifaceted challenges posed by forest fires, ensuring the long-term resilience and health of affected ecosystems while simultaneously safeguarding the well-being of local communities and the environment at large.

II.2. Methodology

This study utilized an integrated approach (figure II.2) to analyze active forest fire propagation and map the burned area. NASA's FIRMS data provided near real-time information on active fire locations, while Sentinel-2 imagery captured before and after the fire (figures II.3 and II.4) was processed to calculate the Normalized Burn Ratio (NBR) and the Normalized Difference Vegetation Index (NDVI).

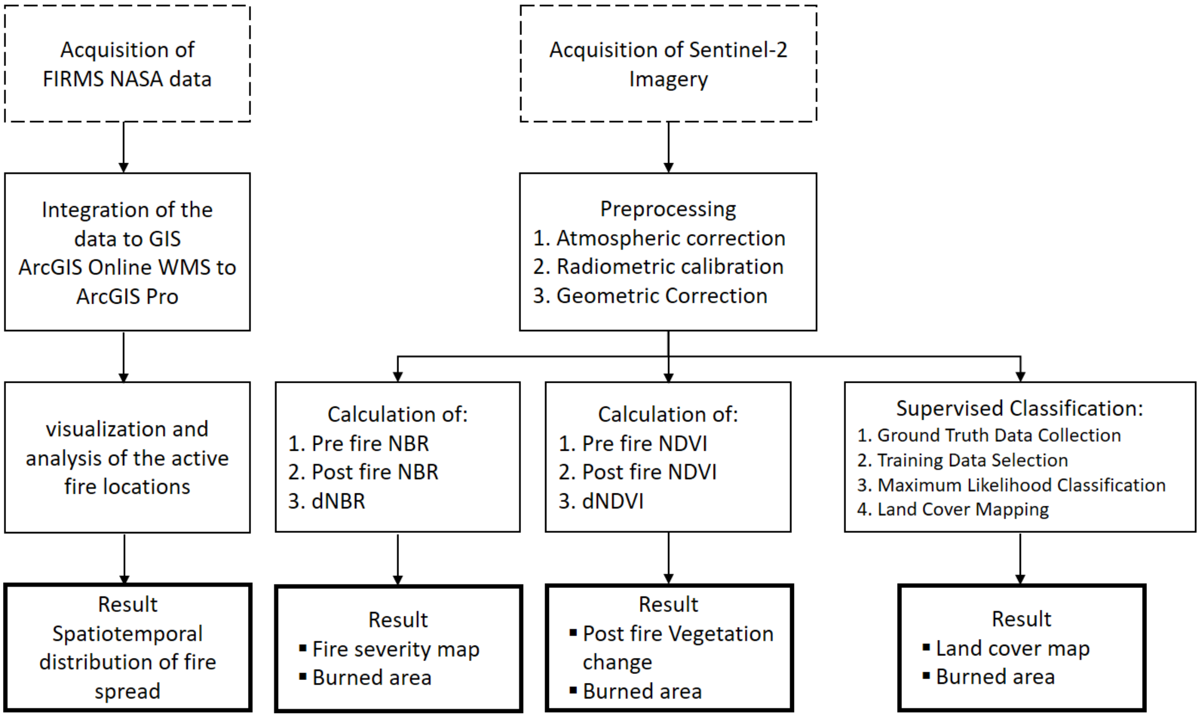

Figure II. 2: Diagram of the proposed methodology (Ben Hichou et al., 2023a)

The differenced NBR (dNBR) and differenced NDVI (dNDVI) were computed to detect fire-induced changes in vegetation. Additionally, a supervised classification using the Maximum Likelihood algorithm was applied to map the burned area in detail.

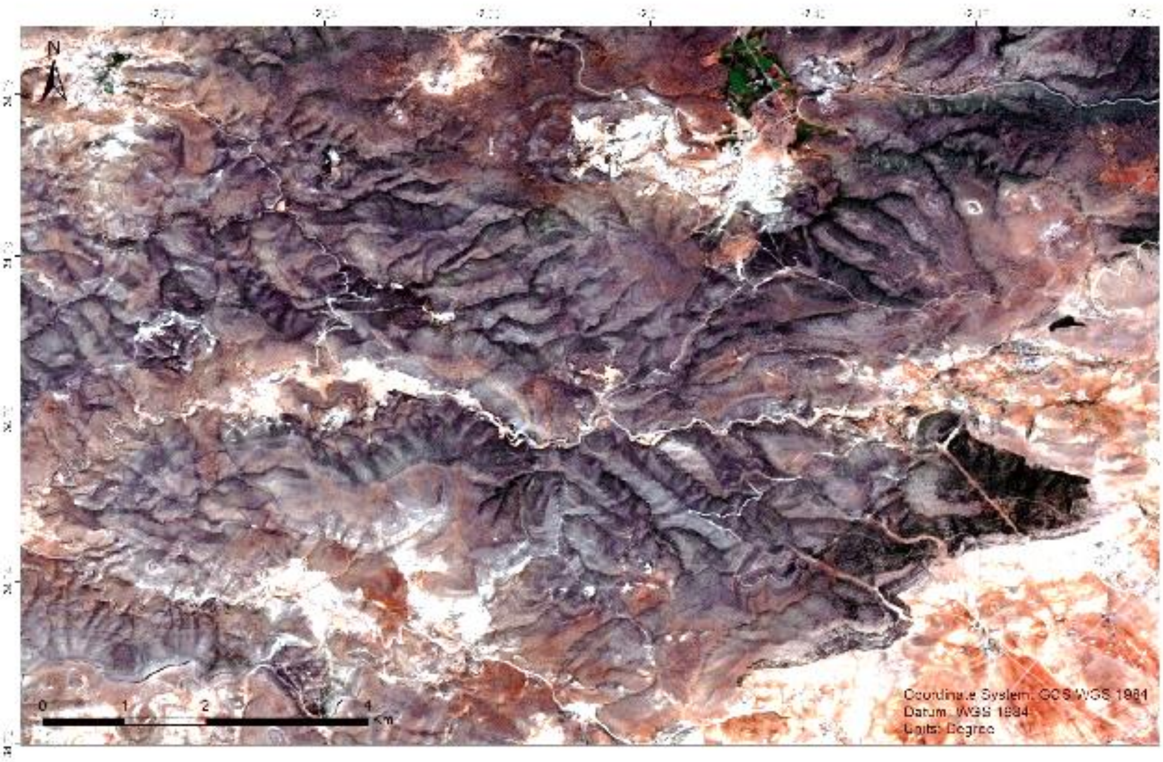

Figure II. 3: Sentinel-2 image before the fire – Acquired on 14/07/2023 (Ben Hichou et al., 2023a)

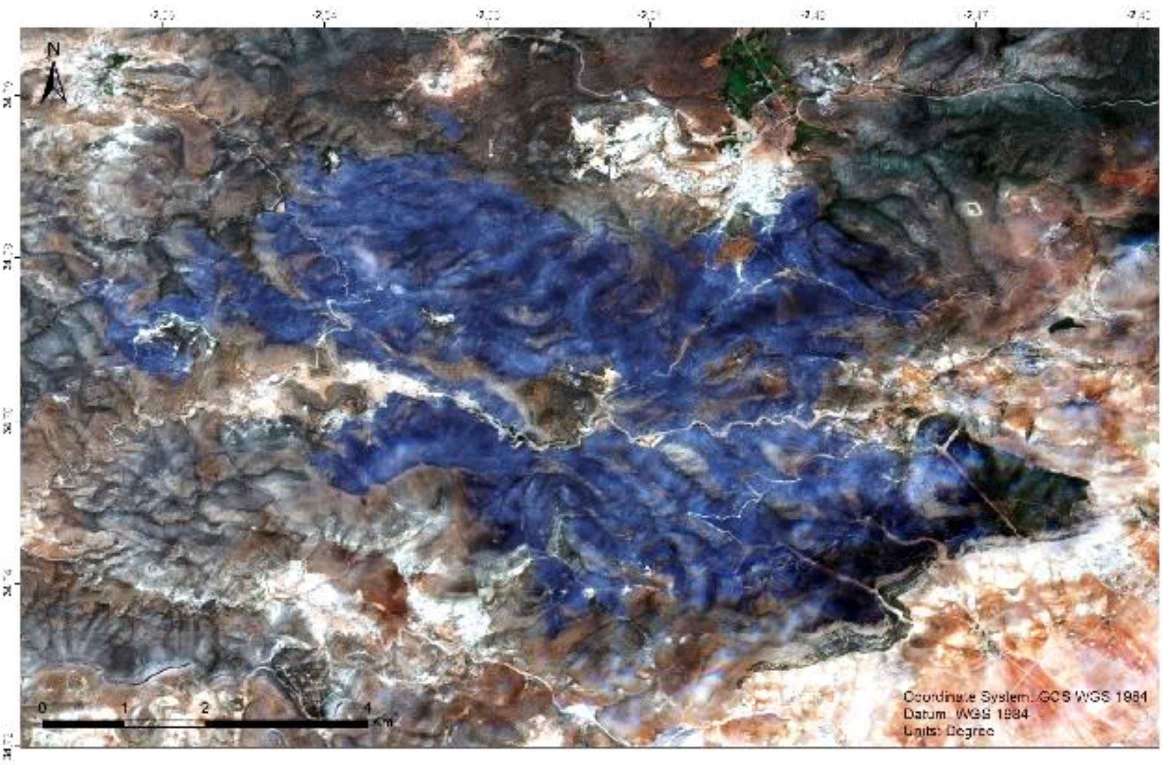

Figure II. 4: Sentinel-2 image after the fire - Acquired on 19/07/2023 (Ben Hichou et al., 2023a)

II.2.1. Analysis of Active Forest Fire Propagation during the Fire Period:

II.2.1.1 Acquisition of NASA FIRMS Data:

NASA's Fire Information for Resource Management System (FIRMS) provided active fire data used to map the areas of active fires near Berkane during the three-day forest fire. The fire-based maps offered through Web Feature Service (WFS) and shared on the ArcGIS Online Atlas was utilized.

The used WFS information pertains to the detectable thermal activity observed by VIIRS satellites over the past 7 days. The data on VIIRS Thermal Hotspots and Fire Activity is generated through NASA's Land, Atmosphere Near real-time Capability for EOS (LANCE) Earth Observation Data, which forms a vital component of NASA's Earth Science Data.

II.2.1.2. Integration of the data to Desktop GIS

The WFS was imported into GIS using ArcGIS Pro. This integration enabled us to create a map with filters on the basemap of the IGIS (Integrated Geographic Information System) of the Province of Berkane, enhancing the visualization and analysis of the active fire locations.

II.2.2. Change Detection and Mapping of the Burned Area after the Fire Period

II.2.2.1. Acquisition and Preprocessing of Sentinel-2 Imagery

Sentinel-2 satellite images were acquired before the fire on July 14, 2023, and after the fire on July 19, 2023. These images have a spatial resolution of 10 meters, which is ideal for accurately mapping the burned area.

Sentinel-2 satellite has various spectral bands (Figure II.5), capturing visible, near-infrared, and shortwave infrared wavelengths. These bands provide key data for diverse applications, including land cover analysis and environmental monitoring.

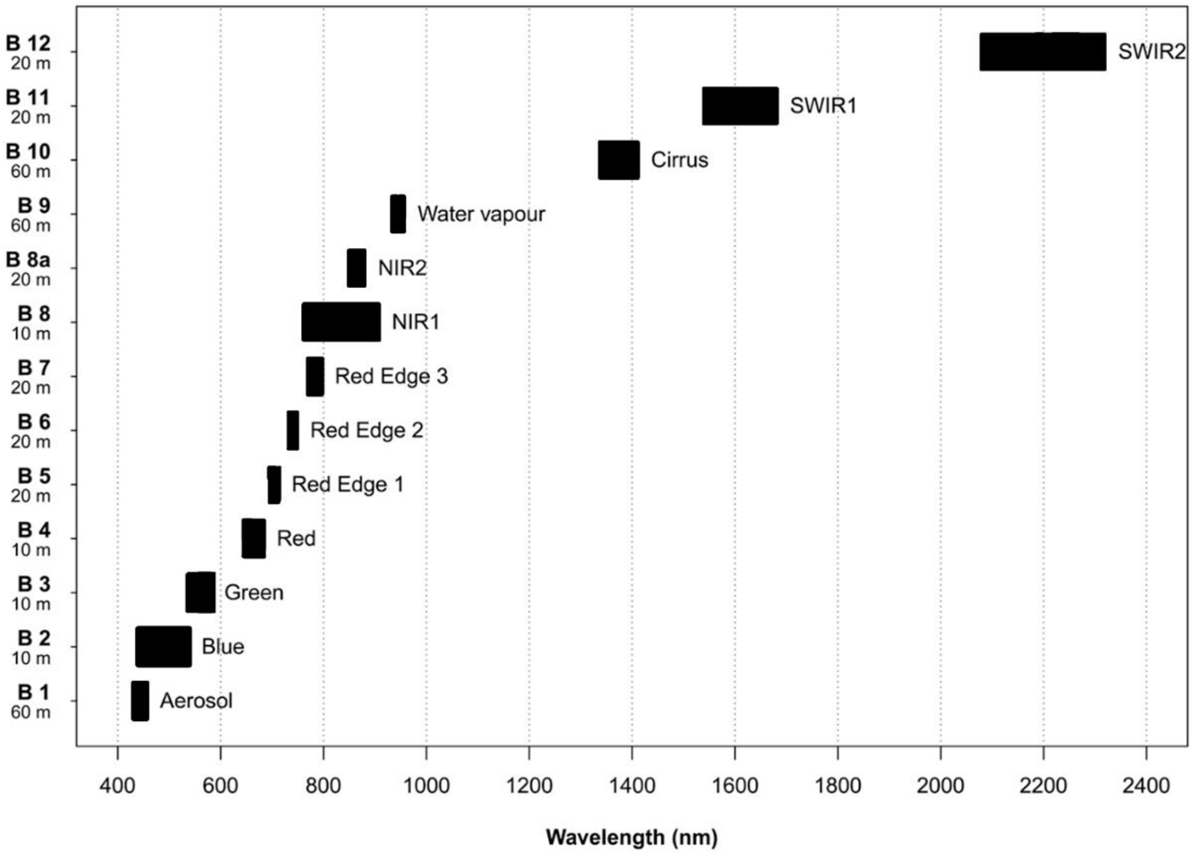

Figure II. 5 : Characteristics of the Sentinel-2 multispectral instrument

The acquired images underwent a series of preprocessing steps, which included atmospheric correction, radiometric calibration, and geometric correction. These essential preparatory measures ensured that the imagery was optimized and ready for accurate calculations of NBR, NDVI, and supervised classification.

II.2.2.2. Calculation of Pre Fire NBR, Post Fire NBR and dNBR

- **Normalized Burn Ratio (NBR):**

The NBR is an essential index used to detect burnt areas in large fire zones. It employs both near-infrared (NIR) and shortwave infrared (SWIR) wavelengths to highlight changes in vegetation caused by fire (Key and Benson, 2005). Healthy vegetation typically exhibits high reflectance in the NIR and low reflectance in the SWIR region, while burnt areas show the opposite behavior with low reflectance in the NIR and high reflectance in the SWIR.

To leverage the spectral differences, NBR utilizes the ratio between NIR and SWIR bands, as shown in the equation (1) below:

$$NBR = \frac{NIR - SWIR}{NIR + SWIR} \quad \text{Eq (1)}$$

A higher NBR value indicates healthy vegetation, while a lower value indicates bare ground or recently burnt areas. Non-burnt areas typically have values close to zero.

- **Burn Severity (dNBR):**

To estimate the severity of the burn, the difference between the pre-fire and post-fire NBR values is computed, leading to the calculation of differenced Normalized Burn Ratio (dNBR). Higher dNBR values correspond to more severe damage, whereas negative dNBR values may indicate regrowth of vegetation following a fire. The equation (2) used to calculate dNBR is illustrated below:

$$dNBR = NBR\ prefire - NBR\ postfire \qquad \text{Eq. (2)}$$

The resulting dNBR image was binarized using the natural break method to identify pixels corresponding to the burned area. These pixels were then converted from raster format to vector format in the form of polygons, facilitating the creation of an accurate burned area map.

The burn severity is estimated using dNBR image. The United States Geological Survey (USGS) has presented a classification table for interpreting burn severity based on dNBR calculations, provided in Table II.1 below.

Table II. 1: Classification of Burn Severity Using dNBR Calculation (Proposed by USGS)

Severity Level	dNBR Range
Unburned	-0.100 to 0.99
Low Severity	0.100 to 0.269
Moderate-low Severity	0.270 to 0.439
Moderate-high Severity	0.440 to 0.659
High Severity	0.660 to 1.300

II.2.2.3. Calculation of Pre Fire NDVI, Post Fire NDVI and dNDVI

The Normalized Difference Vegetation Index (NDVI) is a standardized index allowing you to generate an image displaying greenness (relative biomass). This index takes advantage of the contrast of the characteristics of two bands from a multispectral raster dataset - the chlorophyll pigment absorptions in the red band and the high reflectivity of plant materials in the near-infrared band (Rouse et al., 1973).

The Normalized Difference Vegetation Index (NDVI) is calculated using the equation (3):

$$NDVI = \frac{NIR - R}{NIR + R} \qquad \text{Eq. (3)}$$

where NIR represents the Near Infrared band and R represents the Red band. Similar to the NBR method, the NDVI was calculated for images before and after the fire.

The differenced NDVI (dNDVI) was obtained by subtracting the NDVI Post Fire from the NDVI Pre Fire, enabling the detection of fire-induced changes in vegetation (equation 4).

$$dNDVI = NDVI\, prefire - NDVI\, postfire \qquad \text{Eq. (4)}$$

The resulting dNDVI image was binarized using the natural break method to detect burned areas.

II.2.2.4. Supervised Classification using Maximum Likelihood

A supervised classification was conducted using geospatial artificial intelligence (GeoAI) and Maximum Likelihood algorithm to map land cover, with a specific focus on delineating burned areas. Regions of interest identified during field surveys were used as training samples for the classification (Fisher, 1922). The burned areas were then converted from raster to vector format, represented as polygons, enabling accurate calculation of their total surface area.

For supervised classification to generate a land cover map using Sentinel-2 imagery, optical and infrared bands are commonly employed. Sentinel-2 has multiple spectral bands, including B2 (Blue), B3 (Green), B4 (Red), B8 (Near Infrared), B11 (Mid-Infrared), and B12 (Mid-Infrared). These bands cover wavelengths from visible to infrared, providing valuable information to differentiate and classify various land surfaces such as urban areas, forests, crops, water bodies, etc. The choice of bands depends on the classification type and specific characteristics of the study area.

To create a comprehensive multi-band image, the selected bands are stacked in a specific order based on their respective spectral wavelengths (table II.2). The bands are arranged as follows: B2 (Blue), B3 (Green), B4 (Red), B8 (Near Infrared), B11 (Mid-Infrared), and B12 (Mid-Infrared). Each band is assigned as a separate layer in the new stacked image.

Table II. 2: Corresponding Bands between Sentinel-2 and the Stacked Image

Stucked bands	New order the final stacked image
B2 (Blue)	Band 1
B3 (Green)	Band 2

B4 (Red)	Band 3
B8 (Near Infrared)	Band 4
B11 (Mid-Infrared)	Band 5
B12 (Mid-Infrared)	Band 6

By combining the bands in this manner, the resulting stacked image becomes a valuable resource for land cover analysis and classification. The different layers in the image capture distinct information about the Earth's surface, such as vegetation health, water bodies, urban areas, and soil characteristics. This multi-band approach enables a more detailed and accurate land cover classification, aiding in applications related to environmental monitoring, land use planning, and natural resource management.

II.3. Results and Discussion

II.3.1. Spatiotemporal analysis of the active forest fire

On July 16, 2023, FIRMS (NASA) released information on its near-real-time data portal regarding the start of the propagation of an active forest fire near Douar Dghabcha. During July 17, 2023, the fire rapidly spread to the surrounding areas in the north, northwest, and west of Douar. In response to this critical situation, emergency intervention teams were quickly duplicated on the second day and deployed to the field. Their coordinated efforts helped limit the spread of active fires, mainly concentrated to the north of Douar Beni Oual.

Thanks to the relentless efforts of the teams on the ground and the use of aerial resources such as Canadair aircraft, the active forest fires were brought under control by the end of the third day, July 18, 2023. The teams managed to contain and completely extinguish the flames, thus preventing further spread and protecting the surrounding areas.

This spatiotemporal monitoring map (figure II.6) illustrates the progression of the active forest fire from its origin near Douar Dghabcha to its extinction through the joint efforts of the intervention teams. During the entire course of the forest fire, it should be noted that no settlements were affected and there were no injuries or casualties

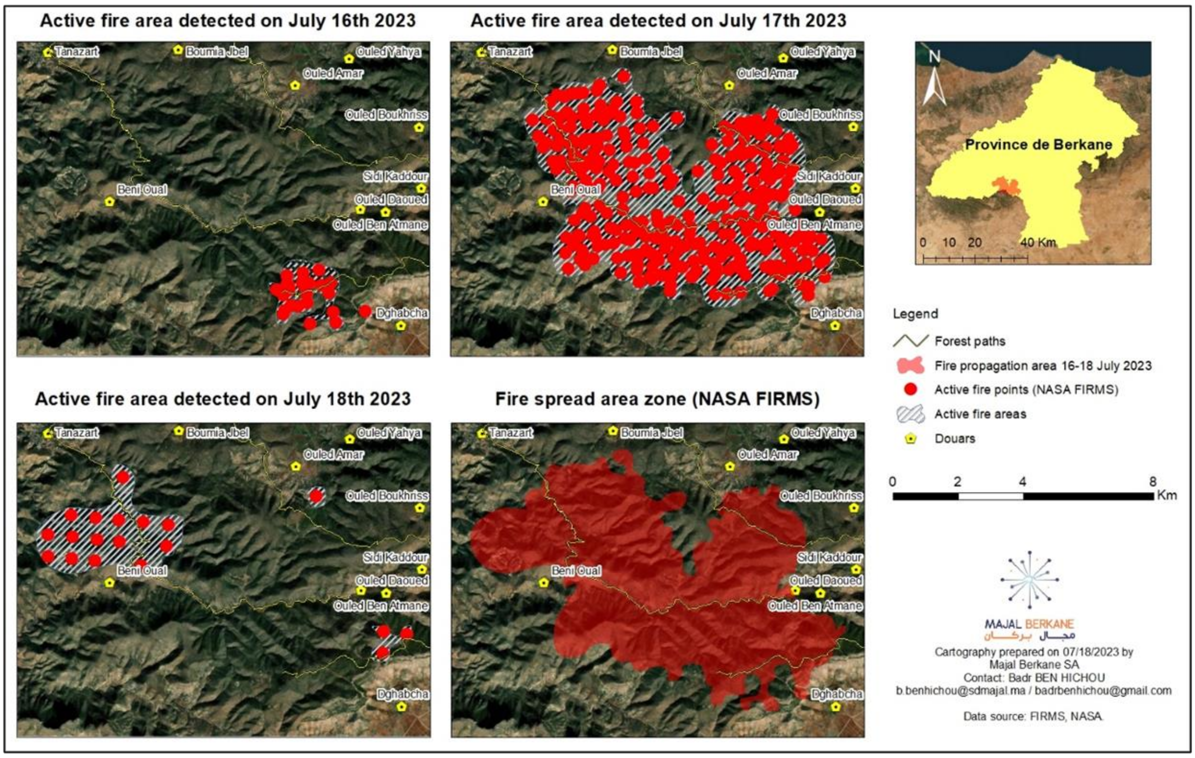

Figure II. 6: Spatio-temporal monitoring of the spread of the forest fire southwest of the city of Berkane. Morocco. (Ben Hichou et al., 2023a)

II.3.2. Normalized Burn Ratio (NBR)

In our analysis, we employed the Normalized Burn Ratio (NBR) to classify the NBR images into 5 distinct classes using natural breaks (figures II.7 and II.8). This classification method effectively highlighted the burned area, evident through the presence of specific NBR values between -0.33 and -0.42. These values were indicative of the fire's impact, aiding in the identification of the affected regions.

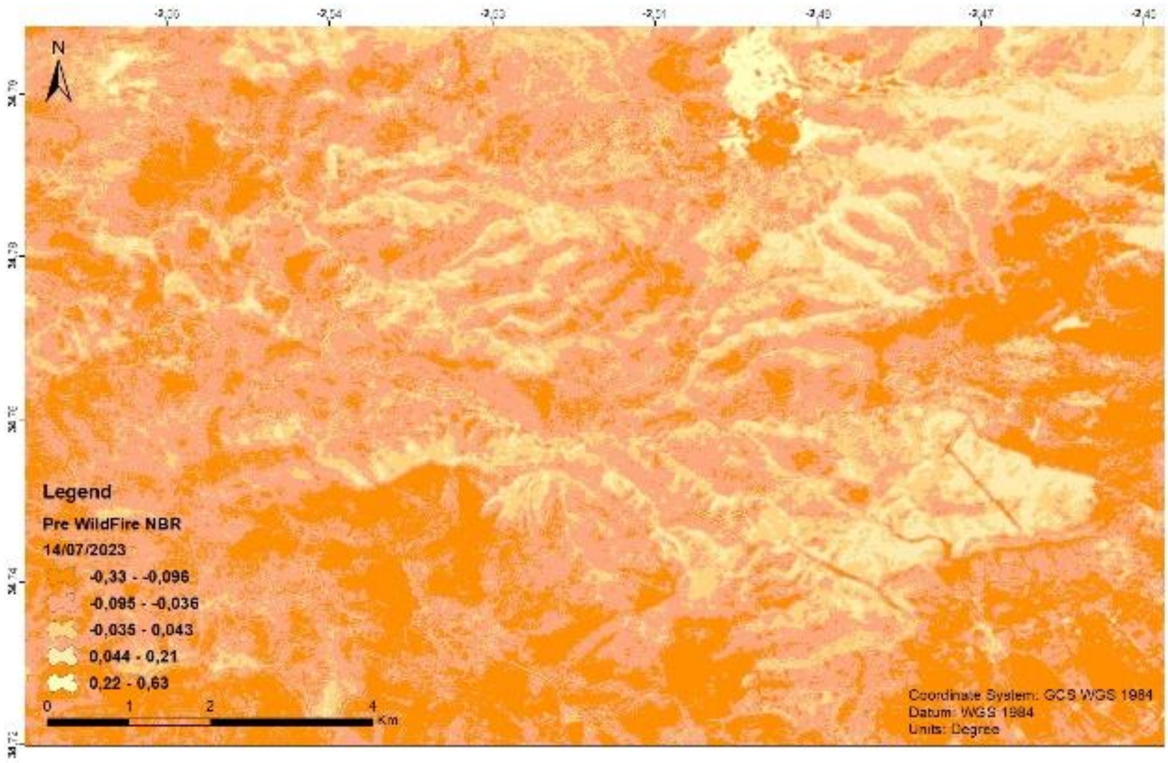

Figure II. 7: Pre-Fire NBR Map (Ben Hichou et al., 2023a)

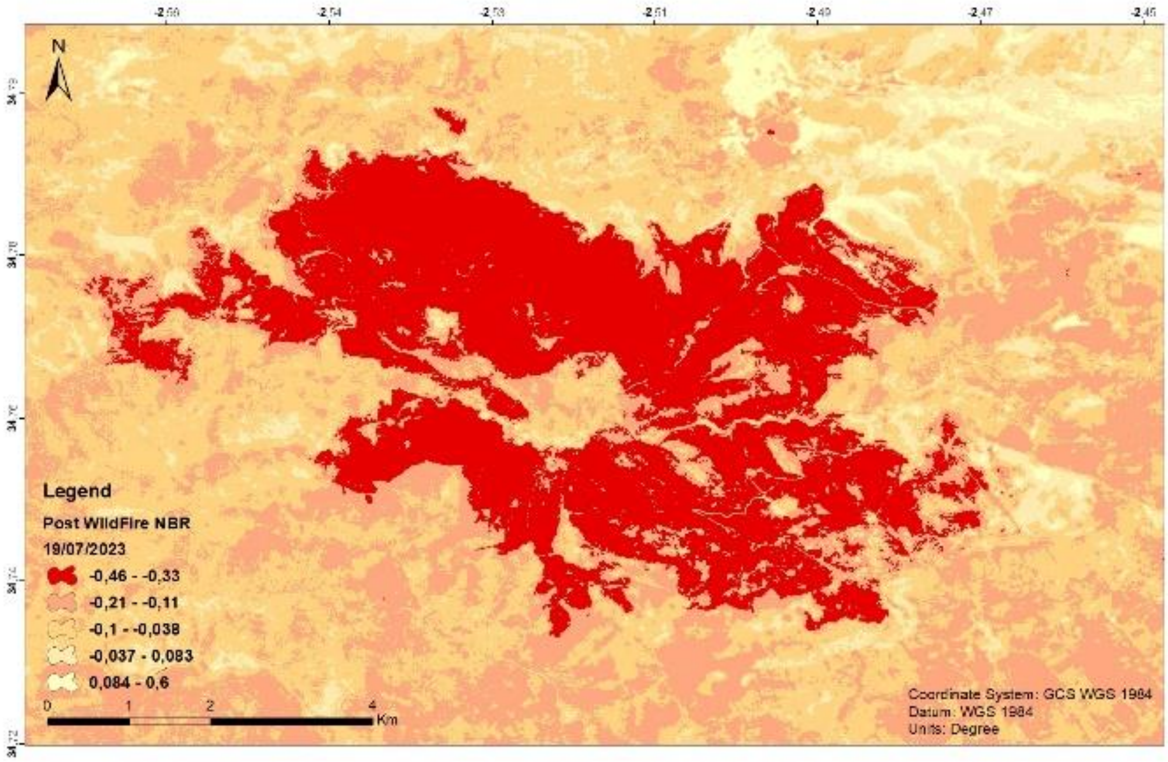

Figure II. 8: Post-Fire NBR Map (Ben Hichou et al., 2023)

II.3.3. Differenced Normalized Burn Ratio (dNBR)

Subsequently, we generated the burned area map using the dNBR (figure II.9), which facilitated a binary classification of the area into burned and unburned regions. The geoprocessing results yielded essential information, indicating that the extent of the burned area covers an approximate total of 3508.12 hectares. Our analysis involved examining the histogram of the dNBR image, where pixel values ranging from 0.131 to 0.568 were attributed to the burned area (figure II.10). Conversely, pixel values falling below 0.131 represented the unburned areas. This approach allowed for a clear delineation of the extent of the fire-affected zone, providing valuable insights into the distribution and severity of the burn.

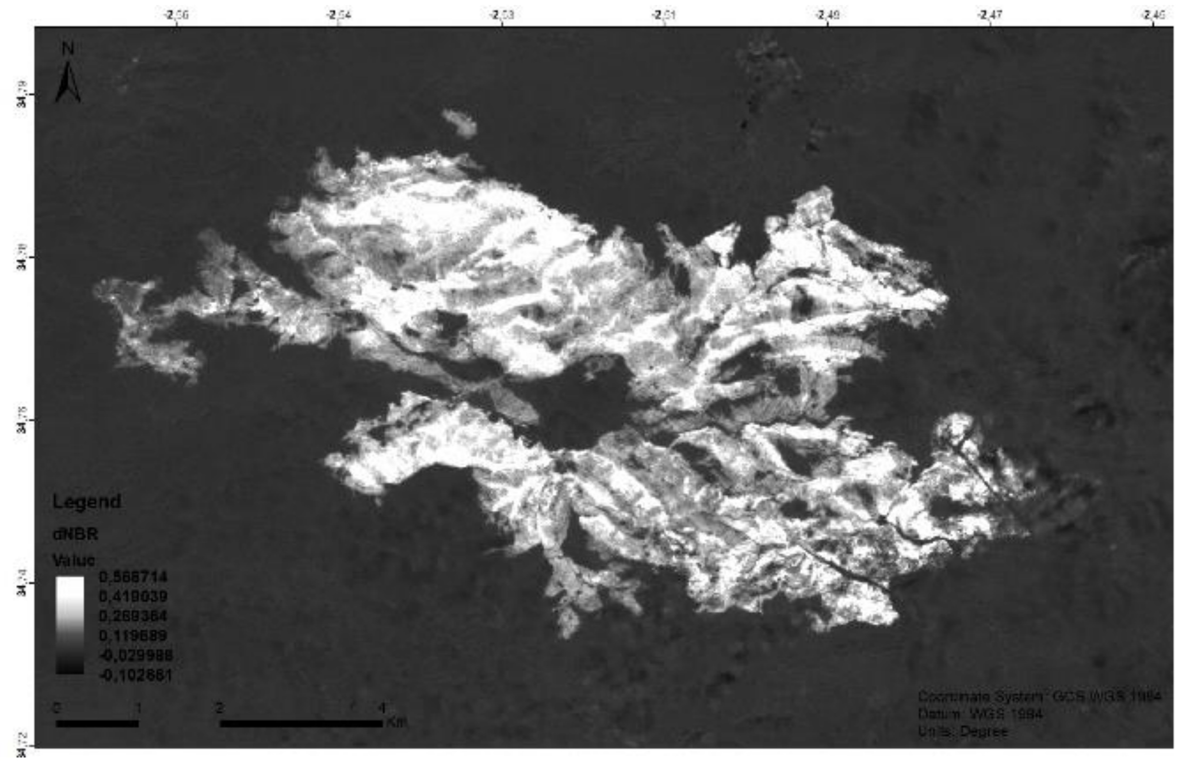

Figure II. 9: dNBR Map in Grayscale (Ben Hichou et al., 2023a)

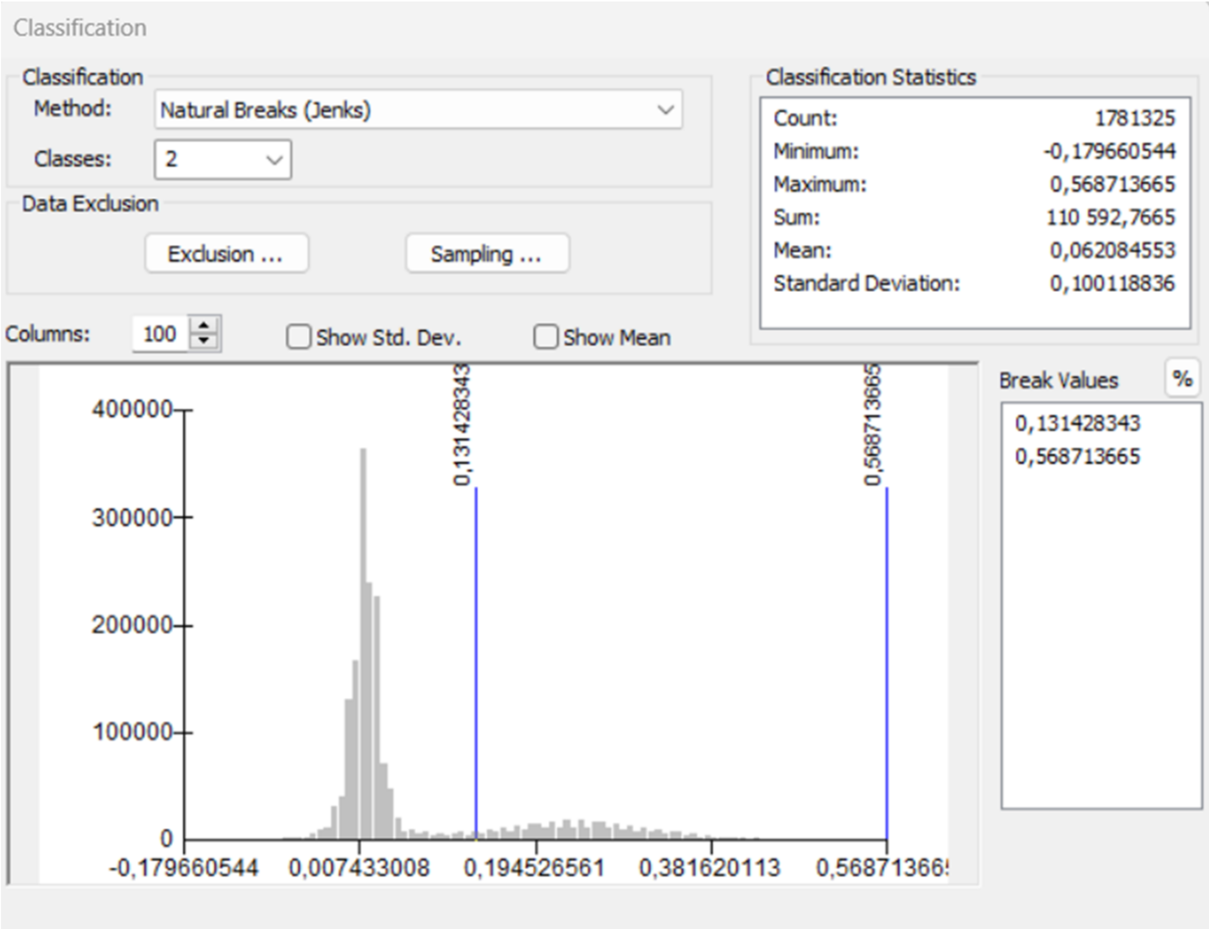

Figure II. 10: Binary Classification of dNBR Pixels Using Natural Break (Ben Hichou et al., 2023a)

Our classification and geoprocessing techniques utilizing NBR and dNBR proved to be effective in accurately identifying and mapping the burned area. These findings are significant for understanding the impact of the wildfire and will aid in developing targeted strategies for post-fire recovery and conservation efforts.

II.3.4. Burn severity map

The burn severity map (figure II.11) was generated by classifying the pixels based on their corresponding dNBR values, resulting in the following categorization:

- Low Severity: This category encompasses dNBR values ranging from 0.100 to 0.269. It represents approximately 65% of the total burned area. Areas falling within this range indicate relatively lower levels of burn severity.
- Moderate-Low Severity: Falling between 0.270 and 0.439 on the dNBR scale, this category covers about 35% of the burned area. It denotes regions with a slightly higher level of burn severity compared to the "Low Severity" category but still represents a moderate impact.

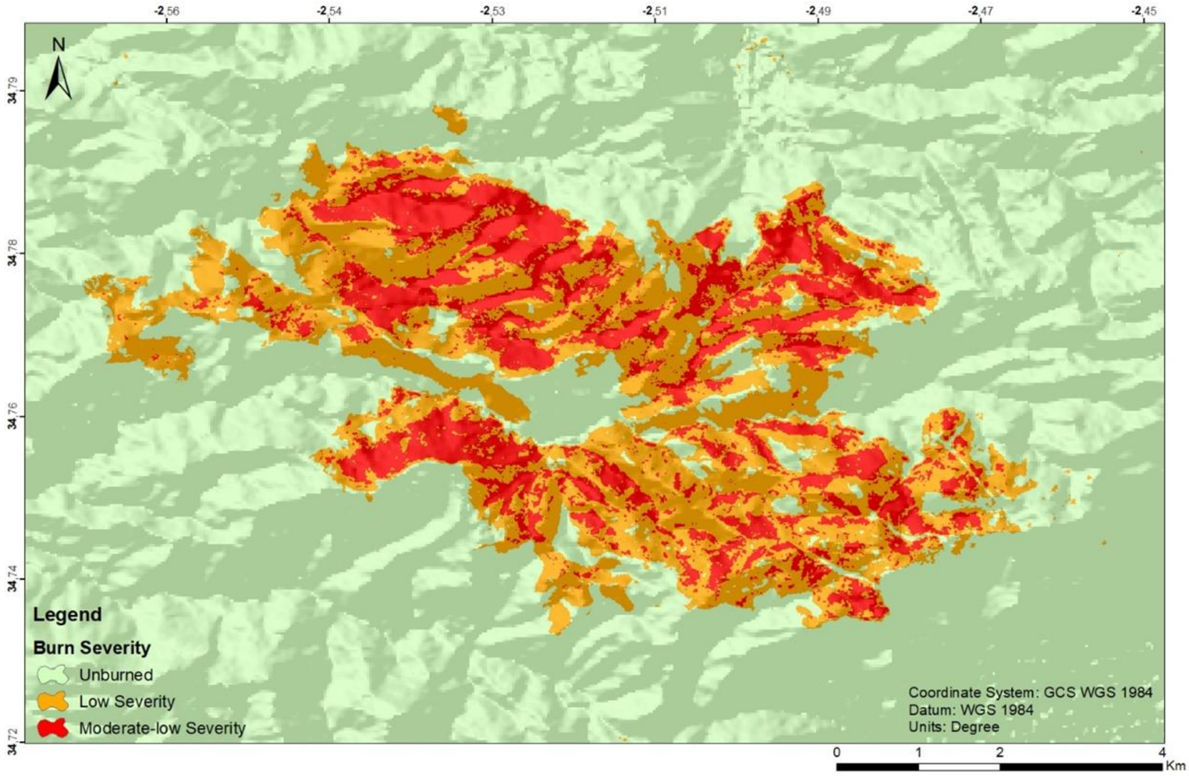

Figure II. 11: Burn severity map (Ben Hichou et al., 2023a)

II.3.5. Normalized Difference Vegetation Index (NDVI)

The results of the NDVI Pre Fire analysis revealed a minimum value greater than 0.0052 (figure II.12), while the NDVI Post Fire showed a minimum value of -0.1097 (figure II.13). These differences in values between the two NDVI images highlight the vegetation changes resulting from the fire.

Significantly, the area impacted by the forest fires, as determined by the NDVI Post Fire, visibly coincides with the area highlighted by the NBR Post Fire.

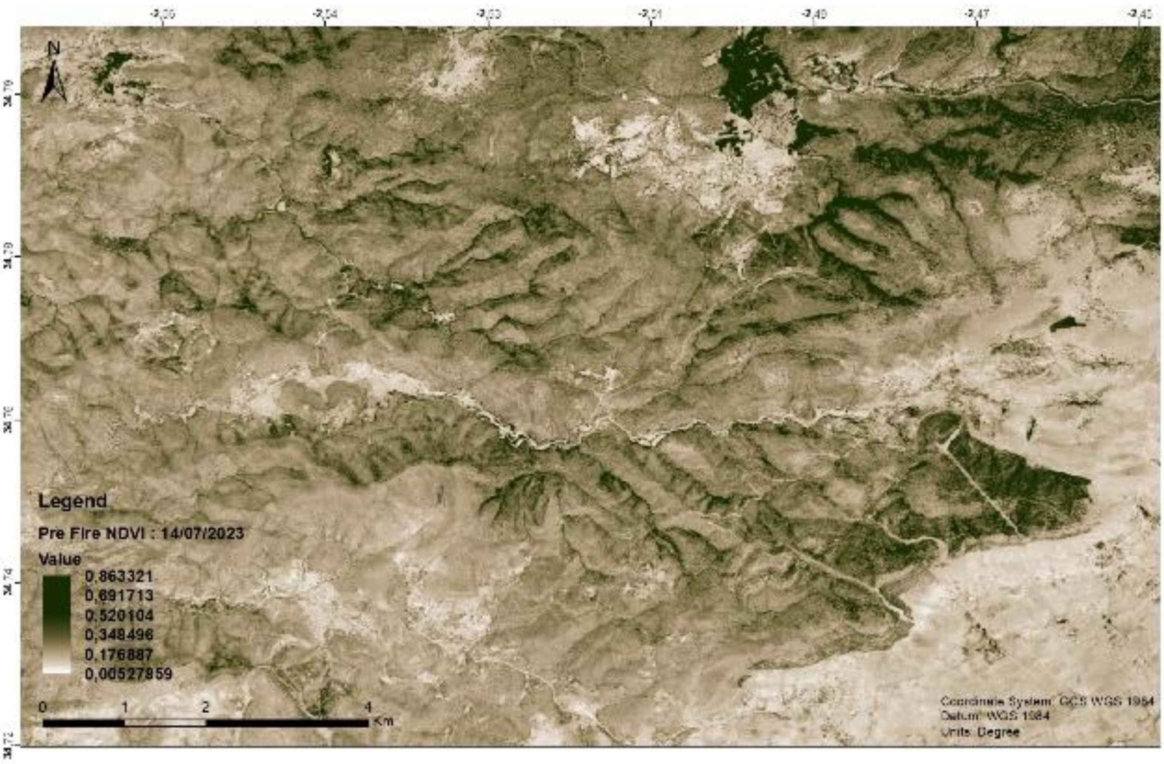

Figure II. 12 : Pre-Fire NDVI Map (Ben Hichou et al., 2023a)

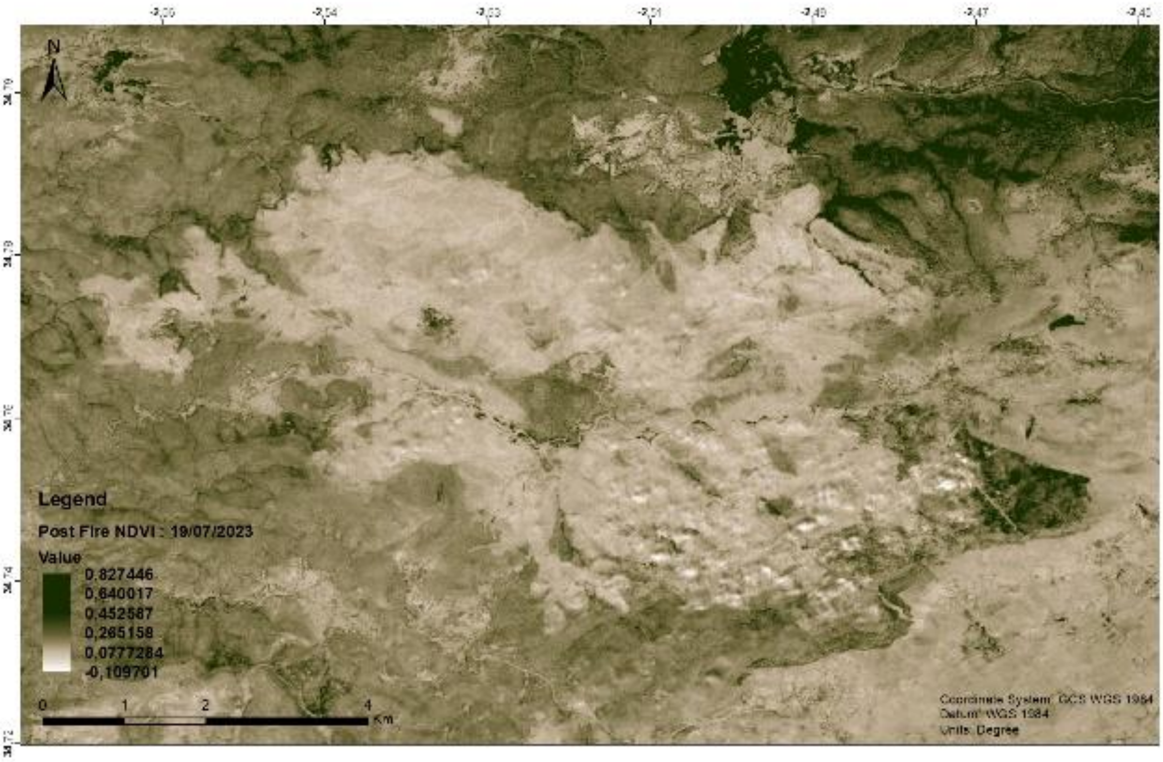

Figure II. 13 : Post-Fire NDVI Map (Ben Hichou et al., 2023a)

II.3.6. Differenced Normalized Difference Vegetation Index (dNDVI)

The dNDVI accurately delineated the pixels of the burned vegetation by classifying the image pixels into two classes using the natural break of its histogram, and allowed us to identify its surface area, which is 3517.98 hectares.

This convergence in identifying the burned area strengthens the reliability of our results and enhances our confidence in the effectiveness of the change detection method used (figure II.14).

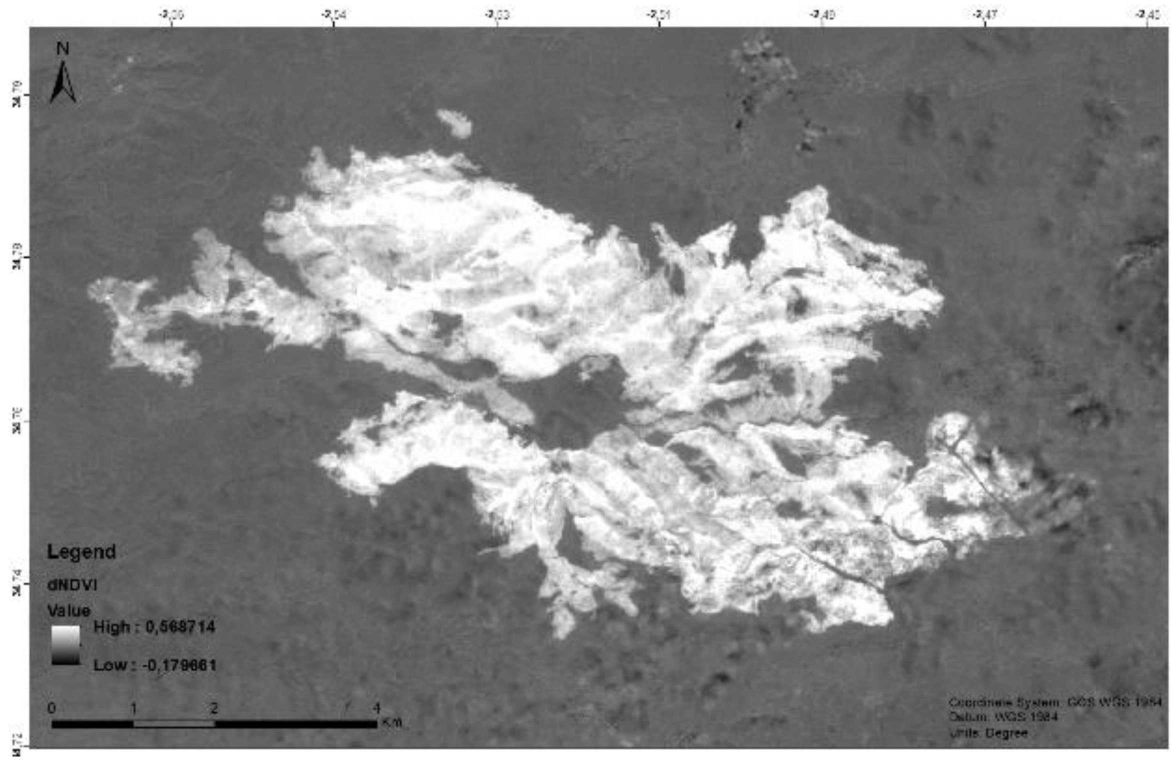

Figure II. 14: dNDVI Map in Grayscale (Ben Hichou et al., 2023a)

II.3.7. Supervised classification

Thanks to our in-depth understanding of the study area and the field visits conducted during the forest fire event, we were able to accurately determine five distinct land cover classes. These classes were utilized as regions of interest in the supervised classification of the Post Fire satellite imagery. The identified land cover classes included the burned area, unburned area (forest), areas covered with alfa vegetation, cultivated areas, and built-up areas.

The scatterplot analysis was performed using relevant spectral bands to highlight the variations between land cover types. In the scatterplot, distinct clusters are evident for each class (region of interest), with the burned area prominently marked within a black circle, showcasing excellent separation of spectral characteristics among different land cover types. This effective capture of unique spectral signatures by the classifier led to a successful classification. Additionally, the analysis revealed minimal overlap between clusters representing different classes, providing further validation of the classification accuracy.

The maximum likelihood classification method was employed to generate a precise land cover map, as each class exhibited unique spectral signatures. This classification method allowed us to effectively differentiate between various land cover types, enhancing the accuracy of our mapping results (figure II.15).

To validate the accuracy of the land cover map, we conducted extensive field visits and performed a rigorous comparison between real-world observations and the classified satellite image. Additionally, we calculated the confusion matrix, which provided us with the Kappa coefficient, a reliable measure of the classification accuracy.

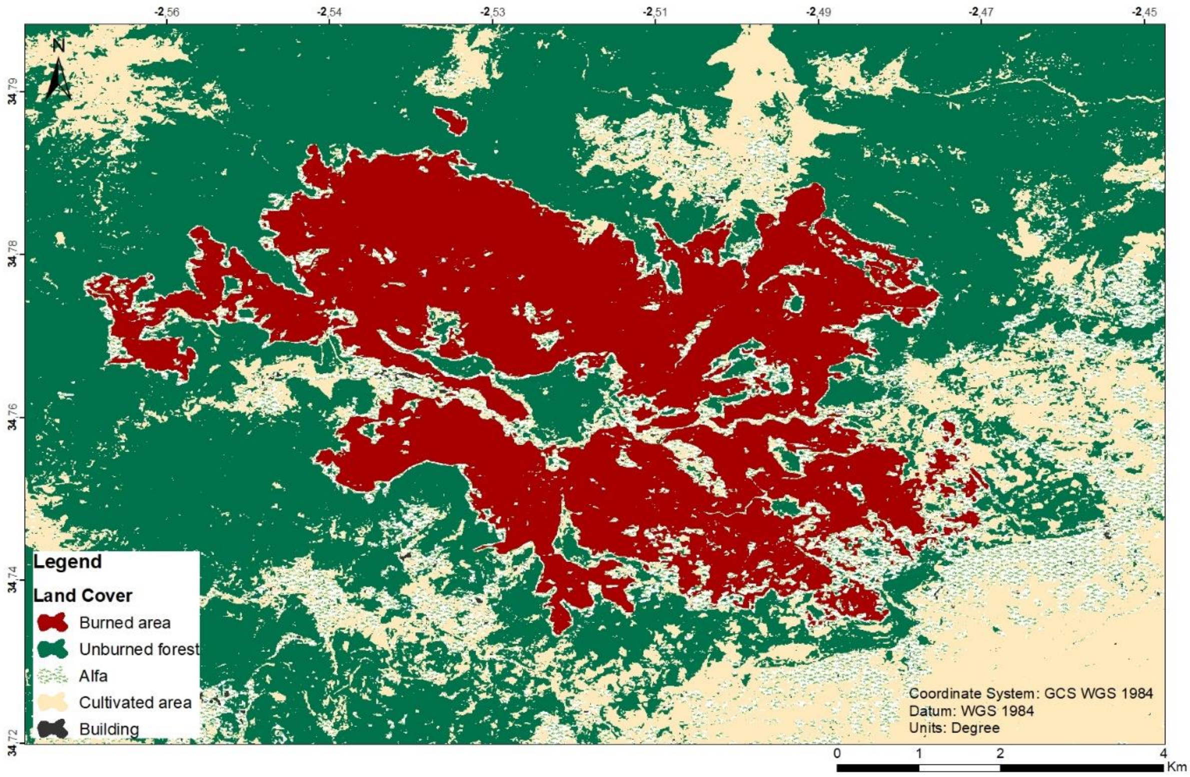

Figure II. 15: Land cover map post fire (Ben Hichou et al., 2023a)

According to our findings, the "burned area" class covered an area of 3113.63 hectares. This information serves as a key component in assessing the extent of the forest fire's impact (figure II.16).

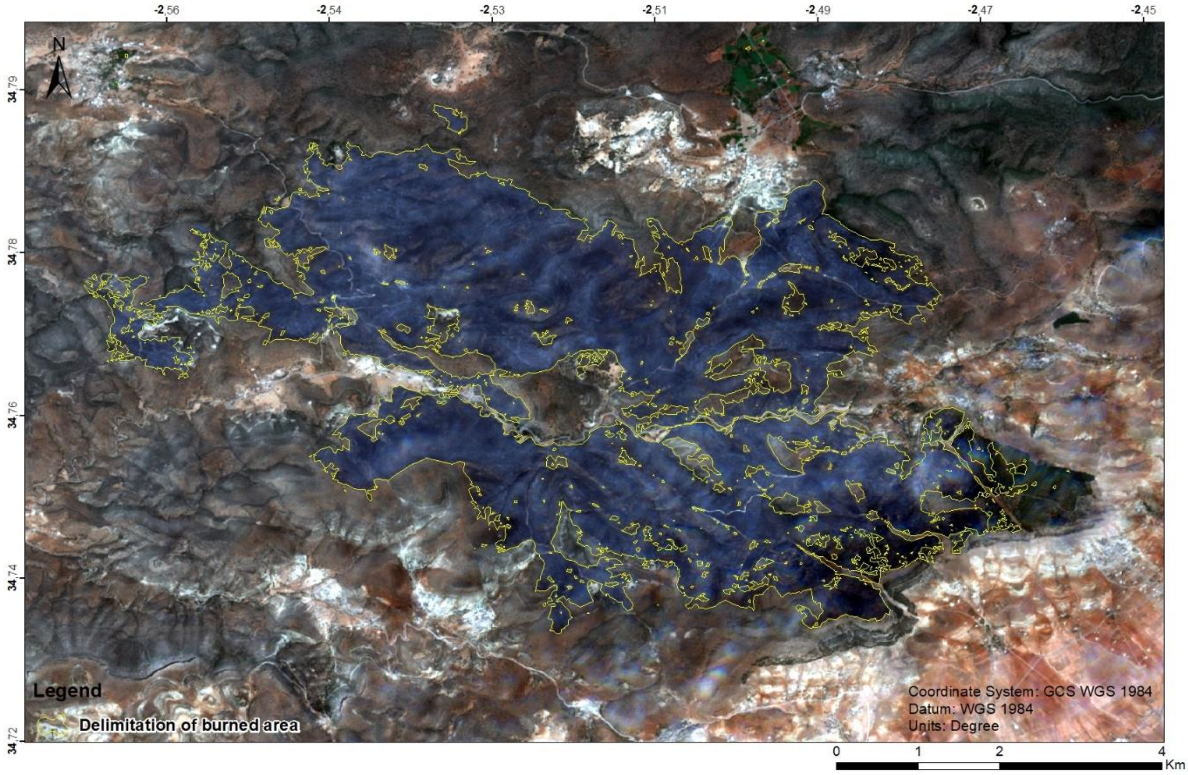

Figure II. 16: Post-fire burned area delimitation on true-color Sentinel 2 image (Ben Hichou et al., 2023a)

The spatiotemporal analysis of the active forest fire near Berkane, Morocco, offers valuable perspectives on the importance of early detection and rapid response, the significance of geospatial analysis in understanding wildfire patterns, and the implications for post-fire recovery and ecosystem management. These perspectives underscore the need for integrated approaches that combine advanced monitoring technologies, effective emergency response strategies, and comprehensive ecological assessments to address the challenges posed by wildfires and ensure the sustainable management of forest ecosystems. Further research and ongoing monitoring efforts are essential to deepen our understanding of the long-term ecological impacts and to guide informed decision-making for ecological restoration and conservation in fire-prone regions.

The recent surge in research on forest fire analysis and mapping using remote sensing techniques has significantly advanced our understanding of how technology can be leveraged to better detect and manage forest fires. The studies mentioned in this chapter and many others have contributed valuable insights into various aspects of this field, each with its unique approach and focus.

One common theme among these studies is the utilization of deep learning and machine learning algorithms to enhance the accuracy and efficiency of forest fire detection and mapping. This approach, as seen in by Ghali (2023), not only streamlines the identification process but also reduces the risk of false positives, ultimately aiding in early intervention and mitigation efforts.

Another noteworthy trend is the integration of multiple data sources, including satellite imagery, aerial imagery, and UAV imagery. Maffei et al. (2021) have pioneered the use of multi-spectral and thermal imagery for forest fire prediction, showcasing the potential of combining different data types to provide a more comprehensive understanding of possible forest fires. This fusion of data sources offers a richer and more detailed perspective on the factors of forest fires.

The research conducted by Collins et al. (2020) introduces an essential dimension to the field by focusing on forest fire severity mapping. Their work highlights the importance of assessing the damage caused by fires, enabling better post-fire land cover change analysis. This contributes to a more holistic understanding of the ecological impact of forest fires.

One of the standout features of our study is the incorporation of FIRMS data to pinpoint active fire locations. This addition is of significant value as it enables near real-time monitoring of forest fires, offering important insights for timely intervention and management. Additionally, our study adopts a supervised classification technique to map burned areas in detail. This method provides better results to understand the post fire change of land cover.

The articles reviewed here collectively highlight the ongoing advancements in forest fire analysis and mapping using remote sensing techniques. These studies demonstrate the importance of leveraging technology to enhance our ability to detect, monitor, and respond to forest fires. Our methodology, which integrates FIRMS data and utilizes supervised classification, represents a significant contribution to this field, enabling more effective forest fire management and ecological assessment.

II.4. Conclusion

The spatiotemporal analysis of the active forest fire highlights the successful efforts of emergency intervention teams in containing and extinguishing the flames, preventing harm to settlements and human lives. The utilization of advanced techniques such as NBR, dNBR, NDVI, and dNDVI proved instrumental in accurately identifying, quantifying, and assessing the extent of the burned area. The supervised classification method further aproaved these results, showcasing the potential of integrated approaches for comprehensive landscape assessment.

Looking ahead, these findings underscore the urgency of early detection and rapid response strategies in wildfire management. The study reinforces the importance of geospatial analysis as a valuable tool for understanding fire patterns and their ecological impacts. Moreover, the insights gained here will guide future strategies for post-fire recovery and ecosystem conservation, emphasizing the need for ongoing research and monitoring efforts in fire-prone regions. By combining technological advancements, effective emergency response, and ecological assessments, we can pave the way for more resilient and sustainable forest ecosystem management practices.

Chapter III: Contribution of the catchment area to the hydrology of a Saharan Wetland, the Imlili Sebkha (Dakhla Region, Morocco): Use of GIS and Satellite Data

III.1. Introduction

Geographic Information Systems (GIS) and satellite data have revolutionized the field of hydrological modeling, offering valuable tools for understanding and managing the intricate relationship between catchment areas and hydrology. In regions with varying hydrological dynamics, such as the Saharan wetlands, like the Imlili Sebkha in the Dakhla region of Morocco, the integration of GIS and satellite data has become pivotal in exploring the contributions of catchment areas to the overall hydrological processes.

The Imlili wetland is an ecological feature nestled in the southern reaches of Morocco, approximately 60 kilometers south of the coastal town of Dakhla. Spanning across the geographical coordinates of 23.202439° to 23.293465° latitude in the north and -15.891996° to -15.946094° longitude in the west, this wetland holds a distinctive place in the region's landscape. It is situated at the confluence of an endoreic hydrographic network, comprising four wadis, one of which stretches over 280 kilometers, alongside several cha'bas. The landscape itself is characterized by an extensive, nearly level basin with salt-enriched sandy soil, categorizing it as a sebkha. However, the intriguing genesis of the Imlili wetland is closely tied to the relatively recent (Holocene) formation of a substantial sandy dam at the lower reaches of the aforementioned hydrographic network, giving it the attributes of a natural dam guelta. It is particularly remarkable as a permanent dune guelta, and it stands as the sole known representative of this distinct feature (Dakki et al., 2020).

One of the most notable indicators of the Imlili wetland's hydrological significance is the presence of the Guinea tilapia (Coptodon guineensis), a cichlid fish known to thrive in environments with a continuous water supply. The occurrence of this species has drawn the attention of numerous researchers, underscoring the importance of understanding the wetland's hydrological dynamics (Qninba et al., 2009; Agnèse et al., 2018; Himmi et al., 2020).

Building upon the foundation laid by previous studies, the present work seeks to delve into a fundamental aspect of the Imlili wetland's hydrological functioning: the analysis of water inputs into its hydrographic network. These inputs are sourced from both pluvial (rainfall-related) and phreatic (groundwater) origins. The balance of these inputs is believed to be significantly influenced by factors such as low pluviometry (limited rainfall), rock fissuring, and soil silting. To unravel the intricacies of this delicate balance, our analysis predominantly relies on the compilation of satellite data, which is supplemented by on-the-ground field surveys conducted on November 27-

28, 2012. These surveys encompassed not only the wetland itself but also its surrounding areas, allowing for a comprehensive investigation of this unique and critical ecosystem.

In the following sections, we will explore the methodologies employed, the data sources harnessed, and the results obtained from our comprehensive analysis of the Imlili Sebkha's hydrological dynamics, shedding light on the vital role of GIS and satellite data in understanding the complex interplay between catchment areas and hydrology in this Saharan wetland.

III.2. Geographical context of the wetland and its catchment area

III.2.1. Physiographic context

The Imlili wetland is situated at an elevation of approximately 36-45 meters above sea level. It occupies a large elongated depression that runs in a NNE-SSW direction, measuring about 10 kilometers in length and 2.6 kilometers in width, covering a total surface area of 17.3 km² (Figure III.1). The shores of this depression are primarily characterized by low cliffs, with their incline occasionally softened by deposits of aeolian dunes. To the south of the depression, these dune deposits have formed a substantial dune field, constantly replenished by sand carried by northern winds. This field has effectively created a natural barrier, occupying a former valley (as documented by Dakki et al. in 2020). Within the Imlili wetland's boundaries, this valley has been filled with sandy-silt deposits, creating a nearly flat surface reminiscent of a sebkha, though it still maintains a slight incline from north to south.

The present layout of the wetland imparts an endoreic nature to its hydrographic network. This network is primarily fed by water sources originating from the Cretaceous and Cenozoic terrains situated to the east and northeast of the sebkha. Towards the northern end of the wetland, it receives inflow from two significant tributaries, Wad Al Hawli and Wad Al Faj. At its southern edge, it is further supplied by another substantial tributary, Wad La'rad, which is of no lesser importance than the two aforementioned sources. Additionally, various other cha'bas contribute to the network's enrichment from the elevated terrains that overlook the sebkha to the east.

The sebkha's basin is punctuated with over 160 shallow, saline groundwater outlets of diverse shapes, primarily located in its northwestern region (as documented by Himmi et al. in 2020). These outlets, despite their vulnerability to filling, never completely run dry simultaneously. This unique characteristic bestows upon the wetland a status of permanence, an attribute distinct to it among sebkhas, as reported by Dakki et al. in 2020. On the northwestern bank and in the southern sector of the sebkha, one can observe intermittent water flow channels, occasionally filled with water and flanked by emergent hydrophytes.

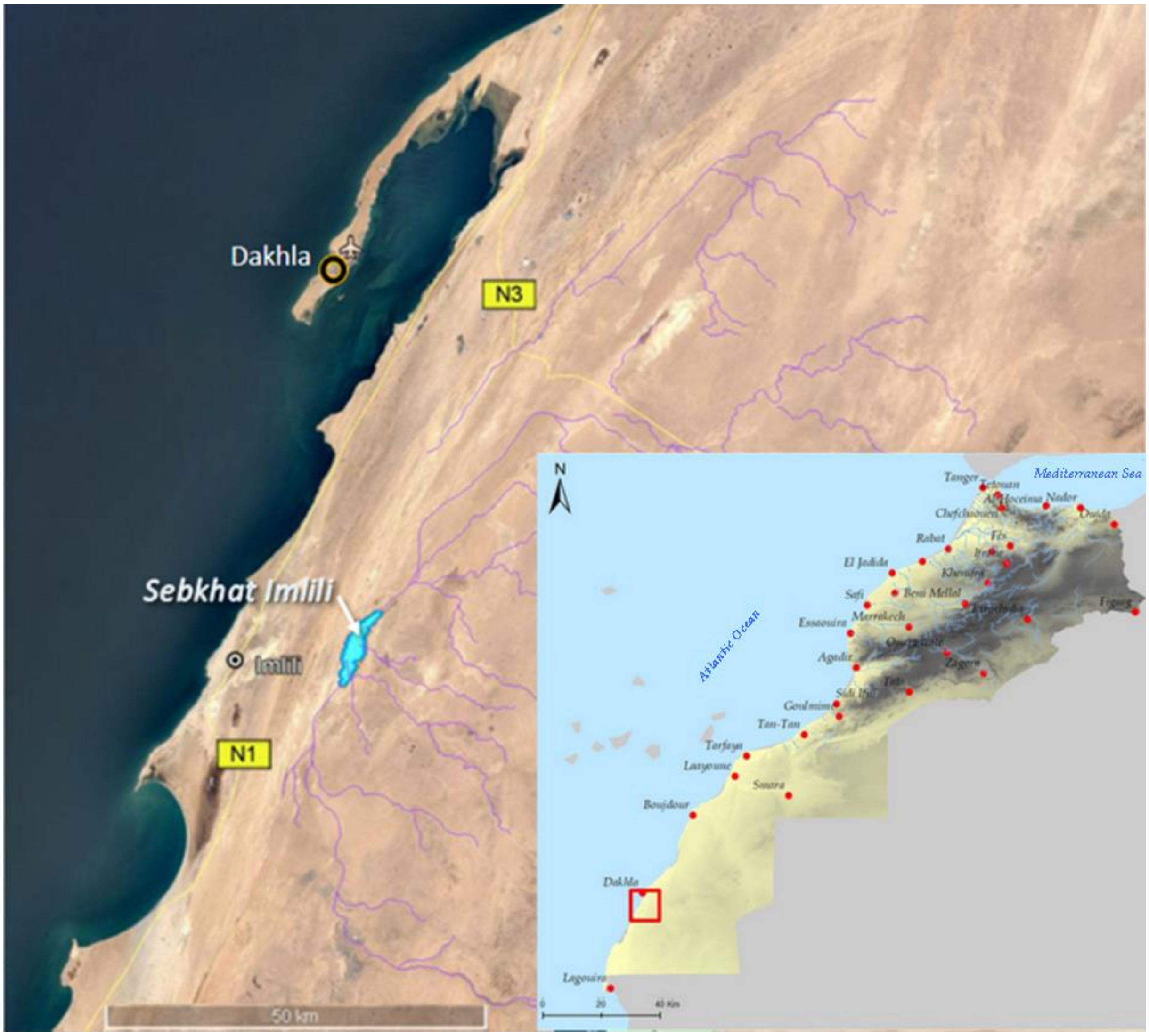

Figure III. 1: Location of the Imlili wetland

III.2.2.Geological Context

The coastal region of Dakhla-Lagwira is located at the southern extremity of the sedimentary basin known as Tarfaya-Laâyoune-Dakhla, which has been forming since the Cretaceous period. Within this basin, you'll find the Imlili sebkha, situated in a lengthy depression that runs in the SSW-NNE orientation, set apart from the Atlantic coast by a plateau roughly 15 kilometers wide. This wetland is surrounded by geological formations of Neogene age, as documented by Rjimati et al. in 2011. These formations include conglomerates, lumachelles, quartzites, calcareous rocks, marly layers, and quartzite sandstones. Frequently, these terrains are covered with aeolian sandbanks, sometimes taking the shape of extensive fields that fill in depressions and wadi beds or are supported by embankments. To the north of the sebkha, the landscape takes on a distinctive ruiniform appearance, with elongated ridges and flat-topped hillocks (garas), shaped significantly by wind activity. Currently, this wind-driven activity counteracts the undulating features of the wadis by reducing the slope of the banks and flattening their beds with predominantly sandy deposits, often creating the appearance of broad, flat-bottomed valleys. The presence of conglomerate and sandy alluvial terraces in most valleys and depressions, along with the extensive nature of these valleys, bears witness to a well-rainfed Holocene history. However, ancient flow channels are often obscured by wind erosion.

The Neogene formations are characterized by their permeability, facilitating the efficient circulation of infiltrated water in the subsoil, thereby establishing a crucial groundwater reservoir, as reported by Hilali et al. in 2020. These formations rest upon layers of Cretaceous-Paleogene age, primarily composed of marl, clay, or sandy-clay, which are generally less permeable to impermeable. Occasionally, quartzite layers are present, sometimes accompanied by intrusions of evaporites.

The layout of the Meso-Cenozoic landforms mirrors the brittle tectonics that characterize the Tarfaya-Laâyoune-Dakhla basin. Of particular note is a lengthy NNE-SSW fault that traverses the depression and extends southward through the wetland, as described by Rjimati et al. in 2011.

III.2.3.Climatic context

The catchment area of the Imlili wetland spans an arid zone where the influence of oceanic air in terms of atmospheric humidification and cooling, while still noticeable in the vegetation cover, is relatively limited. Along the coast, exemplified by the Dakhla station, the average annual rainfall for the period between 1935 and 2005 was a mere 29 millimeters, as documented by Sebbar et al. in 2013. Prior to 1965, this figure was slightly higher at around 37.6 millimeters, according to Quezel's 1965 data. However, over the past four decades, which have been characterized by drought conditions, annual rainfall has significantly decreased, with some years registering averages close to zero, as reported by Hilali et al. in 2020. Even during the wettest years, rainfall barely surpasses 100 millimeters. Rainfall tends to occur in brief, sporadic showers, primarily during the autumn season (associated with the occasional upwelling of the Gulf of Guinea lows and the Anti-Alizes). There are also a few instances of winter thunderstorms (related to the remnants of the North Atlantic lows), with precipitation being virtually negligible for the remainder of the year.

Temperature levels typically range between 10 and 35 degrees Celsius along the coast, but they can soar beyond 40 degrees Celsius in the inland regions, especially when influenced by southeast winds, which intensify evaporation.

In this region, akin to the entire Saharan coastline, wind activity is a frequent occurrence, dominated by prevailing northerly winds, often exhibiting considerable strength, with speeds ranging from 8 to 40 meters per second. These winds not only counteract temperature increases but are primarily acknowledged as the principal agents of erosion and sand transportation, a function well exemplified by the prevalence of dune deposits.

III.3.Material and Methods

The primary objective of this document is to primarily assess the water inflow originating from rainfall. This is accomplished through a simulation of both extreme flow patterns at the wetland level and the average annual surface water inputs. Utilizing daily rainfall data sourced from satellites, these estimations are computed for various weeks throughout the year.

III.3.1.Preparation of the orohydrographic data and geoprocessing

To calculate the flow patterns accurately, an initial demarcation of the Imlili catchment area was necessary. This delineation was carried out using the Digital Terrain Model (DTM) with a 30-meter resolution, specifically the GDEM Aster V2 model. The DTM also facilitated the delineation of the wetland itself and the reconstruction of its hydrographic network (Figure III.2). These tasks were accomplished through the utilization of the "Hydrology" geoprocessing tools within ArcGIS Pro.

It is noteworthy that in order to simulate the entire river system that converges towards the wetland, we selected multiple "low points" around its periphery and created their respective basins. This strategic approach allowed us to incorporate a significant river system, Wad Al Faj, into the sebkha basin, as it flows into the sebkha's northern end, possibly after confluence with Wad Al Hawli. The lower course of this tributary meanders through a wide depression with a gently undulating terrain, interspersed with small ridges and hamadas oriented in a north-south direction. This extensive depression, an extension of the Imlili sebkha to the north, lacks well-defined flow channels, resembling many defunct valleys in the Boujdour-Dakhla region. The trajectory of this tributary, established using the DTM, was further clarified with the assistance of Google Earth. It revealed that the flow could be obstructed by sandy obstacles measuring 2-4 meters in height, which would only yield to exceptional floods (Ben Hichou et al., 2023b).

This meticulous delineation of the catchment area, closely aligned with the site's topographical reality, maximizes the accuracy of our estimations for inputs to the wetland. These inputs encompass surface water that flows during heavy rainfall events and underground water movement, as surface water flow is frequently impeded by dune deposits, promoting infiltration into the subsoil.

Given the limited resolution of the DTM, the modeling was complemented by using a 1:100,000 topographic map. This facilitated the delineation of low-gradient sub-basins located both to the south and north of the wetland. Most of the watercourses in these regions exhibit characteristics of defunct valleys, with poorly defined margins covered in sand, sometimes forming banks that can obstruct the flow. In certain instances, these features give rise to graras, which are shallow depressions with fine sediments that support the growth of shrub and herbaceous vegetation, at times forming dense vegetation, or even small sebkhas (Ben Hichou et al., 2023b).

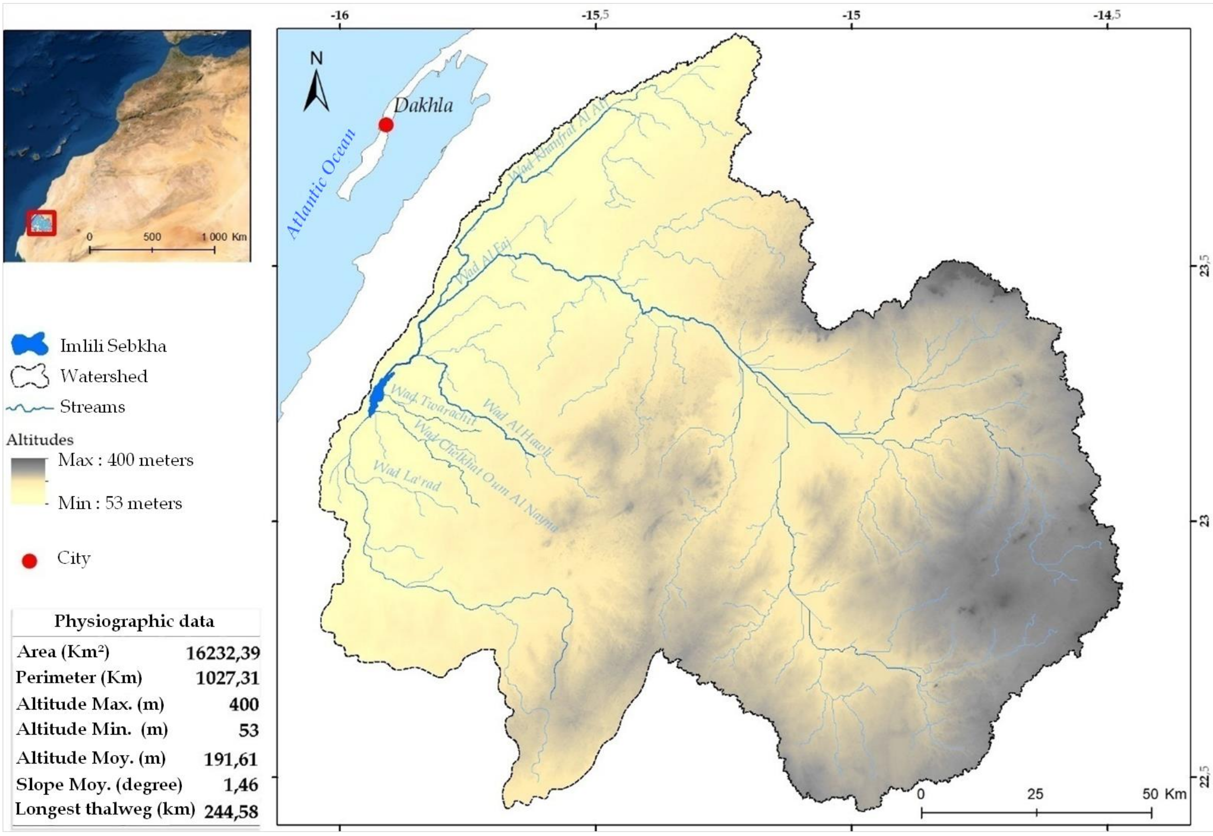

Figure III. 2: Orohydrography of the Imlili wetland watershed (Ben Hichou et al., 2023b)

III.3.2.Estimated volumes of water received by the wetland

To determine the average annual surface water contributions from the catchment to the wetland, we evaluate the catchment's water balance. This assessment is conducted using the lowest point of the wetland, situated in proximity to its southern extremity, as the reference point (outlet). The calculation is rooted in the following equation (1):

$$P + S = R + E + I \qquad (1)$$

- P : Precipitation in mm ;
- S : Accumulation from the previous rainy period in mm ;
- R: Height of runoff in mm ;
- E: Evaporation in mm;

- I: Infiltration in mm.

The quantity of water that arrives at the wetland during a rainfall event is directly related to the catchment area and the average runoff height (R), which, in turn, is influenced by the runoff coefficient (RC). The calculation for this volume is as follows (2):

$$V = A \times R = A \times RC \times P \qquad (2)$$

- V : Volume of water runoff in m^3 ;
- A: Catchment area in m^2 ;
- R: Average height of runoff in mm;
- P: Precipitation in mm;
- RC: Runoff coefficient in %.

We derived precipitation data from satellite-based simulations (Chirps V2 images in 5 x 5 km^2 pixels) with daily frequency spanning 35 years (1981 to 2015). These data were extracted from within the catchment boundary polygon.

The runoff coefficient (RC) is determined through an assessment of soil infiltration rates, land slope, and land use. In Morocco, this coefficient has been empirically estimated for various soil types, as indicated in Table III.1.

Table III. 1: Recommended values for the runoff coefficient based on soil type, slope and land occupation rate.

Nature of the soil	Sandy			Clay		
Slope	Flat	Undulating	Steep	Flat	Undulating	Steep
Land use (%)	2	2-7	> 7	2	2-7	> 7
Runoff coefficient	0.10	0.15	0.20	0.17	0.22	0.35

Within the Imlili catchment area, the prevailing land use type that can be applied to the entire region is "steppe vegetation" (Figure III.3). This generalization is based on a map created through supervised classification of LandSat 8 images captured by the OLI (Operational Land Imager) sensor, employing remote sensing software. These images were obtained during the wettest period of the year, as determined by rainfall analysis.

The runoff coefficient varies across the catchment area, with a value of 10% in the lower western regions, covering approximately 60% of its total surface area, and 15% in the eastern, higher elevated areas (as illustrated in Figure III.4). Only on a few minor ridges, which constitute an insignificant portion of the total surface area, does this coefficient reach 20%.

The Quaternary soils' permeability, in conjunction with the prevalence of sandy soils within the catchment area, hinders the long-term accumulation of surface water reserves. This is especially pertinent given the region's rainfall pattern characterized by brief showers interspersed with extended dry periods. As a result, it is reasonable to assume that the parameter S (representing the accumulation of the previous rainy period) has a value close to zero. Likewise, during the rainy season, the atmosphere is humid, and evaporation can be considered negligible (E ≈ 0).

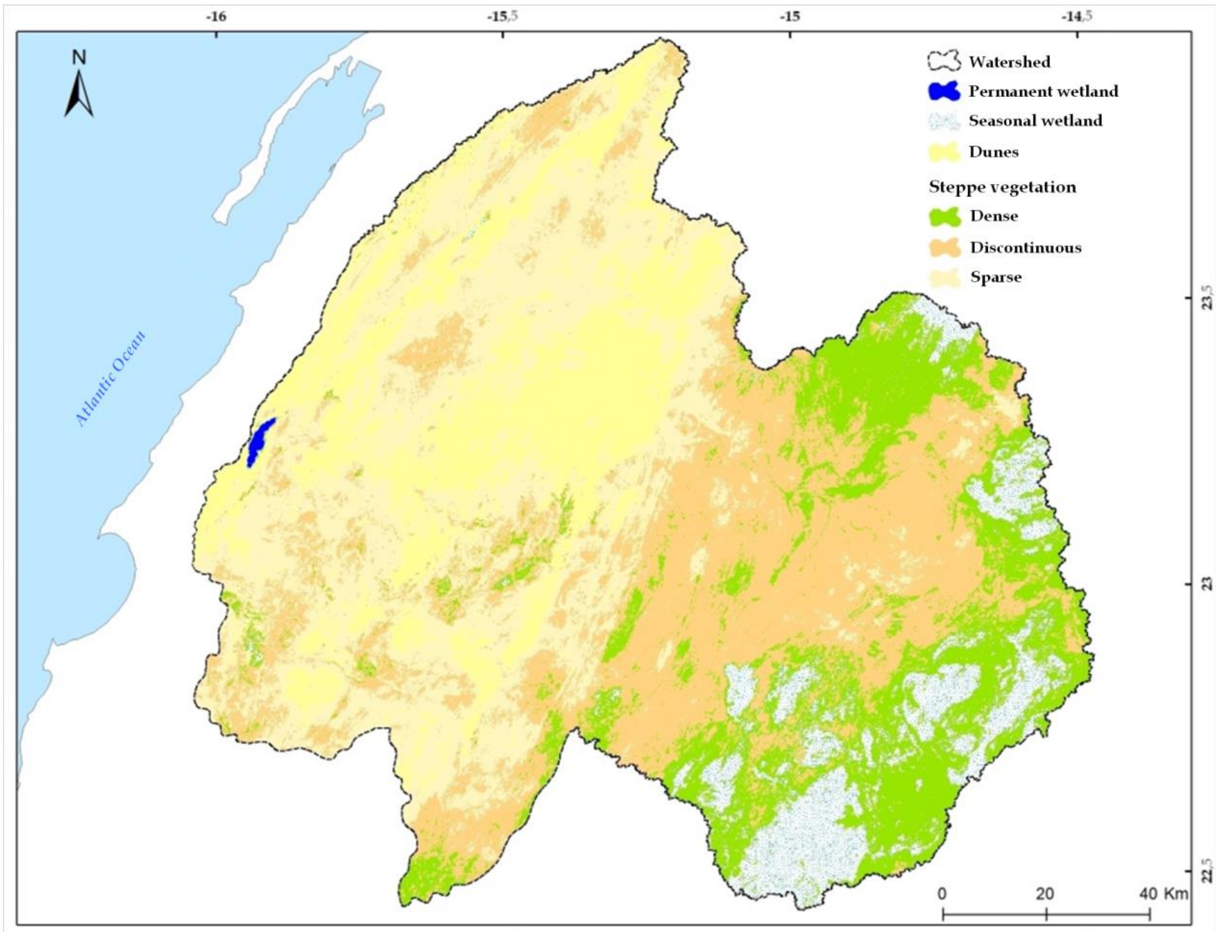

Figure III. 3: Land use types (habitats) in the Imlili watershed. (Ben Hichou et al., 2023b)

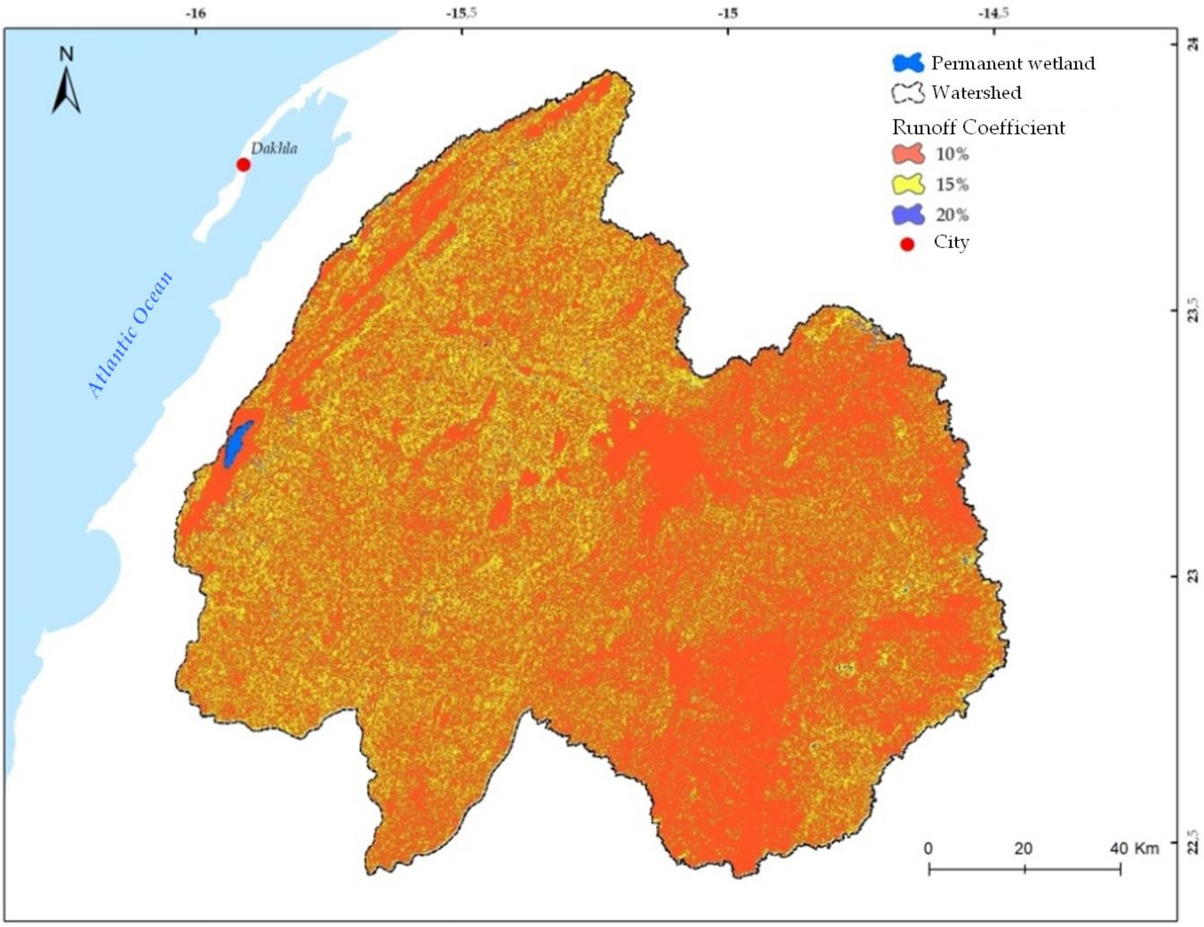

Figure III. 4: Variation of the runoff coefficient in the Imlili watershed. (Ben Hichou et al., 2023b)

Simulation of extreme flows

Conventional calculation methods typically rely on empirical formulas that take into account two key characteristics of the catchment area: its size, represented by the surface area, and its topographic gradient, denoted by the average slope of the longest river. These parameters are determined using ArcGIS Pro, utilizing the Aster GDEM V2 digital elevation model and the 1:100,000 topographic map.

The methodology employed in this study involves a combination of the Hazan-Lazarevic formula (Hazan et al., 1969) and the Fuller 1 formula (Fuller, 1914) for extrapolating flow data. These authors are reported to have used data from approximately fifteen hydrological stations situated in different basins, assumed to cover various regions within Morocco.

The Hazan-Lazarevic formula computes the millennial flow generated downstream of a catchment as a function of its surface area and two specific parameters (k1 and k2):

$$\mathbf{Qt(1000) = k1 \times S^{k2}}$$

Where:

Qt(1000) represents the peak flow (in cubic meters per second) with a recurrence period of 1000 years, and

S is the watershed area (in km^2).

The values of the parameters k1 and k2 are contingent upon the geographical location of the basin, which is indicative of its average annual rainfall. For the Saharan coastal area, K1 = 9.38 and k2 = 0.74.

The conversion of millennial flood flows into flows with shorter recurrence periods (T) is determined using the Fuller formula (3):

$$Q_t(T) = \frac{Q_{(1000)} \times (1 + a \times \log(T))}{1 + a \times \log(1000)} \tag{3}$$

$Q_t(T)$: Peak recurrence flow rate T (in m^3/s) ;

a : Regional coefficient that varies with the location of the concerned basin (for the Saharan area, the Water Department recommends $a = 1$).

III.4.Result and discussion

III.4.1.Hydrological summary: surface water input to the wetland

Due to the limited rainfall in the Saharan region, the assessment of water inflow into the wetland was conducted during the wettest periods of the year. To identify potential timeframes of concentrated rainfall, the calculation interval was reduced to one week (Ben Hichou et al., 2023b). The graph displayed in Figure III.5 illustrates the fluctuations in average weekly rainfall, computed from a daily dataset spanning the period from 1981 to 2015.

Rainfall in this region occurs sporadically in the form of showers. The wettest period encompasses weeks 36 to 39, which roughly corresponds to the month of September. Notable showers occur at the end of August and during the winter season, with the highest rainfall observed in the initial and final weeks of September, measuring 3.97 mm and 3.15 mm, respectively. The average annual volume of water that is assumed to reach the wetland over the period from 1981 to 2015 amounts to 23.2 million cubic meters per year. This translates to approximately 2.9 million cubic meters per week during the 'September-October' timeframe and 4.929 million cubic meters per week during the wettest month, spanning weeks 36 to 39.

Given the catchment area's low gradient (as depicted in Figure III.6) and the prevalence of sandbanks, the time of concentration for rainfall is notably high, reaching 74.86

minutes. Consequently, the flow velocity during showers is relatively low. This implies that after heavy rainfall, the majority of rainwater reaching the sebkha primarily originates from the edges of the wetland. The remaining portion of the rainfall is expected to infiltrate into the wadi underflows or gradually evaporate over time. The numerous small depressions visible in the wadi beds accumulate this water over short durations and are believed to contribute to this infiltration.

In this context, precipitation plays a more significant role in recharging the water table, which predominantly converges on the wetland aquifer, rather than directly filling the wetland through surface runoff.

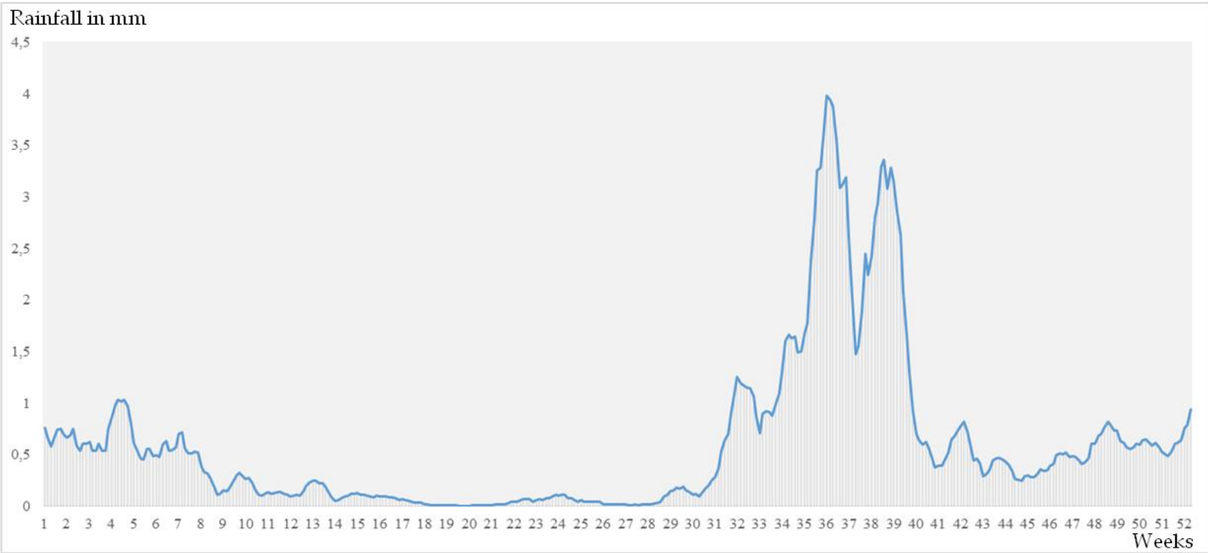

Figure III. 5: : Determination of the wettest period in the Imlili watershed. (Ben Hichou et al., 2023b)

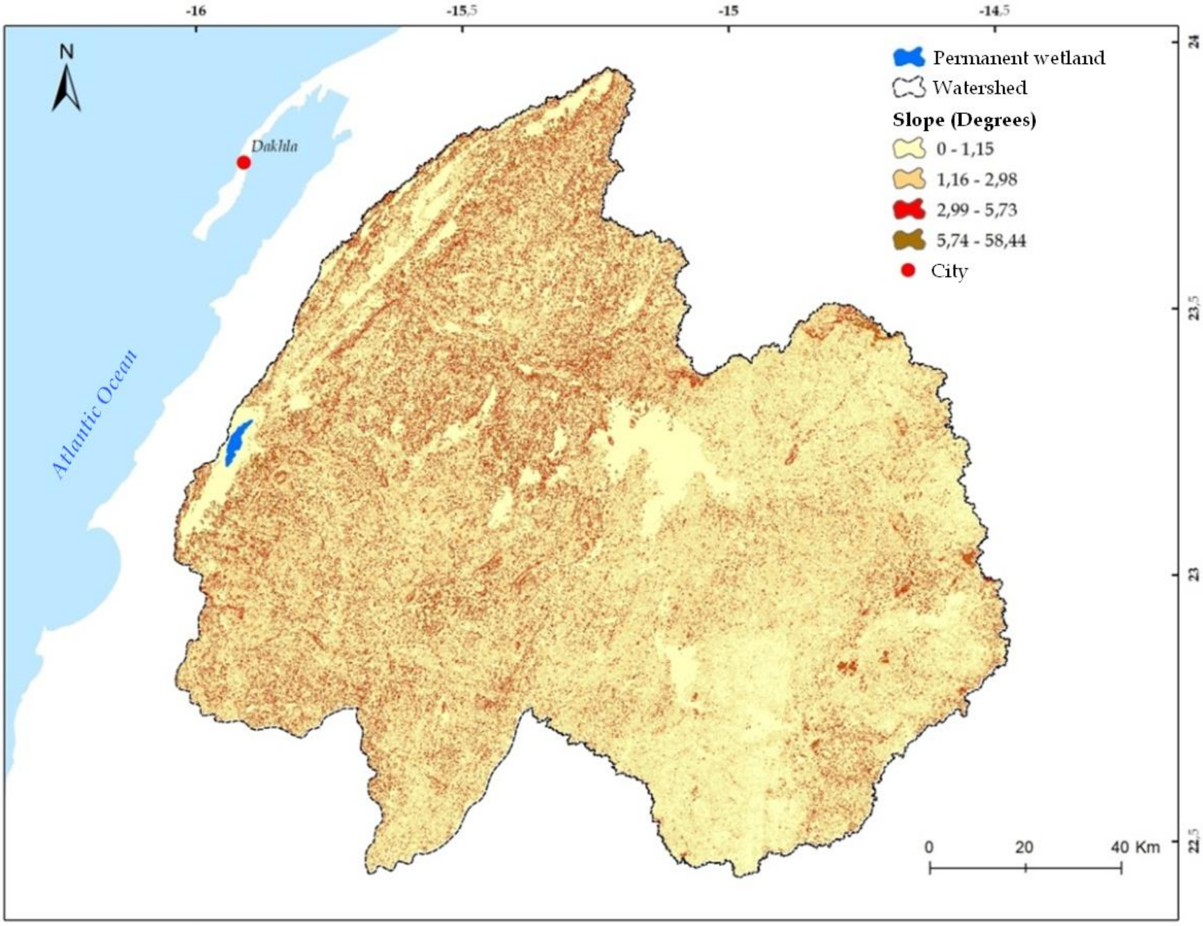

Figure III. 6: Slope variation in the Imlili wetland catchment area. (Ben Hichou et al., 2023b)

III.4.2.Peak flow

The extreme flows, estimated for various return periods, provide a comprehensive perspective on the extraordinary floods, as depicted in Figure III.7. These floods warrant attention not only for the considerable volumes of water they bring to the wetland but also for the potential materials they might carry from the catchment, such as sand, silt, gravel, and organic matter.

Despite the gentle incline of the wadi beds, these major floods have the potential to displace numerous sandy barriers, allowing a substantial portion of their water to reach the sebkha. This could result in the significant transportation of materials, including sand and occasionally silt, downstream towards the thalwegs and possibly into the wetland. However, it's worth noting that these flows may still be unable to overcome certain impassable obstacles. These obstacles play a role in retaining rainwater upstream of the wetland, thereby facilitating the recharge of the sebkha aquifer.

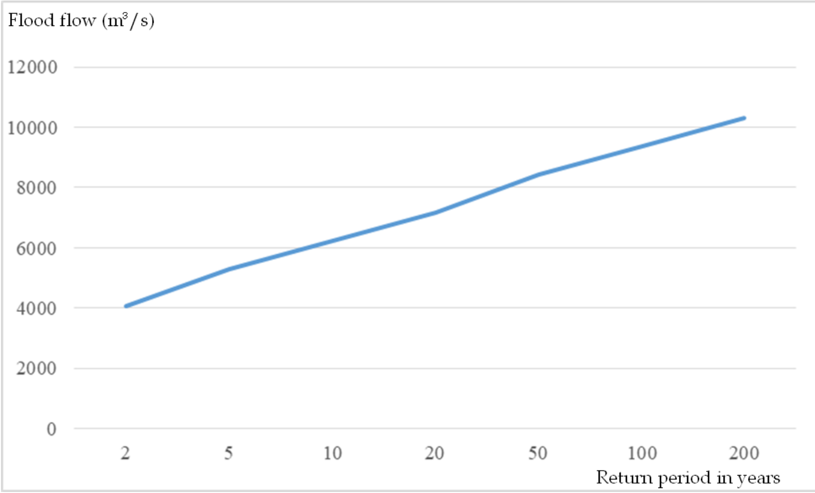

Figure III. 7: Variation of peak flows according to return periods. Source: Personal study. (Ben Hichou et al., 2023b)

The Imlili wetland's sustained existence is attributed to the upward movement of groundwater through shallow cavities in its shallows. Due to the gentle slope of the land and the accumulation of sediment on runoff surfaces, the majority of rainwater is absorbed into the subsoil. Only a small portion of surface water resulting from significant storms manages to reach the wetland. Nevertheless, occasional replenishment of the wetland by surface water is confirmed by evidence of flooding (up to several decimeters in height) and visible runoff, as observed by locals and visitors, as well as the wetland's vegetation (Ibn Tattou, 2020). These surface inflows are most likely to occur in early autumn (Figure IV.5), as the wetland experiences limited rainfall during spring and summer (weeks 09-31).

The wetland's enduring nature is thus closely tied to the emergence of the surface water table, which is assumed to have relatively ample reserves, even during recent drought periods. This indicates that rainwater is not entirely lost to evaporation and is largely absorbed by the surface aquifers, facilitated by the permeability of the majority of the land (composed of Cenozoic deposits) and sandy soils. Additionally, during floods, rainwater inundates a portion of the wetland, including the cavities that connect to the water table, contributing to the replenishment of the underlying aquifer.

III.5.Conclusion

This study's significance lies in its exploration of the irrigation mechanisms of the Imlili wetland, with a specific focus on the sustainability of the groundwater sources that bestow upon it the characteristic of being a perennial sebkha. The role of rainwater in the hydrological processes of Saharan wetlands, often underestimated due to the arid climate, is reassessed upwards in the case of the Imlili sebkha, recognizing its rapid infiltration into the subsoil.

Furthermore, the study extends its scope to encompass the Wad Al Faj network as part of the catchment area, acknowledging that modeling this network might present challenges in the digital field model. Notably, in the region drained by this network to the north of the wetland, defining flow areas can be problematic, especially when they might be obstructed by temporary sandy barriers.

This extension, even if we acknowledge that its direct contributions to the Imlili wetland may be limited, is valuable in recognizing the network's role in recharging the water table and not overlooking its potential surface contributions to the wetland during periods of heavy rainfall.

Chapter IV: Assessing the Impact of Artificial Dams on Hydro-Sedimentary Regime: A Case Study of Hassan Ad-Dakhil Reservoir in the Ziz Basin, Morocco

IV.1. Introduction

Mudflats are a very important component of natural wetlands, mainly in estuaries, large marshlands and lakes, and in river flood plains. Their formation is due to inland waters, loaded with suspended particles drained from the the catchment area by surface runoff downstream. These sediments constitute flat zones of accumulation of fine materials generally rich in organic matter, which plays a major role in the regeneration of nutrients (Pearson et al., 2021) and the trophic scheme of the ecosystem.

The mobilization and export of soil fragments by the water during flood events is a natural erosion process involved in the composition of the particulate flow downstream of a (Venarsky et al.2022; Bai et al., 2020). In the studied watershed, the erosion is influenced by anthropogenic activities, among which dams have a direct impact on the hydro-sedimentary dynamics of the aquatic ecosystems; indeed, they block both water and sediment fluxes, creating thus a stagnant reservoir with active sedimentation upstream to them, and by drying long downstream sectors (Yang et al., 2020).

The material flows generated during extreme hydrological events are transferred and lead to the formation of nutrient-rich alluvial plains, which are set in motion by the action of rainfall and runoff (Hamilton et al., 2022).

There are many studies around the world assessing the impact of artificial dams on the hydro-sedimentary functioning of streams (Kastridis et al., 2022; Guan et al., 2022; Özşahin, 2023; Yuan et al., 2022; Zeng et al., 2022; Wang et al., 2021; Vericat & Batalla, 2004; Sanz et al., 2001; Ibàñez et al., 1996; Altaiee, 1990). Some of them concluded that the efficiency of large dams in blocking soil fragments can reach 99% (Williams et al., 1984), while Altaiee, (1990) found that in the Monsul dam on the Tigris River, 95% of the suspended sediment load mobilized during flood periods remain trapped.

Several dams have been built in Morocco, mainly to meet agricultural, energy, and watering needs, which also releases significant amounts of accumulated sediment. These discharges in the form of occasional events have a strong impact on downstream ecosystems. Given that the released sediments are typically fine and are easily drained by the flow, releases may have an effect on hydro-sedimentary processes in the river channel (Liu et al., 2023). The sudden and massive suspension of sediments in the modified system increases the rate of sediment loading, which can cause stress on aquatic ecosystems (Petts, 1984). For Helmi, (2023) and Zhao, (2021), the river is directly impacted by the way the sediment is released. The assessment and control of the hydro-sedimentary regime of a catchment requires the analysis and integration of the different factors that promote erosive processes (rainfall erosivity, terrain topography, soil erodibility and land cover). GIS as geospatial tools allows, through well-established equations, the integration of these different factors (Domazetović et al., 2019; El Jazouli et al. 2019; Sinshaw, 2021).

The application case chosen for this work is Hassan Ad-Dakhil reservoir, located in the Ziz basin (Figure IV.1). Its solid flow, mainly due to rainwater and more specially to floods, end up in this reservoir, while they fed the large downstream valley, corresponding to one of the largest oases in the world. Therefore, in order to quantify the hydro-sedimentary dysfunctions caused by this dam to the oasis, we used deterministic methods of erosion to quantify the sediment volumes trapped in the dam. Our objective is to test how these methods offer a general approach for quantifying the impact of artificial dams on the hydro-sedimentary regime.

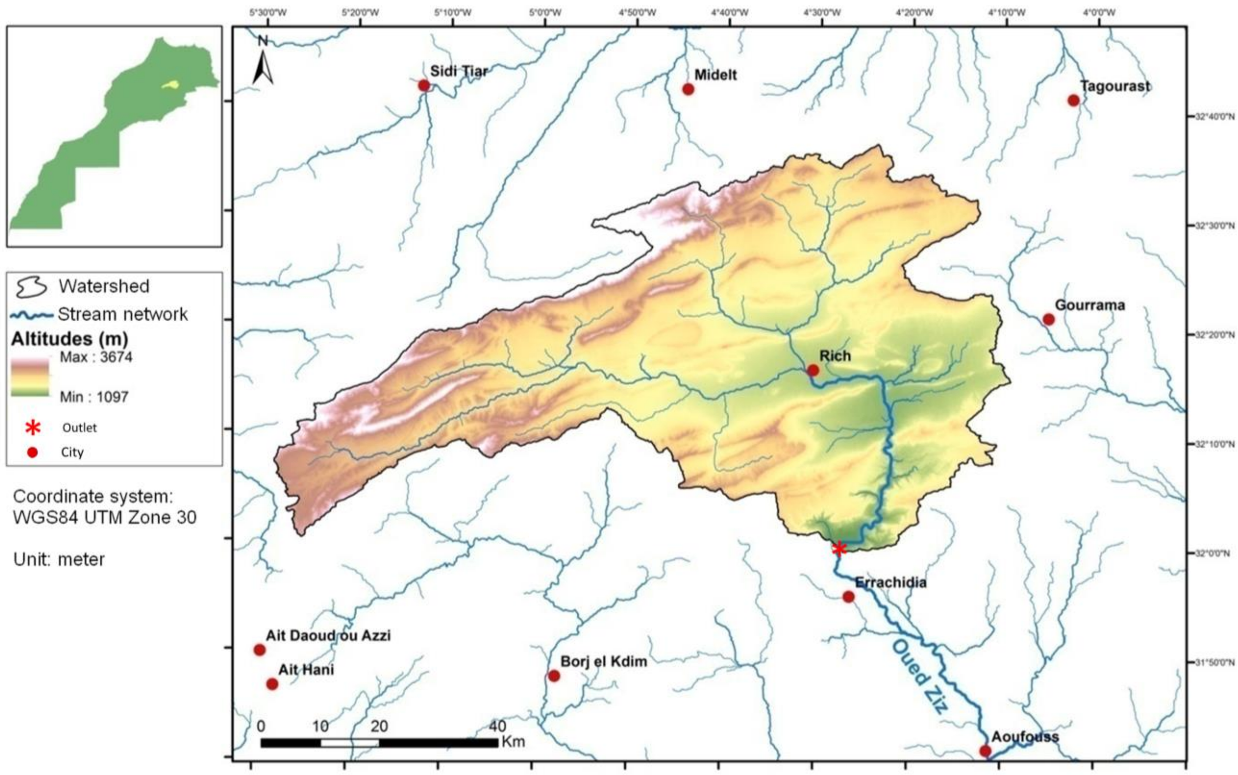

Figure IV. 1: Geographical location of the study area (Ben Hichou et al., 2023c)

The Hassan Ad-Dakhil Dam, built in 1971 on the Ziz River channel, is located in a hilly environment characterized by rocky outcrops, ranging from a basin low of 1097 m to a maximum altitude of 3674 m, as calculated by geoprocessing using the local Digital Elevation Model. According to data from the Guir Ziz Rheris Hydraulic Basin Agency (ABHGZR), the reservoir at Hassan Ad-Dakhil received 1,446,808.5 m^3 of dry sediment per year on average from 2010 to 2021. Based on measurements made on the ground, 1 m^3 of the sediment that is moved during floods weighs 14.7 kg. The Ziz River and its tributaries meander through small, generally agriculturally zoned channels with little in the way of natural flora.

IV.2.Material and Methods

The methodology involves estimating the sediment inputs captured within an artificial water reservoir by simulating the transport of solid particles in its surrounding area. This simulation is achieved by employing formulas that calculate the sediment delivery ratio at the reservoir, such as the average annual sediment emission equation or the Williams Emission Coefficient, which assess land movement (Williams, 1977).

To execute these approaches (Figure IV.2), available remote sensing data were utilized in conjunction with a Geographic Information System (GIS), enabling the integration of multiple parameters and their processing as data layers. The coupling of the RUSLE method with GIS facilitated the mapping of erosive factors (figures IV.3, IV.4, IV.5, and IV.6) and their organization within a geographical database. This enabled the execution of necessary treatments and operations to identify areas prone to water erosion.

The soil map of the catchment area of the Hassan Ad-Dakhil Dam (Figure IV.5) is a digitized subset of the soil map of Morocco.

In the studied catchment area, the average annual rainfall is 290 mm. This value was computed by analyzing the mean annual rainfall data from 1981 to 2021, obtained from the 40-year quasi-real satellite data of Chirps V2 (Funk et al., 1977).

IV.2.1.Soil Erosion Modelling

Several studies have been carried out on remote sensing and erosion quantification (Abdelhadi et al., 2022; Salvacion, 2023; Diani et al., 2023; Aouichaty et al., 2022; Ougougdal et al., 2020; Tahouri et al., 2022). Among the most applied models in this quantification, we have chosen the RUSLE model, which is an empirical model for the quantification of soil erosion of Wischmeier (Wischmeier et al., 1978) by correcting certain inaccuracies. This model considers erosion as the result of the multiplication of six parameters in the form:

$$\mathbf{A=R\times K\times LS\times C\times P}$$

Where:

A: Land loss rate in tonnes per hectare per year (t/ha/yr);

R: Rainfall erosivity in megajoule millimetre per hectare hour (MJ.mm/ha. h);

K: Soil erodibility in tonne hour per megajoule millimetre (t.h/ MJ.mm);

LS: Length of slope and inclination (m * %);

C: Land cover factor (without unit);

P: Factor considering the anti-erosion practices (without unit).

In this modelling, we have processed each parameter and integrated it in the form of a geo-referenced layer. All these layers allowed to end up with maps representing each component. And through the application of the RUSLE model (Figure IV.2), we obtained a map representing the sensitivity of soils to erosion at the dam catchment.

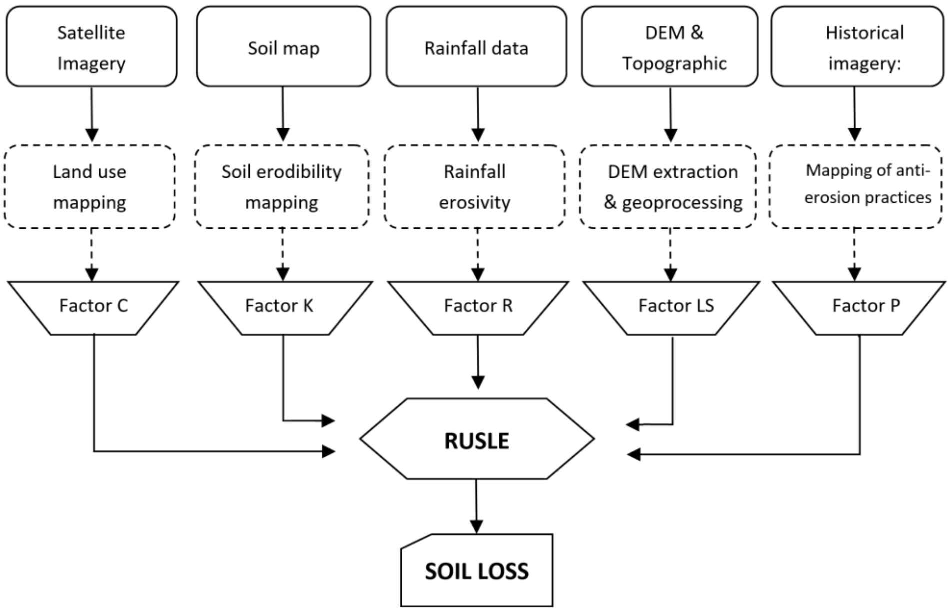

Figure IV. 2: Water erosion modelling method (Ben Hichou et al., 2023c)

IV.2.2. Land Cover and C-Factor Calculation

The method consists of analyzing the land cover from a satellite image and validating the analyses by comparing the spatial distribution of the remotely mapped habitats with the existing habitats determined in the field during several field trips.

In a first step, we extracted the part of the image covering only the area in question, according to the boundary of the studied catchment. A pre-processing of the Landsat 8 OLI image was done by applying a succession of essential operations that precede the classification, namely, radiometric correction of the image and improvement of its quality. The field data allowed us to identify the areas of interest, and the spectral signature of the different habitats, to launch a supervised classification, for which we chose the maximum likelihood estimation (MLE) algorithm. The confusion matrix and the Kappa index validated the classification. In addition, to assess the reliability of the mapping, a field mission to complete the validation was essential. The verification was carried out by travelling in the field, using the Trimble GPS field tablet PC.

The land cover map was drawn up based on the results of the classification. This allowed us to identify the C-factor for each habitat type mapped. This factor varies between 0 for areas where the effect of surface erosion is nil, and 1 for areas directly exposed to the risk of degradation (Ben Hichou et al., 2023c).

IV.2.3.Soil Erodibility Mapping

The K factor is a function of the texture, the organic matter content of the soil and the permeability of the soil. These data for the Hassan Ad-Dakhil Dam catchment area were extracted from the soil samples described in the soil map of Morocco (Ben Hichou et al., 2023c). The method of Wischmeier for the determination of this factor is defined by the following equation.

$$\mathbf{K = 2,8\ 10^{-7} M^{1,14}(12 - OM) + 0,0043(b - 2) + 0,0033(c - 3)}$$

M: (% fine sand + % silt)* (100- % clay)

OM: Organic matter

b: Soil structure index

c: Soil permeability

IV.2.4.Rainfall Erosivity Mapping

The R-factor is the representation of the erosivity of rain or erosive aggressiveness of rain, being the product of two characteristics of a rain shower: kinetic energy and maximum intensity in 30 minutes. This factor is defined by the equation of Wischmeier [32]:

$$\mathbf{R = E \times I_{30}}$$

E: kinetic energy of the rainfall

$\mathbf{I_{30}}$: maximum rainfall intensity in 30 minutes expressed in mm/hour.

For our case, and for the calculation of the rainfall erosivity factor, we based ourselves on the formula of Arnoldus (1977), because he only takes into consideration the average monthly and annual rainfall available, his formula is defined by the following equation:

$$\mathbf{Log\ R = 1.744 \times Log\left(\frac{Pi^2}{P}\right) + 1.299}$$

R: the rainfall aggressiveness index in units/year

P: average annual precipitation of the observation period in (mm)

Pi: Average monthly precipitation in (mm)

IV.2.5. Topographical Factors

The topographical factor depends on both the length of the slope (L) and its inclination. The amount and speed of runoff increases with the continuous accumulation on the slope and its steepness (S) (Ben Hichou et al., 2023c). The LS factor is defined by Wischmeier as follows:

$$\mathbf{LS} = \left(\frac{\mathbf{X}}{\mathbf{22.1}}\right)^{\mathbf{m}} \times (\mathbf{0.065} + \mathbf{0.045\ S} + \mathbf{0.0065\ s^2})$$

X: the length of the slope (m)

s: the slope (%)

m: slope coefficient

The values of X and s are calculated from the DTM. The calculation of the X-value, the flow accumulation was derived from the DTM after performing the flow direction and filling processes in the GIS.

X = (flow accumulation × resolution)

The m coefficient was determined according to the slope ranges given by Wischmeier. It has two values (0.4 or 0.5), respectively for slopes over 5% or between 3% and 5%.

IV.2.6. Anthropogenic Erosion Control Practices

Factor P describes the soil conserving human activities that are practiced in a catchment to control soil water erosion. It generally varies from 0 to 1 depending on the practice adopted. However, given the absence of anti-erosion practices in the study catchment, this factor is taken as a unit value of 1

IV.2.7. Sediment Supply and Model Validation

This step consists of determining the portion of the eroded material that was able to reach the reservoir. The proportion of sediment transported to the reservoir (net erosion) by the rate of erosion-sensitive soils (gross erosion) constitutes the sediment delivery ratio (SDR).

$$\mathbf{SDR} = \frac{\mathbf{net\ erosion}}{\mathbf{gross\ erosion}}$$

The gross erosion calculated by the RUSLE equation does not consider the sediment load transported by surface runoff. The estimation of net erosion at the watershed outlet was done by calculating the most used sediment delivery ratio for the conversion of gross erosion of a watershed into net erosion at its outlet (Ben Hichou et al., 2023c). The model of Williams used to determine this ratio is expressed as follows

$$\mathbf{SDR} = \mathbf{1.366} \times \mathbf{10^{-11}} [\mathbf{DA}]^{-\mathbf{0,0998}} \left[\frac{\mathbf{R}}{\mathbf{L}}\right]^{\mathbf{0,3629}} [\mathbf{CN}]^{\mathbf{5,444}}$$

SDR: Sediment delivery ratio (ratio);

DA: Drainage area (km^2);

L: Longest River (km);

R: Average gradient (m);

CN: SCS runoff curve number.

The validation of the result obtained was carried out by comparing the simulated rate of sediments trapped at the Hassan Ad-Dakhil dam with their rate measured by the Guir Ziz Rheris Hydraulic Basin Agency (ABHGZR).

IV.2.8.Geoprocessing

The geoprocessing tools in GIS has been adopted as a powerful tool to implement the RUSLE method for mapping crucial factors related to soil erosion (figures IV.3, IV.4, IV.5, IV.6 et IV.7). The system enables the creation of a land cover map (Factor C), a digitized soil map extracted from the soil map of Morocco, a map indicating rainfall erosivity (Factor R), and a topographic factor map (Factor LS). By integrating these mapped factors, GIS facilitates the assessment of soil erosion risk and provides valuable insights for effective erosion control and land management strategies (Ben Hichou et al., 2023c).

In this study, we found the absence of anti-erosion interventions in the catchment area, we therefore assigned the value 1 to the general average for the P factor, over the whole area.

Bare soil occupies 70% of the surface area of the studied catchment, and its other parts have low vegetation cover. This is due to the low to very low rainfall, with a long dry season and frequent droughts.

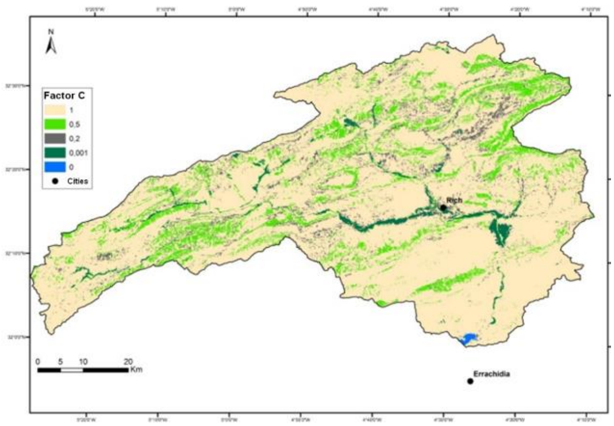

Figure IV. 3: Map of factor Factor C (Land cover)(Ben Hichou et al., 2023c)

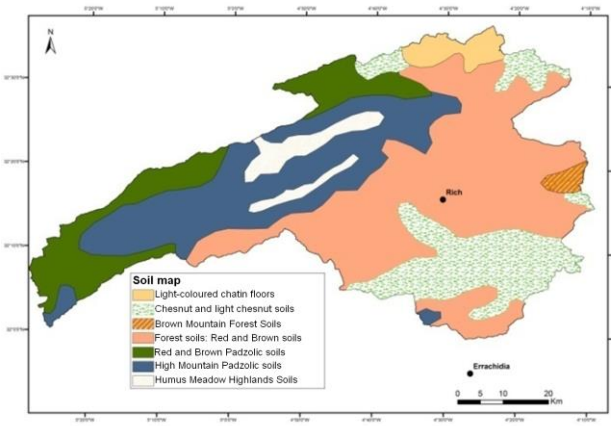

Figure IV. 4: Soil map (extracted from the soil map of Morocco, redigitalized) (Ben Hichou et al., 2023c)

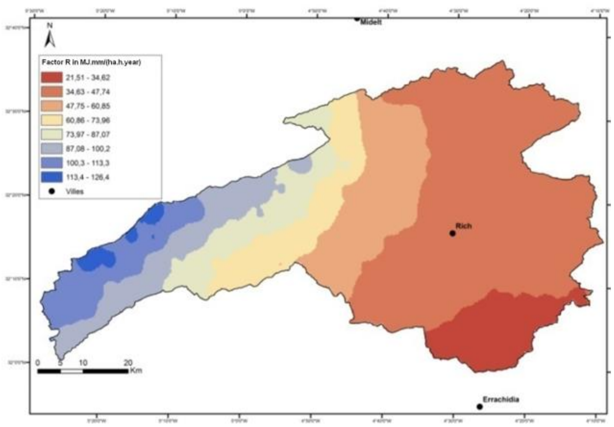

Figure IV. 5: Map of rainfall erosivity (R) (Ben Hichou et al., 2023c)

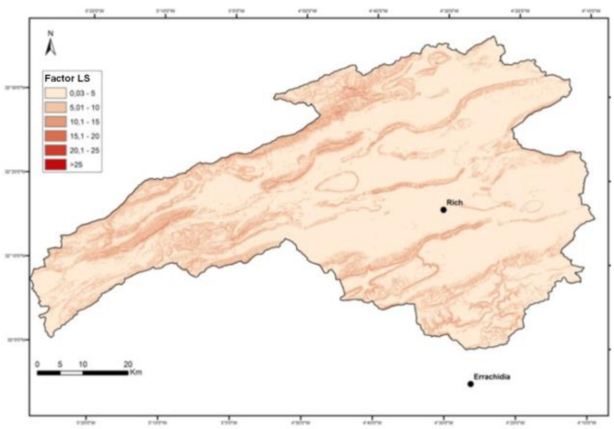

Figure IV. 6: Map of topographic factor (LS) (Ben Hichou et al., 2023c)

The land cover map (Figure IV.3) shows the distribution of C-factor values ranging from 0 to 1 with 87.8% of the catchment area having very low vegetation cover. Each value corresponds to a type of land cover (Table *IV*.1).

Table IV. 1: Land Cover C values

Land cover type	C Index
Water	0
Dense vegetation	0.001
Building	0.2
Vegetation cover	0.5
Bare soil	1

Soil erodibility is directly related to several factors: soil texture and structure, permeability, and organic matter. It is low for stable soils in the middle of the catchment and high for fragile soils in the east and south of the catchment (Ben Hichou et al., 2023c).

IV.3.Results and Discussion

The reservoir studied receives most of the rainfall that feeds the Ziz basin (Figure IV.7). As essential agent of soil erosion, the floods generated by these precipitations bring sediments that renew the riverbank soils upstream of the dam, and a great part of these sediments remains accumulated in the reservoir. Downstream of the dam, the lower branches of the Ziz basin, the water and sediment volumes were highly reduced since the dam was constructed, but still great during exceptional great floods. The area receives relatively low precipitations throughout the year, with a maximum in the western mountainous area, and most of the rainfall in concentrated in the winter months (November-February). The average annual precipitation in the studied catchment is around 220mm, with some areas receiving as little as 150mm per year near the outlet of the watershed. Most of the precipitation falls in the form of sporadic showers, with occasional thunderstorms (Ben Hichou et al., 2023c).

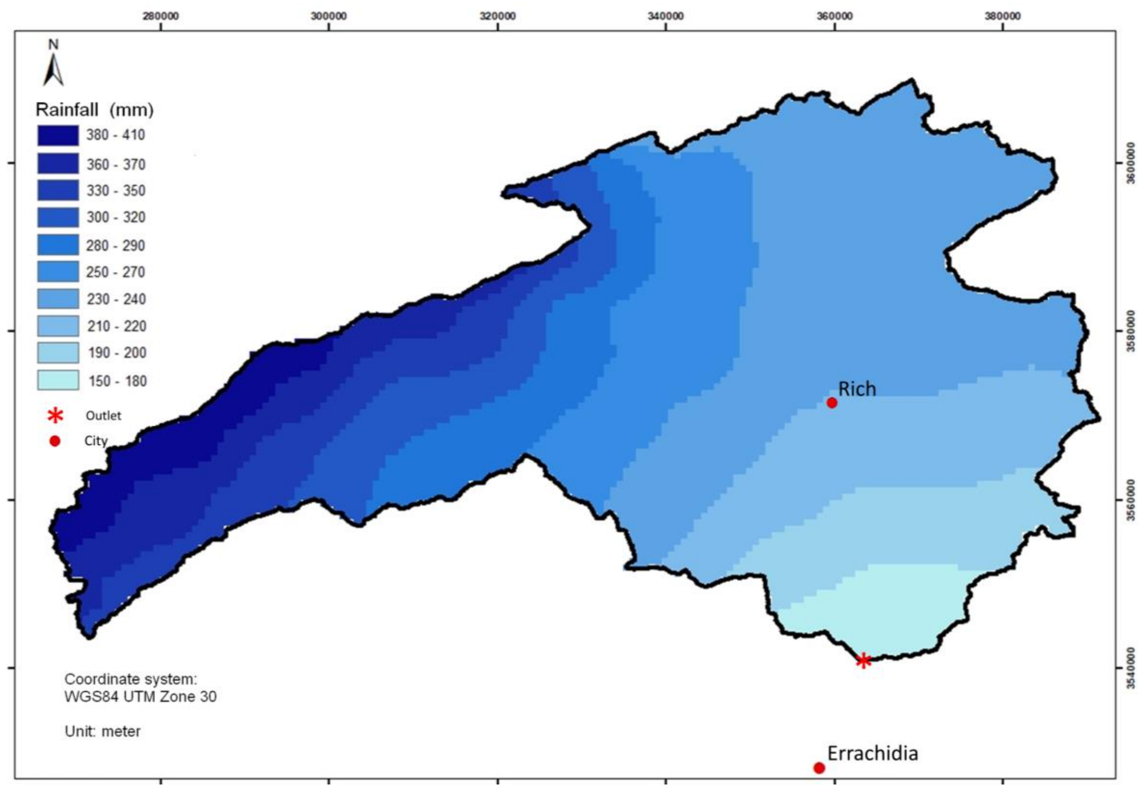

Figure IV. 7: Annual average 1981-2021 of the precipitations in the Ziz basin upstream to Hassan Ad-Dakhil dam (based on data extracted from Chirps V2) (Ben Hichou et al., 2023c)

The study area consists mainly of the following land cover elements:

- Bare silty and sandy soils, sometimes gravelly;
- Vegetation and cultivated areas corresponding to the irrigated plots on either side of the Oued Ziz and its tributaries;

- Built-up area corresponding to the centre of Rich and its outlying districts;
- Water at the level of the rivers and the dam.

According to the results obtained, we note that the average rate of soils sensitive to water erosion is 4.82 tn/ha/year, which amounts to 2117257.3 tn/year for the entire catchment area (Figures IV.8 and table IV.2).

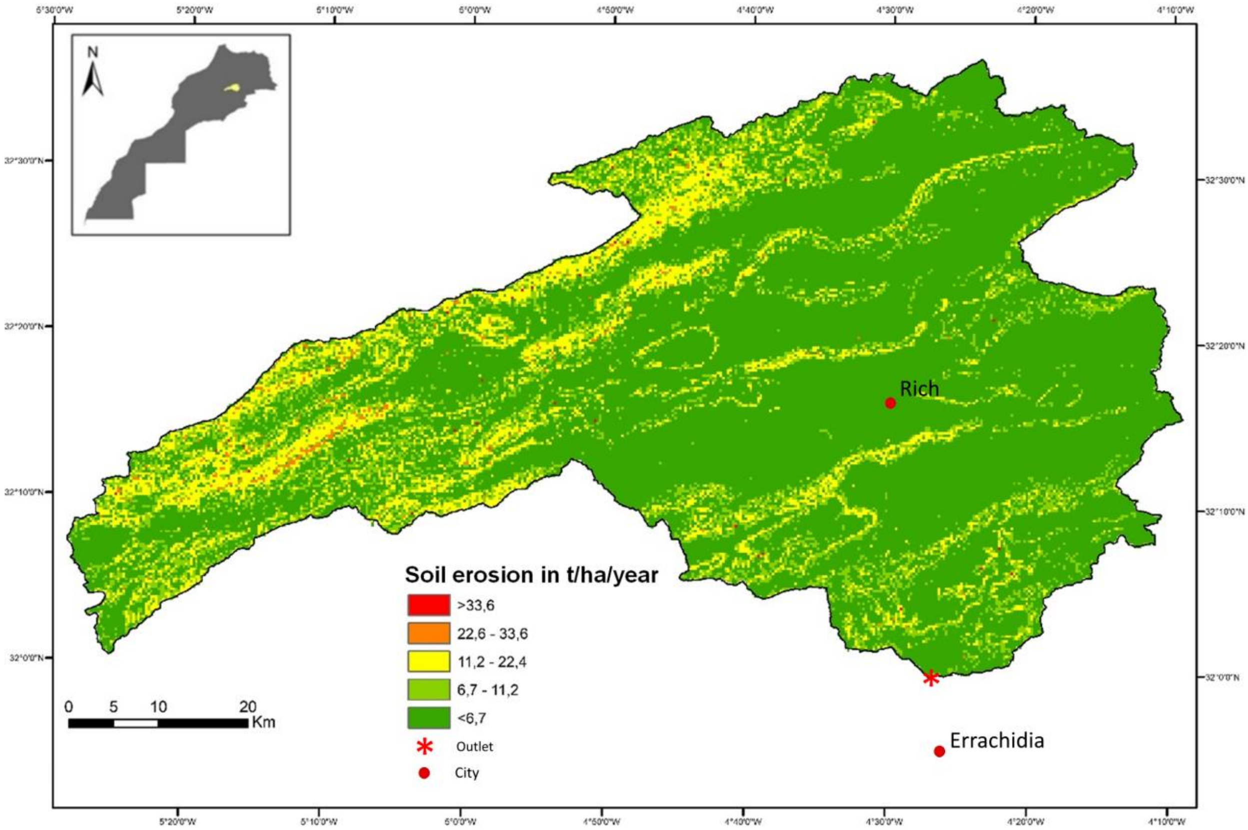

Figure IV. 8: Map of soil sensitivity to water erosion (Ben Hichou et al., 2023c)

Table IV. 2: Statistics of soils sensitive to water erosion in the Hassan Ad-Dakhil Dam catchment area

Soil loss rate (T/Ha/Year)	Surface in Ha	Pourcentage
< 6.7	328148	74.70%
6.70 – 11.20	56584	12.88%
11.2 – 22.40	52056	11.85%
22.40 – 33.60	2091	0.48%
> 33.6	386	0.09%
Average erosion rate: 4.82 t/ha/year		

The estimated rate of sediment trapped in the reservoir is calculated by multiplying the gross erosion value by the sediment delivery ratio value which is calculated using the equation of William.

The result of this estimation was compared with the measured net erosion (Table IV.3).

Table IV. 3: Estimated and measured net erosion values at Hassan Ad-Dakhil Dam

Estimated net erosion (m^3/year)	**1440915**
Measured net erosion (m^3/year)	1446808
Similarity ratio Estimated/measured	0.996

We meticulously validated the model we employed to estimate net soil erosion by comparing our estimation results with on-site measurements from the ABHGZR. This validation process revealed a staggering 99.6% similarity between the two sets of values, highlighting an impressive level of alignment. According to our model's calculations, the yearly surface runoff in the studied catchment contributes to the transport of approximately 1,440,915.00 m^3 of soil to the reservoir. By adopting this methodology, we've managed to offer a comprehensive evaluation of soil erosion and sedimentation mechanisms (Ben Hichou et al., 2023c).

The estimations we derived are not only reliable but also notably accurate, particularly in gauging sediment delivery rates. These findings hold significant implications for forecasting sedimentation rates and formulating tailored strategies for sediment management within the dam's vicinity. These findings contribute to the assessment of the operational longevity of the dam in the absence of dredging. Consequently, our integrated methodology emerges as a valuable instrument for the concurrent preservation of both the dam's operational efficiency and the ecological equilibrium of its surrounding environment.

IV.4. Conclusion

The use of RUSLE approach and Williams' model, in conjunction with GIS and Remote Sensing technology, enabled a full study of soil erosion and sedimentation processes in the pilot area, which is the Hassan Ad-Dakhil Dam catchment area. The study projected an annual sediment delivery rate of 2,117,257.3 tonnes and a volume of 1,440,915.00 m^3 of soil being drained into the reservoir each year by assessing several characteristics such as land cover, soil erodibility, and rainfall. The validation of the model used to estimate net erosion revealed a significant degree of consistency with in-situ observations, indicating the approach's dependability and accuracy. The obtained results can be used to anticipate sedimentation rates and establish appropriate sediment management measures for the dam and surrounding area.

The research's methodology has the potential to make a significant contribution to ecological preservation and sustainability by offering a solid framework for assessing and mitigating soil erosion and sedimentation issues in dam catchment areas and beyond.

Chapter V: Incorporating Sentinel 2 Data into a GIS System for MEDALUS Model-Based Mapping of Degradation-Prone Areas

V.1. Introduction

In Morocco, soil degradation is a pressing national concern, posing a significant risk to the country's natural resources. The SMBA basin has been identified as one of the basins most vulnerable to soil degradation under the National Watershed Management Plan (*Plan National d'Aménagement des Bassins Versants*).

Erosion is a central factor contributing to this degradation. When the soil loses its ability to absorb rainfall, excess water runs off its surface, carrying away soil particles and creating gullies and ravines. Human activities such as overgrazing, intensified agriculture, deforestation, and urbanization further exacerbate soil degradation.

The Erosion Sensitivity Index (ESI) draws inspiration from the methodology developed by experts in the MEDALUS (Mediterranean Desertification and Land Use) project. This index leverages remote sensing and Geographic Information System tools. Some other models, often referred to as hybrid or semi-empirical models, combine empirical and physical measurements collected in the field, like the Soil and Water Assessment Tools (SWAT) developed by Arnold and his colleagues in 1996.

Given the diverse climate conditions across Morocco, detecting degraded areas and monitoring the evolution of erosive processes to quantify and map areas at risk of degradation are essential. This requires integrating data related to all elements influencing or mitigating this phenomenon, including climate, soil, and terrain characteristics.

The sub-basin of Sidi Mohamed Ben Abdellah, located in the western part of northern Morocco and bounded to the north by the Sebou watershed and to the south by the watershed of Oued Oum-Rbia, faces the Atlantic Ocean to the west. Covering an area of approximately 10,000 km^2, this region is highly susceptible to soil degradation, particularly due to recent climate changes and the pressures of urbanization and deforestation resulting from demographic growth.

In these dry and arid lands, water erosion is the primary cause of severe degradation. To mitigate its consequences, erosion control methods are imperative.

Numerous studies have been conducted in the SMBA basin, which is the focus of our research. These studies encompass various disciplines, including geomorphology (Beaudet, 1986), pedology (Ghanem, 1981), siltation of dams (Lahlou, 1986), and sediment analysis (Ben Mohammadi, 1991), as well as soil loss mapping through the application of the USEL model (Wischmeier and Smith, 1978); (Ouakil et al., 2021), among others. It is crucial to position our study within the context of these diverse research endeavors on soil loss within this watershed. Indeed, understanding soil loss in watersheds demands a multidisciplinary approach, involving geology, pedology, hydrology, socio-economics, climate, and more.

Our study area applies the MEDALUS model, utilizing a comprehensive dataset representing all the contributing factors to this phenomenon. This dataset includes a land use map generated from a mosaic of satellite images (SENTINEL2) covering the entire study area, records from rainfall stations, a soil map, and a slope map derived from the Digital Terrain Model.

V.2. Study Area

Situated in the central northwestern region of Morocco, the study area encompasses the sub-basin of Sidi Mohamed Ben Abdellah, covering an extensive area of approximately 10,000 km², a significant portion of the country's total landmass. This region is positioned in the northwestern quadrant of Morocco, as illustrated in Figure V.1. The northern boundary of our basin is defined by the Sebou watershed, while the southern boundary is delineated by the Oum-Rbia watershed, with its western border extending to the Atlantic Ocean.

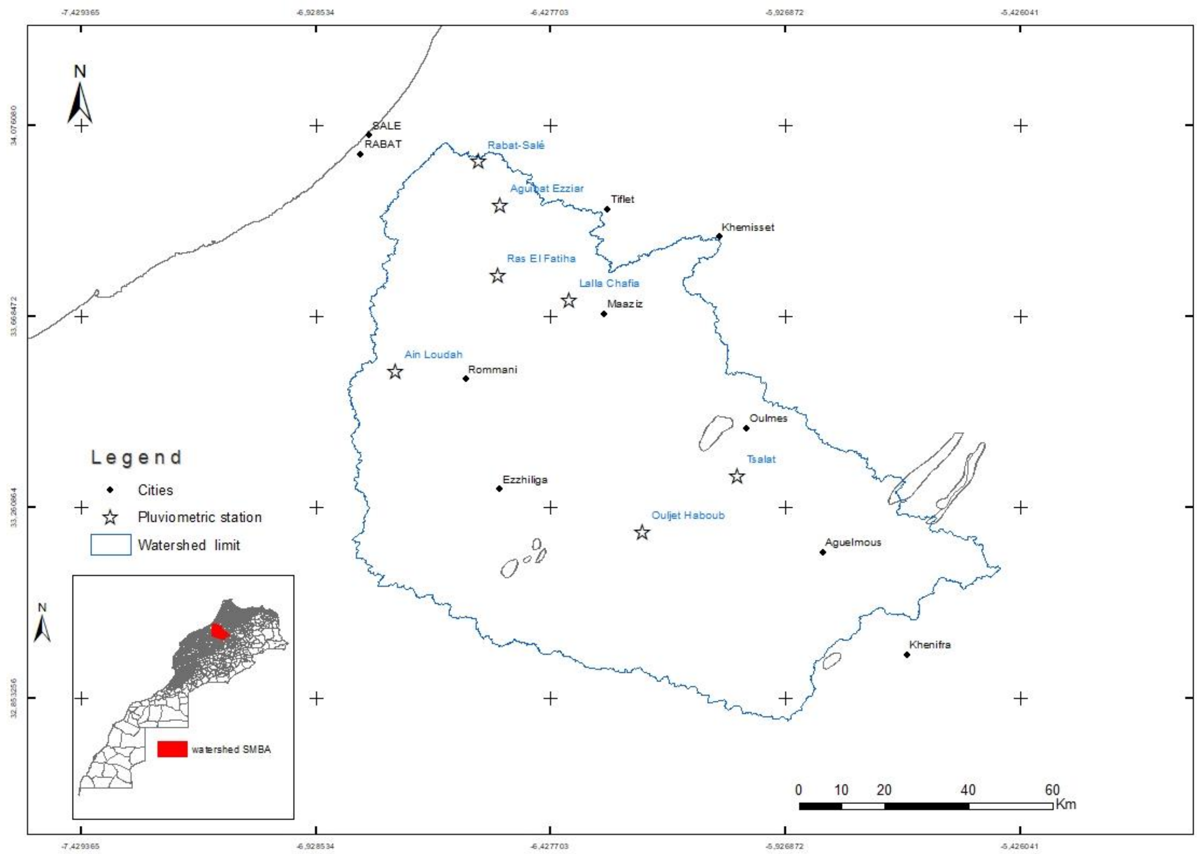

Figure V. 1: Geographic location map

V.2.1. Climate in the SMBA Basin

The climate in the SMBA watershed is characterized as semi-arid, predominantly distinguished by prolonged dry periods and occasional, limited rainfall during the wet season. Climate patterns within the basin are shaped by various factors, including altitude—particularly noteworthy in the northern region where altitudes can reach up to 1,630 meters (as shown in figure V.2)—and the basin's exposure to the Atlantic Ocean. This exposure contributes to both moisture influx and temperature moderation.

Average annual temperatures within the basin typically range between 15°C and 18°C along the coastline, while mountainous areas experience slightly cooler temperatures ranging from 15°C to 17°C.

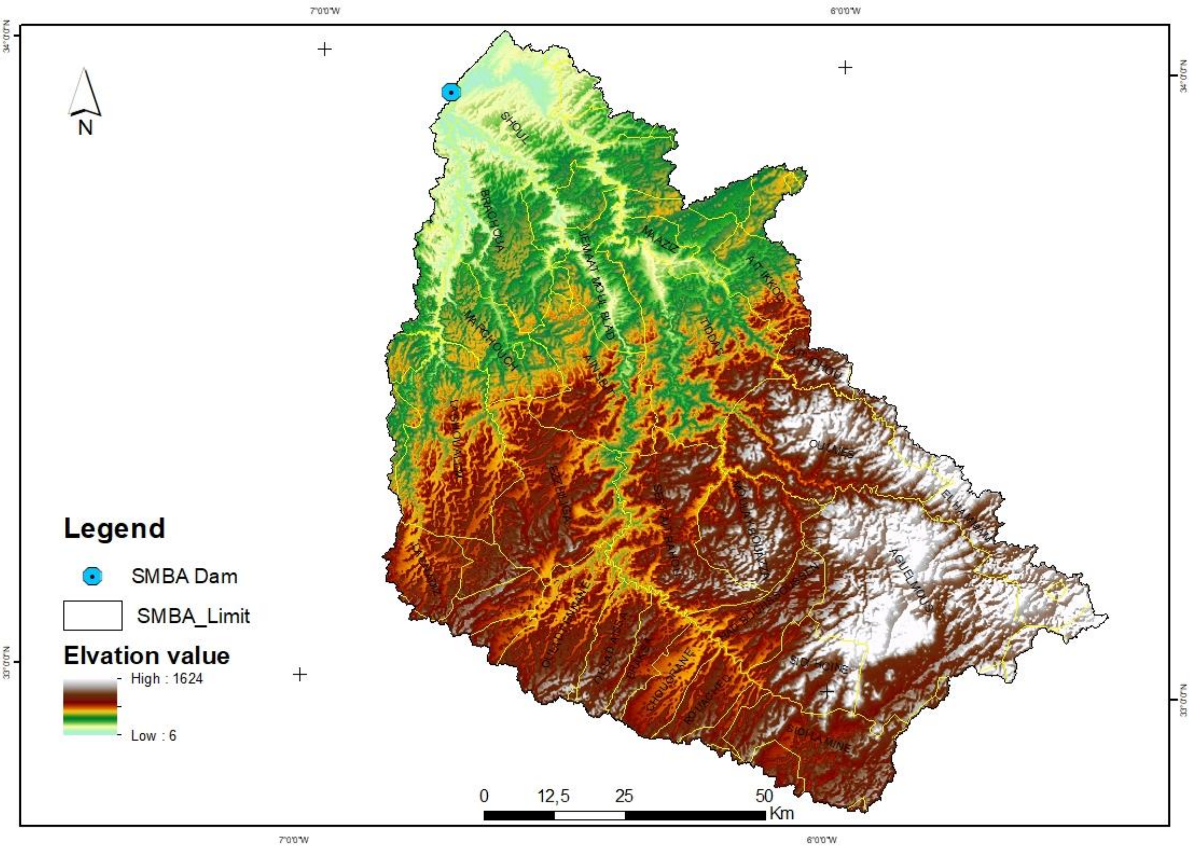

Figure V. 2: Spatial distribution of elevations in the watershed

During the summer season, temperatures can soar to levels exceeding 45°C, primarily attributed to the Chergui winds, a hot wind originating from the Sahara (Table V.1).

Table V. 1: Average monthly annual precipitation for the period 1980-2009(SIGMED,2014)

Stations	Sept	Oct	Nov	Dec	Jan	Feb	Mar	Apr	May	Jun	Jul	Aug	Annual total
Sidi Jabbour	12,4	29	45,2	48,1	45,4	41,9	36,5	30,3	17,5	6,9	0,9	0,8	314,9
Aguibat Ezziar	9,5	34,8	68,7	76,1	67,8	56,6	46,6	42,7	22,4	6,9	0,5	0,9	433,5
Ras El Fatiha	10,3	31,1	60,5	69,9	59,1	53	45,3	37,4	16,1	5,3	0,8	1,4	390,2
Lalla Chafia	12,1	30,4	49,2	52,8	51	45,4	40,9	40,1	17,6	5,2	0,3	0,6	345,6
Ouljet Haboub	11,9	22	33,3	40,5	30,6	37,6	33,6	28,4	17,6	9,5	3,5	3,9	272,4
Ain Loudah	11	28,7	54,3	56,9	54,3	50,1	38	33,2	16,6	3,9	0,9	1,2	349,1
Tsalat	16,3	34,8	62,7	77,9	67,5	64,7	55,6	42,6	27,9	11,1	5,6	4,6	471,3
Rabat-Salé	8,6	42,8	67,3	104,8	79	61,3	52	55,2	20,4	4	0,2	1,2	496,8
Max	16,3	42,8	68,7	104,8	79	54,7	55,6	55,2	27,9	11,1	5,6	4,6	526,3
Min	8,6	22	33,3	40,5	30,6	37,6	33,6	28,4	16,1	3,9	0,2	0,6	255,4
Monthly average	11,5	31,7	55,2	65,9	56,8	51,3	43,6	38,7	19,5	6,6	1,6	1,8	384,2

The basin exhibits a distinct climatic pattern, featuring a rainy season spanning from October to May, followed by a dry season from June to September with relatively modest precipitation levels. The highest amount of rainfall occurs in December, while the lowest is recorded in July.

Within the watershed, two prevailing wind patterns influence the climate:

- Winter rains are brought by winds associated with polar air masses that affect Mediterranean regions.
- The Chergui winds, on the other hand, originate from the Sahara Desert and carry dry, hot air that contributes to arid conditions along the coastal plains (as illustrated in Figure V.3).

Martonne's aridity index :

$I=P/(T+10)$

With:

P: Total annual precipitation

T: Average annual temperature

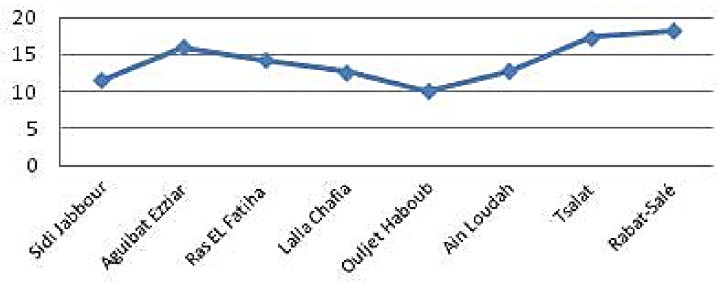

Figure V. 3: variation of the Marton index

Rainfall erosivity:

The equation used for calculating the rainfall erosivity factor is as follows:

$$\mathbf{Log\ R=1.744\times Log\ (Pi^2/P)+1.299}$$

Where:

R: the rainfall aggressiveness index in units/year

P: Average annual precipitation of the observation period in (mm)

Pi : Average monthly precipitation in (mm)

Based on Martonne's classification, the basin exhibits a semi-arid climate (as depicted in Figure V.4), with values ranging from a minimum of 10 to a maximum of 18.25, particularly observed in the Rabat-Salé regions.

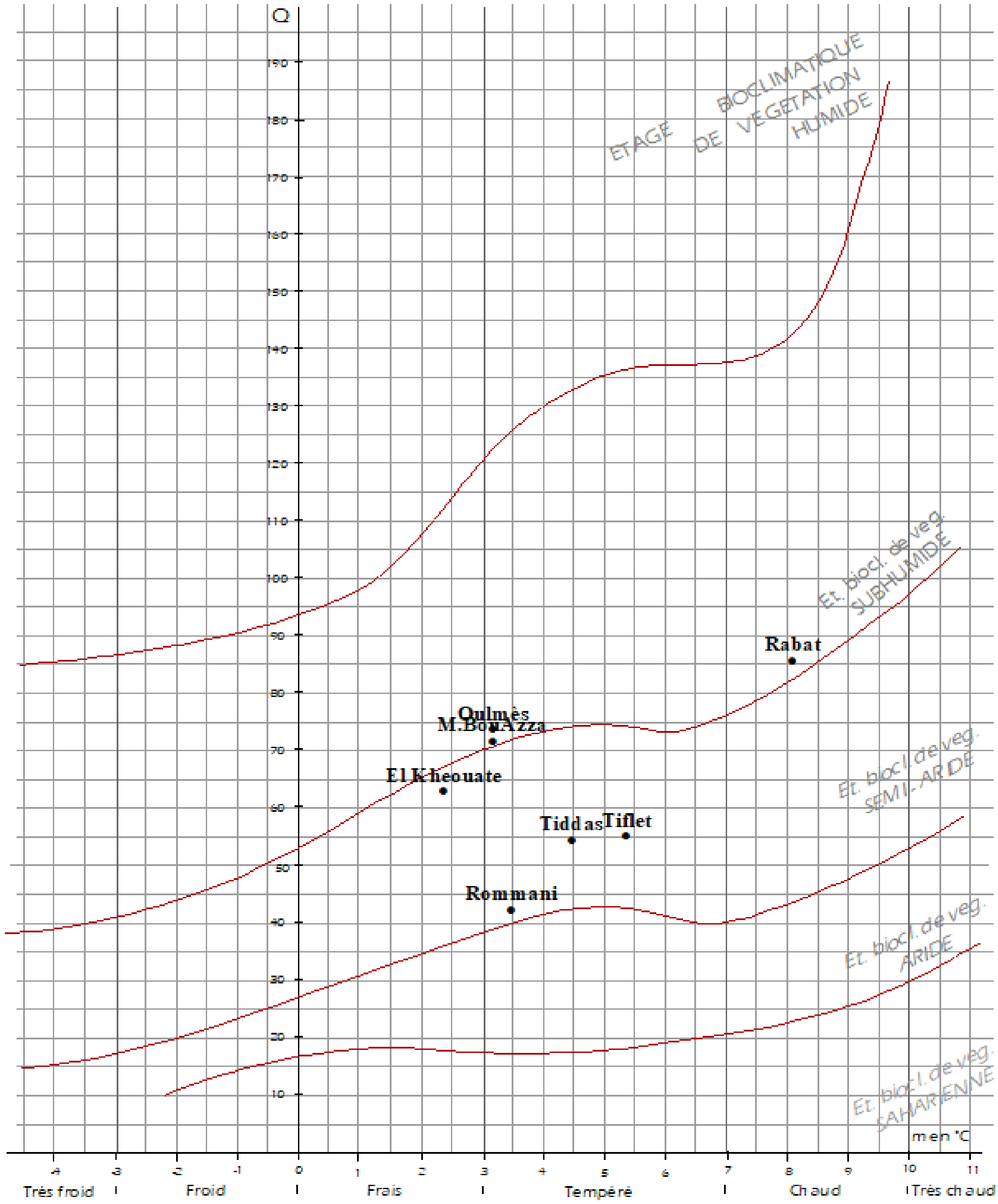

Figure V. 4: Emberger Rainfall Quotient

To enhance the precision of aridity assessment throughout the year, researchers employs a monthly aridity index calculated using the following formula:

$$I=12P/(T+10)$$

The analysis of this index at the watershed level reveals the following findings:

1. The months of June, July, and August constitute an "arid" season, with July being the most severe, recording a temperature of 24.5°C.
2. September, with an index of 2.86, is categorized as an arid month with a semi-arid inclination due to relatively higher rainfall compared to June, July, and August.
3. The remaining months exhibit lower aridity levels, primarily owing to their relatively greater precipitation.
4. December, January, and February are the least arid months, with indices ranging from 34.82 to 39.13. This distinction is attributed to the significant rains characterizing this time of the year.

To establish a meaningful connection between vegetation cover and climate, it is essential to determine the duration of the dry season. According to Gaussen's criteria, any month in which the total rainfall (P in mm) is equal to or less than twice the average monthly temperature in degrees Celsius is considered a biologically dry month (Bagnouls and Gaussen, 1953) (Figure V.5).

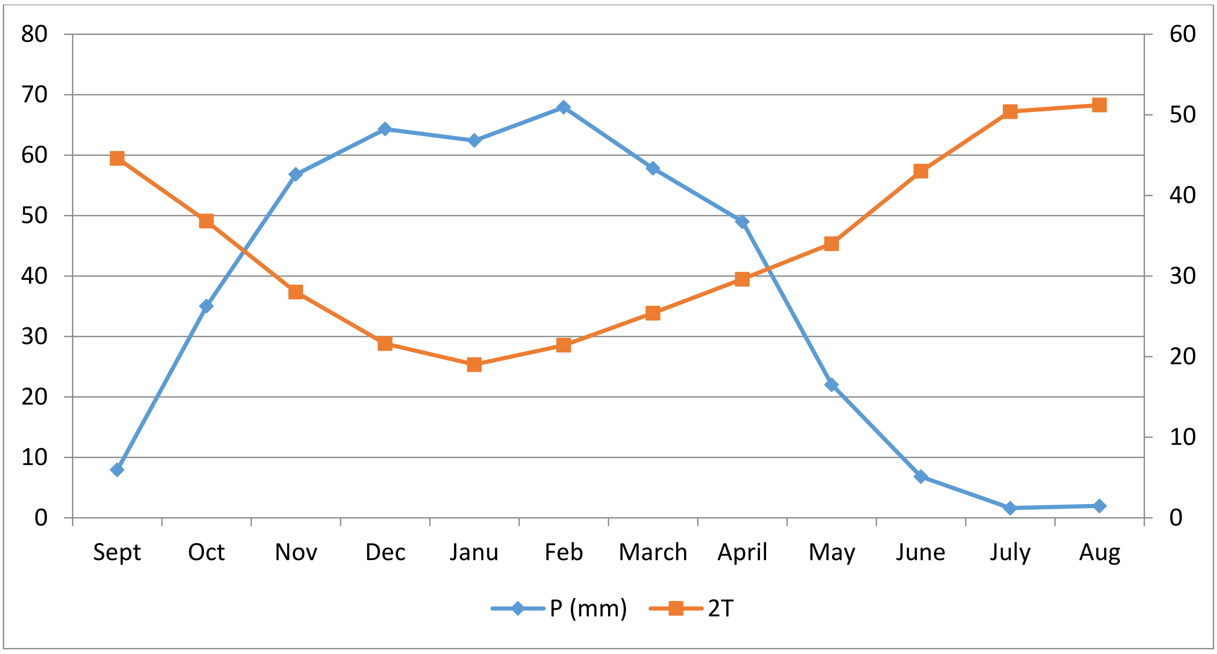

Figure V. 5: Ombrothermic Diagram

V.2.2. Geology of the Study Area

In the latter case, the primary geological considerations revolve around the lithology and tectonic makeup of the underlying bedrock. The Bouregreg watershed, as a whole, is situated within the Moroccan central massif, which stands out as the northernmost and most significant of the Hercynian basement bulges in Atlantic Morocco. The SMBA watershed encompasses the entirety of the Moroccan Central Massif, accounting for a substantial 90% of its geological structure. As we move from the upstream to the downstream sections of the basin, as detailed in Table V.2 (Ben Mohammadi, 1991) and illustrated in Figure V.6, we can distinguish the following geological features:

- The Kasba Tadla-Azrou anticlinorium, constituting the upper part of the Bouregreg watershed, is, in essence, a complex amalgamation of faulted anticlines of varying magnitudes. Here, rocks ranging from the Precambrian to the Devonian eras are exposed, interspersed with discordant and synclinal depressions from the Carboniferous period (Termier, 1936; Bouabdelli, 1989). The central-eastern part of this intricate geological setting is overlaid by Permian continental strata from Khenifra through angular unconformity.
- The synclinorium of Fourhal, extending from the north of Boujad to the Causse d'Agourai, exposes sandstones and shales of Visio, Namur, and Westphalia to erosion (Tahiri, 1991). On its eastern flank, there's a granitic intrusion at Ment.
- The Khouribga-Oulmès anticlinorium, located at the core of the Bouregreg watershed, is oriented in a NE-SW direction. It features primarily schistose and quartzite layers from the Ordovician and Silurian periods. Some detrital and/or carbonate scarps from the Carboniferous era rest upon these layers (Piqué, 1979; Chakiri, 1991; Tahiri, 1991). Several granitoid massifs are also present in this region, including Zaër, Oulmès, and Moulay Bou Azza.
- The synclinorium of Khémisset-Rommani is a substantial synclinal mass primarily composed of schistosandstone layers from the Lower Carboniferous (Tournaisian and Viséen) and clay and basalt from the Triassic. At times, anticlines within this region expose Devonian formations (Chakiri, 1991; Zahraoui, 1991).
- The Rabat-Tiflet anticlinorium is a remarkable geological structure oriented in an East-West direction. It reveals cataclastic granite and Caledonian metamorphic rocks, emerging through fractures and geological disruptions (Piqué, 1979; El Hassani, 1990).

Table V. 2: Results of the planimetry of the lithological formations of the Bouregreg watershed

Lithological formations	Area in Km²	Percentage
Schist	7066	72,1
Quartzite	942	9 ,6
Sandstone and Limestone	502	5,1
Granites	470	4,8
Clays and basalts	413	4,3
Marls	407	4,1

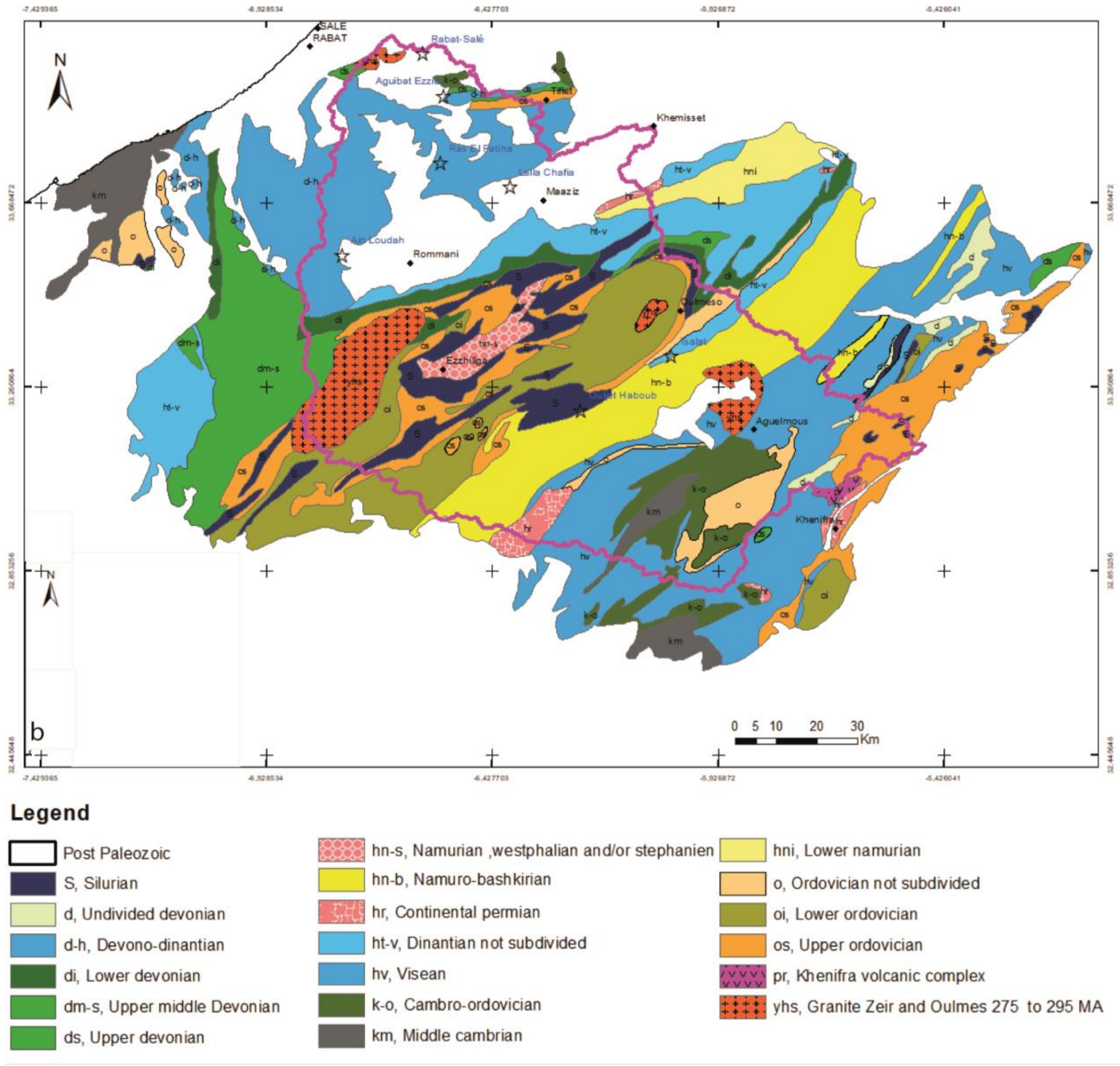

Figure V. 6: Geologic Map

V.3. Methodology

Our aim is to employ the MEDALUS model to map areas at risk of degradation. To achieve this goal, we utilize a dataset to enrich our database and prepare the necessary parameters (indicators) for model deployment.

Assessing and mitigating erosion risks entails analyzing and integrating various factors that contribute to erosive processes, including terrain topography, soil erodibility, and land use patterns.

We sourced Sentinel 2 acquisitions, accessible through the Glovis database (https://glovis.usgs.gov), as the foundational data for mapping land cover in our study area. To accomplish this, we applied a classification method based on the imagery's Red-

Green-Blue-Infrared (R-G-B-IR) mode, encompassing a combination of four spectral bands.

For the morphological assessment of our region, the downloadable Digital Terrain Model Raster, available on the internet, serves as the foundational dataset. This model features a 30-meter resolution.

Utilizing Geographic Information Systems (GIS), we can integrate diverse factors and apply mathematical equations to the data values, ultimately generating a risk map that reflects sensitivity to erosion.

In our data processing and analysis, we harnessed various tools and software applications (Table V.3).

Table V. 3: Data and materiel used

Data	Software
- Satellite Image Sentinel 2 (RVBPIR)	- Geomatica 2018
- Precipitation data	- Erdas Emagines 2015
- Bioclimatic static recording	- Arc Gis 10.8
- Geological map	
- Soil map	

The MEDALUS method used in the framework of the DISMED project (2003) for the purpose of producing a desertification sensitivity map for the Mediterranean countries, is based on the integration of four factors (soil, vegetation, climate, land use) (figure V.7).

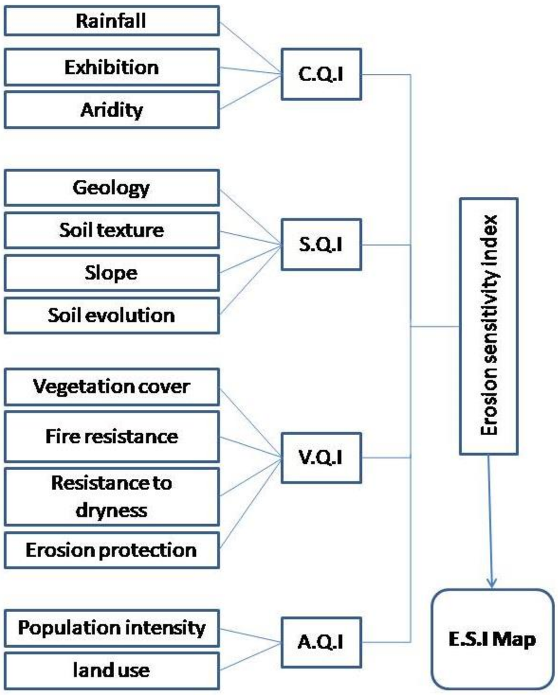

Figure V. 7: Methodology of application of the MEDALUS model

The choice of the MEDALUS method was based mainly on the amount of data required and the simplicity of implementation, it is a reasonable method both qualitative and quantitative.

ISE =(IQS * IQV * IQC * IQA)

With:

ESI: Erosion sensitivity index

SQI: Soil Quality Index

IQC: Climate Quality Index

AQI: Development Quality Index

V.4. Result and Discussion

V.4.1. The Climate Quality Index (CQI)

Climatic conditions wield a profound influence on the acceleration of erosive processes, underscoring their pivotal role in shaping the landscape. This influence is further underscored by the vital role that the quality of the climate plays in this context. The quality of climate is evaluated by scrutinizing several key parameters that directly impact the availability of water resources. These crucial parameters encompass the amount of precipitation, the degree of exposure to climatic elements, and the prevailing aridity levels within a given region.

Within this multifaceted evaluation, the interplay of these three key parameters is instrumental in determining the overall quality of the climate. It is through a complex and comprehensive process that this quality index for the climate is derived. This process involves the integration of data from three distinct layers of information: exposure (EXP), total precipitation (PP), and the aridity index (IA).

$$\mathbf{IQC} = (\mathbf{EXP} \times \mathbf{PP} \times \mathbf{IA})^{1/3}$$

This comprehensive assessment involves the examination of three critical layers, each delving into key aspects of a region's climatic and environmental conditions. The first layer, known as the exposure layer, is dedicated to gauging a region's susceptibility to various climatic elements and environmental factors. It seeks to uncover vulnerabilities that may exist and their implications for the area.

Moving to the second layer, we encounter the total precipitation data. This layer focuses on the accumulation of rainfall over time in a given region. By scrutinizing historical precipitation records, it sheds light on the availability of water resources, a critical factor in understanding a region's climate dynamics.

The third and final layer in this assessment is the aridity index, which serves as a vital component in the evaluation. This index offers valuable insights into the aridity levels of the region, indicating its capacity to retain moisture. It provides critical information about the region's dryness and its ability to support vegetation and ecosystems.

When researchers and scientists diligently analyze and interconnect these three layers of data, they gain a holistic comprehension of the climate quality within a specific region. This profound understanding equips them with the knowledge needed to identify and address the risks associated with erosive processes, which have the potential to profoundly impact both the environment and the surrounding ecosystems.

To create the exposure map, we source data from the Digital Terrain Model and rainfall records from local weather stations. As for the aridity assessment, we employ the Global Aridity Index and potential evapotranspiration data, both of which are modeled using information accessible through the WorldClim Global Climate Data platform and https://cgiarcsi.community. This choice is underpinned by two key reasons: firstly, the endorsement of this index by the United Nations, affirming its universal applicability, and secondly, its user-friendliness, making it a practical choice for our analysis.

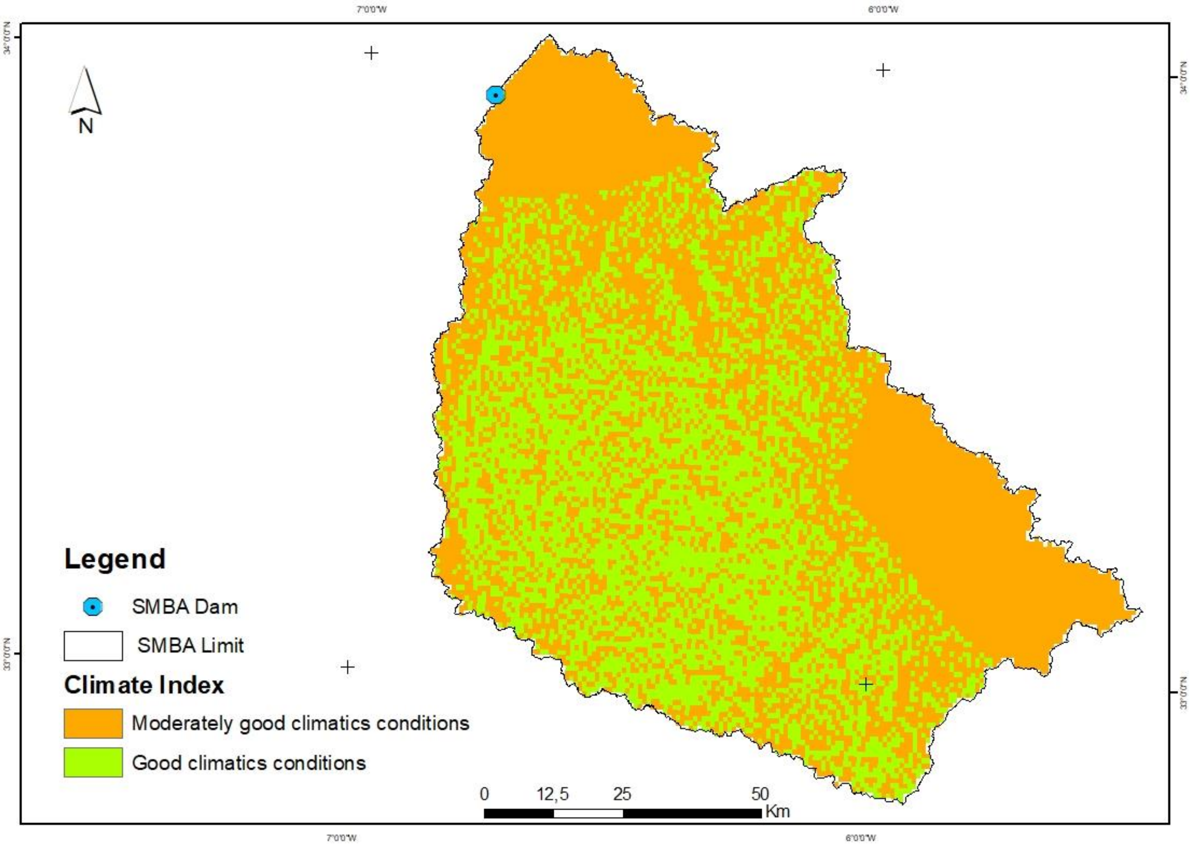

Figure V. 8: Climate Quality Map

It's worth mentioning that approximately 30% of our zone exhibits favorable climatic conditions, while the remaining 70% experiences average conditions. This outcome is indicative of the influence of three key factors: rainfall, aridity, and exposure.

V.4.2. Soil Quality Index (SQI)

The Soil Quality Index (SQI) is calculated by integrating data related to parent materials (PM), land slope (Slope), and soil horizon evolution to compensate for the absence of depth (ES) and texture (TEXT) information, as represented by the following equation:

$$\boldsymbol{IQS = (RE \times ES \times TEXT \times Pente)^{1/4}}$$

The layer intersections were instrumental in generating the Soil Quality Map (SQI). It is important to note that this index primarily reflects soil quality in relation to susceptibility to desertification rather than assessing the inherent agronomic suitability of the soil (refer to Figure V.9).

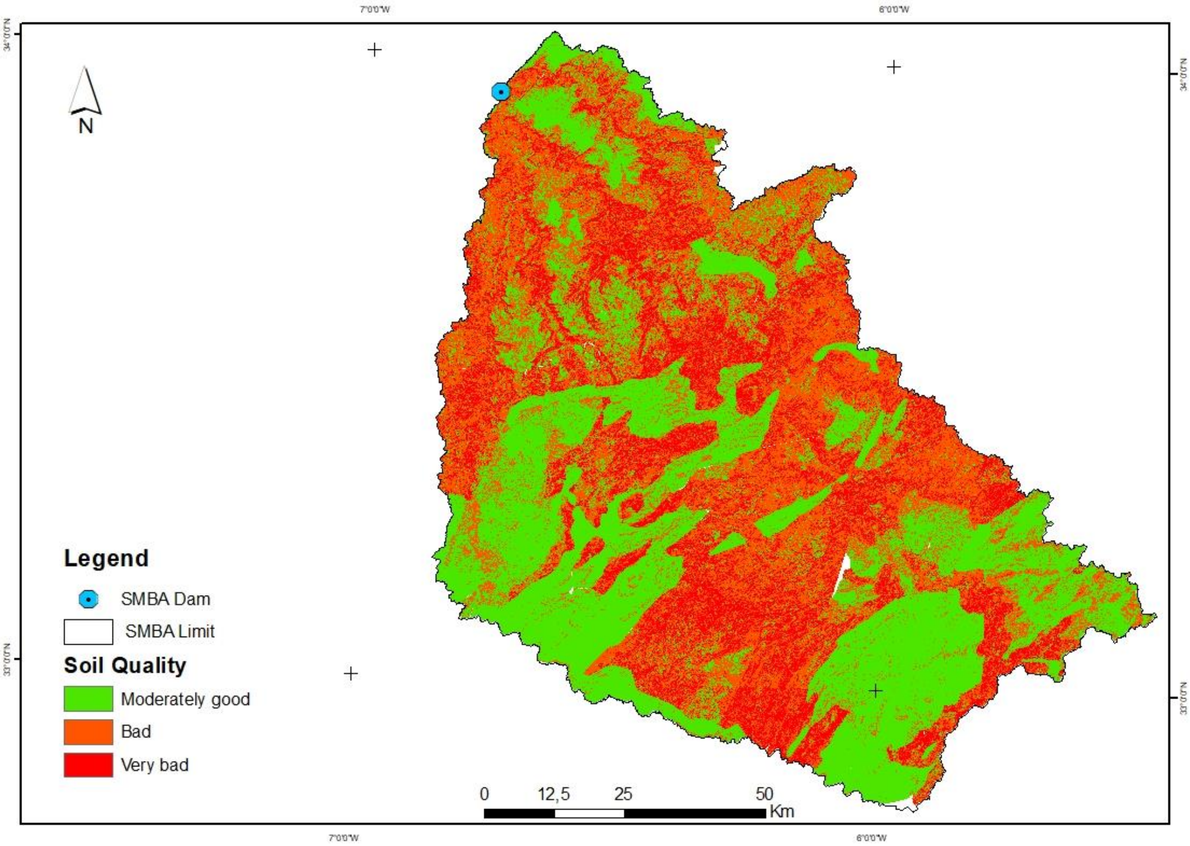

Figure V. 9: Soil Quality Map

The Soil Quality Index (SQI) results reveal that the majority of the land within the basin is characterized as having an average quality in terms of vulnerability to degradation, accounting for 60% of the area. Upstream, the soil quality is moderately good, attributed to the coherent parent materials and favorable texture for infiltration.

V.4.3. The Vegetation Quality Index (VQI)

To create the vegetation index map, we utilized data from the Sentinel 2 satellite. The S2 acquisitions were pre-processed to generate an image with four bands (R, V, B, PIR) suitable for analysis. This image was then employed to determine land cover through a supervised classification approach. This classification method relies on a dataset of known land cover points (ground truth) and utilizes the maximum likelihood statistical algorithm to identify spectral signatures, resulting in distinct land cover classes with optimal statistical separability (Figure V.10).

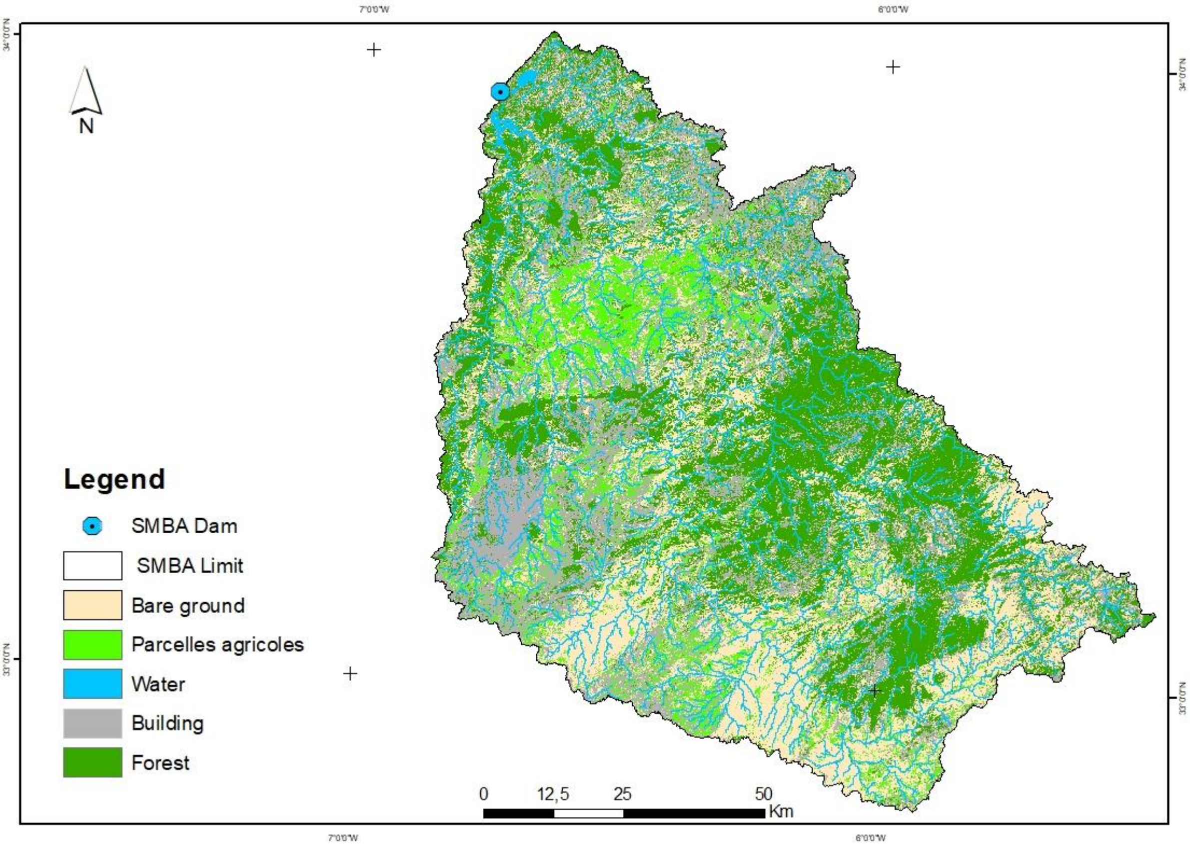

Figure V. 10: Land use map

The land use map illustrates the diverse classes found within the Bouregreg basin. It's evident that cork oak predominantly occupies the lower regions of the basin, forming both sparse and dense forests as well as varying-density matorrals. Additionally, areas dedicated to cereal cultivation can be observed. This diversity plays a pivotal role in enhancing soil stability and its resilience against degradation risks.

The development of the Vegetation Quality Index involves the amalgamation of several factors, including land use patterns, resistance to drought, protection against forest fires, and erosion control systems in agricultural zones, as depicted in Figure V.11.

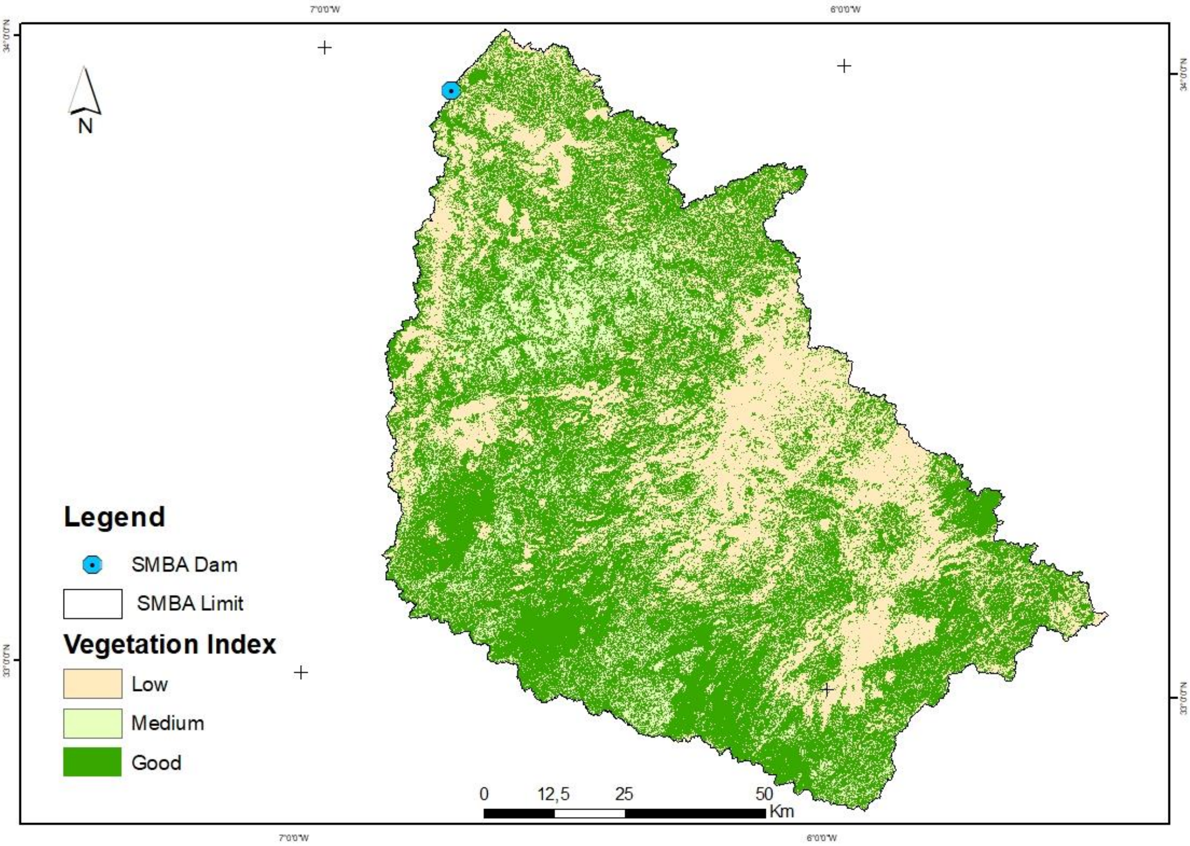

Figure V. 11: Vegetation quality index map

The map is generated through the reclassification of vegetation data derived from the land cover map, and it involves the incorporation of various parameters that influence the quality of vegetation cover in alignment with Medalus standards. The table displays the weighting of vegetation cover as per the MEDALUS standards (Table V.4).

Table V. 4: Vegetation cover weighting according to MEDALUS standards

Classe	Description	Score
1	Good	1
2	Medium	1,66
3	Low	2

V.4.4. The Management System Quality Index (MSQI)

A particularly intriguing facet of the Medalus model lies in its incorporation of socio-economic factors into the examination of land degradation. Consequently, the Land Management System Quality Index is computed based on three key parameters: the intensity of agricultural land use (IUTA), the intensity of rangeland use (IUTP), and population pressure (DP).

Table V. 5: Anthropic pressure according to the MEDALUS laws

Class	Description	Index
1	Extreme (>1000hbts/Km²)	2
2	High (1000 >D>100hbts/Km²)	1,66
3	Medium (100>D>50hbts/Km²)	1,5

The Quality Index of the Management System map is generated by the multiplicative combination of three indices: DP, IUTA, and IUTP. This outcome allows for the categorization of our area into three classes: Good, Average, and Low. It is notable that a significant portion of the land lacks effective anti-erosion management systems.

V.4.5. Creation of the Desertification Sensitivity Map (ISE)

The desertification sensitivity map is constructed by consolidating data from four indices related to soil (SQI), vegetation (VQI), climate (CQI), and management system (SAQI). This map is subsequently reclassified according to Medalus model standards, as depicted in Figure V.12. The resulting Desertification Sensitivity Index is then used to establish four sensitivity classes, as presented in the table V.6.

Table V. 6: Medalus desertification sensitivity classification standards

Class	Description	Index	Surface %
1	Stable	<1,17	25,89
2	Potential	1,17-1,23	37,72
3	Fragile	1,23-1,38	26,79
4	Critique	>1,38	9,58

V.4.6. Desertification Sensitivity Map

Based on the obtained results, it's evident that only approximately 25% of the land can be considered relatively stable, typically encompassing forested areas and lower-altitude regions. The remaining 75% is susceptible to degradation risks, as illustrated in Figure V.12. It's important to highlight that the significant migration of the population to urban areas (urbanization) and unregulated land use practices (overgrazing) have exacerbated the soil's sensitivity to desertification.

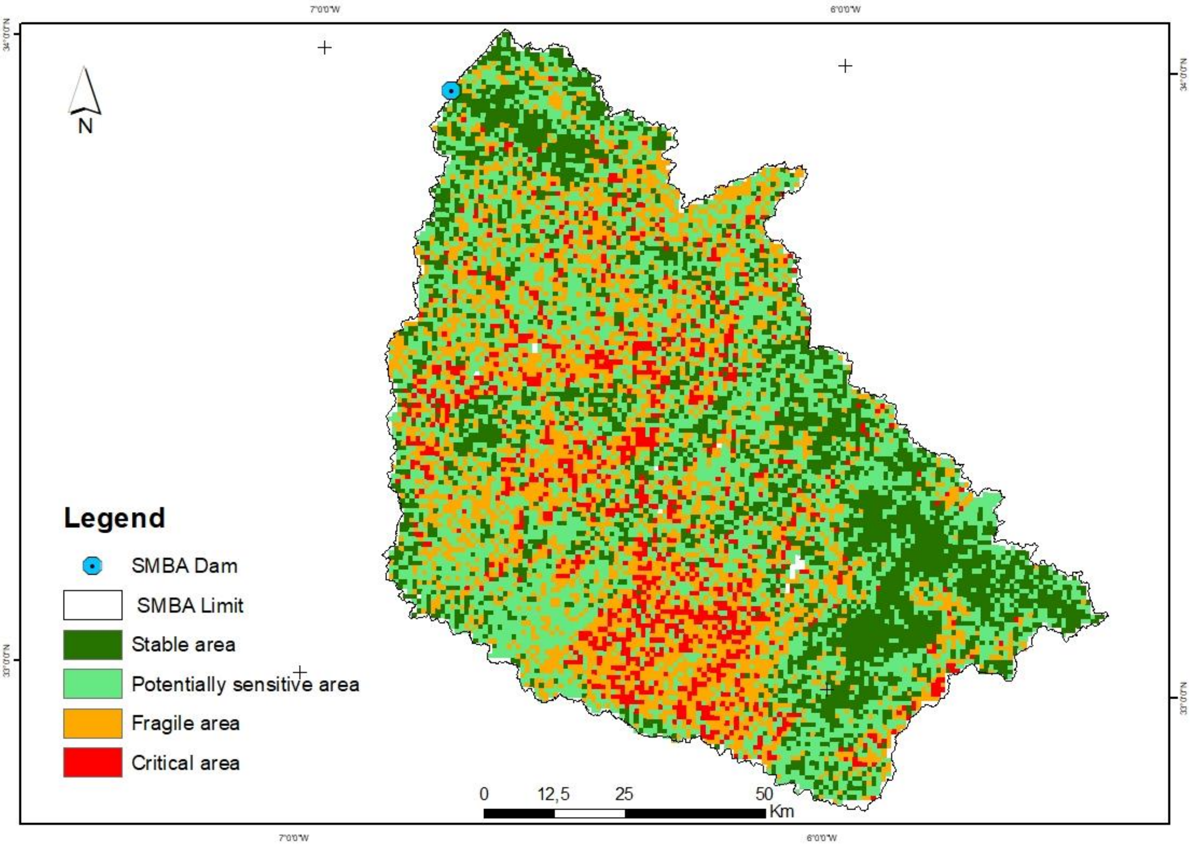

Figure V. 12: Desertification Sensitivity Map

V.5. Conclusion

The Sidi Mohemed Ben Abdellah basin is situated in the humid region of Morocco, yet it's considered a semi-arid basin where rainfall plays a pivotal role in shaping land use patterns. Unfavorable climatic conditions have contributed to the degradation of vegetation cover, thereby increasing soil erosion risk. Additionally, the significant population migration to urban areas and unregulated land utilization have further heightened the soil's susceptibility to desertification.

The land use map, derived from Sentinel 2 satellite image processing, classifies the area into five categories. Water bodies cover 10%, while vegetation occupies about 25%. Human-influenced areas are divided into agricultural zones (15%) and buildings (20%). The remaining 40% is characterized as barren land.

The geomorphology is characterized by altitudes ranging from 1600 to 6 meters from east to west, featuring fragile soils that are particularly prone to erosion. Spatial remote sensing and geographic information systems serve as essential tools for monitoring land cover changes, enabling a deeper understanding of the erosion phenomenon and facilitating the application of adaptive strategies.

The results obtained highlight a continuous increase in the proportion of degraded land. This trend is not solely attributed to climate disruptions (primarily temperature and precipitation fluctuations) but also to haphazard land use stemming from the rapid demographic growth and urban migration. Any effective adaptation strategy necessitates a multidisciplinary approach to better manage this phenomenon.

Chapter VI: Classification of Estuarine Wetlands and Watershed Characteristics Extraction using GIS Techniques: Case of coastal strip of Yemen

VI.1. Introduction

Estuaries represent semi-enclosed coastal water bodies that maintain a direct link to the open sea, characterized by the mixing of seawater and freshwater from land runoff, as initially defined by Pritchard in 1967. This definition underscores the incredible diversity of habitats found within estuaries, shaped by both marine and inland influences, rendering them ecologically, socially, and culturally rich ecosystems (Stuip et al. 2002; MEA 2005; McCartney et al. 2010; Scharin et al. 2016).

The study of estuaries has played a crucial role in advancing ecological understanding, particularly in deciphering the dynamics and threats facing these intricate ecosystems (Mitsch and Gosselink 2000; Bruland 2008; Lellis-Dibble et al. 2008; Elliott and Whitfield 2011). Unfortunately, it is disheartening to note that nearly half of the world's wetlands have experienced degradation since 1900, with many, especially estuarine ecosystems, facing irreversible losses (O'Connor and Crowe 2005; Davidson 2014; Dahl 1990; Noss et al. 1995). This degradation is exacerbated in arid regions like Yemen due to the adverse impacts of climate change, including recurring droughts (Ranjan et al. 2006; Barnard and Thuiller 2008; Erwin 2008; Elasha 2010; Crooks et al. 2011).

This situation poses a range of challenges, including water scarcity, limited economic opportunities, food insecurity, community conflicts, and a significant loss of biodiversity (Verner et al., 2013; AlMahfadi et al., 2016). Therefore, it is imperative for nations to proactively integrate wetlands, especially estuaries, into their development strategies (Parry et al. 2007; Elliott and Whitfield 2011; Tulu and Desta 2015) while gaining a comprehensive understanding of their functioning and implementing sustainable practices.

The journey toward this understanding naturally begins with the inventory and classification of wetlands (Brinson 1993; Gopal and Sah 1995; Scott and Jones 1995; Allee et al. 2000; Finlayson et al. 2002; Junk et al. 2013; Zoltai et al. 1975). However, classifying estuarine ecosystems is particularly challenging due to their intricate mosaic of habitats and ecological mechanisms (Elliott and McLusky 2002; Elliott and Whitfield 2011; Valle-Levinson 2010; Day et al. 2012) and the complexities of their management (Simpson 2002).

Yemen, home to a minimum of 451 estuaries along the Red Sea, Gulf of Aden, and Arabian Sea, is believed to host a significant share of coastal biodiversity within the Arabian Peninsula (PERSGA 2003, 2004; EPA 2004; Lavergne 2012; Al-Mahfadi and

Dakki 2020). Nonetheless, conserving this biodiversity faces substantial challenges, primarily due to the absence of scientific, technical, and legislative tools (NBSAPY 2005; EPA 2009). Given this knowledge gap, the present study aims to establish an initial classification for all of Yemen's estuaries as a foundational step in their management.

This classification primarily relies on remote sensing (RS) data, predominantly gathered through Geographic Information Systems (GIS). Most of these datasets not only pertain to the estuaries and their immediate surroundings but also encompass their respective catchment areas. With this approach, our secondary goal is to assess the effectiveness of these tools and catchment area data in the classification of estuaries. We are guided by two hypotheses: (1) in situations where acquiring on-site estuarine data is impractical, as is the case in Yemen, RS can serve as a viable alternative to field data collection (Populus et al. 1995; Ozesmi and Bauer 2002; Rebelo et al. 2009; Perennou et al. 2018), and (2) the characteristics of estuarine ecosystems are significantly influenced by their watershed features (Ladson 1999; Kondolf et al. 2003; Chessman et al. 2006; Gregory 2006; Thornton et al. 2007; Harvey et al. 2008; Day et al. 2012).

VI.2. Methodology

To establish a classification system for Yemeni estuaries, we explored two primary approaches. The first approach involves integrating these estuaries into an existing classification system that covers the Red Sea, the Gulf of Aden, and the Arabian Sea regions. Our investigation uncovered several hierarchical classification schemes designed for global wetlands (Brinson 1993; Jay et al. 2000; Allee et al. 2000; RAMSAR 2010, 2011; Pittman et al. 2011; Valle-Levinson 2011). Some other schemes were tailored to the Palearctic region (Finlayson and Van der Valk 1995; Devillers and Devillers-Terschuren 1996; Devillers et al. 2001; Davies et al. 2004; Evans 2012). The MedWet classification scheme (Farinha et al. 1996) was adapted from the US wetland classification system (Cowardin et al. 1979) to suit Mediterranean wetlands. However, all of these classifications rely on field data, which are currently unavailable in Yemen due to the country's unstable circumstances.

The second approach involves creating a region-specific classification scheme by utilizing a set of carefully selected estuarine attributes organized in a binary matrix (estuaries × attributes). This matrix is then processed with suitable classification algorithms (Gopal and Sah 1995; Scott and Jones 1995; Pittman et al. 2011; Alaoui et al. 2017; Smith et al. 1995; Rebelo 2009; Dvorett et al. 2012; Martin et al. 2011). In our research, we have chosen the second approach. Regardless of the method chosen, our primary objective is to maximize the acquisition of physical attributes while minimizing the need for field visits.

Therefore, our classification system, based on the hydromorphic characteristics of the river's terminal course and its watershed, primarily relies on remote sensing (RS) and

Geographic Information Systems (GIS). We also incorporate occasional on-site observations in addition to the limited existing literature. This literature is dispersed and relatively scarce in international and regional reports, such as those from IUCN (Barratt et al. 1987), FAO (Sanders and Morgan 1989), and PERSGA (e.g., PERSGA 2003, 2004, 2019), as well as a handful of published studies focusing on marine ecosystems and significant ecological threats (Evans 1994; Lavergne 2012; Al-Mahfadi and Dakki 2016, 2019).

To confirm the feasibility of our approach, we examined classifications constructed using RS data (Sader et al. 1995; Rebelo 2009; Rebelo et al. 2009; Miller et al. 2004). However, several other sources (Davidson and Finlayson 2007; Pittman et al. 2011; Valle-Levinson 2011; Schoch et al. 2014; Perennou et al. 2018) indicate that the utilization of these methods has significantly enhanced scientists' capabilities to describe earth patterns, including wetlands, across both large and detailed spatial scales. This improvement is attributed not only to the wealth of data that RS can offer for wetland inventories and typologies (Sader et al. 1995; Populus et al. 1995; Wright and Bartlett 1999; Ozesmi and Bauer 2002; Zubair 2006; Ahmad and Erum 2012) but also for monitoring and managing these valuable ecosystems (Wanzie 2003; Zeng et al. 2006; Hushulong 2012; Schoch et al. 2014).

VI.1.1.Identification and Inventory of Estuarine Wetlands

To ensure a comprehensive inclusion of all estuaries within our classification system, we embarked on an exhaustive inventory process. Initially, we identified estuaries by creating a complete watershed map for the entire country using a Digital Elevation Model (DEM) with a 30-meter resolution, specifically the GDEM Aster V2 model, utilizing Geographic Information System (GIS) tools. Subsequently, we designated the lowest point within each hydrographic network as the approximate location of the corresponding estuary. Given the relatively low resolution of the DEM, the initial locations were subjected to verification in a secondary phase and subsequently refined for all estuaries using satellite imagery captured between 1980 and 2020 from the Google Earth web browser and ESRI's Basemap library.

Each estuary was then uniquely identified by its geographical coordinates, assigned a code, and provided with a provisional name. These provisional names typically corresponded to the river's name or the nearest locality name, primarily sourced from topographic maps. Most estuaries were readily identifiable as elongated water channels aligned with the direction of the river's flow, occasionally appearing as parallel coastal grooves filled with water, even if seasonally. These estuaries were distinguishable from the upstream riverbeds, which were generally dry. They were often separated from the sea by sediment sills influenced by hydro-wind dynamics. In the case of broader estuaries, multiple channels were observed, sometimes resembling expansive ponds fed by distinct watercourses.

However, the identification process was not always straightforward. Several smaller watersheds generated automatically from the DEM did not exhibit any estuary and were consequently excluded from the inventory. In other instances, especially in the western region of the country, locating estuaries proved challenging. These estuaries were identified through the Digital Elevation Model as large, arid valleys, and their delineation on satellite imagery was often complex. Many of these valleys had been affected by wind-induced silt deposition. The likelihood of water accumulation in these wadis was very low, especially when their riverbeds were only slightly damp. In such cases, their locations were determined based on the general topography, vegetation density, and the presence of agricultural fields.

In rare cases, the presence of mangroves provided clues to the existence of estuaries. In situations where mangroves were absent, it was inferred that these valleys did not harbor estuaries.

VI.1.2.Criteria for Classification

In our endeavor to classify estuarine wetlands, we exclusively relied on physical descriptors pertaining to both their immediate surroundings and the characteristics of their watersheds (see Table VI.1). The majority of these descriptors were derived from satellite data, including digital elevation models, rainfall patterns, Google Earth imagery, and other available general maps such as geological information. However, we selectively retained only those descriptors that were quantifiable, albeit occasionally with some degree of imprecision (refer to Appendix 1).

VI.1.3.Watershed Descriptors

The descriptors associated with the watershed and utilized in the classification (Table VI.1) were extracted from the Digital Elevation Model (DEM) using Arc-GIS. These tools enabled the determination of hydrographic networks, the delineation of watersheds (including sub-basins), and the calculation of various geometric characteristics. Among these characteristics were key descriptors such as watershed area, perimeter, maximum altitude, mainstream river length, and slope, as exemplified in Figure VI.1.

In certain cases, particularly along the western coast, generating these geometric characteristics for some estuaries posed challenges. After traversing mountainous terrain, several rivers transition into low-lying coastal plains where their beds divide into two channels, often clearly visible in images. This geomorphological intricacy results in two (or more) estuaries belonging to the same river basin, thereby sharing nearly identical watershed characteristics. To address this complexity within the GIS models, we delineated these watersheds separately and recognized that their upstream boundaries and attributes were quite similar, while their terminal courses and estuaries remained distinct.

Rainfall emerged as a significant watershed descriptor due to its profound influence on the hydromorphic features of the estuaries. We expressed this descriptor as the annual average precipitation within the watershed, calculated using simulated rainfall data sourced from CHIRPS (Climate Hazards Group, Infra-Red Precipitation with Station data) V2 images for the period '1981–2014,' which encompasses multiple dry phases.

Geology of the watershed played a pivotal role in shaping both the river network and the physiography of the estuaries. It also determined the physicochemical attributes of the water. In this study, we employed the 'dominant rocks' concerning their primary mineral composition as a significant criterion for estuary classification. We categorized this qualitative attribute into five distinct classes (Table VI.1), grouping geological outcrops with similar 'petrographic nature,' as defined in the geological map of Yemen (Van der Gun and Ahmed 1995). For each estuary, we computed the total area covered by each petrographic class within the watershed and identified the dominant class as a classification attribute. The area was calculated using Arc-Map, finding the intersection between rock polygons (Figure VI.2) and the watershed polygon. While we acknowledge that these quantitative data may not be highly precise, both the clustering and ordination algorithms we employed are relatively robust against data value variations. Moreover, a high degree of precision was not essential since the original data had been transformed into categories.

VI.1.4.Local Descriptors

Local descriptors encompass parameters characterizing the estuary itself and the immediate environment that exerts influence on its hydrology and physical characteristics. This environment, referred to as the 'stream terminal section' (STS), pertains to the stream bed where the presence of water is discernible during specific periods of high flows and/or high tides, as evidenced by historical images. The upstream limit of this section is typically delineated by the presence of water traces or variations in vegetation density, and occasionally by a change in slope. It is important to note that the vast majority of Yemeni wadis display a consistently dry bed upstream of their respective STS.

To define these local descriptors, the initial step involves delineating the STS using available images, primarily sourced from Google Earth. These images are chosen based on existing features that indicate the maximum submersion of the STS. Four geometric descriptors associated with the boundaries of the STS can then be measured (in Figure VI.3):

- Area: This descriptor is presented as a geometric parameter of the delineation polygon.
- Length: It represents the measured distance between the coastline and the upper limit of the STS.
- Width: This descriptor corresponds to the distance between the edges of the STS at its widest point.
- Height: It is characterized by the altitude of the upstream limit of the STS.

Given the potential imprecision of altitudes provided by Google Earth and the variability in streambed water presence, these measurements are regarded as rough estimates.

Other local descriptors are associated with the surrounding seawater environment. Three of these descriptors, deduced from available images, are as follows:

- Sea Tide Amplitude: This descriptor, playing a crucial role in estuarine hydrology, was provided by the Civil Aviation and Meteorology Authority. We utilized the average values for the '2006-2016' decade from the nearest station (among the ten national stations), considering the limited number of available stations.
- Sea Connection: This is a qualitative descriptor indicating the frequency of connections between estuarine and seawaters. In arid regions, this rhythm reflects both the energy and frequency of river flow and the dynamics of tides that facilitate such connections. We categorized these connections into three categories:
    - Permanent/Semi-Permanent Connection: This category includes estuaries experiencing either a permanent or frequent river flow or active marine dynamics that regularly subject the estuary to high tide seawater. Distinguishing between these two situations can be challenging, particularly when the estuary channel is not well-defined. In such cases, the coastal area assumes a lagoon-like appearance with reduced marine energy and a dense biological carpet, often comprising mangroves or sea meadows.
    - Seasonal Connection: This connection pattern is considered the norm for estuaries of major rivers. These rivers typically experience intense seasonal floods due to seasonal rains, leading to periods of substantial water flow. However, the lower course is usually dry most of the time.
    - Occasional Connection: Occasional connection is a common situation in Yemen, given the prevalence of small, arid catchment areas primarily located on coastal slopes and lowlands. This characteristic also extends to some major rivers, where dams intercept floods and reduce their impact on estuaries, causing intermittent connections to the sea. These criteria help distinguish intermittent open/closed estuaries from permanent ones.

- Sea Exposition: This descriptor identifies the sea to which the estuary is connected, recognizing different hydrodynamic characteristics. The coastal waters bordering Yemen are subdivided into five distinct regions, primarily influenced by the Indian Ocean:
    - Red Sea (Coast of Intracontinental Sea);
    - Bab Al Mandeb Strait (Part of the Red Sea Slightly Influenced by the Pacific Ocean);
    - Gulf of Aden (Coast of a Large Sea Exposed to Medium Energy);
    - Arabian Sea (Continental Coast Largely Open to Pacific Influence);
    - Socotra/Indian Ocean (Coast of a Highly Dynamic Ocean, Specific to Socotra Island).
- Water Regime: Water regime is another significant descriptor related to estuarine ecosystems. In its simplest form, this descriptor signifies the duration and timing of water presence in the estuary. It is used to account for the fact that many stream terminal sections remain dry for several months, while others are continuously wet, with or without marine influence. Three situations are considered:
- Permanent/Semi-Permanent: This class implies the presence of water in all images, although there is no conclusive evidence that this presence is permanent.
- Very Probably Seasonal: This category includes images showing water in the estuary, particularly during wet seasons.
- Occasional: Occasional connection characterizes estuaries where water is intermittently present, but remains dry in most images, dependent on rainfall within the watershed.
- Geology of the Lower Part of the Watershed (Dominant Geological Outcrops): The dominant rocks in the lower watershed significantly influence estuary physiography. We applied the same methodology used for watershed geology (as described above) to this attribute. The reference area covers the estuary's surroundings, including the nearest slopes, generally within altitudes of 10-20 meters.

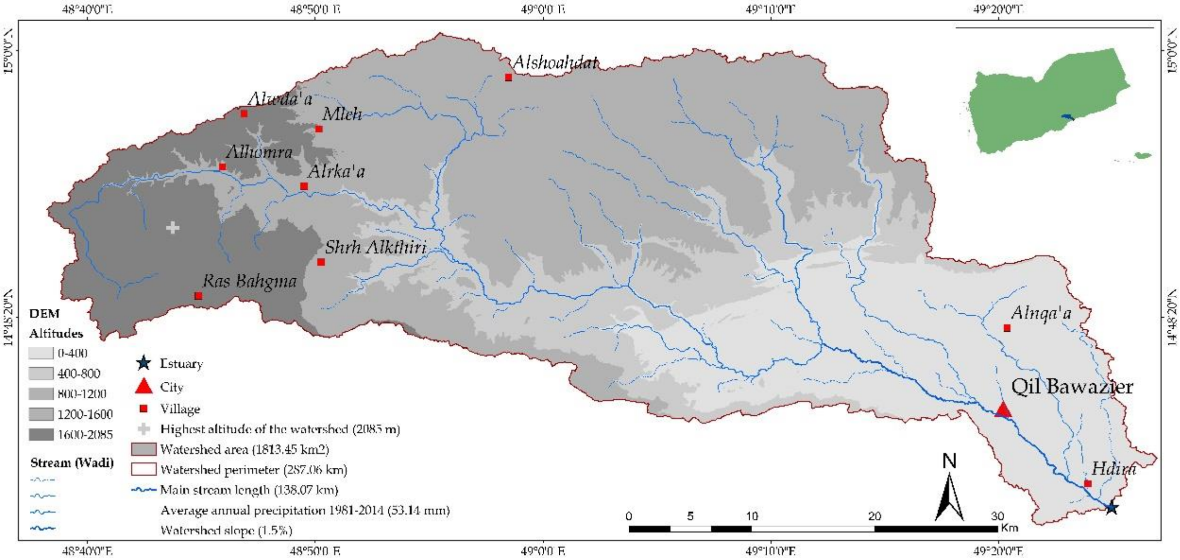

Figure VI. 1: Watershed classification descriptors (example of Wadi Hadramawt).

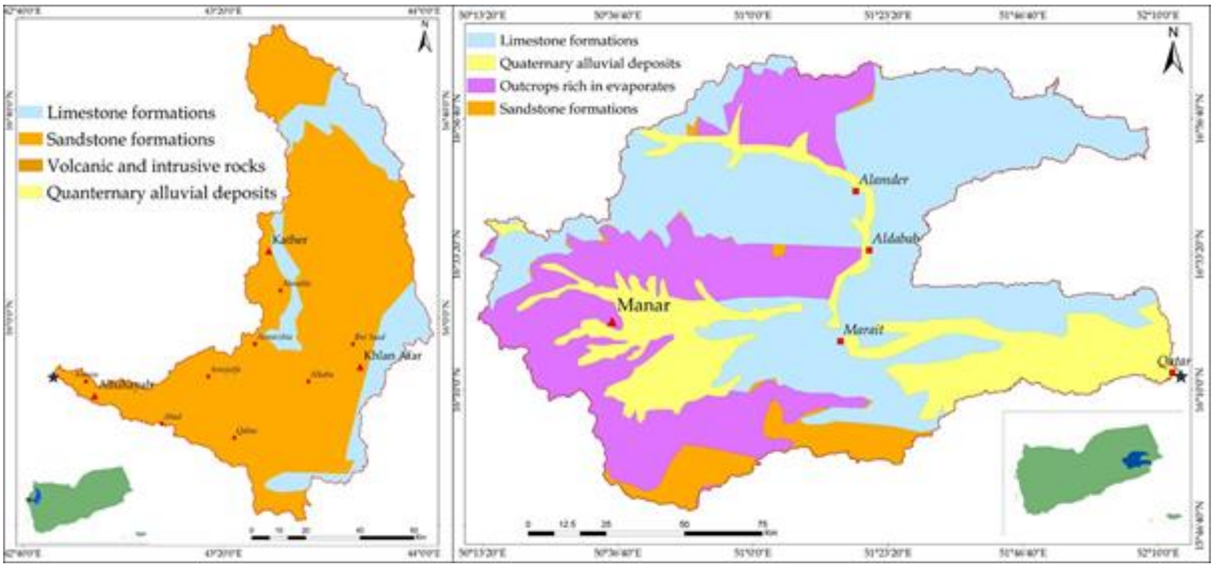

Figure VI. 2: Simplified examples of dominant rocks: Wadi Mawr, Alhodaidah (left) and Wadi Dahawn, Almahra (right)

Figure VI. 3: Measuring geometric descriptors in the stream terminal section: three examples of estuarine configuration, in wet and dry conditions.

VI.1.5.Matrix of Classification Criteria

Before applying the classification tools, we conducted an analysis using the Pearson correlation coefficient (PCC) to identify potential high redundancy among parameters in terms of their significance in the classification process. The coefficient revealed a perfect correlation between the area and the watershed perimeter (as depicted in Figure VI.4). Consequently, we opted to exclude the perimeter from the matrix as it offers less utility compared to the area. Although a high correlation of 0.98 was observed between the watershed area and the stream terminal section (STS) area, these two attributes pertain to distinct zones and hold different levels of significance in the classification. Additionally, we noted a notable correlation of 0.67 between the length and width of the STS. However, this correlation does not justify the high redundancy between these attributes.

Table VI. 1: Description of the parameters used as classification criteria

Codes	Criteria	Meaning	Class 1	Class 2	Class 3	Class 4	Class 5
Watershed descriptors							
WA	Watershed Area (km²)	Watershed area, calculated using 'Hydrology' tool in ArcGIS	<50	51-350	351-705	751-1800	> 1800
WM	Watershed mainstream length (km)	Length of mainstream in the watershed, calculated using 'Hydrology' tool in ArcGIS	<20	20-50	50-100	100-250	>250
WH	Watershed Maximum altitude (m)	The highest altitude in the whole watershed, calculated using DEM model in ArcGIS	<400	401-800	801-1400	1401-2000	>2000
WO	Watershed Slope (%)	Average slope of the mainstream in the watershed (WH/WM*100)	<2	2.1-4	4.1-10	10.1-24	>24
WG	Watershed dominant geological outcrops	Dominant type of rocks in the watershed*	Alluvial deposits	Volcanic/intrusive rocks	Sandstone formations	Limestone formations	Evaporate Outcrops
WP	Average annual precipitation	Average annual rainfall in the watershed for the '1981-2014' period (see text)	<50	51-100	101-150	151-200	>200
Local descriptors (relative to the stream terminal section-STS)							
EA	STS Area (ha)	STS area, estimated from its delineation polygon at	<6	6-16	16.1-50	51.1-150	>150
EL	STS length (km)	Approximate distance from the coastline to the upstream limit of the STS	<0.5	0.5-1.0	1.0-2.5	2.5-4.0	>4
EH	STS height (m)	Altitude at the upstream limit of the STS	<4	4-6	6.1-8	8.1-10	>10
EW	STS Width (m)	Maximum distance between the STS edges, at its maximum submersion	<45	46-82	83-250	251-450	>450
HT	High Tide level (m)	Average sea tide amplitude for the 2006-2016 decade, at the nearest station	1	2	2.2	2.4	...
SC	Sea Connection	Rhythm of connection between the estuary and the sea	Permanent/semi-permanent	Seasonal	Occasional	...	...
FT	Water regime	Water regime, described with three possible situations: 1. Permanent/semi-permanent, 2. Seasonal, 3. Occasional					
SE	Sea exposition	Sea to which the estuary is connected	Red Sea	Bab Al Mandab	Gulf of Aden	Arabian Sea	Socotra/ Ind. Ocean
EG	Estuary dominant geological outcrops	Dominant type of rocks in the surroundings of the stream terminal section	Alluvial deposits	Volcanic/intrusive rocks	Sandstone formations	Limestone formations	Evaporate Outcrops

The final matrix encompasses 15 attributes, both quantitative and qualitative (Table VI.1). Of these, six attributes are associated with the watershed, while nine are linked to the estuary and its immediate surroundings. These parameters are presumed to play a pivotal role in the functionality of estuarine wetlands. However, it's important to note that we do not assert that other factors, such as river flow, dams, urbanization, etc., lack significance for classification. Rather, their utilization was not feasible for various reasons, including the unavailability of data from remote sensing or official databases and the impracticality of measurement without physical field visits.

Furthermore, it's acknowledged that the original quantitative data may contain inaccuracies, primarily due to the methods used for measurement and the limited resolution of images covering Yemen and the Digital Elevation Model (DEM). As a result, these data have been transformed into three to five modalities or classes (Table VI.1). The delineation of these class boundaries is typically based on a logical subdivision and strives to maintain a balance in the number of estuaries within each class, with illustrative examples provided in Figure VI.5. This transformation yields a cohesive qualitative dataset amenable to analysis via factorial methods.

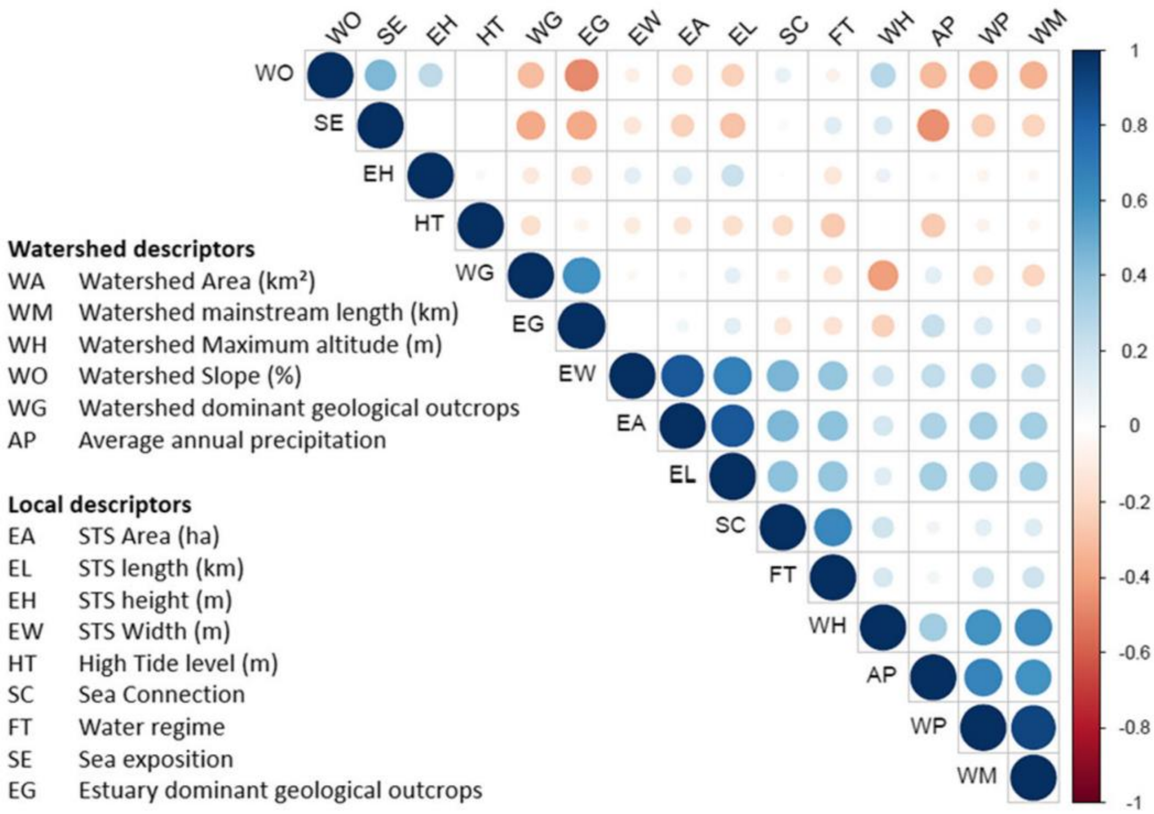

Figure VI. 4: Correlations between the criteria

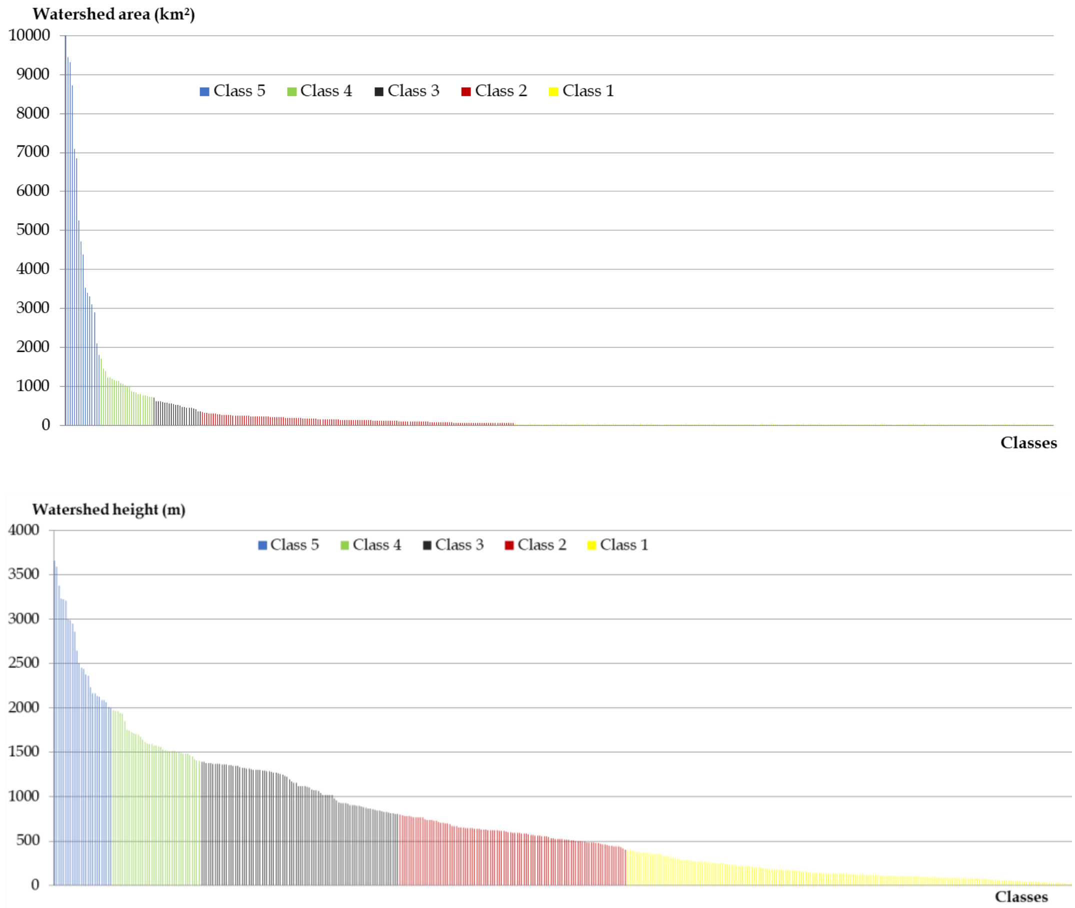

Figure VI. 5: Examples of criteria segmentation method in the average annual: watershed area (top) and watershed height (below).

VI.1.6.Classification Algorithm: Analysis Process

From the plethora of available clustering methods, we have chosen to employ two complementary techniques for the classification of Yemen's estuaries: factorial analysis (Benzécri et al. 1973; Hill 1973) and a generic clustering methodology (Alaoui et al. 2017). Factorial analysis serves as an effective ordination method that arranges the variables (descriptors) and individual estuaries within a meaningful framework defined by a series of axes, known as "factors," which elucidate this organization. This approach enables the exploration of correlations between various elements and can unveil unexpected gradients. In this study, we have utilized multiple factorial analysis (MFA), which can accommodate diverse data sets, incorporating both qualitative and quantitative variables (Lebart et al. 1977; Abdi et al. 2012). However, MFA plots may not always clearly delineate clusters, particularly for larger matrices.

To address this limitation and to organize the individual estuaries into groups based on their similarities, we have turned to the generic methodology for clustering (GMC). This approach employs an unsupervised classification method, the MCDBSCAN algorithm (Alaoui et al. 2017), to define clusters.

These two methods are considered complementary because while GMC identifies clusters that may be challenging to distinguish using MFA, MFA aids in illustrating and explaining the organization of these clusters within the primary planes.

The classification outcomes are visually presented by mapping estuaries and descriptors (criteria) onto the initial two planes of the Multiple Factorial Analysis (MFA), namely F1-F2 and F1-F3. These plots serve to encapsulate both the commonalities between estuaries and the associations between criteria. The significance of the three axes is explored through the projection of descriptors onto these planes.

Similarly, the clusters established via the GMC approach are visually distinguished on these planes using distinctive symbols and ellipses for each cluster. Furthermore, these clusters are depicted on a national map by displaying their corresponding watershed polygons.

VI.3.Results

VI.3.1.MFA Ordination of the Estuaries

The initial MFA analysis of the complete data matrix, encompassing 451 estuaries, identified one isolated estuary, referred to as 'Hadramawt.' This particular estuary stands out due to its substantial size and an exceptionally large watershed. Subsequently, a second analysis was conducted, considering this estuary as a supplementary element.

The first three axes of this analysis collectively account for 26% of the total inertia in the analysis, with individual contributions of 10.8%, 8.6%, and 6.6%. Although these contributions may appear relatively modest, the results depicted on the initial two planes, F1-F2 (Figure VI.6) and F1-F3 (Figure VI.7), reveal a consistent dispersion pattern among the estuaries. The projection of descriptors onto these two planes (Figures VI.8, VI.9, VI.10, and VI.11) underscores the significance of this dispersion.

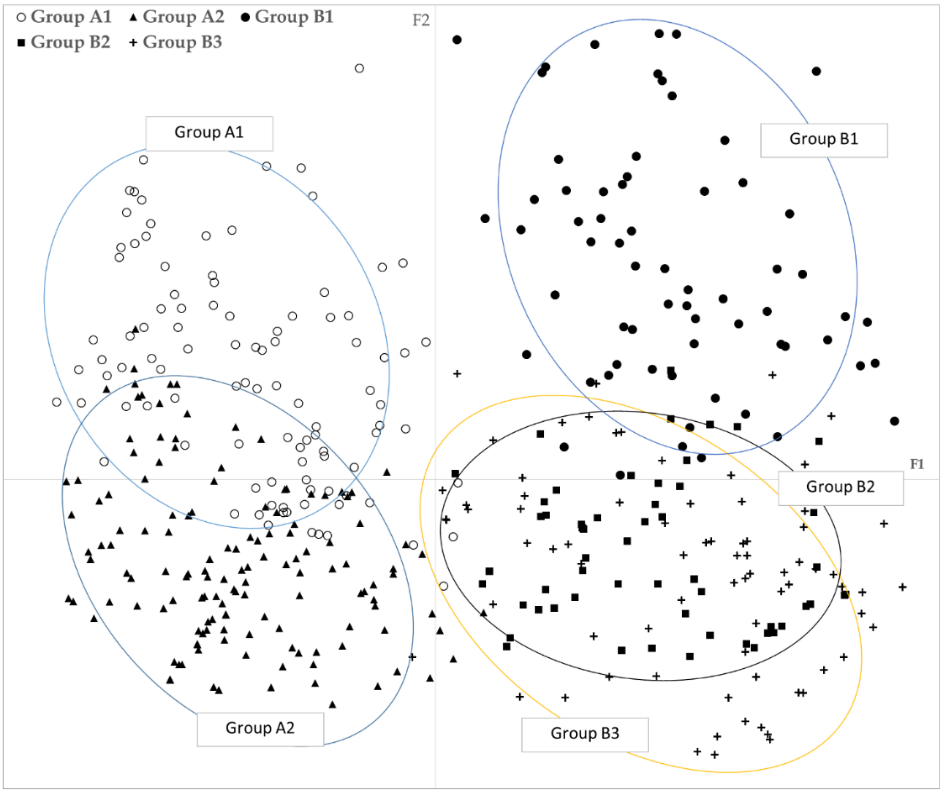

Figure VI. 6: Classification of Yemen's estuaries, using the GCM and the MFA: projection of estuaries' clusters on MFA plans F1-F2

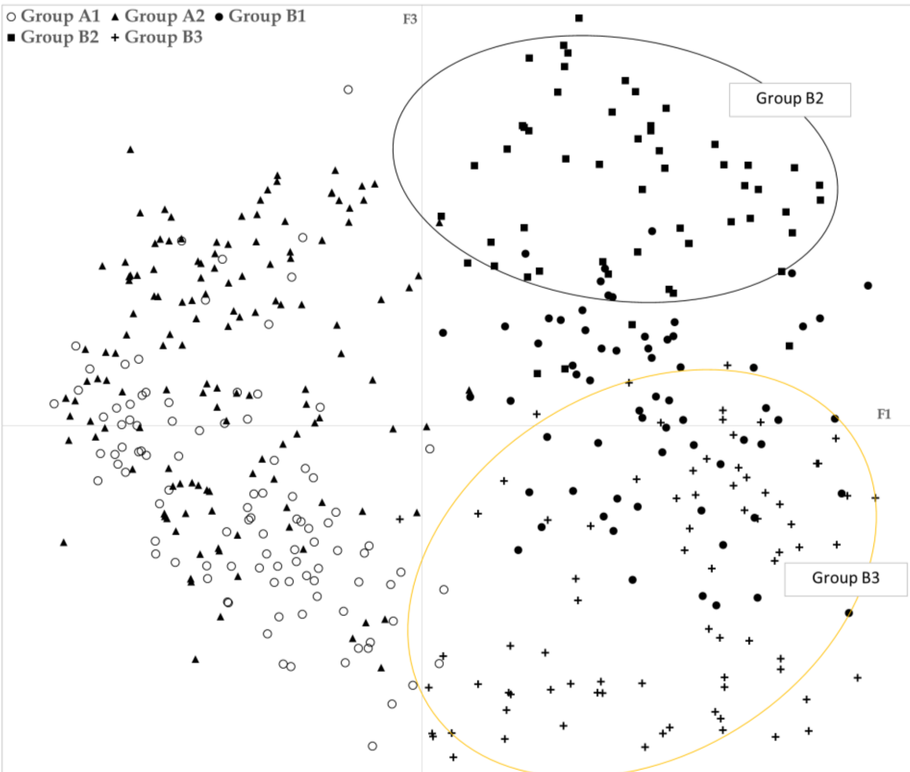

Figure VI. 7: Classification of Yemen's estuaries, using the GCM and the MFA: projection of estuaries and of B2 and B3 clusters on MFA plans F1-F3

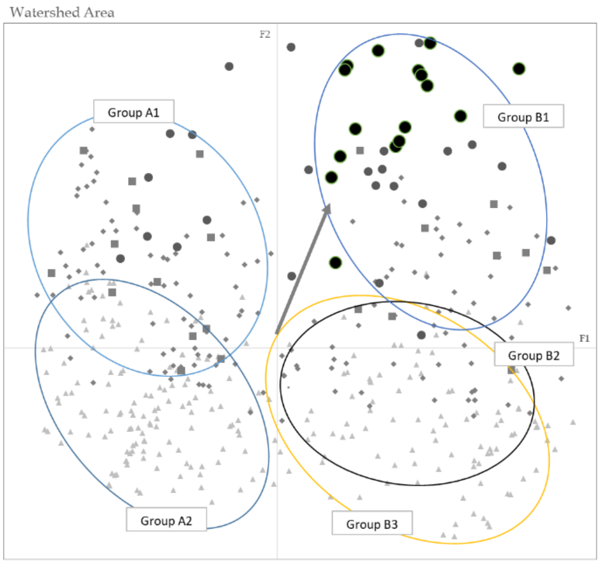

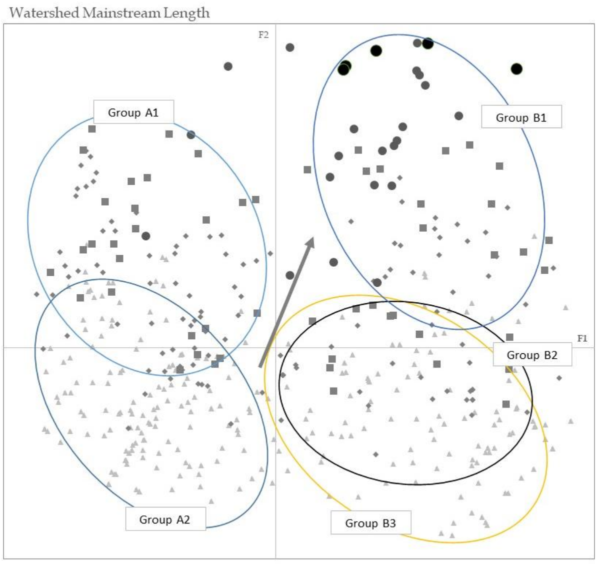

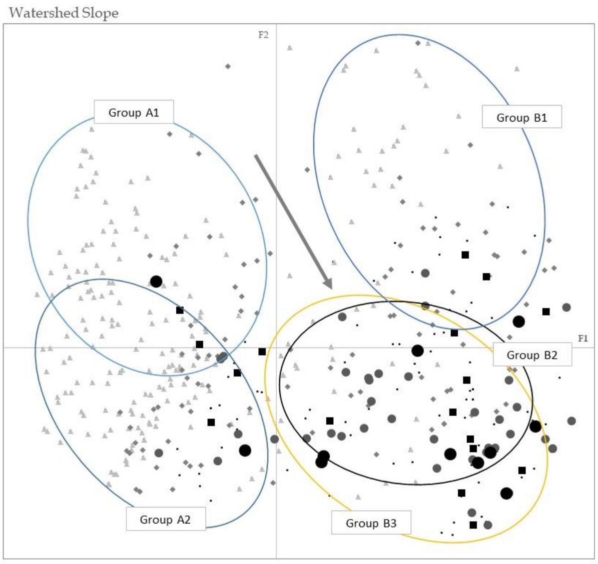

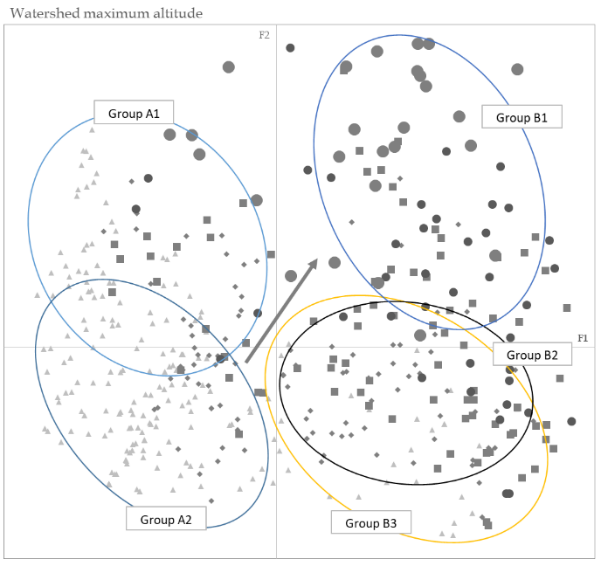

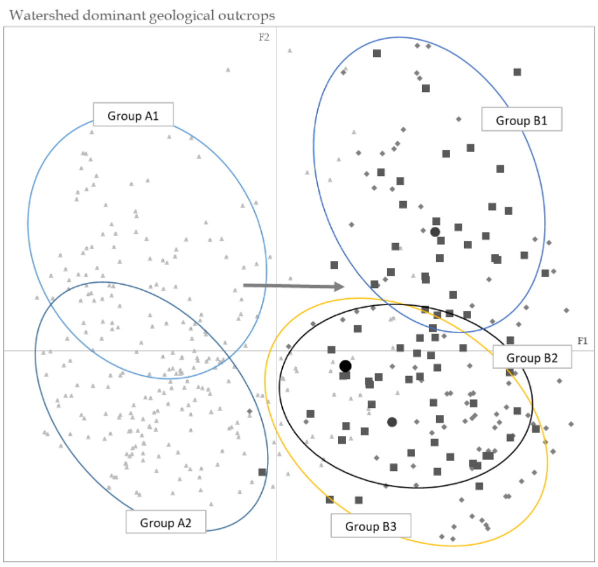

Legend

Codification of descriptors (details in text)

- Class 1
- Class 2
- Class 3
- Class 4
- Class 5
- Estuaries' clusters/groups

Direction of significant variation of a descriptor in the MFA plan 'F1-F2'

Figure VI. 8: Descriptors' contribution to the explanation of MFA axes (F1-F2) and the GCM clusters/groups.

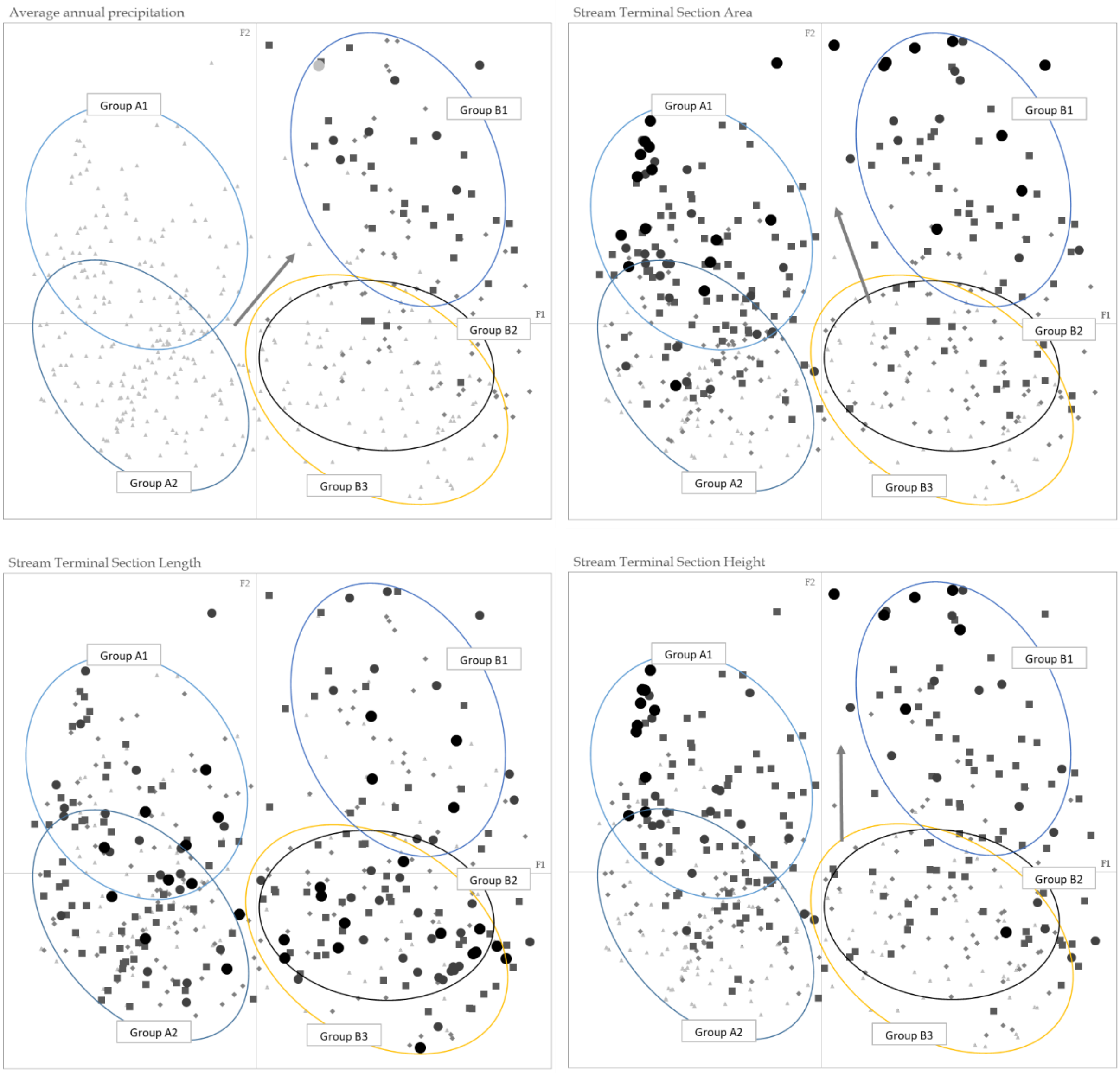

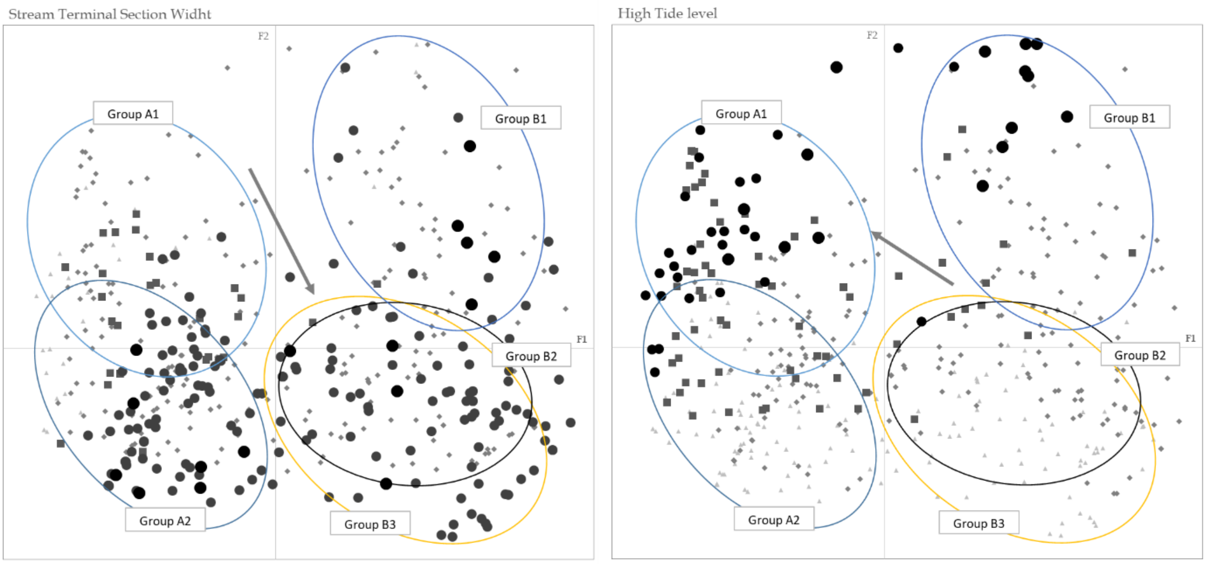

Figure VI. 9: Descriptors' contribution to the explanation of MFA axes (F1-F2) and the GCM clusters/groups (continued).

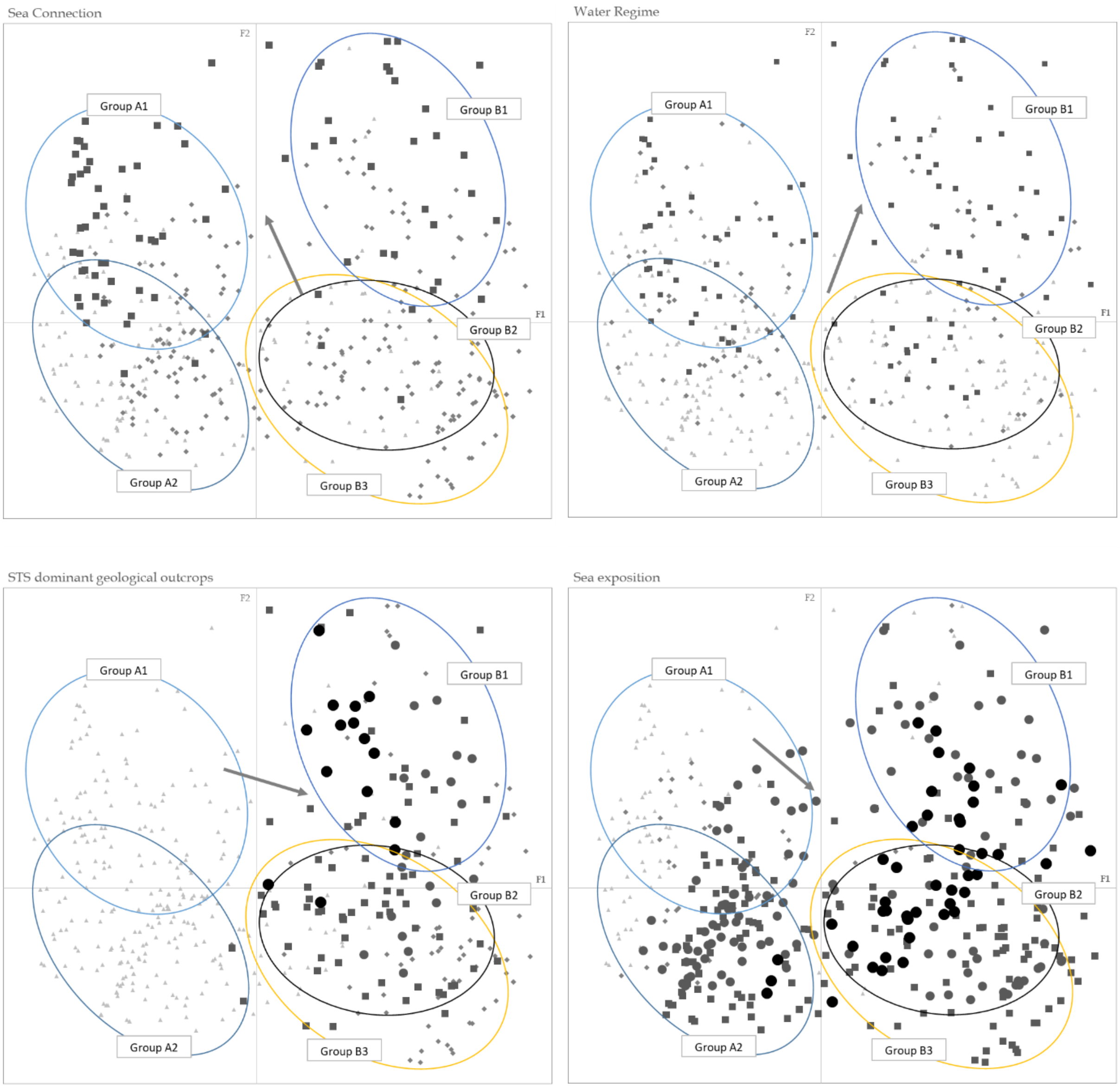

Figure VI. 10: Descriptors' contribution to the explanation of MFA axes (F1-F2) and the GCM clusters/groups (continued)

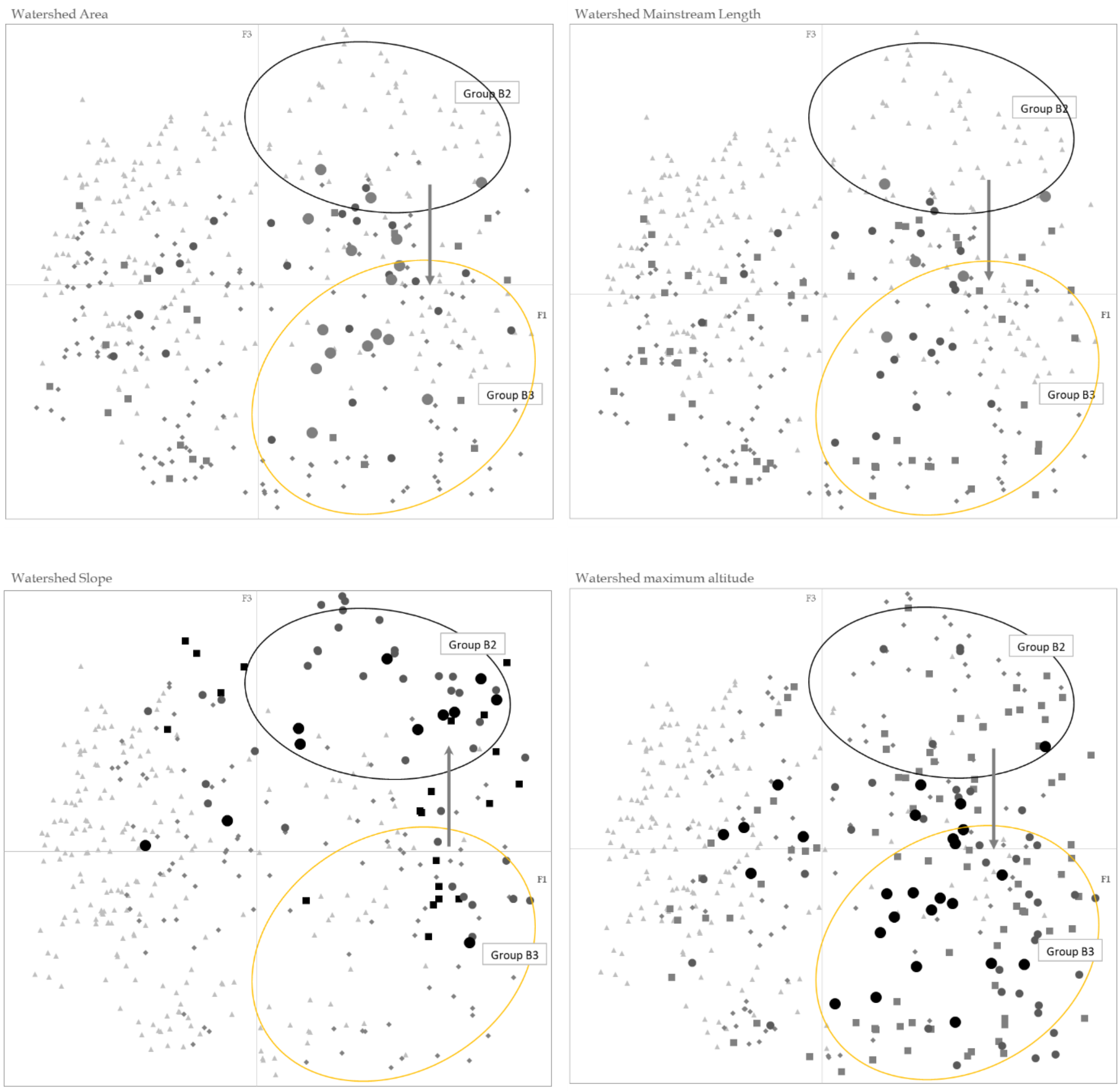

Figure VI. 11: Descriptors' contribution to the explanation of MFA axes (F1-F3) and the GCM Clusters/Groups 2 and 3 (see legend in Figure VI. 8).

The F1 axis primarily reflects a geological differentiation between two major groups. The first group, characterized by negative coordinates on this axis, is associated with dominant Quaternary alluvial deposits within both the entire watershed area and its lower section. The second group encompasses various geological formations found throughout the country.

Descriptors that exhibit substantial variations along the F2 axis are linked to estuary size (area, width, and length), watershed attributes (area, length, and height), as well as local hydrology (sea connection and water regime). However, it's important to note that all other descriptors simultaneously exhibit variations along these two axes, contributing to the differentiation of one or more groups from the rest. Notably, the length of the stream terminal section remains the sole parameter with unclear correlation to these axes, possibly due to measurement imprecisions.

The F3 axis warrants consideration due to its distinguishing role between groups B2 and B3 (Figure VI.7), despite their overlap in the F1-F2 plane. This separation was achieved through the clustering method (GMC). Four descriptors, all linked to the watershed, exhibit variations along this axis (Figure VI.11). Among these, two descriptors (area and length) distinctly oppose the two groups, while altitude and slope exhibit less distinct separations, further influenced by the two additional descriptors (slope and maximum elevation).

VI.3.2.Classification of Estuaries

The classification process, aided by the MFA and GMC methodologies, led to the categorization of Yemen's estuaries into six distinct types, as visually depicted in Figures VI.6 and VI.7. These types are briefly characterized below and visually represented on the country map using their watershed polygons (Figure VI.12).

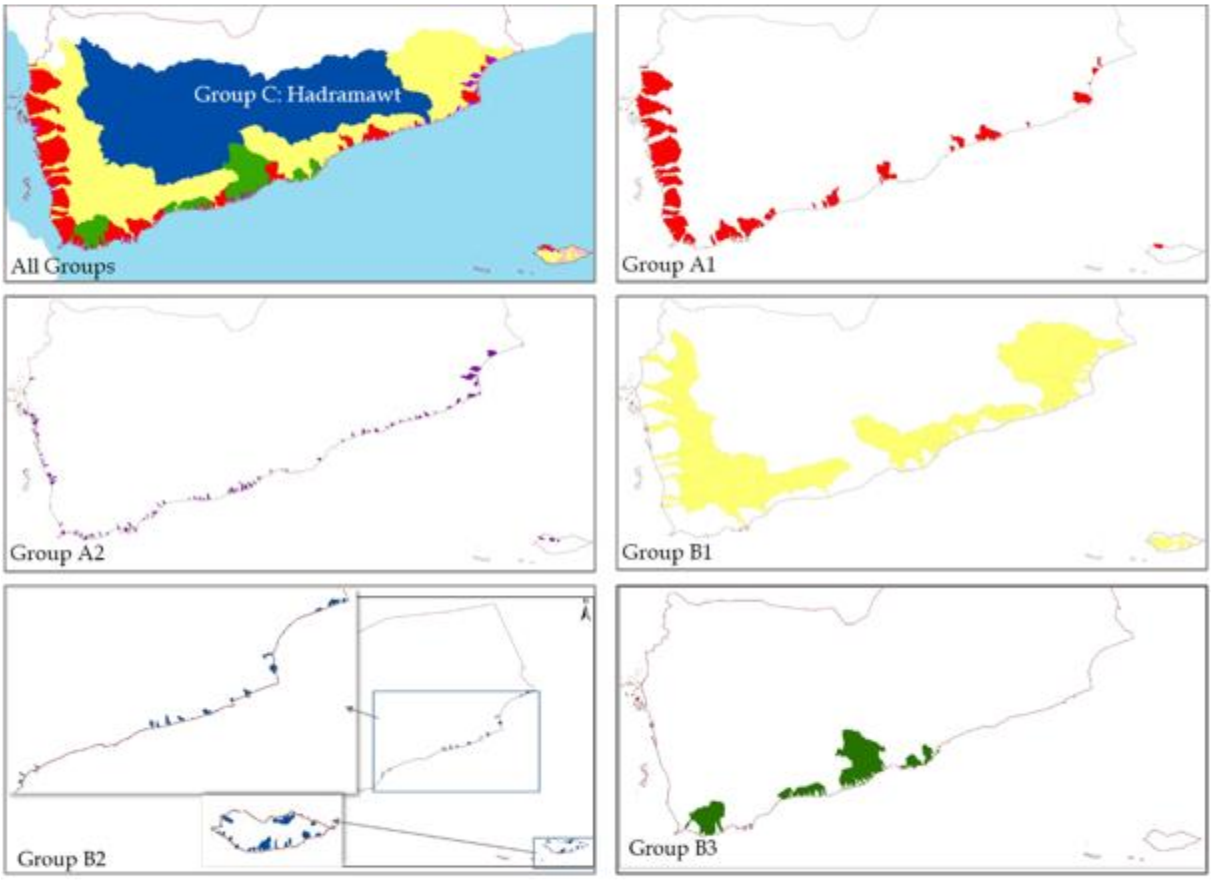

Figure VI. 12: Geographical distribution of the estuarine groups/types.

Group A1: Small Estuaries with Lowland and Foothill Watersheds

This category encompasses small estuaries, predominantly located along the country's Western Red Sea coast. These estuaries, each covering an area of less than 6 hectares, exhibit water regimes significantly influenced by river floods, with approximately 62% intermittently separated from the sea by sedimentary barriers. Roughly half of these estuaries experience seasonal or occasional submersion. Permanent ones typically manifest as depressions containing ponds, while others resemble sea inlets with hydrology largely dictated by marine tides and storms. These estuaries generally feature watersheds that extend from the coastal plain to the mountain foothills, with elevations rarely exceeding 800 meters. The mainstream length typically remains below 100 km, and the slope is less than 4%. The predominant geological feature in these watersheds is Quaternary alluvial deposits, both in the entire area and its coastal zone.

Group A2: Very Small Estuaries with Strictly Small Coastal Watersheds

In this group, the estuaries are characterized by minimal watersheds that do not extend onto the coastal plains and slopes. Their stream length is less than 20 km, with maximum elevations typically ranging from 100 to 200 meters, occasionally exceeding 400 meters. The average slope is correspondingly low, usually below 4%. These estuaries, numbering around 148 along Yemen's coast, occupy a limited area of less than 6 hectares. Their watersheds are marked by Quaternary alluvial deposits, both across the entire area and the coastal zone. These wetlands generally remain dry, with intermittent connections to the sea in approximately half of the cases. Many do not exhibit classic estuarine characteristics and are primarily identified through the analysis of streambed traces in various images.

Group B1: Medium-Sized Estuaries with Large Watersheds and Seasonal or Occasional Sea Connections

This category comprises estuaries present along the entire coastline of Yemen, including the Socotra coast. These estuaries exhibit diverse but rarely small sizes, typically featuring seasonal or occasional water regimes. Their watersheds are characterized by large or medium sizes, draining high mountains that exceed altitudes of 1500 meters, particularly in the western regions of the country. Despite their high elevation, these watersheds maintain a moderate average mainstream slope, typically not exceeding 10%. This suggests the presence of deep valleys carved by rivers at higher altitudes. The dominant geological features in most watersheds are sandstone or volcanic/intrusive rocks, alongside non-negligible Quaternary alluvial deposits. Precipitation within these watersheds is generally less than 100 mm, but the higher recorded precipitations in Yemen, exceeding 200 mm, predominantly occur in the upland regions of these watersheds. Due to irregular rainfall and the substantial number of dams and water diversions, these estuaries receive inland waters for brief periods, with their lower courses frequently drying up outside of the wet seasons.

Group B2: Arabian Sea Small Estuaries with Sloping, Small, and Arid Basins

Most of the estuaries in this group are situated along the Arabian Sea and the Socotra Island. They feature very small and sloping watersheds, with maximum stream lengths of about 20 km and exceptionally extending beyond 50 km^2 in area. These watersheds drain coastal mountains dominated by resistant rocks. They are predominantly marked by sandstone and/or volcanic/intrusive rocks across their entire area and lower sections, with occasional occurrences of Quaternary alluvial deposits. These estuaries are typically dry or maintain small ponds, with approximately 84% experiencing intermittent inundation from high tides or rainfall. In areas suitable for agriculture, despite the limited size and short watering periods of these wadis, the surroundings are densely populated. Groundwater is available near the coastal mountain bases but does not significantly contribute to the estuary's hydrology.

Group B3: Small Estuaries of the Gulf of Aden

This group consists of estuaries specific to the Gulf of Aden coast. These estuaries typically exhibit small sizes, with the majority not exceeding 16 hectares and a significant portion falling below 6 hectares. Approximately 89% of these estuaries appear to be permanently or semi-permanently flooded, primarily due to the high amplitude of sea tides (averaging about 2.4 meters) and frequent storms. Their upstream beds are often dry, but roughly 64% of these estuaries are intermittently blocked by low sedimentary dikes. These estuaries primarily feature small watersheds, generally less than 350 km^2 in size, with moderate to low slopes, although 43% exhibit steep slopes extending to the mountain slopes overlooking the sea. The geological composition varies but predominantly comprises volcanic/intrusive rocks, with sandstone outcrops replacing them in 31% of cases in the lower courses.

Group C: The Hadramawt Estuary

This unique estuary in Yemen stands apart due to its permanent exposure to the sea's dynamics. It boasts a substantial size exceeding 210.49 hectares and features a long terminal section stretching over 7.66 kilometers. The estuary's watershed covers almost 40% of the country, encompassing an area of 140.740 km^2, with a maximum length of 882 km and a relatively high slope. Indeed, it represents the largest and highest basin in the Arabian Peninsula, with elevations reaching up to 3657 meters.

VI.4. Discussion

This chapter presents a significant hydromorphic classification of Yemen's estuaries, primarily utilizing accessible satellite data, which has been distilled into 15 physiographical descriptors. This classification has unveiled six distinct estuary types, predominantly differentiated by a select few descriptor categories. The watershed and estuary sizes, particularly expressed through area, length, and height, alongside the dominant rock outcrops in both the watershed and lowland, play pivotal roles in these differentiations. Sea exposition, which encompasses tide amplitude, seems to have a relatively secondary impact on this classification. These findings reaffirm the pivotal role of river catchment area characteristics in shaping estuaries, as established by prior studies (Ladson 1999; Kondolf et al. 2003; Chessman et al. 2006; Gregory 2006; Thornton et al. 2007; Harvey et al. 2008; Day et al. 2012).

While the role of rainfall in the catchment area, which significantly influences stream hydrology, was expected to be a key determinant, its influence appears to be overshadowed by the high prevalence of dams and intensive water diversion for agriculture. This significantly reduces the flow in lower stream courses. However, this role may be implicitly integrated within the correlation between estuarine and catchment area sizes. This correlation remains evident even in the face of recent droughts, a prominent expression of climate change, and human pressures. It has persisted since the Quaternary period, primarily due to pluvial episodes.

Despite the absence of river flow attributes, it is evident, through time series of images, that water regimes are predominantly seasonal in most estuaries. This is a consequence of both the seasonality of rainfall under global warming, leading to frequent droughts, and excessive water withdrawal and dam constructions. Furthermore, the severe depletion of coastal aquifers amplifies water scarcity (Briscoe 1999; NWRA 2005; Shah et al. 2009). Notably, lower watershed zones have been subject to human occupation and aquifer pumping for millennia, further emphasizing the role of sea connection over water inputs from inland or ground sources in maintaining water permanency in estuaries.

The exchange frequency between estuaries and the sea remains challenging to define with available images. However, water permanency in estuaries can also result from frequent estuary closures, transforming them into natural reservoirs with high salinity. These intermittently open/closed estuaries, known as 'estuarine gueltas' in North Africa, are prevalent and characteristic of arid regions facing substantial climate change and water abstraction, such as Yemen. Nevertheless, they do not emerge as distinct types in our classification, as they are well-distributed across all groups.

The geographical location of estuaries plays a secondary role in our classification, as two groups of small estuaries (B2 and B3) are found on different coasts with varying sea hydrodynamics (the Arabian Sea and the Gulf of Aden). However, marine descriptors that are meant to differentiate these seas (e.g., tide amplitude) are diluted in the classification by non-marine descriptors.

The categories established in our hydromorphic classification do not neatly align with existing wetland typologies, which typically focus on detailed descriptors specific to the internal characteristics of estuaries (hydrology, sediments, vegetation, etc.). Nonetheless, we believe that our categories could represent the highest levels of these typologies. In particular, open/closed estuaries, highly prevalent in arid zones, are not prominently featured in Palearctic wetland typologies. We advocate for their inclusion in global typologies, as they are widespread in arid regions and have been extensively characterized in regions such as South Africa, South America, Southern Asia, Australia, New Zealand, California, and North Western Africa.

In light of these findings and the increasing volume of satellite data, remote sensing appears to be a promising approach for preliminary classifications of estuaries, especially in remote and inaccessible regions. While certain key hydrological attributes are lacking, the selected watershed descriptors prove to be valuable classification criteria, along with STS parameters. However, this preliminary classification does not replace those based on descriptors internal to wetlands (e.g., hydrology, sediments, habitats, and vegetation), which currently require field investigations. In any case, catchment area descriptions are essential for wetland inventories, monitoring, management, and conservation. Therefore, integrating catchment characteristics into estuarine classifications, leveraging freely available satellite data and technical tools, would significantly enhance the overall understanding and management of estuarine ecosystems.

VI.5. Conclusion

This study offers a robust conceptual framework, especially valuable in situations where the absence of bibliographic data and the challenges of conducting on-site visits to estuaries create significant hurdles. These conditions posed major obstacles during our research in Yemen's troubled environment. Despite some limitations in data precision, the classification results provide initial insights into the distinctions among Yemen's estuaries, particularly concerning their hydromorphic behavior. It underscores that these distinctions are closely intertwined with watershed size and geology.

These findings open the door to future scientific inquiries that could advance satellite data measurement and automate certain data collection processes, such as monitoring water regimes, wetland areas, and sea connections. Another avenue for research could involve enriching the classification descriptors with new relevant parameters encompassing geomorphological, hydrological (average water flow and exceptional floods), sedimentary (bottom granulometry and sand barrier composition), ecological (habitats), and anthropogenic (water and land usage) attributes.

It's worth emphasizing that this study has produced a comprehensive geodatabase covering 451 Yemen estuaries, containing at least 20 parameters, some of which may not have been prominently featured in our results but are nonetheless valuable. This geodatabase also includes additional resources, such as estuary and catchment delineations, perimeters, watershed shapes, and more. It serves as a crucial foundation for a comprehensive national inventory of Yemen's estuaries, which is a project we are committed to pursuing in the future. We hope that the security situation will improve, enabling us to conduct field visits, as our work aims to gather new local descriptors of estuaries using existing high-resolution imagery.

Chapter VII: Conclusion

VII.1. Conclusion

The amalgamation of geomatics, remote sensing, GIS and GeoAI has undeniably ushered in a new era of understanding and addressing multifaceted environmental challenges. As we delve into the nuanced realms of Earth's ecosystems, these technologies stand out as powerful tools, transcending traditional boundaries and opening up avenues for innovative solutions.

One of the striking aspects illuminated by the collective findings is the role of these technologies in comprehending the intricate dynamics of forest fire propagation. By employing geomatics and remote sensing, researchers can monitor and analyze the spread of wildfires in real-time, aiding in the development of more effective firefighting strategies. The integration of GIS technologies further allows for the creation of detailed fire risk maps, facilitating proactive measures to mitigate the impact of these destructive events.

The exploration of wetland hydrology represents another frontier where geoinformation technologies have proven instrumental. These technologies enable scientists to monitor changes in wetland ecosystems, track water flow patterns, and assess the impact of human activities on these delicate environments. The insights gained through such analysis contribute not only to the preservation of biodiversity but also to the sustainable management of water resources.

The examination of dam-induced sedimentation emerges as a critical application of these integrated technologies. By leveraging geomatics and remote sensing, researchers can assess sedimentation levels around dams, helping to predict potential environmental consequences and the dam’s lifespan. GIS plays a pivotal role in visualizing and analyzing the data, enabling decision-makers to implement measures that minimize the ecological impact of sedimentation on downstream ecosystems.

Mapping degradation-prone areas is a paramount concern in the realm of environmental management, and geoinformation technologies emerge as indispensable tools in this endeavor. The ability to collect, process, and analyze spatial data allows for the identification of vulnerable regions, facilitating targeted interventions for soil conservation, reforestation, and sustainable land use planning.

Estuarine classification, an area traditionally fraught with complexities, benefits immensely from the integration of these technologies. Geoinformation technologies aid in the precise delineation of estuarine boundaries, and they provide valuable information on land cover. GIS ties these diverse datasets together, offering a comprehensive understanding of estuarine ecosystems and supporting conservation efforts in these critical coastal zones.

The collective findings underscore not only the versatility but also the synergy achieved through the integration of geoinformation technologies. As we continue to grapple with the intricacies of environmental challenges, these tools stand as beacons of innovation, guiding us towards more informed and effective strategies for the conservation and sustainable management of our planet's precious ecosystems.

Chapter II highlights the successful application of advanced techniques for forest fire analysis, emphasizing the importance of early detection and rapid response strategies in wildfire management. The study reinforces geospatial analysis as a key tool for understanding fire patterns and their ecological impacts, guiding future strategies for recovery and conservation.

Chapter III contributes significantly to the understanding of Saharan wetlands, emphasizing the role of catchment areas in sustaining groundwater sources. The study recognizes the importance of rainwater in hydrological processes and extends its scope to acknowledge the potential contributions of surface water from the stream network during heavy rainfall.

In Chapter IV, the assessment of artificial dams on the hydro-sedimentary regime provides a comprehensive framework for studying soil erosion and sedimentation processes. The methodology, validated against in-situ observations, offers a reliable tool for anticipating sedimentation rates and implementing measures for ecological preservation and sustainability.

Chapter V, focused on mapping degradation-prone areas, utilizes Sentinel 2 data and GIS techniques to reveal the impact of climatic conditions, population migration, and land use on soil erosion. The results emphasize the need for multidisciplinary approaches to manage and adapt to the continuous increase in degraded land.

Chapter VI, despite challenges in Yemen's troubled environment, provides valuable insights into estuarine classification and highlights the interconnectedness of distinctions among estuaries with watershed size and geology. The study lays the foundation for a comprehensive national inventory of Yemen's estuaries, showcasing the potential for future scientific inquiries and data enrichment.

Collectively, these chapters not only contribute to the advancement of environmental science but also emphasize the importance of ongoing research, monitoring efforts, and multidisciplinary approaches to address complex ecological challenges. The integration of technological advancements, effective emergency response, and ecological assessments serves as a pathway toward more resilient and sustainable environmental management practices.

VII.2. Recommendations and Suggestions for Future Research

By pursuing the recommendations below, researchers can further enhance the capabilities of geoinformation technologies, integrating IoT and machine learning to contribute to more robust environmental management strategies and fostering sustainable practices for the future.

1. **Interdisciplinary Collaboration:** Encourage collaborative research endeavors that bring together experts from diverse fields such as ecology, meteorology, and sociology. Interdisciplinary collaborations can provide a more holistic understanding of environmental challenges and enhance the applicability of geomatics, remote sensing, and GIS technologies.
2. **Real-Time Monitoring and Early Warning Systems:** Investigate the development of more advanced real-time monitoring systems for environmental phenomena, particularly in the context of forest fire propagation. The integration of cutting-edge technologies, such as Internet of Things (IoT) and machine learning, could enhance the accuracy and timeliness of early warning systems, improving our ability to respond swiftly to emerging environmental threats.
3. **Long-Term Monitoring of Wetland Ecosystems:** Conduct longitudinal studies to monitor changes in wetland ecosystems over extended periods. This would provide insights into the long-term effects of human activities, climate change, and conservation efforts on wetland hydrology. Longitudinal data can inform sustainable water resource management practices and contribute to the development of adaptive strategies for preserving biodiversity.
4. **Predictive Modeling for Dam-Induced Sedimentation:** Focus on the development of predictive models that utilize geomatics, remote sensing, GIS data, IoT sensors, and machine learning algorithms to forecast dam-induced sedimentation. By understanding the factors influencing sedimentation rates, researchers can develop proactive measures to minimize ecological impact and inform dam construction and maintenance practices.
5. **Fine-Scale Mapping of Degradation-Prone Areas:** Explore the potential for higher resolution mapping to identify degradation-prone areas at a finer scale. This could involve the use of advanced satellite imagery, drone technology, IoT devices, and machine learning algorithms to capture more detailed spatial data. Fine-scale mapping would enhance the precision of interventions, allowing for targeted and efficient soil conservation, reforestation, and land use planning.
6. **Integration of Social and Economic Factors:** Incorporate social and economic variables into environmental mapping and analysis. Understanding the human dimensions of environmental challenges is crucial for developing sustainable

solutions. Future research should explore ways to integrate socioeconomic data into geospatial analyses, combined with IoT and machine learning capabilities, providing a more comprehensive understanding of the interconnectedness between human activities and environmental changes.

7. **Advancements in Estuarine Monitoring Techniques:** Investigate novel monitoring techniques for estuarine ecosystems, such as the incorporation of advanced sensors, remote sensing technologies, IoT devices, and machine learning algorithms. Continuous monitoring of estuarine boundaries, water quality, and vegetation cover can provide real-time data, contributing to more effective conservation and management strategies for these ecologically sensitive coastal zones.
8. **Ethical and Privacy Considerations:** Address ethical and privacy considerations associated with the use of geospatial technologies, IoT, and machine learning. Future research should explore frameworks for responsible data collection and sharing, ensuring that the benefits of these technologies are balanced with concerns related to privacy, data security, and potential misuse.

Thesis References

Abbaspour, K. C., Yang, J., Maximov, I., Siber, R., Bogner, K., Mieleitner, J., … Srinivasan, R. (2007). Modelling hydrology and water quality in the pre-alpine/alpine Thur watershed using SWAT. Journal of Hydrology, 333(2–4), 413–430. doi:10.1016/j.jhydrol.2006.09.014

Abdi, H., Williams, L. J., & Valentin, D. (2013). Multiple factor analysis: principal component analysis for multitable and multiblock data sets. Wiley Interdisciplinary reviews: computational statistics, 5(2), 149-179.

Agnèse J.F., Louizi H., Gilles A., Berrada-Rkhami F., Benhoussa A., Qninba A. & Pariselle A. (2018). A euryhaline fish, lost in the desert: The unexpected metapopulation structure of Coptodon guineensis (Günther, 1862) in the Sebkha of Imlili. C. R. Biologies, 341, pp. 75–84.

Ahmad S. & Erum S. (2012). Remote Sensing and GIS Application in Wetland Change Analysis: Case Study of Kaliar Kahar. Sci., Tech. and Dev., 31, 3, pp. 251-259.

Ahmed El Hassani. (1990). La bordure nord de la chaîne hercynienne du Maroc, chaîne "calédonienne" des Sehoul et plateforme nord-mesetienne. Sciences de la Terre. UNIVERSITE LOUIS PASTEUR STRASBOURG FRANCE. Français. NNT.

Aiello, A., Adamo, M., & Canora, F. (2015). Remote sensing and GIS to assess soil erosion with RUSLE3D and USPED at river basin scale in southern Italy. Catena, 131, 174–185. DOI: 10.1016/j.catena.2015.04.003

Alaoui A. Teeaki B., Olengoba-Ibara B. & Zerouaoui J. (2017). A Generic Methodology for Clustering to Maximises Inter-Cluster Inertia. Intern. J. Adv. Computer Sci. Appl., 8, 11, pp. 187-191. DOI: 10.14569/IJACSA.2017.081125

Allee R., Dethier M., Brown D., Deegan L., Ford R., Hourigan T., Maragos J., Schoch C., Sealey K., Twilley R., Weinstein M., Yoklavich M. (2000). Marine and estuarine ecosystem and habitat classification. NOAA Technical Memorandum. NMFSF/SPO-43, pp 1-14.

Al-Mahfadi A. & Dakki M. (2016). Causes and effects of coastal wetlands degradation in Yemen. Int. J. IIOABJ, 7, Suppl 1, pp. 548-553.

Al-Mahfadi A. & Dakki M. (2019). Vulnerability of Al-Hodidah wetlands in Yemen: main socioeconomic causes. Science Direct: Materials Today: Proceedings, 13, pp. 517-524. DOI: 10.1016/j.matpr.2019.04.008

Al-Mahfadi A. & Dakki M. (2020). Scientific elements for a Yemeni wetland conservation strategy: overview of the main factors explaining the diversity and characteristics of wetlands. Bull Inst. Sci., Rabat, Sci. Vie, 42.

Altaiee, T. (1990). The influence of a dam on the downstream degradation of a river bed: case study of the Tigris River. Hydrology in mountainous regions II: artificial reservoirs, water and slopes proceedings of two International Symposia, 27 Aug.-1 Sep Vol 194, 153-160.

Al-Zahrani, M., Al-Areeq, A., & Sharif, H. O. (2017). Estimating urban flooding potential near the outlet of an arid catchment in Saudi Arabia. Geomatics Natural Hazards and Risk, 8(2), 672–688. doi:10.1080/19475705.2016.1255668

Amarnath, G. (2014). An algorithm for rapid flood inundation mapping from optical data using a reflectance differencing technique. Journal of Flood Risk Management, 7(3), 239–250. doi:10.1111/jfr3.12045

Amengual, A., Romero, R., Gómez, M., Martín, A., & Alonso, S. (2007). A hydrometeorological modeling study of a flash-flood event over Catalonia, Spain. Journal of Hydrometeorology, 8(3), 282–303. doi:10.1175/jhm577.1

Amos, C., Petropoulos, G. P., & Ferentinos, K. P. (2019). Determining the use of Sentinel-2A MSI for wildfire burning & severity detection. International Journal of Remote Sensing, 40(3), 905–930. doi:10.1080/01431161.2018.1519284

Andrews, P. L. (1986). BEHAVE: fire behavior prediction and fuel modeling system-BURN Subsystem, part 1. doi:10.2737/int-gtr-194

Aouichaty N., Bouslihim Y., Hilali S., Zouhri A., Koulali Y. (2022). Estimation of water erosion in abandoned quarries sites using the combination of RUSLE model and geostatistical method. Scientific African, 16, e01153,. DOI: 10.1016/j.sciaf.2022.e01153

Arjasakusuma, S., Kusuma, S. S., Vetrita, Y., Prasasti, I., & Arief, R. (2022). Monthly Burned-Area Mapping using Multi-Sensor Integration of Sentinel-1 and Sentinel-2 and machine learning: Case Study of 2019's fire events in South Sumatra Province, Indonesia. Remote Sensing Applications: Society and Environment, 27, 100790.

Arnold J. G., Srinivasan R., Muttiah R. S., Williams J. R., (1996). Large-aerea hydrologic modeling and assessment : Part I Medel development. Journal of American Water Resources Association

Arnold, J. G., & Fohrer, N. (2005). SWAT2000: current capabilities and research opportunities in applied watershed modelling. Hydrological Processes, 19(3), 563–572. doi:10.1002/hyp.5611

Arnoldus, H.M.J. (1977) Methodology Used to Determine the Maximum Potential Range Average Annual Soil Loss to Sheet and Rill Erosion in Morocco. Assessing Soil Degradation, FAO Soils Bulletin (FAO), 34, 39-48.

Ascoli, D., Plana, E., Oggioni, S. D., Tomao, A., Colonico, M., Corona, P., … Barbati, A. (2023). Fire-smart solutions for sustainable wildfire risk prevention: Bottom-up initiatives meet top-down policies under EU green deal. International Journal of Disaster Risk Reduction: IJDRR, 92(103715), 103715. doi:10.1016/j.ijdrr.2023.103715

Athanasiou, M., Bouchounas, T., Korakaki, E., Tziritis, E., Xanthopoulos, G., & Sitara, S. (2022). Introducing the use of fire for wildfire prevention in Greece: pilot application of prescribed burning in Chios island. In Advances in Forest Fire Research 2022 (pp. 1487–1494). doi:10.14195/978-989-26-2298-9_227

Badar, B., Romshoo, S. A., & Khan, M. A. (2013). Integrating biophysical and socioeconomic information for prioritizing watersheds in a Kashmir Himalayan lake: a remote sensing and GIS approach. Environmental Monitoring and Assessment, 185(8), 6419–6445. doi:10.1007/s10661-012-3035-9

Bagnouls, F. and Gaussen, H. (1953) Saison sèche et indice xérothermique. Doc. Carte port. Vég. Art. 8. Toulouse, 47 p.

Bai, L., Wang, N., Jiao, J., Chen, Y., Tang, B., Wang, H., ... Wang, Z. Chen, Y., Yan, X., Wang, Z. (2020). Soil erosion and sediment interception by check dams in a watershed for an extreme rainstorm on the Loess Plateau, China. International Journal of Sediment Research, 35(4), 408-416. DOI: 10.1016/j.ijsrc.2020.03.005

Barmpoutis, P., Papaioannou, P., Dimitropoulos, K., & Grammalidis, N. (2020). A review on early forest fire detection systems using optical remote sensing. Sensors (Basel, Switzerland), 20(22), 6442. doi:10.3390/s20226442

Barnard P. & Thuiller W. (2008). Introduction to Global change and biodiversity: Future challenges. Biology Letters4, pp. 553-555. DOI: 10.1098/rsbl.2008.0374

Barratt L., Dawson-Shepherd A., Ormand R. & McDowell R., 1987. Yemen Arab Republic Marine Conservation Survey, Volume 1, Distribution of habitats and species along the YAR coastline, IUCN, Red Sea and Gulf of Aden Environmental Programme/TMRU, UK.

Beaudet, G. (1969) Le plateau central marocain et ses bordures: étude géomorphologique. Thèse de Lettres.Imprimerie française, Rabat.

Ben Hichou, B., Mhammdi, N., Dakki, M. (2023a). Integrated Geomatics and Remote Sensing Analysis of Forest Fire Propagation and Land Cover Change: Berkane, Morocco. Ecological Engineering & Environmental Technology, 24(9). DOI: 10.12912/27197050/174254

Ben Hichou, B., Mhammdi, N., Ouakil, A., Qninba, A., Dakki, M. (2023b). Contribution of the Catchment Area to the Hydrology of a Saharan Wetland, the Imlili Sebkha

(Dakhla Region, Morocco) – Use of GIS and Satellite Data. Ecological Engineering & Environmental Technology, 24(4), 88-96. DOI: 10.12912/27197050/161951

Ben Hichou, B., Dakki, M., Mhammdi, N. (2023c) Determining the Impact of a Dam on the Natural Hydro-Sedimentary Dynamics Using Remote Sensing and GIS: Case of the Hassan Ad-Dakhil Dam (South-East Morocco), IEEE Asia-Pacific Conference on Geoscience, Electronics and Remote Sensing Technology (AGERS), Surabaya, Indonesia, 2023, pp. 12-18, DOI: 10.1109/AGERS61027.2023.10490533.

Bennet, B.M., Hoffman, D., Prakashi, C. (1989). Observer Mechanics—A Formal Theory of Perception, Academic Press: Cambridge, MA, USA.

Bernardi, D., Schippa, L. (2014). A mobile bed 1D numerical model to support Red River (VietNam basin management. In: Proceedings of the 7th International Conference on Fluvial Hydraulics. DOI: 10.1201/b17133-229

Bhatti, M.T., Ashraf, M., Anwar, A.A. (2021). Soil erosion and sediment load management strategies for sustainable irrigation in arid regions. Sustainability 13 (6 , 3547. DOI: 10.3390/su13063547

Biggin, D. S. (1996). A comparison of ERS-1 satellite radar and aerial photography for river flood mapping. Water and Environment Journal: The Journal, 10(1), 59–64. doi:10.1111/j.1747-6593.1996.tb00009.x

Bizzi, S., et al. (2015). On the control of riverbed incision induced by run-of-river power plant. Water Resour. Res. 51 (7 , 5023-5040. Conservancy, C.S.C., 2007. San Clemente Dam Removal Project Technical Assistance, p. 7. DOI: 10.1002/2014WR016237

Bouabdelli M., 1989 - Tectonique et sédimentation dans un bassin orogénique: le sillon viséen D'Azrou-Khénifra (Est du Massif hercynien central du Maroc). Thèse Doctorat es-Sciences, Strasbourg, 259p.

Brean W. Duncan, Guofan Shao, Frederic W. Adrian. (2009). Delineating a managed fire regime and exploring its relationship to the natural fire regime in East Central Florida, USA: A remote sensing and GIS approach, Forest Ecology and Management, Volume 258, Issue 2, Pages 132-145, ISSN 0378-1127.

Brinson M. M. (1993). A Hydrogeomorphic classification for wetlands. Technical Report WRP-DE-4, U.S. Army Engineer Waterways Experiment Station, Vicksburg, MS. Pp0-68.

Briscoe J. (1999). Water resources management in Yemen: results of a consultation. Off. memo., World Bank, Washington.

Bruland G. L. (2008). Coastal wetlands: function and role in reducing impact of land-based management. Natural Resources and Environmental Management

Department, University of Hawaii Manoa, USA. pp 1-39. DOI: 10.2495/978-1-84564-091-0/04

Chakiri S., 1991 - Le Paléozoïque de la région de Tsili-Tiddas (Maroc central occidental),Stratigraphie, Sédimentologie et évolution structurale hercynienne. Thèse de 3ème Cycle, Univ. Rabat, 227p.

Chalkias, C., Stathopoulos, N., Kalogeropoulos, K., & Karymbalis, E. (2016). Applied hydrological modeling with the use of geoinformatics: Theory and practice. In Empirical Modeling and Its Applications. doi:10.5772/62824

Chappell, A., Webb, N. P., Guerschman, J. P., Thomas, D. T., Mata, G., Handcock, R. N., … Butler, H. J. (2018). Improving ground cover monitoring for wind erosion assessment using MODIS BRDF parameters. Remote Sensing of Environment, 204, 756–768. doi:10.1016/j.rse.2017.09.026

Chen, Z., Liu, Z., Yin, L., Zheng, W. (2022). Statistical analysis of regional air temperature characteristics before and after dam construction. Urban Clim 41, 101085. https:// doi.org/10.1016/j.uclim.2022.101085.

Chessman BC, Fryirs KA, Brierley GJ. (2006). Linking geomorphic character, behaviour and condition to fluvial biodiversity: implications for river management. Aquat. Conserv. Mar. Freshw. Ecosystems, 16, pp. 267-288. DOI: 10.1002/aqc.724

Choudhari, K., Panigrahi, B., Chandra, J.P. (2014). Simulation of rainfall-runoff process using HEC-HMS model for Balijore Nala watershed, Odisha, India. Int. J. Geomat. Geosci. 2014, 5, 253–265.

Chowdary, V. M., Chakraborthy, D., Jeyaram, A., Murthy, Y. V. N. K., Sharma, J. R., & Dadhwal, V. K. (2013). Multi-criteria decision making approach for watershed prioritization using analytic hierarchy process technique and GIS. Water Resources Management, 27(10), 3555–3571. doi:10.1007/s11269-013-0364-6

Chris Suh Wanzie. (2003). Wetland conservation and development in the Sahel of Cameroon. Jean-Yves Jamin, Lamine Seiny Boukar, Christian Floret. Cirad - Prasac, 6 p., hal-00137946.

Collins, L., McCarthy, G., Mellor, A., Newell, G., & Smith, L. (2020). Training data requirements for fire severity mapping using Landsat imagery and random forest. Remote Sensing of Environment, 245, 111839.

Colson, D., Petropoulos, G. P., & Ferentinos, K. P. (2018). Exploring the potential of sentinels-1 & 2 of the Copernicus mission in support of rapid and cost-effective wildfire assessment. International Journal of Applied Earth Observation and Geoinformation: ITC Journal, 73, 262–276. doi:10.1016/j.jag.2018.06.011

Cowardin L. M., Carter V., Golet F. C. & LaRoe E.T., 1979. Classification of wetlands and deep-water habitats of the United States. U.S. Department of Interior, Fish and Wildlife Service FWS/OBS-79/31. Washington, D.C.

Crooks S., Herr D., Tamelander J., Laffoley D. & Vandever J. (2011). Mitigating climate change through restoration and management of coastal wetlands and near-shore marine ecosystems: challenges and opportunities. Environment Department Paper, 121, World Bank, Washington, pp 1-47.

Dahl T. E. (1990). Wetlands Losses in the United States 1780's to 1980's. US Fish and Wildlife Service, National Wetlands Inventory Project, Washington, D.C. pp1-11.

Dakki M., El Fellah B. & Qninba A. (2020). Rivers' natural reservoirs: new inputs to the classification of Mediterranean and Saharan wetlands. Bull. Inst. Sci., Rabat, Ser. Sci. Vie, 42,pp.1-14.

Dalezios, N. R., Petropoulos, G. P., & Faraslis, I. N. (2020, April 13). Concepts and methodologies of environmental hazards and disasters. Techniques for Disaster Risk Management and Mitigation, pp. 1–22. doi:10.1002/9781119359203.ch1

Davidson N.C. (2014). How much wetland has the world lost? Long-term and recent trends in global wetland area. CSIRO Publishing. Marine and Freshwater Research. DOI: 10.1071/MF14173

Davies CE., Moss D. & Hill MO. (2004). EUNIS Habitat classification Revised 2004. European Environment Agency, European Topic Centre on Nature Protection and Biodiversity, pp1-270.

Day J.W., Ya'ñez-Arancibia, Kemp A.W.M. and Crump B.C. (2012). Introduction to estuarine ecology. In: Day J.W. et al. (Ed). Estuarine Ecology, 2nd Edition, Wiley-Blackwell, pp. 1-19. DOI: 10.1002/9781118412787.ch1

De Jong, S.M. Applications of reflective remote sensing for land degradation studies in a Mediterranean environment. Ph.D. Thesis, Utrecht University, Utrecht, The Netherlands, 1994.

De Vente, J., & Poesen, J. (2005). Predicting soil erosion and sediment yield at the basin scale: Scale issues and semi-quantitative models. Earth-Science Reviews, 71(1–2), 95–125. doi:10.1016/j.earscirev.2005.02.002

Deekshatulu, B.L., Lohani, B.N., Narayan, L.R.A. Disaster warning and assessment by remote sensing. In Proceedings of the Southeast Asian Conference on Soil Engineering, Taipei, Taiwan, 19–28 May 1980, pp. 819–824.

Devillers P. & Devillers-Terschuren J., (1996). A classification of Palaearctic habitats. Nature and Environment, 78, Council of Europe, Strasbourg, pp. 9-157.

Devillers P., Devillers-Terschuren J., Vander-Linden C., (2001). PHYSIS Palaearctic Habitat Classification. Updated to 10 December 2001. Institut royal des Sciences Naturelles, Bruxelles.

Dewan, A. M., Kumamoto, T., & Nishigaki, M. (2006). Flood hazard delineation in greater Dhaka, Bangladesh using an integrated GIS and remote sensing approach. Geocarto International, 21(2), 33–38. doi:10.1080/10106040608542381

Dewan, A., Corner, R., Saleem, A., Rahman, M. M., Haider, M. R., Rahman, M. M., & Sarker, M. H. (2017). Assessing channel changes of the Ganges-Padma River system in Bangladesh using Landsat and hydrological data. Geomorphology (Amsterdam, Netherlands), 276, 257–279. doi:10.1016/j.geomorph.2016.10.017

Diani, K., Ettazarini, S., Hahou, Y., El Belrhiti, H., Allaoui, W., Mounir, K., & Gourfi, A. (2023). Identification of Soil Erosion Sites in Semiarid Zones: Using GIS, Remote Sensing, and PAP/RAC Model. In Handbook of Hydroinformatics (pp. 169-183). DOI: 10.1016/B978-0-12-821961-4.00003-8

Ding, Y., Wang, M., Fu, Y., Zhang, L., & Wang, X. (2023). A wildfire detection algorithm based on the dynamic brightness temperature threshold. Forests, 14(3), 477. doi:10.3390/f14030477

Domazetović, F., Šiljeg, A., Lončar, N., & Marić, I. (2019). Development of automated multicriteria GIS analysis of gully erosion susceptibility. Applied Geography, 112, 102083. DOI: 10.1016/j.apgeog.2019.102083

Dvorett D., Bidwell, J., Davis, C. & DuBois, C. (2012). Developing a hydrogeomorphic wetland inventory: reclassifying national wetlands inventory polygons in geographic information systems. Wetland, 32, pp. 83-93. DOI: 10.1007/s13157-011-0247-7

Eckelmann, W., Baritz, R., Bialousz, S., Bielek, P., Carré, F., Hrušková, B., Jones, R.J., Kibblewhite, M., Kozak, J., Le Bas, C., et al. (2006). Common Criteria for Risk Area Identification According to Soil Threats, Office for Official Publications of the European Communities: Brussels, Belgium.

El Jazouli, A., Barakat, A., Khellouk, R., Rais, J., & El Baghdadi, M. (2019). Remote sensing and GIS techniques for prediction of land use land cover change effects on soil erosion in the high basin of the Oum Er Rbia River (Morocco). Remote Sensing Applications: Society and Environment, 13, 361-374. DOI: 10.1016/j.rsase.2018.12.004

Elasha B. O., (2010). Mapping of Climate Change Threats and Human Development Impacts in the Arab Region. UNDP Regional Bureau for Arab States, Arab Human Development Report, Research Paper Series. 40pp.

Elliott M. & McLusky D. S., (2002). The need for definitions in understanding estuaries. Estuarine, Coastal and Shelf Science, 55, 6, pp.815-827. DOI: 10.1006/ecss.2002.1031

Elliott M. & Whitfield A.K., (2011). Challenging paradigms in estuarine ecology and management. Estuarine, Coastal and Shelf Science, 94, pp.306-314. DOI: 10.1016/j.ecss.2011.06.016

EPA (Environmental Protection Agency), (2005). Wetland Mapping and Classification Methodology: Overall Framework. A Method to Provide Baseline Mapping and Classification for Wetlands in Queensland, Version 1.2. Queensland Government, Brisbane.

EPA (Environmental Protection Authority). (2009). The 4th National Report: Assessing Progress towards the 2010 Target - The 4th National CBD Report. Ministry of Water and Environment, Yemen. 100pp.

Erwin K., (2008). Wetlands and global climate change: the role of wetland restoration in a changing world. Wetlands Ecol. Management, 17, pp.71-84. DOI: 10.1007/s11273-008-9119-1

Evans D. (2012). The EUNIS habitats classification - past, present and future. Revista de Investigacion Marina, 19, 2, pp.28-29.

Evans MI. (ed.), (1994). Important Bird Areas in the Middle East. BirdLife Conservation Series No.2. BirdLife International, Cambridge, 410pp.

Evans, A., Lamine, S., Kalivas, D., Petropoulos, G.P. (2018). Exploring the Potential of EO data and GIS for Ecosystem Health Modelling in Response to Wildfire: A Case Study in Central Greece. Environ. Eng. Manag.

Fang, X., Wang, Q., Wang, J., Xiang, Y., Wu, Y., Zhang, Y. (2021). Employing extreme value theory to establish nutrient criteria in bay waters: A case study of Xiangshan Bay. J. Hydrol. DOI: 10.1016/j.jhydrol.2021.127146.

FAO. (1994). Organisation des Nations Unis pour l'Alimentation et l'Agriculture. Introduction à la gestion conservatoire de l'eau, de la biomasse et de la fertilité des sols (CGES). Bulletin Pédologique de la FAO n°70, 420p

Farinha JC., Costa L., Zalidis G., Mantzavelas A., Fitoka E., Hecker N. & Tomàs-Vives P., 1996. Mediterranean wetland inventory: Habitat Description System. MedWet Publication, ICN/Wetlands International/Greek Biotope Wetland Centre, Publication N° III.

Fernandez, P., Delgado, E., Lopez-Alonso, M., & Poyatos, J. M. (2018). GIS environmental information analysis of the Darro River basin as the key for the management and hydrological forest restoration. The Science of the Total Environment, 613–614, 1154–1164. doi:10.1016/j.scitotenv.2017.09.190

Ferreira, R. M., Franca, M. J., Leal, J. G., & Cardoso, A. H. (2009). Mathematical modelling of shallow flows: Closure models drawn from grain-scale mechanics of sediment transport and flow hydrodynamics. Canadian journal of civil engineering, 36(10), 1605-1621.

Finlayson C.M. & Van der Valk A. G., (1995). Wetland classification and inventory: a summary. Plant Ecology 118, 1, pp.185-192. DOI: 10.1007/BF00045199

Fisher, R. A. (1922). On the mathematical foundations of theoretical statistics. Philosophical Transactions of the Royal Society of London. Series A, Containing Papers of a Mathematical or Physical Character, 222, 309-368.

Fistikoglu, O., & Harmancioglu, N. B. (2002). Water Resources Management, 16(6), 447–467. doi:10.1023/a:1022282125760

Forkuo, E.K. (2011). Flood hazard mapping using Aster image data with GIS. Int. J. Geomat. Geosci. 2011, 1, 932–950.

Fortin, J.-P., Turcotte, R., Massicotte, S., Moussa, R., Fitzback, J., & Villeneuve, J.-P. (2001). Distributed watershed model compatible with remote sensing and GIS data. I: Description of model. Journal of Hydrologic Engineering, 6(2), 91–99. doi:10.1061/(asce)1084-0699(2001)6:2(91)

Fugura, A.A., Billa, L., Pradhan, B., Mohamed, T.A., Rawashdeh, S. (2011). Coupling of hydrodynamic modeling and aerial photogrammetry-derived digital surface model for flood simulation scenarios using GIS: Kuala Lumpur flood, Malaysia. Disaster Adv. 2011, 4, 20–28.

Fuller W.E. (1914). Flood flows [Section]//Trans. Soc. Civ. Eng. Vol. LXXVII.

Funk, C., Peterson, P., Landsfeld, M., Pedreros, D., Verdin, J., Shukla, S., Husak, G., Rowland, J., Harrison, L., Hoell, A., Michelsen, J. (2015). The Climate Hazards Infrared Precipitation with Stations - A New Environmental Record for Monitoring Extremes. Scientific Data, 2(1), 1-21. DOI: 10.1038/sdata.2015.66

Ganasri, B. P., & Ramesh, H. (2016). Assessment of soil erosion by RUSLE model using remote sensing and GIS - A case study of Nethravathi Basin. Geoscience Frontiers, 7(6), 953–961. doi:10.1016/j.gsf.2015.10.007

Gao, G., Liang, Y., Liu, J., Dunkerley, D., & Fu, B. (2023). A modified RUSLE model to simulate soil erosion under different ecological restoration types in the loess hilly area. International Soil and Water Conservation Research. DOI: 10.1016/j.iswcr.2023.08.007

Ge, D., Yuan, H., Xiao, J., Zhu, N. (2019). Insight into the enhanced sludge dewaterability by tannic acid conditioning and pH regulation. Sci. Total Environ. 679, 298-306. DOI: 10.1016/j.scitotenv.2019.05.060.

Ghali R, Akhloufi MA. (2023). Deep Learning Approaches for Wildland Fires Remote Sensing: Classification, Detection, and Segmentation. Remote Sensing. 2023; 15(7):1821.

Ghanem Haddou ,1981 Contribution à la connaissance des sols du Maroc : classification genese et répartition des sols des régions des Zaers de la Basse-Chaouia et des Sehouls (Meseta Atlantique Marocaine)

Gillespie, T. W., Chu, J., Frankenberg, E., & Thomas, D. (2007). Assessment and prediction of natural hazards from satellite imagery. Progress in Physical Geography, 31(5), 459–470. doi:10.1177/0309133307083296

Giordano, A., Bonfils, P., Briggs, D. J., de Sequeira, E. M., de Laburu, C. R., & Yassoglou, N. (1991). The methodological approach to soil erosion and important land resources evaluation of the European community. Soil Technology, 4(1), 65–77. doi:10.1016/0933-3630(91)90040-t

Gioti, E., Riga, C., Kalogeropoulos, K., Chalkias, C. A GIS-based flash flood runoff model using high resolution DEM and meteorological data. EARSeL eProceedings 2013, 12, 33–43.

Gopal B.& Sah M. (1995). Inventory and Classification of Wetlands in India. Vegtatio, 118, Kluwer Academic Publishers, Belgium, pp. 39-48. DOI: 10.1007/978-94-011-0427-2_5

Granville, K., Woolford, D. G., Dean, C. B., & McFayden, C. B. (2022). Wildland fire prevention: the impact of the Modifying Industrial Operations Protocol on the growth of industrial forestry-caused wildland fires in Ontario, Canada. International Journal of Wildland Fire, 31(9), 825–834. doi:10.1071/wf22074

Gregory K.J. (2006). The human role in changing river channels. Geomorphology, 79, pp.172-191. DOI: 10.1016/j.geomorph.2006.06.018

Guan, Q., Feng, L., Tang, J., Park, E., Ali, T. A., & Zheng, Y. (2022). Trends in river total suspended sediments driven by dams and soil erosion: A comparison between the Yangtze and Mekong rivers. Water Resources Research, 58(10), e2022WR031979. DOI: 10.1029/2022WR031979

Hamilton, S. K. (2022). Flood Plains of Large Rivers. Encyclopedia of Inland Waters (Second Edition), Elsevier, 290-300. ISBN 9780128220412. DOI: 10.1016/B978-0-12-819166-8.00091-8

Handmer, J.W., Milne, J. Flood maps as public information. In Proceedings of the Floodplain Management Conference, Canberra, Australia, 7–10 May 1980, Conference Series 4. Australian Water Resources Council: Canberra, Australia, Australian Government Publishing Service: Canberra, Australia, 1981, pp. 1–26.

Harvey GL, Clifford NJ, Gurnell AM. (2008). Towards an ecologically meaningful classification of the flow biotope for river inventory, rehabilitation, design and appraisal purposes. J Environ Management, 88, pp.638-650. DOI: 10.1016/j.jenvman.2007.03.039

Hazan R. et Lazarevic D., Détermination des débits maximum et hydrogramme de crues [Rapport]. - Rabat : Office National des Irrigations, 1969. - pp. 354-361.

Haznedar, B., Kilinc, H. C., Ozkan, F., & Yurtsever, A. (2023). Streamflow forecasting using a hybrid LSTM-PSO approach: the case of Seyhan Basin. Natural Hazards, 117(1), 681-701. DOI: 10.1007/s11069-023-05877-3

Hegg, B. (2020). Burn out and backfire/backfiring. In Encyclopedia of Wildfires and Wildland-Urban Interface (WUI) Fires (pp. 1–3). doi:10.1007/978-3-319-51727-8_264-1

Helmi, A. M. (2023). Quantifying catchments sediment release in arid regions using GIS-based Universal soil loss equation (USLE). Ain Shams Engineering Journal, 14(8), 102038. DOI: 10.1016/j.asej.2022.102038

Hilali M., Baki S., Benaissi L., Emran A., Bahaj T., Eddahby L. (2020). Caractérisation hydrologique et hydrogéologique d'une sebkha soumise à un climat de type saharien : Cas de la sebkha d'Imlili (Province Oued Eddahab, Maroc). In : Qninba et al. (Eds) : Sebkhat Imlili, une zone humide saharienne relique. Région Dakhla-Oued Eddahab/Inst. Sci. Rabat, Ass. Nat. Init. Dakhla, pp. 3-18.

Hill M.O., 1973. Reciprocal averaging: An eigenvector method of ordination. Journal of Ecology, 61, 2, pp. 237-249. DOI: 10.2307/2258931

Himmi O., Bayed A., El Agbani M.A., El Belle T., Khayya M.L. et Qninba. A. (2020). Biodiversité aquatique de la Sebkha d'Imlili. In : Qninba et al. (Eds). Sebkhat Imlili, une zone humide saharienne relique. Région Dakhla-Oued Eddahab/Inst. Sci. Rabat, Ass. Nat. Init. Dakhla, pp. 71-83.

Hollingsworth, L. T. (2020). Backing Fire. In Encyclopedia of Wildfires and Wildland-Urban Interface (WUI) Fires (pp. 1–6). doi:10.1007/978-3-319-51727-8_185-1

Huang, S., Li, J., & Xu, M. (2012). Water surface variations monitoring and flood hazard analysis in Dongting Lake area using long-term Terra/MODIS data time series. Natural Hazards (Dordrecht, Netherlands), 62(1), 93–100. doi:10.1007/s11069-011-9921-6

Huang, Y., Ba'rdossy, A., Zhang, K. (2019). Sensitivity of hydrological models to temporal https://hess.copernicus.org/articles/23/2647/2019/

Hubert-Moy, L., Ganzetti, I., Bariou, R., & Mounier, J. (1992). Une cartographie des zones inondables en Ille-et-Vilaine par télédétection. Norois, 155(1), 337–347. doi:10.3406/noroi.1992.6438

Hushulong Q. (2012). The Problems of Wetlands in Our Country and the Researches. International Conference on Future Electrical Power and Energy Systems. Energy Procedia, 17, pp 462-466. DOI: 10.1016/j.egypro.2012.02.121

Ibàñez, C., Prat, N., & Canicio, A. (1996). Changes in the hydrology and sediment transport produced by large dams on the lower Ebro river and its estuary. Regulated Rivers: Research & Management, 12(1), 51-62. DOI: 10.1002/(SICI)1099-1646(199601)12:1<51::AID-RRR376>3.0.CO;2-I

Ibn Tattou M. (2020). Contribution à l'étude de la flore et de la végétation de Sebkhat Imlili (Sahara océanique). In : Qninba et al. (Eds) : Sebkhat Imlili, une zone humide saharienne relique. Région Dakhla-Oued Eddahab/Inst. Sci. Rabat, Ass. Nat. Init. Dakhla, pp. 49-61.

Ireland, G., & Petropoulos, G. P. (2015). Exploring the relationships between post-fire vegetation regeneration dynamics, topography and burn severity: A case study from the Montane Cordillera Ecozones of Western Canada. Applied Geography (Sevenoaks, England), 56, 232–248. doi:10.1016/j.apgeog.2014.11.016

Ireland, G., Volpi, M., & Petropoulos, G. (2015). Examining the capability of supervised machine learning classifiers in extracting flooded areas from Landsat TM imagery: A case study from a Mediterranean flood. Remote Sensing, 7(3), 3372–3399. DOI: 10.3390/rs70303372

Jang, E. (2017). Sediment Discharge Assessment for Rivers Using Model Tree in Data Mining. University of Myongji Yongin, Korea. DOI: 10.1080/02626667.2023.2221790

Jay D. A., Geyer, W. R. & Montgomery, D. R. (2000). An ecological perspective on estuarine classification. In: Hobbie, J.E. (Ed.), Estuarine Science: a synthetic approach to research and practice. Island Press, Washington, pp.149-176.

Jeyaseelan, A. (2003). Droughts and Floods Assessment and Monitoring Using Remote Sensing and GIS, Satellite Remote Sensing and GIS Applications in Agri-Cultural Meteorology, World Meteorological Organization: Dehra Dun, India, Geneva, Switzerland.

Jha, M.K., Paudel, R.C. (2010). Erosion predictions by empirical models in a mountainous watershed in Nepal. J. Spat. Hydrol. 2010, 10, 89–102.

Jia, Y., Wang, H., Zhou, Z., Qiu, Y., Luo, X., Wang, J., … Qin, D. (2006). Development of the WEP-L distributed hydrological model and dynamic assessment of water resources in the Yellow River basin. Journal of Hydrology, 331(3–4), 606–629. doi:10.1016/j.jhydrol.2006.06.006

Jiao, Z., Zhang, Y., Mu, L., Xin, J., Jiao, S., Liu, H., & Liu, D. (2020). A YOLOv3-based learning strategy for real-time UAV-based forest fire detection. 2020 Chinese Control And Decision Conference (CCDC). Presented at the 2020 Chinese Control And Decision Conference (CCDC), Hefei, China. doi:10.1109/ccdc49329.2020.9163816

Joyce, K. E., Belliss, S. E., Samsonov, S. V., McNeill, S. J., & Glassey, P. J. (2009). A review of the status of satellite remote sensing and image processing techniques for mapping natural hazards and disasters. Progress in Physical Geography, 33(2), 183–207. doi:10.1177/0309133309339563

Julien, P.Y. (2018). River Mechanics. Cambridge University Press. DOI: 10.1017/9781316107072

Junk W. J., Piedade M. T. F., Lourival R., Wittmann F., Kandus P., Lacerda L. D., Bozelli R. L., Esteves F. A., Cunha C. N., Maltchik L., Schongart J., Schaeffer-novelli Y. & Agostinho A. A., (2013). Brazilian wetlands: their definition, delineation, and classification for research, sustainable management, and protection. Aquatic Conserv. Mar. Freshw. Ecosystems. DOI: 10.1002/aqc.2386

Kala, C. P. (2023). Environmental and socioeconomic impacts of forest fires: A call for multilateral cooperation and management interventions. Natural Hazards Research.

Kalivas, D. P., Petropoulos, G. P., Athanasiou, I. M., & Kollias, V. J. (2013). An intercomparison of burnt area estimates derived from key operational products: the Greek wildland fires of 2005–2007. Nonlinear Processes in Geophysics, 20(3), 397–409. doi:10.5194/npg-20-397-2013

Kalogeropoulos, K., Chalkias, C., Pissias, E., & Karalis, S. (2011). Application of the SWAT model for the investigation of reservoirs creation. In Advances in the Research of Aquatic Environment (pp. 71–79). doi:10.1007/978-3-642-24076-8_9

Kalogeropoulos, K., Karalis, S., Karymbalis, E., Chalkias, C., Chalkias, G., Katsafados, P. (2013). Modeling Flash Floods in Vouraikos River Mouth, Greece. In Proceedings of the MEDCOAST Conference Proceedings2013, Marmaris, Turkey, 30 October–3 November 2013, Volume II, pp. 1135–1146.

Kalogeropoulos, K., Stathopoulos, N., Psarogiannis, A., Penteris, D., Tsiakos, C., Karagiannopoulou, A., Krikigianni, E., Karymbalis, E., Chalkias, C. (2016).A GIS-based method for flood risk assessment. In Proceedings of the European Geosciences Union General Assembly 2016, Vienna, Austria, 17–22.

Kalogeropoulos, K., Stathopoulos, N., Psarogiannis, A., Pissias, E., Louka, P., Petropoulos, G. P., & Chalkias, C. (2020). An integrated GIS-hydro modeling methodology for surface runoff exploitation via small-scale reservoirs. Water, 12(11), 3182. doi:10.3390/w12113182

Kalogeropoulos, Kleomenis, & Chalkias, C. (2013). Modelling the impacts of climate change on surface runoff in small Mediterranean catchments: empirical evidence from Greece. Water and Environment Journal: The Journal, 27(4), 505–513. doi:10.1111/j.1747-6593.2012.00369.x

Kang, W., Jang, E. K., Yang, C. Y., & Julien, P. Y. (2021). Geospatial analysis and model development for specific degradation in South Korea using model tree data mining. Catena, 200, 105142. DOI: 10.1016/j.catena.2021.105142

Karamesouti, M., Petropoulos, G. P., Papanikolaou, I. D., Kairis, O., & Kosmas, K. (2016). Erosion rate predictions from PESERA and RUSLE at a Mediterranean site before and after a wildfire: Comparison & implications. Geoderma, 261, 44–58. doi:10.1016/j.geoderma.2015.06.025

Karydas, C. G., & Panagos, P. (2018). The G2 erosion model: An algorithm for month-time step assessments. Environmental Research, 161, 256–267. doi:10.1016/j.envres.2017.11.010

Karydas, C. G., Panagos, P., & Gitas, I. Z. (2014). A classification of water erosion models according to their geospatial characteristics. International Journal of Digital Earth, 7(3), 229–250. doi:10.1080/17538947.2012.671380

Kastridis, A., Margiorou, S., & Sapountzis, M. (2022). Check-dams and silt fences: Cost-effective methods to monitor soil erosion under various disturbances in forest ecosystems. Land, 11(12), 2129. DOI: 10.3390/land11122129

Key, C. H., & Benson, N. C. (2005). Landscape assessment (LA): Sampling and analysis methods. In Entwistle, P.G., DeBano, L.F., Neary, D.G. (Tech. Coords.), Proceedings: Restoration of American Southwest Ponderosa Pine Forests, General Technical Report. RMRS-GTR-150, 73-84. Fort Collins, CO: U.S. Department of Agriculture, Forest Service, Rocky Mountain Research Station.

Khomsi, K., Mahe, G., Sinan, M., Snoussi, M. (2014). Evolution des évènements chauds rares dans les bassins versants de Tensift et Bouregreg. In : Laouina, A. & Mahe, G. (Eds.), Gestion durable des terres. Proceedings de la réunion multi-acteurs sur le bassin du Bouregreg. CERGéo, Faculté des Lettres et Sciences Humaines, Université

Mohammed V-Agdal, Rabat, 28 mai 2013. Edité par ARGDT, Rabat, Maroc, ISBN 978-9954-33-482-9, 37-52.

Kimbrough, L. (2022). Forest Fires Are Getting Worse, 20 Years of Data Confirm. Monfabay. Available online: https://news.mongabay.com/2022/08/forest-fires-are-getting-worse-according-to-new-20-year-analysis/ (accessed on 17 August 2022).

Knebl, M. R., Yang, Z.-L., Hutchison, K., & Maidment, D. R. (2005). Regional scale flood modeling using NEXRAD rainfall, GIS, and HEC-HMS/RAS: a case study for the San Antonio River Basin Summer 2002 storm event. Journal of Environmental Management, 75(4), 325–336. doi:10.1016/j.jenvman.2004.11.024

Knorr, W., Pytharoulis, I., Petropoulos, G.P., Gobron, N. (2011). Combined Use of Weather Forecasting and Satellite Remote Sensing Information for Fire Risk, fire and fire impact monitoring. Comput. Ecol. Softw. 2011, 1, 112–120.

Kondolf GM, Montgomery DR, Piegay H, Schmitt L. (2003). Geomorphic classification of rivers and streams. In: Kondolf GM, Piegay H Eds. Tools in Fluvial Geomorphology. Wiley & Sons, pp. 171-204. DOI: 10.1002/0470868333.ch7

Kosmopoulos, P., Kazadzis, S., El-Askary, H., Taylor, M., Gkikas, A., Proestakis, E., … El-Khayat, M. (2018). Earth-Observation-based estimation and forecasting of particulate matter impact on solar energy in Egypt. Remote Sensing, 10(12), 1870. doi:10.3390/rs10121870

Kothyari, U.C. Erosion and sediment problems in India. In Proceedings of the Exeter Symposium on Erosion and Sediment Yield: Global and Regional Perspectives, IAHS Publication No. 236, ISI: Exeter, UK, 1996, pp. 531–540.

Kourgialas, N. N., Karatzas, G. P., & Nikolaidis, N. P. (2010). An integrated framework for the hydrologic simulation of a complex geomorphological river basin. Journal of Hydrology, 381(3–4), 308–321. doi:10.1016/j.jhydrol.2009.12.003

Kulsoontornrat, J., Ongsomwang, S. (2021). Suitable land-use and land-cover allocation scenarios to minimize sediment and nutrient loads into kwan phayao, upper ing watershed, Thailand. Appl. Sci. 11 (21 , 10430. DOI: 10.3390/app112110430

Lacroix, M. P., Martz, L. W., Kite, G. W., & Garbrecht, J. (2002). Using digital terrain analysis modeling techniques for the parameterization of a hydrologic model. Environmental Modelling & Software: With Environment Data News, 17(2), 125–134. doi:10.1016/s1364-8152(01)00042-1

Ladson T. (1999). An index of stream condition: manual for catchment managers. Waterways Unit, Depart. Nat. Res. Env., Victoria, 30 pp.

Lal, R. (2001). Soil degradation by erosion. Land Degradation and Development, 12(6), 519–539. doi:10.1002/ldr.472

Lal, R. (2003). Soil erosion and the global carbon budget. Environment International, 29(4), 437–450. doi:10.1016/S0160-4120(02)00192-7

Lavergne E. (2012). Estuarine fish biodiversity of Socotra Island (N.W. Indian Ocean): from the fish community to the functioning of Terapon jarbua populations. Biodiversity and Ecology, Univ. Bretagne occidentale, Brest, France.

Lebart L., Morineau A. & Tabard N. (1977). Techniques de la description statistique, méthodes et logiciels pour l'analyse des grands tableaux. Bordas Ed., Paris, 351pp.

Lee, G.-S., & Lee, K.-H. (2006). Scaling effect for estimating soil loss in the RUSLE model using remotely sensed geospatial data in Korea. Hydrology and Earth System Sciences Discussions, 3(1), 135–157. doi:10.5194/hessd-3-135-2006

Leh, M., Bajwa, S., & Chaubey, I. (2013). Impact of land use change on erosion risk: An integrated remote sensing, geographic information system and modeling methodology. Land Degradation and Development. doi:10.1002/ldr.1137

Lekkas, E. (2000). Natural and Technological Disasters, Access Pre-Press, Available online: https://www.researchgate.net/publication/226053524_Natural_and_Technological_Disasters (accessed on 2 February 2021).

Lellis-Dibble K.A., McGlynn K.E., & Bigford T.E. (2008). Estuarine Fish and Shellfish Species in U.S. Commercial and Recreational Fisheries: Economic Value as an Incentive to Protect and Restore Estuarine Habitat. National Marine Fisheries Service, NOAA Technical Memorandum NMFS-F/SPO-90. 94pp.

Li, H., Zhang, T., Tsang, D. C., & Li, G. (2020). Effects of external additives: Biochar, bentonite, phosphate, on co-composting for swine manure and corn straw. Chemosphere, 248, 125927. DOI: 10.1016/j.chemosphere.2020.125927

Liu, C.-C., Wu, A.-M., Yen, S.-Y., & Huang, C.-H. (2009). Rapid locating of fire points from Formosat-2 high spatial resolution imagery: example of the 2007 California wildfire. International Journal of Wildland Fire, 18(4), 415. doi:10.1071/wf08026

Liu, E., Chen, S., Yan, D., Deng, Y., Wang, H., Jing, Z., Pan, S. (2022). Detrital zircon geochronology and heavy mineral composition constraints on provenance evolution in the western Pearl River Mouth basin, northern south China sea: A source to sink approach. Mar. Petrol. Geol. 145, 105884. DOI: 10.1016/j. marpetgeo.2022.105884.

Liu, J., Zheng, H., Shen, Y., Xing, B., & Wang, X. (2023). Variation in sediment sources and the response of suspended sediment grain size in the upper Changjiang Basin following the large dam constructions. Science of The Total Environment, 166869. DOI: 10.1016/j.scitotenv.2023.166869

Liu, K., Li, Z., Yao, C., Chen, J., Zhang, K., Saifullah, M. (2016). Coupling the k-nearest neighbor procedure with the Kalman filter for real-time updating of the hydraulic DOI: 10.1016/j.ijsrc.2016.02.002

Maantay, J., & Maroko, A. (2009). Mapping urban risk: Flood hazards, race, & environmental justice in New York". Applied Geography (Sevenoaks, England), 29(1), 111–124. doi:10.1016/j.apgeog.2008.08.002

Macedo, D. R., Hughes, R. M., Kaufmann, P. R., & Callisto, M. (2018). Development and validation of an environmental fragility index (EFI) for the neotropical savannah biome. The Science of the Total Environment, 635, 1267–1279. doi:10.1016/j.scitotenv.2018.04.216

Maffei, C., Lindenbergh, R., & Menenti, M. (2021). Combining multi-spectral and thermal remote sensing to predict forest fire characteristics. ISPRS Journal of Photogrammetry and Remote Sensing, 181, 400-412.

Mahe, G. Benabdelfadel, H. Dieulin ,C. Elbaraka, M. Ezzaouini , M . Khomsi, k. Rouche, N. Sinan, M. Snoussi, M. Trabi, A. Zerouali, A. (2014) Evolution des débits liquides et solides du Bouregreg. Quantification des MES au Bassin versant du Bouregreg, méthode MUSLE

Mahe, G., Aksoy, H., Brou, Y.T, Meddi, M., Roose, E. (2013) Relationships between man, environment and sediment transport: a spatial approach. Revue des Sciences de l'Eau, 26, 3, 235-244.

Martin G.I., Kirkman L.K. & Hepinstall-Cymerman J. (2011). Mapping geographically isolated wetlands in the Dougherty Plain, Georgia, USA. Wetlands. DOI: 10.1007/s13157-011-0263-7

McCartney M., Rebelo L-M., Senaratna-Sellamuttu S. & de Silva S. (2010). Wetlands, agriculture and poverty reduction., Colombo, Sri Lanka. IWMI Research Report 137, 26pp. Doi: 10.5337/2010.230. DOI: 10.5337/2010.230

McColl, C., & Aggett, G. (2007). Land-use forecasting and hydrologic model integration for improved land-use decision support. Journal of Environmental Management, 84(4), 494–512. doi:10.1016/j.jenvman.2006.06.023

McGee, T. K., & Cabling, L. P. B. (2022). Preventing wildfires with fire permits in rural Edson, Alberta. International Journal of Wildland Fire, 31(6), 599–606. doi:10.1071/wf20177

McNeil, B. E., de Beurs, K. M., Eshleman, K. N., Foster, J. R., & Townsend, P. A. (2007). Maintenance of ecosystem nitrogen limitation by ephemeral forest disturbance: An assessment using MODIS, Hyperion, and Landsat ETM+. Geophysical Research Letters, 34(19). doi:10.1029/2007gl031387

MEA (Millennium Ecosystem Assessment). (2005). Ecosystems and Human Well-being: Wetlands and Water Synthesis. World Resources Institute, Washington, DC, pp 1-67.

Melesse, A. M., & Graham, W. D. (2004). Storm runoff prediction based on a spatially distributed travel time method utilizing remote sensing and gis. Journal of the American Water Resources Association, 40(4), 863–879. doi:10.1111/j.1752-1688.2004.tb01051.x

Melissa B. Jenkins, Anna W. Schoettle, Jessica W. Wright, Karl A. Anderson, Joseph Fortier, Linh Hoang, Tony Incashola Jr., Robert E. Keane, Jodie Krakowski, Dawn M. LaFleur, Sabine Mellmann-Brown, Elliott D. Meyer, ShiNaasha Pete, Katherine Renwick, Robert A. (2022). Sissons, Restoring a forest keystone species: A plan for the restoration of whitebark pine (Pinus albicaulis Engelm.) in the Crown of the Continent Ecosystem, Forest Ecology and Management, Volume 522, 120282, ISSN 0378-1127.

Mendes, J., & Maia, R. (2016). Hydrologic modelling calibration for operational flood forecasting. Water Resources Management, 30(15), 5671–5685. doi:10.1007/s11269-016-1509-1

Menmohammadi Aicha. (1991). Erosion et sédimentation dans le bassin versant de l'oued Bou-Regreg (S.L.)

Miller, J.R., Turner, M.G., Smithwick, E.A.H., Dent, C.L. & Stanley, E.H. (2004). Spatial extrapolation: the science of predicting ecological patterns and processes. BioScience, 54, pp. 310-320. DOI: 10.1641/0006-3568(2004)054[0310:SETSOP]2.0.CO;2

Milliman, J. D., & Syvitski, J. P. M. (1992). Geomorphic/tectonic control of sediment discharge to the ocean: The importance of small mountainous rivers. The Journal of Geology, 100(5), 525–544. doi:10.1086/629606

Mitsch W.J. & Gosselink J.G., (2000). The value of wetlands: importance of scale and landscape setting. Special Issue: The Values of Wetlands: Landscape and Institutional Perspectives. Ecological Economics, 35, pp 25-33. DOI: 10.1016/S0921-8009(00)00165-8

NBSAPY. (2005). National Biodiversity Strategy and Action Plan for Yemen. Environ. Prot. Authority. Min. Water and Env., Yemen, UNDP/GEF/IUCN. YEM/96/G31. Pp1-70.

Nearing, M.A., Pruski, F.F., O'neal, M.R. (2004). Expected climate change impacts on soil erosion rates: A review. J. Soil Water Conserv. 2004, 59, 43–50.

Neugirg, F., Stark, M., Kaiser, A., Vlacilova, M., Della Seta, M., Vergari, F., … Haas, F. (2016). Erosion processes in calanchi in the Upper Orcia Valley, Southern Tuscany, Italy based on multitemporal high-resolution terrestrial LiDAR and UAV surveys. Geomorphology (Amsterdam, Netherlands), 269, 8–22. doi:10.1016/j.geomorph.2016.06.027

Nigel, R., & Rughooputh, S. (2010). Mapping of monthly soil erosion risk of mainland Mauritius and its aggregation with delineated basins. Geomorphology (Amsterdam, Netherlands), 114(3), 101–114. doi:10.1016/j.geomorph.2009.06.013

Nikolaos, S., Kleomenis, K., Elias, D., Panagiotis, S., Panagiota, L., Vagelis, P., & Christos, C. (2019). A robust remote sensing–spatial modeling–remote sensing (R-M-R) approach for flood hazard assessment. In Spatial Modeling in GIS and R for Earth and Environmental Sciences (pp. 391–410). doi:10.1016/b978-0-12-815226-3.00017-x

Nolè, A., Rita, A., Spatola, M. F., & Borghetti, M. (2022). Biogeographic variability in wildfire severity and post-fire vegetation recovery across the European forests via remote sensing-derived spectral metrics. Science of The Total Environment, 823, 153807.

Noss R., La Roe E. & Scott M. (1995). Endangered Ecosystems of the United States: A Preliminary Assessment of Loss and Degradation. Univ. Idaho, Department of Fish and Wildlife Moscow, Idaho.

NWRA (National Water Resources Authority). (2005). Annual Report. Ministry of Water and Environment. Yemen, 45 pp.

O'Connor N. & Crowe T., (2005). Biodiversity Loss and Ecosystem Functioning: Distinguishing Between Number and Identity of Species. Ecology, 86, 7, pp.1783-1796. DOI: 10.1890/04-1172

Oldeman, L.R., Van Engelen, V.W.P., Pulles, J.H.M. (1990). The extent of human induced soil degradation. In Annex 5 of World Man of the Status of Human-Induced Soil Degradation: An. Explanatory Note, 2nd ed., Oldeman, L.R., Hakkeling, R.T.A., Sombroek, W.G., Eds., International Soil Reference and Information Center: Wageningen, The Netherlands.

Oris, F., Asselin, H., Ali, A. A., Finsinger, W., & Bergeron, Y. (2014). Effect of increased fire activity on global warming in the boreal forest. Environmental Reviews, 22(3), 206–219. doi:10.1139/er-2013-0062

Ouakil, A., Ben Hichou, B., Kaoutar, E., Taha, A., Jamal, C., Hicham, E. (2022). Coupling of Space Remote Sensing and GIS for Detection of Areas at Risk of Degradation (Sidi Mohammed Ben Abdellah Dam Case (Morocco)). Ecological Engineering & Environmental Technology, 23(6), 161-172. DOI: 10.12912/27197050/152953

Ougougdal H. A., KHEBIZA M. Y., MESSOULI M., BOUNOUA L. (2020). Delineation of vulnerable areas to water erosion in a mountain region using SDR-InVEST model: A case study of the Ourika watershed, Morocco. Scientific African, 10, e00646. DOI: 10.1016/j.sciaf.2020.e00646

Ozesmi S.L. & Bauer, M.E. (2002). Satellite Remote Sensing of Wetlands. Wetlands Ecology and Management, 10, pp.381-402. DOI: 10.1023/A:1020908432489

Özşahin, E. (2023). Climate change effect on soil erosion using different erosion models: A case study in the Naip Dam basin, Türkiye. Computers and Electronics in Agriculture, 207, 107711. DOI: 10.1016/j.compag.2023.107711

Paiva, R. C. D., Collischonn, W., & Buarque, D. C. (2013). Validation of a full hydrodynamic model for large-scale hydrologic modelling in the Amazon. Hydrological Processes, 27(3), 333–346. doi:10.1002/hyp.8425

Pandey, V., Srivastava, P. K., & Petropoulos, G. P. (2020). The contribution of earth observation in disaster prediction, management, and mitigation: A holistic view. In Techniques for Disaster Risk Management and Mitigation (pp. 47–62). Wiley. DOI: 10.1002/9781119359203.ch4

Park, S., Oh, C., Jeon, S., Jung, H., & Choi, C. (2011). Soil erosion risk in Korean watersheds, assessed using the revised universal soil loss equation. Journal of Hydrology, 399(3–4), 263–273. doi:10.1016/j.jhydrol.2011.01.004

Parry M.L., Canziani O.F., Palutikof J.P., van der Linden P.J. & Hanson C.E. (Eds.). (2007). Climate Change 2007: Impacts, Adaptation and Vulnerability. Contribution of Working Group II to the Fourth Assessment Report of the IPCC, Cambridge University Press, 811 pp.

Payra, S., Sharma, A., & Verma, S. (2023). Application of remote sensing to study forest fires. In Atmospheric Remote Sensing (pp. 239-260). Elsevier.

Pearson, R. G., Connolly, N. M., Davis, A. M., & Brodie, J. E. (2021). Fresh waters and estuaries of the Great Barrier Reef catchment: Effects and management of anthropogenic disturbance on biodiversity, ecology, and connectivity. Marine Pollution Bulletin, 166, 112194. DOI: 10.1016/j.marpolbul.2021.112194

Pellegrini, A. F. A., Anderegg, W. R. L., Paine, C. E. T., Hoffmann, W. A., Kartzinel, T., Rabin, S. S., … Pacala, S. W. (2017). Convergence of bark investment according to fire and climate structures ecosystem vulnerability to future change. Ecology Letters, 20(3), 307–316. doi:10.1111/ele.12725

Pelletier, J. D., Mayer, L., Pearthree, P. A., House, P. K., Demsey, K. A., Klawon, J. E., & Vincent, K. R. (2005). An integrated approach to flood hazard assessment on alluvial fans using numerical modeling, field mapping, and remote sensing. Geological Society of America Bulletin, 117(9), 1167. doi:10.1130/b25544.1

Perennou C., Guelmami A., Paganini M., Philipson P., Poulin B., Strauch A., Tottrup C., Truckenbrodt J. & Geijzendorffer I. (2018). Mapping Mediterranean wetlands with remote sensing: a good-looking map is not always a good map. David A. Bohan AJD Guy Woodward and Michelle Jackson, editor. Advances in Ecological Research, 58, pp.243-277. DOI: 10.1016/bs.aecr.2017.12.002

Perissinotto R., Stretch D.D., Whitfield A.K., Adams J.B., Forbes A.T. & Demetriades N.T. (2010). Ecosystem functioning of temporary open/closed estuaries in South Africa. In Crane J.N. & Solomon A.E. (Eds). Estuaries: Types, movement patterns and climatical impacts. Nova Science Publishers, Env. Sci., Engin. & Techn. Series, pp. 1-69.

PERSGA. (2003). Regional Action Plan for the Conservation of Coral Reefs in the Red Sea and Gulf of Aden. PERSGA, Jeddah, Saudi Arabia.

PERSGA. (2004). Regional Action Plan for the Conservation of Mangroves in the Red Sea and Gulf of Aden. PERSGA, Jeddah, Saudi Arabia.

PERSGA. (2019). Regional action plan for the sustainable management of scattered marine waste in the Red Sea and Gulf of Aden. PERSGA Report RP.0091.

Petropoulos, G. P., Kontoes, C. C., & Keramitsoglou, I. (2012). Land cover mapping with emphasis to burnt area delineation using co-orbital ALI and Landsat TM imagery. International Journal of Applied Earth Observation and Geoinformation: ITC Journal, 18, 344–355. doi:10.1016/j.jag.2012.02.004

Petts, G. E. (1984). Impounded rivers: perspectives for ecological management. Wiley.

Pierson-Wickmann, A. C., Gruau, G., Jardé, E., Gaury, N., Brient, L., Lengronne, M., ... & Lambert, T. (2011). Development of a combined isotopic and mass-balance approach to determine dissolved organic carbon sources in eutrophic reservoirs. Chemosphere, 83(3), 356-366. DOI: 10.1016/j.chemosphere.2010.12.014

Pimentel, D. (2006). Soil erosion: A food and environmental threat. Environment Development and Sustainability, 8(1), 119–137. doi:10.1007/s10668-005-1262-8

Piqué A., 1979 - Evolution structurale d'un segment de la chaîne hercynienne: la Meseta marocaine Nordoccidentale. Sci. Géol., Mém., Strasbourg. 56, 253p.

Pissias, E., Psarogiannis, A., Kalogeropoulos, K. (2013). Water savings-a necessity in a changing environment. The case of small reservoirs. In Proceedings of the WIN4life Conference, Tinos, Greece, 19–21.

Pittman SJ, Connor DW, Radke L. & Wright DJ. (2011). Application of Estuarine and Coastal Classifications in Marine Spatial Management. In: Wolanski E and McLusky DS (eds.) Treatise on Estuarine and Coastal Science, Vol 1. Waltham: Academic Press. pp163-205. DOI: 10.1016/B978-0-12-374711-2.00110-8

Polykretis, C., Alexakis, D. D., Grillakis, M. G., & Manoudakis, S. (2020). Assessment of intra-annual and inter-annual variabilities of soil erosion in Crete island (Greece) by incorporating the dynamic “nature” of R and C-factors in RUSLE modeling. Remote Sensing, 12(15), 2439. doi:10.3390/rs12152439

Populus J., More AU F., Coquelet, D., & Xavier, J. P. (1995). An assessment of environmental sensitivity to marine pollutions: solutions with remote sensing and Geographical Information Systems (GIS). International Journal of Remote Sensing 16, pp.3-15, DOI: 10.1080/01431169508954368. DOI: 10.1080/01431169508954368

Poser, K., Dransch, D. (2010). Volunteered geographic information for disaster management with application to rapid flood damage estimation. Geomatica 2010, 64, 89–98.

Price, O. (2019). Bushfires. In Encyclopedia of Wildfires and Wildland-Urban Interface (WUI) Fires (pp. 1–5). doi:10.1007/978-3-319-51727-8_151-1

Priya, R. S., & Vani, K. (2019). Deep learning based forest fire classification and detection in satellite images. 2019 11th International Conference on Advanced Computing (ICoAC). Presented at the 2019 11th International Conference on Advanced Computing (ICoAC), Chennai, India. doi:10.1109/icoac48765.2019.246817

Pulvirenti, L., Pierdicca, N., Chini, M., & Guerriero, L. (2011). An algorithm for operational flood mapping from Synthetic Aperture Radar (SAR) data using fuzzy logic. Natural Hazards and Earth System Sciences, 11(2), 529–540. doi:10.5194/nhess-11-529-2011

Qninba A., Ibn Tattou M., M. Radi, A. El Idrissi Essougrati, H. Bensouiba., S. Ben Moussa, T. Ougga, J. Bouzrou, I. Azaguagh, J. Bensbai et M.L. Khayya. (2009).

Sebkhet Imlily, une zone humide originale dans le Sud marocain. Bull. Inst. Sci., Rabat, Section Sci. Vie, 31, pp. 51-55.

Quan, Q., Gao, S., Shang, Y., Wang, B. (2021). Assessment of the sustainability of Gymnocypris eckloni habitat under river damming in the source region of the Yellow River. Sci. Total Environ. 778, 146312. DOI: 10.1016/j.scitotenv.2021.146312

Quezel P. (1965). La végétation du Sahara du Tchad à la Mauritanie. Geobotanica selecta, Stuttgart, 2, p. 333.

RAMSAR. (2010). Handbook 15 Wetlands Inventory. A Ramsar framework for wetland inventory and ecological character description. Ramsar Handbooks for the wise use of wetlands 4th edition.

RAMSAR. (2011). Convention on wetlands. Wetland Ecosystem Services.

Ranaee, E., Shoushtari, M. M., & Quchani, S. R. (2009). The combination of HEC-Geo-HMS, HEC-HMS and MIKE11 software utilize in a two branches river flood routing modeling. 2009 Second International Conference on Environmental and Computer Science. Presented at the 2009 Second International Conference on Environmental and Computer Science, Dubai, UAE. doi:10.1109/icecs.2009.62

Ranjan P., Kazamaa S., Sawamoto M. (2006). Effects of climate change on coastal fresh groundwater resources, Global Environmental Change, 16, pp. 388-399. DOI: 10.1016/j.gloenvcha.2006.03.006

Rayegani, B., Barati, S., Sohrabi, T. A., & Sonboli, B. (2016). Remotely sensed data capacities to assess soil degradation. Egyptian Journal of Remote Sensing and Space Sciences, 19(2), 207–222. doi:10.1016/j.ejrs.2015.12.001

Rebelo L-M. (2009). Mapping inland wetlands in Africa using long waveband radar: The ALOS Kyoto and Carbon Initiative. International Water Management Institute. Addis Ababa, Ethiopia. pp 1-7.

Rebelo L-M., Finlayson C.M. & Nagabhatla N. (2009). Remote sensing and GIS for wetland inventory, mapping and change analysis. Journal of Environmental Management, 90, pp. 2144-2153. DOI: 10.1016/j.jenvman.2007.06.027

Rjimati E., Zemmouri A. (2011). Notice explicative de la carte géologique du Maroc au 1/100000 ; feuille Imlili. Notes et Mémoires du Service Géologique, N°491 bis.

Rouse Jr., J. W., Haas, R. H., Schell, J. A., & Deering, D. W. (1973). Monitoring vegetation systems in the Great Plains with ERTS. In Third Earth Resources Technology Satellite-1 Symposium, 10-14 December 1973, Greenbelt, Maryland (Vol. 1, pp. 309-317). NASA.

Rozalis, S., Morin, E., Yair, Y., & Price, C. (2010). Flash flood prediction using an uncalibrated hydrological model and radar rainfall data in a Mediterranean watershed under changing hydrological conditions. Journal of Hydrology, 394(1–2), 245–255. doi:10.1016/j.jhydrol.2010.03.021

Rozos, D., Skilodimou, H. D., Loupasakis, C., & Bathrellos, G. D. (2013). Application of the revised universal soil loss equation model on landslide prevention. An example from N. Euboea (Evia) Island, Greece. Environmental Earth Sciences, 70(7), 3255–3266. doi:10.1007/s12665-013-2390-3

Ryan M. Perkl. (2016). Geodesigning landscape linkages: Coupling GIS with wildlife corridor design in conservation planning, Landscape and Urban Planning, Volume 156, Pages 44-58, ISSN 0169-2046.

Sader S. A., Ahl D. & Liou W. S., 1995. Accuracy of Landsat-TM and GIS rule-based methods for forest wetland classification in Maine. Remote Sensing of Environment 53, pp.134-142. DOI: 10.1016/0034-4257(95)00085-F

Said, Y. A., Petropoulos, G. P., & Srivastava, P. K. (2015). Assessing the influence of atmospheric and topographic correction and inclusion of SWIR bands in burned scars detection from high-resolution EO imagery: a case study using ASTER. Natural Hazards (Dordrecht, Netherlands), 78(3), 1609–1628. doi:10.1007/s11069-015-1792-9

Salvacion, A. R. (2023). Soil Erosion Modeling under Future Climate Change: A Case Study on Marinduque Island, Philippines. In Water, Land, and Forest Susceptibility and Sustainability (pp. 381-398). DOI: 10.1016/B978-0-323-91880-0.00012-X

Sanders A.P.L. & Morgan, G.R. (1989). Review of the fisheries resources of the Red Sea and the Gulf of Aden. FAO Fisheries Technical Paper. No, 304. Rome, FAO.pp.1-126.

Sanz, M. M. E., Avendaño, S. C., & Cobo, R. R. (2001). Influencia del complejo de embalses Mequinenza-Ribarroja-Flix (río Ebro) en la morfología del cauce situado aguas abajo.

Schoch G. C., Albert D. M. & Shanley C. S. (2014). An Estuarine Habitat Classification for a Complex Fjordal Island Archipelago. Estuaries and Coasts, 37, pp. 160-176. DOI 10.1007/s12237-013-9622-3. DOI: 10.1007/s12237-013-9622-3

Scott D. A. & Jones T.A., 1995. Classification and inventory of wetlands: A global overview. Vegetatio, 118, Kluwer Academic Publishers, Belgium, pp. 3-16. DOI: 10.1007/978-94-011-0427-2_2

Sebbar A. (2013). Etude de la variabilité et de l'évolution de la pluviométrie au Maroc (1935-2005): Réactualisation de la carte des précipitations. Thèse Doc. Fac. Sci. Ben M'sik, Casablanca, 187 pp.

Setia, R., Dhaliwal, S. S., Singh, R., Kumar, V., Taneja, S., Kukal, S. S., & Pateriya, B. (2021). Phytoavailability and human risk assessment of heavy metals in soils and food crops around Sutlej river, India. Chemosphere, 263, 128321. DOI: 10.1016/j.chemosphere.2020.128321

Shah T.N., Hoogesteger J., Villholth K. and Giordano M. (2009). Groundwater: a global assessment of scale and significance. Annual Review of Environment and Resources, 34, 7, pp. 1-26

Shen, D., Chen, X., Nguyen, M., & Yan, W. Q. (2018). Flame detection using deep learning. 2018 4th International Conference on Control, Automation and Robotics (ICCAR). Presented at the 2018 4th International Conference on Control, Automation and Robotics (ICCAR), Auckland. doi:10.1109/iccar.2018.8384711

Shu, L., Ng, J. C., Tang, W., Zhao, Y., Sun, L., & Zhang, H. (2021). Assessment methodology applied to arsenic pollution in lake sediments combining static and dynamic processes. Chemosphere, 277, 130260. DOI: 10.1016/j.chemosphere.2021.130260

Sinshaw, B. G., Belete, A. M., Mekonen, B. M., Wubetu, T. G., Anley, T. L., Alamneh, W. D., ... Atanaw, S. B. (2021). Watershed-based soil erosion and sediment yield modeling in the Rib watershed of the Upper Blue Nile Basin, Ethiopia. Energy Nexus, 3, 100023. DOI: 10.1016/j.nexus.2021.100023

Skakun, S., Kussul, N., Shelestov, A., & Kussul, O. (2014). Flood hazard and flood risk assessment using a time series of satellite images: a case study in Namibia. Risk Analysis: An Official Publication of the Society for Risk Analysis, 34(8), 1521–1537. doi:10.1111/risa.12156

Smith D., Ammann A., Bartoldus C. & Brinson M. (1995). An Approach for Assessing Wetland Functions Using Hydrogeomorphic Classification, Reference Wetlands, and Functional Indices. Wetlands Research Program Technical Report WRP-DE-9, U.S. Army Corps of Engineers Washington, DC, 20314-1000.

Smith, K. (2001). Environmental Hazards Assessing Risk and Reducing Disaster, 3rd ed., Routledge: London, UK.

Smith, K., Petley, D.N. (2009) Environmental Hazards: Assessing Risk and Reducing Disaster, 5th ed., Routledge: Abingdon, UK,.

Sousa, D., Cruz-Jesus, F., Sousa, A., & Painho, M. (2021). A multivariate approach to assess the structural determinants of large wildfires: evidence from a Mediterranean country. International Journal of Wildland Fire, 30(4), 241. doi:10.1071/wf20119

Srivastava, P. K., Petropoulos, G., Suman, S., Singh, S. K., Islam, T., & Loka, D. (2019). Deriving forest fire probability maps from the fusion of visible/infrared satellite data and geospatial data mining. doi:10.31219/osf.io/8kzcn

Stamellou, E., Kalogeropoulos, K., Stathopoulos, N., Chalkias, C., Katsafados, P. (2017). Flood Assessment via analytical Hierarchy model, GIS & Cellular Automata. In Proceedings of the 11th International Hydrogeological Congress of Greece, Athens, Greece, 4–6 October 2017.

Stancalie, G., & Craciunescu, V. (2005). Contribution of earth observation data supplied by the new satellite sensors to flood disaster assessment and hazard reduction. In Geo-information for Disaster Management (pp. 1315–1332). doi:10.1007/3-540-27468-5_91

Stathopoulos, N., Kalogeropoulos, K., Polykretis, C., Skrimizeas, P., Louka, P., Karymbalis, E., & Chalkias, C. (2017). Introducing flood susceptibility index using remote-sensing data and geographic information systems. In Remote Sensing of Hydrometeorological Hazards (pp. 381–400). doi:10.1201/9781315154947-18

Stathopoulos, N., Louka, P., Kalogeropoulos, K., Karymbalis, E., Papadopoulos, A., Chalkias, C. (2017). Flood Impact Assessment via SAR data analysis and GIS. Applications in Sperchios River Basin Greece. In Proceedings of the 2nd Conference of GIS and Spatial Analysis in Agriculture and Environment, Athens, Greece, 25–26 May 2017.

Stathopoulos, N., Lykoudi, E., Vasileiou, E., Rozos, D., & Dimitrakopoulos, D. (2017). Erosion vulnerability assessment of sperchios river basin, in East Central Greece — A GIS based analysis. Open Journal of Geology, 07(05), 621–646. doi:10.4236/ojg.2017.75043

Stipanicev, D., Bodrozic, L., & Stula, M. (2007). Environmental intelligence based on advanced sensor networks. 2007 14th International Workshop on Systems, Signals and Image Processing and 6th EURASIP Conference Focused on Speech and Image Processing, Multimedia Communications and Services. Presented at the 2007 14th International Workshop on Systems, Signals and Image Processing and 6th EURASIP Conference focused on Speech and Image Processing, Multimedia Communications and Services, Maribor, Slovenia. doi:10.1109/iwssip.2007.4381190

Stone, M., Krishnappan, B. G., Silins, U., Emelko, M. B., Williams, C. H., Collins, A. L., & Spencer, S. A. (2021). A new framework for modelling fine sediment transport in rivers includes flocculation to inform reservoir management in wildfire impacted watersheds. Water, 13(17), 2319. DOI: 10.3390/w13172319

Stuip M.A.M., Baker C.J. & Oosterberg W. (2002). The Socio-economics of Wetlands. Wetlands International and RIZA, The Netherlands, 28pp.

Tahiri A. (1991) - Le Maroc central septentrional: Stratigraphie, Sédimentologie et Tectonique du Paléozoïque; Un exemple de passage des zones internes aux zones externes de la chaîne hercynienne du Maroc. Doctorat ès-Sciences, Univ de Bretagne Occidentale, Brest, France, 300p.

Tahouri J., Sadiki A., Karrat L. H., Johnson V. C., Weng Chan N., Fei Z., Te Kung H. (2022). Using a modified PAP/RAC model and GIS-for mapping water erosion and causal risk factors: Case study of the Asfalou watershed, Morocco. International Soil and Water Conservation Research, 10(2), 254-272, 2022. DOI: 10.1016/j.iswcr.2021.07.003

Tapia-Silva, F.O., Nuñez, J.M., López-López, D. (2007). Using SRTM DEM, Landsat ETM+ images and a distributed rainfall-runoff model to define inundation hazard maps on urban canyons. In Proceedings of the 32nd International Symposium on Remote Sensing of Environment: Sustainable Development Through Global Earth Observations, San José, Costa Rica, 25–29 June 2007, p. 4.

Tehrany, M. S., Pradhan, B., & Jebur, M. N. (2013). Spatial prediction of flood susceptible areas using rule based decision tree (DT) and a novel ensemble bivariate and multivariate statistical models in GIS. Journal of Hydrology, 504, 69–79. doi:10.1016/j.jhydrol.2013.09.034

Termier H. (1936). Etudes géologiques sur le Maroc Central et le Moyen Atlas septentrional. Notes et M. Serv. Des Mines et de la carte géologique - Rabat, n°.33, t.III

Thomas, J., Joseph, S., & Thrivikramji, K. P. (2018). Assessment of soil erosion in a tropical mountain river basin of the southern Western Ghats, India using RUSLE and GIS. Geoscience Frontiers, 9(3), 893–906. doi:10.1016/j.gsf.2017.05.011

Thorne, R., & Woo, M.-K. (2006). Efficacy of a hydrologic model in simulating discharge from a large mountainous catchment. Journal of Hydrology, 330(1–2), 301–312. doi:10.1016/j.jhydrol.2006.03.031

Thornton E., Neave M. and Rayburg S. (2007). Hydraulic geometry in river channel networks as a method for the assessment of river condition.

Tralli, D. M., Blom, R. G., Zlotnicki, V., Donnellan, A., & Evans, D. L. (2005). Satellite remote sensing of earthquake, volcano, flood, landslide and coastal inundation hazards. ISPRS Journal of Photogrammetry and Remote Sensing: Official

Publication of the International Society for Photogrammetry and Remote Sensing (ISPRS), 59(4), 185–198. doi:10.1016/j.isprsjprs.2005.02.002

Tulu F. D. & Desta M. A. (2015). Human Development and Wetland Conservation Policy. Intern. J. Environmental Sciences, 4, 3, pp. 126-138.

U.S. EPA. (2016). Climate Change Indicators: Wildfires, EPA: Washington, DC, USA.

Valle-Levinson A. (2011). Classification of Estuarine Circulation. In: Wolanski E and McLusky DS (Eds.) Treatise on Estuarine and Coastal Science, Vol 1, Waltham Academic Press, pp. 75-86. DOI: 10.1016/B978-0-12-374711-2.00106-6

Van Beek, C. L., Tóth, T., Hagyó, A., Tóth, G., Recatalá Boix, L., Añó Vidal, C., … Oenema, O. (2010). The need for harmonizing methodologies for assessing soil threats in Europe. Soil Use and Management, 26(3), 299–309. doi:10.1111/j.1475-2743.2010.00280.x

Van der Gun J. & Ahmed A. (1995). The water resources of Yemen. A summary and digest of available information. Technical Report WRY35, Ministry of Oil and Mineral Resources, Sana'a, Yemen. pp 1-106.

Van Der Knijff, J. M., Younis, J., & De Roo, A. P. J. (2010). LISFLOOD: a GIS-based distributed model for river basin scale water balance and flood simulation. Geographical Information Systems, 24(2), 189–212. doi:10.1080/13658810802549154

Van Remortel, R. D., Hamilton, M. E., & Hickey, R. J. (2001). Estimating the LS factor for RUSLE through iterative slope length processing of digital elevation data within arclnfo grid. Cartography, 30(1), 27–35. doi:10.1080/00690805.2001.9714133

Venarsky, M. P., Lowe, V., Frid, C. L., & Burford, M. A. (2022). Flow regimes among rivers influence benthic biota biodiversity but not abundance or biomass in intertidal mudflats and sandflats in wet-dry tropical estuaries. Estuarine, Coastal and Shelf Science, 271, 107858. DOI: 10.1016/j.ecss.2022.107858

Vericat, D., & Batalla, R. J. (2004). Efectos de las presas en la dinámica fluvial del curso bajo del río Ebro. Cuaternario y Geomorfología, 18(1-2), 37-50.

Verner D. & Breisinger C., eds. (2013). Economics of Climate Change in the Arab World: Case Studies from the Syrian Arab Republic, Tunisia, and the Republic of Yemen. World Bank, Washington. DOI: 10.1596/978-0-8213-9846-3

Viana-Soto A, Aguado I, Salas J, García M. (2020). Identifying Post-Fire Recovery Trajectories and Driving Factors Using Landsat Time Series in Fire-Prone Mediterranean Pine Forests. Remote Sensing. 2020; 12(9):1499.

Volpi, M., Petropoulos, G. P., & Kanevski, M. (2013). Flooding extent cartography with Landsat TM imagery and regularized kernel Fisher's discriminant analysis. Computers & Geosciences, 57, 24–31. doi:10.1016/j.cageo.2013.03.009

Wahlstrom, M., & Guha-Sapir, D. (2015). The human cost of weather-related disasters 1995–2015. Geneva, Switzerland: UNISDR.

Walling, D.E., Fang, D. (2003). Recent trends in the suspended sediment loads of the world's rivers. Global Planet. Change 39 (1 , 111-126. DOI: 10.1016/S0921-8181(03)00020-1

Walling, D.E., Webb, B.W. (1996). Erosion and sediment yield: A global overview. In Erosion and Sediment Yield: Global and Regional Perspectives Proceedings of the Exeter Symposium, Walling, D.E., Webb, B.W., Eds., IAHS Publication No. 236, ISI: Exeter, UK, 1996, pp. 3–19.

Wang, L., Cuthbertson, A. J., Zhang, S. H., Pender, G., Shu, A. P., & Wang, Y. Q. (2021). Graded bed load transport in sediment supply limited channels under unsteady flow hydrographs. Journal of Hydrology, 595, 126015. DOI: 10.1016/j.jhydrol.2021.126015

Wang, S., Zhang, K., Chao, L., Li, D., Tian, X., Bao, H., Xia, Y. (2021). EXploring the utility of radar and satellite-sensed precipitation and their dynamic bias correction for integrated prediction of flood and landslide hazards. J. Hydrol. (Amst. 603, 126964. DOI: 10.1016/j.jhydrol.2021.126964.

Wang, Y. (2004). Using Landsat 7 TM data acquired days after a flood event to delineate the maximum flood extent on a coastal floodplain. International Journal of Remote Sensing, 25(5), 959–974. doi:10.1080/0143116031000150022

Webster, T. L., Forbes, D. L., Dickie, S., & Shreenan, R. (2004). Using topographic lidar to map flood risk from storm-surge events for Charlottetown, Prince Edward Island, Canada. Canadian Journal of Remote Sensing/Journal Canadien de Teledetection, 30(1), 64–76. doi:10.5589/m03-053

Weng, Q. (2001). Modeling urban growth effects on surface runoff with the integration of remote sensing and GIS. Environmental Management, 28(6), 737–748. doi:10.1007/s002670010258

Wheater, H., Jakeman, A., Beven, K. (1993). Progress and Directions in Rainfall-Runoff Modelling.

White, W.R. (2000). Flushing of sediments from reservoirs. Thematic Review IV, 5. DOI: 10.1680/eosfr.29538

Whitfield A.K. (1992). A characterization of Southern African estuarine systems. South Afr. J. Aquatic Sci., 18, 1/2, pp. 89-103. DOI: 10.1080/10183469.1992.9631327

Whitfield A.K., Bate G.C., Adams J.B., Cowley P.D., Froneman P.W., Gama P.T. et al. (2012). A review of the ecology and management of temporarily open/closed estuaries in South Africa, with particular emphasis on river flow and mouth state as primary drivers of these systems. Afr. J. Marine Sci., 34, pp. 163-180. DOI: 10.2989/1814232X.2012.675041

Whyte, A., Ferentinos, K. P., & Petropoulos, G. P. (2018). A new synergistic approach for monitoring wetlands using Sentinels -1 and 2 data with object-based machine learning algorithms. Environmental Modelling & Software: With Environment Data News, 104, 40–54. doi:10.1016/j.envsoft.2018.01.023

Williams J. R., Jones C. A., Dyke P. T. (1984). A modeling approach to determining the relationship between erosion and soil productivity. Transactions of the ASAE, 27(1), 129-0144, 1984.

Williams, J. R. (1977). Sediment delivery ratios determined with sediment and runoff models. In: Erosion and Solid Matter Transport in Inland Waters (Proc. Paris Symp., July 1977), 168-179. IAHS Publ. no. 122.

Wischmeier, W.H., Smith, D.D. (1978). Predicting Rainfall Erosion Losses: A Guide to Conservation Planning, Agriculture Handbook No. 537, USDA: Washington, DC, USA.

Wright D. & Bartlett D. (1999). Marine and coastal geographical information systems. Taylor & Francis, Peterborough. 320pp. DOI: 10.4324/9780203484739

Xie, W., Li, X., Jian, W., Yang, Y., Liu, H., Robledo, L.F., Nie, W. (2021). A novel hybrid method for landslide susceptibility mapping-based geodetector and machine learning cluster: A case of Xiaojin county, China. ISPRS Int. J. Geo-Inf. 10 (2 , 93. DOI: 10.3390/ijgi10020093.

Xin, Q., Olofsson, P., Zhu, Z., Tan, B., & Woodcock, C. E. (2013). Toward near real-time monitoring of forest disturbance by fusion of MODIS and Landsat data. Remote Sensing of Environment, 135, 234–247. doi:10.1016/j.rse.2013.04.002

Xu, L., Xu, X., & Meng, X. (2013). Risk assessment of soil erosion in different rainfall scenarios by RUSLE model coupled with Information Diffusion Model: A case study of Bohai Rim, China. Catena, 100, 74–82. doi:10.1016/j.catena.2012.08.012

Yang, J., et al. (2022). Heavy metal pollution in agricultural soils of a typical volcanic area: risk assessment and source appointment. Chemosphere, 135340. DOI: 10.1016/j.chemosphere.2022.135340

Yang, Y., Zheng, J., Zhu, L., Zhang, H., & Wang, J. (2020). Influence of the Three Gorges Dam on the transport and sorting of coarse and fine sediments downstream of the dam. Journal of Hydrology, 128654. DOI: 10.1016/j.jhydrol.2022.128654

Yin, L., Wang, L., Keim, B.D., Konsoer, K., Zheng, W. (2022). Wavelet analysis of dam injection and discharge in three gorges dam and reservoir with precipitation and river discharge. Water 14 (4 , 567. DOI: 10.3390/w14040567

Yuan, S., Li, Z., Chen, L., Li, P., & Zhang, Z. (2022). Influence of check dams on flood hydrology across varying stages of their lifespan in a highly erodible catchment, Loess Plateau of China. Catena, 210, 105864. DOI: 10.1016/j.catena.2021.105864

Yue, Z., Zhou, W., Li, T. (2021). Impact of the Indian Ocean dipole on evolution of the subsequent ENSO: Relative roles of dynamic and thermodynamic processes. J. Clim. 34 (9 , 3591-3607. DOI: 10.1175/JCLI-D-20-0487.1

Zahraoui, M. (1991) - La plate-forme carbonatée dévonienne du Maroc occidental et sa dislocation hercynienne. Thèse ès Sciences, Univ. Bretagne Occidentale, Brest, 261 p.

Zeng T. Q., Zhou Q., Cowell P. & Huang H. (2006). Coastal GIS: Functionality Versus Applications. Aquaculture, 3, pp.101-121.

Zeng, Y., Meng, X., Zhang, Y., Dai, W., Fang, N., & Shi, Z. (2022). Estimation of the volume of sediment deposited behind check dams based on UAV remote sensing. Journal of Hydrology, 612, 128143. DOI: 10.1016/j.jhydrol.2022.128143

Zhang, J., Shang, Y., Liu, J., Lu, J., Wei, S., Wan, Z., ... & Fu, J. (2021). Optimisation of reservoir operation mode to improve sediment transport capacity of silt-laden rivers. Journal of Hydrology, 594, 125951. DOI: 10.1016/j.jhydrol.2020.125951

Zhang, Q. G., Huang, R. Q., Liu, Y. X., Su, X. P., Li, G. Q., & Nie, W. (2016). A physically—based geometry model for transport distance estimation of rainfall-eroded soil sediment. Applied Sciences, 6(2), 34. DOI: 10.3390/app6020034

Zhao, F., Song, L., Peng, Z., Yang, J., Luan, G., Chu, C., Xie, Z. (2021). Night-time light remote sensing mapping: construction and analysis of ethnic minority development index. Rem. Sens. Basel, Switz. 13 11 , 2129. DOI: 10.3390/rs13112129

Zhao, Y., Hu, C., Zhang, X., Lv, X., Yin, X., & Wang, Z. (2021). Response of sediment discharge to soil erosion control in the middle reaches of the Yellow River. Catena, 203, 105330. DOI: 10.1016/j.catena.2021.105330